Pharmacognostic Studies of Natural Deep Eutectic Solvents

BY

YANG LIU
M.S., Key Laboratory of Forest Plant Ecology, Ministry of Education, China 2010
B.S., College of Life Sciences, Northeast Forestry University, China 2007

THESIS

Submitted as partial fulfillment of the requirements
for the degree of Doctor of Philosophy in Pharmacognosy
in the Graduate College of the
University of Illinois at Chicago, 2018

Chicago, Illinois

Defense Committee:
Dr. Guido F. Pauli, Chair and Advisor
Dr. Shao-Nong Chen
Dr. James B. McAlpine
Dr. Djaja D. Soejarto
Dr. Jimmy Orjala
Dr. J. Brent Friesen
Dr. David S. Seigler, University of Illinois at Urbana-Champaign

DEDICATION

This dissertation is dedicated to my family, Yu Zhang and Sophia T. Liu, whose love and support allowed the current endeavor to become a reality.

ACKNOWLEDGMENTS

This dissertation was only made possible with the help and guidance from many scientific researchers. I appreciate all their efforts for the achievements in my dissertation.

Initially, I gratefully acknowledge my thesis committee – (Dr. Guido F. Pauli, Dr. Shao-Nong Chen, Dr. James B. McAlpine, Dr. Djaja D. Soejarto, Dr. Jimmy Orjala, Dr. J. Brent Friesen, and Dr. David S. Seigler) – for their vigorous support and professional assistance. They provided guidance in related areas that helped me accomplish my research goals. I was especially fortunate to have as the advisor of my dissertation and chairperson of my thesis committee, Dr. Guido Pauli, who oversaw the development of my proposal, and provided instructions important to the implementation of the hypothesized research. Because of him, I have directly obtained all possible scientific realization. Of all the kindness that Dr. Pauli has shown me, I am most indebted for his management skills, providing a freedom for my study and for my experimental environment, and allowing me to acquire a unique insight into the natural product research and to keep me productive. Regarding this dissertation, Dr. Pauli has made many suggestions, what I regard as the most significant results of the present research. Moreover, Dr. Pauli has introduced me to cutting-edge technologies, such as quantitative NMR and countercurrent separation (countercurrent chromatography and centrifugal partitioning chromatography), and other key instruments and procedures.

In the past five years, I become proficient in countercurrent separation. Drs. Guido Pauli, J. Brent Friesen, Shao-Nong Chen, James McAlpine, Charlotte Simmler, Jonathan Bisson, Rene Ramos, Rasika Shrikant Phansalkar, and Joowon

Nam, PhD candidates Laura Tyler and Mary Choules have shown me enormous kindness by supporting me with instructions and guidance, and giving me the opportunity to conduct research using droplet countercurrent chromatography, countercurrent chromatography, and centrifugal partition chromatography. I am most grateful to Drs. Pauli, Friesen and McAlpine for the example they set by dedicating so much of their personal and professional time to advancement of theoretical discussion in endeavors where the solvent system selection strategy in countercurrent separation can be developed. It has been truly wonderful to work with Dr. Dianpeng Li, Dr. Kemal Duric, Ms. Qingfei Fan, and Ms. Ting Tang. I really appreciate the cooperation with Dr. Scott G. Franzblau, Dr. Birgit U. Jaki, and Dr. Edyta Grzelak in Institute for Tuberculosis Research - UIC College of Pharmacy. We worked together and attempted to develop a novel strategy, combining with the solvent system selection method and bioautography. Especially, Dr. Grzelak is a brilliant biologist and chemist, and an exceptionally hard worker. It was a great privilege to have worked with her on this project; she always is calm and willing to talk about whatever issue we have. Moreover, I am grateful for support from the team at Cherry Instruments – Wrightwood Technologies (Chicago, IL) in particular by Mr. Samuel Pro and Mr. Warren Friedel.

I have also gained experience in NMR applications, such as quantitative ^{1}H NMR and quantitative ^{13}C NMR. I really appreciate the support from Drs. Guido Pauli, Jimmy Orjala, Brian T. Murphy, Chun-Tao Che, David C. Lankin, Shao-Nong Chen, Aleksej Krunic, Ben Ramirez, Robert Kleps, Jose Napolitano, Charlotte Simmler, Rene Ramos, Shihui Dong, Feng Qiu, Rasika Shrikant Phansalkar, Joowon Nam,

Gonzalo Rodolfo, Larry L. Klein, Tanja Goedecke, Ming Zhao, and Karina Szymulanska, and Ms. Isoo Youn. It would be impossible to overcome some tough but important work without the advice provided by Drs. Pauli and David C. Lankin. Especially, Dr. Lankin can help me to find the answers of my questions on NMR each time. And I can always obtain a direct answer or some potential solutions. Moreover, I am really grateful for USP Global Fellowship from the U.S. Pharmacopeial Convention, which provided financial support for my quantitative NMR research.

In my priority project on natural eutectic solvents, I received much support from our cooperators in College of Pharmacy and/or UIC/NIH Botanical Center: (i) Formulation group (Dr. Richard Gemeinhart and Dr. Yu Zhang). Dr. Yu Zhang has nicely spent a lot of time on discussion with me, and eventually developed a novel formulation (hydrogel) to observe the potential natural eutectic function in (bio)polymers. I am really grateful for all of her hard working for supporting my dissertation; (ii) LC-MS group (Drs. Richard van Breemen, Dejan Nikolic, Alyssa Sprouse, Guannan Li, Yongchao Li, and Lingyi Huang). Dr. Dejan Nikolic regularly provided nearly instant results, and I am grateful even more importantly for his easy-going manner and willingness to share his profuse knowledge of analytical and medicinal chemistry; (iii) Pharmacology group (Drs. Judy Bolton, Birgit Dietz, Shuai Wang, and Huali Dong). I really had an excellent cooperation with Dr. Shuai Wang. We worked together to investigate the licochalcone A function *in vitro* and *in vivo*, and discovered a licochalcone A-based NADES. I am really grateful for Dr. Wang's hard work, and wonderful discussion.

Moreover, I really appreciate the general supports from Dr. Djaja Soejarto,

Dr. Daniel Kulakowski, and Jahir Garzon. This experience was wonderful memory in the past five years. I am grateful for the service of Medicinal Chemistry and Pharmacognosy department office, such as Arletta Harris, Kimberly Huang, Mei Zhang, Dan Lu, Elizabeth Ryan, and Colleen Piersen.

I would like to thank the funding support by grant P50 AT00155 from the Office of Dietary Supplements (ODS) and National Center for Complementary and Integrative Health (NCCIH) of the National Institutes of Health (NIH), and USP Global Fellowship from U.S. Pharmacopeia. I am appreciative to the Department of Medicinal Chemistry and Pharmacognosy in the College of Pharmacy, at the University of Illinois at Chicago, particularly for offering me the Teaching/Research Assistantship to cover a tuition waiver and stipend during my nearly six-year study.

My partner, Dr. Yu Zhang, has been a pillar of support, both personally and professionally, and I am truly fortunate and immensely grateful to have her in my life.

YL

PREFACE

This dissertation is concerned primarily with the roles of natural deep eutectic solvents (NADES) and the NADES phenomenon in natural products research. To date, the NADES matrix in producing plant material, and in corresponding preparations are not understood very well. The present study involves a thorough review of existing literature as well as experimental evidence that extends the current knowledge on NADES. One aspect that is unclear from the literature regards the intermolecular interactions of NADES components in the matrix. This is analyzed via the assistance of new study models, such as the water loss and the hydrogel models. A potential involvement of NADES in poly-pharmacology actions was also uncovered via the multi-component NADES systems, the hydrogel model, and the hydrolysis model. All study models used throughout the present work aim to observe the potential NADES properties and functions in natural product research, rather than pursuing NADES applications. Thus, details of natural products chemistry and related studies are the focus of this work, whereas pharmacological aspects are not involved in this dissertation. One of the aims of this work is to enhance the basic knowledge for future *in vitro* and *in vivo* studies involving NADES. Resulting insights are based on the experimental data obtained. In addition, future NADES pharmacological studies will benefit from the technologies (e.g., countercurrent chromatography and quantitative NMR) developed and evaluated in this study. Collectively, the outcomes of the present work should help better understanding the NADES roles, and the corresponding functions in traditional medicine and botanical dietary supplement applications.

CONTRIBUTION OF AUTHORS

To clarify how each author has contributed to each individual research paper, I assign a person's name against the following roles or tasks: conception or design of the work, data collection, data analysis and interpretation, drafting the article, critical revision of the article, and final approval of the version to be published.

(1) Liu Y., Zhang Y., Chen, S.N., Friesen J.B., Nikolić D., Choules M.P., McAlpine J.B., Lankin, D.C., Gemeinhart R.A., and Pauli, G.F. (2018) The influence of natural deep eutectic solvents on bioactive natural products: studying interactions between a hydrogel model and *Schisandra chinensis* metabolites. Fitoterapia. In Press.

Conception or design of the work: Liu Y. and Zhang Y.

Data collection: Liu Y., Zhang Y., and Nikolić D.,

Data analysis and interpretation: Liu Y., Zhang Y., and Chen, S.N.

Drafting the article: Liu Y. and Zhang Y.

Critical revision of the article: Friesen J.B., Choules M.P., McAlpine J.B., Lankin, D.C., Gemeinhart R.A., and Pauli, G.F.

Final approval of the version to be published: Liu Y., Zhang Y., Chen, S.N., Friesen J.B., Nikolić D., Choules M.P., McAlpine J.B., Lankin, Gemeinhart R.A., and Pauli, G.F.

(2) Liu Y., Friesen J.B., McAlpine J.B., Lankin, D.C., Chen, S.N., and Pauli, G.F. (2018) Natural Deep Eutectic Solvents: Properties, Applications, and Perspectives. J. Nat. Prod. 81 (3): 679–690.

Conception or design of the work: Liu Y. and Pauli, G.F.

Data collection: Liu Y.

CONTRIBUTION OF AUTHORS (continued)

Data analysis and interpretation: Liu Y., Chen, S.N., and Pauli, G.F.

Drafting the article: Liu Y. and Pauli, G.F.

Critical revision of the article: Liu Y., Friesen J.B., McAlpine J.B., Lankin, D.C., Chen, S.N., and Pauli, G.F.

Final approval of the version to be published: Liu Y., Friesen J.B., McAlpine, Lankin, D.C., Chen, S.N., and Pauli, G.F.

(3) Liu Y., Friesen J.B., Grzelak, E.M., Fan, Q., Tang, T., Durić, K., Jaki, B.U., McAlpine, J.B., Franzblau, S.G., Chen, S.N., and Pauli, G.F. (2017) Sweet Spot Matching: A TLC-based Countercurrent Solvent System Selection Strategy. J. Chromatogr. A 1504: 46-54.

Conception or design of the work: Liu Y., Friesen J.B., and Pauli, G.F.

Data collection: Liu Y., Friesen J.B., Grzelak, E.M., Fan, Q., Tang, T., Durić, K., and Chen, S.N.

Data analysis and interpretation: Liu Y., Friesen J.B., and Pauli, G.F.

Drafting the article: Liu Y., Friesen J.B., and Pauli, G.F.

Critical revision of the article: Liu Y., Friesen J.B., Grzelak, E.M., Fan, Q., Tang, T., Durić, K., Jaki, B.U., McAlpine, J.B., Franzblau, S.G., Chen, S.N., and Pauli, G.F.

Final approval of the version to be published: Liu Y., Friesen J.B., Grzelak, E.M., Fan, Q., Tang, T., Durić, K., Jaki, B.U., McAlpine, J.B., Franzblau, S.G., Chen, S.N., and Pauli, G.F.

(4) Liu Y., Garzon, J., Friesen, J.B., Zhang, Y., McAlpine, J.B., Lankin, D.C., Chen, S.N., and Pauli, G.F. (2016) Countercurrent assisted quantitative recovery of metabolites from plant-associated natural deep eutectic solvents. Fitoterapia.

112:30-37.

Conception or design of the work: Liu Y., Garzon, J. and Zhang, Y.

Data collection: Liu Y. and Garzon, J.

Data analysis and interpretation: Liu Y., Zhang, Y., Chen, S.N., and Pauli, G.F.

Drafting the article: Liu Y., Zhang, Y., and Pauli, G.F.

Critical revision of the article: Liu Y., Garzon, J., Friesen, J.B., Zhang, Y., McAlpine, J.B., Lankin, D.C., Chen, S.N., and Pauli, G.F.

Final approval of the version to be published: Liu Y., Garzon, J., Friesen, J.B., Zhang, Y., McAlpine, J.B., Lankin, D.C., Chen, S.N., and Pauli, G.F.

(5) Liu, Y., Friesen, J.B., McAlpine, J.B., and Pauli, G.F. (2015) Solvent System Selection Strategies in Countercurrent Separation, Planta Med. 81: 1-10.

Conception or design of the work: Liu, Y., Friesen, J.B., and Pauli, G.F.

Data collection: Liu, Y., Friesen, J.B., and Pauli, G.F.

Data analysis and interpretation: Liu, Y., Friesen, J.B., McAlpine, J.B., and Pauli, G.F.

Drafting the article: Liu, Y., Friesen, J.B., McAlpine, J.B., and Pauli, G.F.

Critical revision of the article: Liu, Y., Friesen, J.B., McAlpine, J.B., and Pauli, G.F.

Final approval of the version to be published: Liu, Y., Friesen, J.B., McAlpine, J.B., and Pauli, G.F.

(6) Liu, Y., Chen, S.N., McAlpine, J.B., Klein, L.L., Friesen, J.B., Lankin, D.C., and Pauli, G.F. (2014) Quantification of a botanical negative marker without an identical standard: ginkgotoxin in *Ginkgo biloba*, J. Nat. Prod. 77(3):611-617.

Conception or design of the work: Chen, S.N. and Pauli, G.F.

CONTRIBUTION OF AUTHORS (continued)

Data collection: Liu, Y. and Klein, L.L.

Data analysis and interpretation: Liu, Y., Chen, S.N., McAlpine, J.B., Klein, L.L., Friesen, J.B., Lankin, D.C., and Pauli, G.F.

Drafting the article: Liu, Y., Chen, S.N., McAlpine, J.B., Friesen, J.Band Pauli, G.F.

Critical revision of the article: Liu, Y., Chen, S.N., McAlpine, J.B., Klein, L.L., Friesen, J.B., Lankin, D.C., and Pauli, G.F.

Final approval of the version to be published: Liu, Y., Chen, S.N., McAlpine, J.B., Klein, L.L., Friesen, J.B., Lankin, D.C., and Pauli, G.F.

TABLE OF CONTENTS

TABLE OF CONTENTS (continued)

TABLE OF CONTENTS (continued)

LIST OF TABLES

LIST OF TABLES (continued)

LIST OF FIGURES

LIST OF FIGURES (continued)

LIST OF FIGURES (continued)

LIST OF FIGURES (continued)

LIST OF EQUATIONS

LIST OF ABBREVIATIONS

Å	Ångstrom
Ac	Acetonitrile (in CCS solvent system)
AQ	Data acquisition time (in seconds) for the NMR spectra
At	Acetone (in CCS solvent system)
BDS	Botanical dietary supplement
n-BuOH	*n*-butanol
CCC	Countercurrent chromatography
CCS	Countercurrent separation
DCM	Dichloromethane
δ	Chemical shift (ppm)
CPC	Centrifugal partition chromatography
$Cr(acac)_3$	Chromium(III) acetylacetonate
D1	Relaxation delay (in NMR experiments)
D8	Mixing time (in NMR experiments)
DMSO-d_6	Deuterated dimethyl sulfoxide (in NMR experiments)
DS	Dummy scans (in NMR experiments)
E	Ethyl acetate (in CCS solvent system)
EC	External calibrant (in NMR experiments)
Et	Ethanol (in CCS solvent system)
EtOAc	Ethyl acetate
EtOH	Ethanol
EO	Essential oil

FID	Free induction decay
GUESS	Generally useful estimation of solvent systems
H	*n*-Hexane (in CCS solvent system)
Hep	*n*-Heptane (in CCS solvent system)
HMDB	Human Metabolome Database
HPLC	High-performance liquid chromatography
HSCCC	High-speed countercurrent chromatography
IC	Internal calibrant
IR	Infrared spectroscopy
Iso	Isopropanol (in CCS solvent system)
K	Partition coefficient
λ	Wavelength (nm)
LG	Lorentzian–Gaussian window function in NMR
LOD	Limit of detection
LOQ	Limit of quantification
LP	Lower phase
M	Methanol (in CCS solvent system)
Ma	Methyl acetate (in CCS solvent system)
Me	Methyl group
MeOH	Methanol
MP	Mobile phase
MS	Mass spectrometry

MTBE	Methyl *tert*-butyl ether (in CCS solvent system)
NADES	Natural deep eutectic solvent(s) (used as both singular and plural in this work)
NMR	Nuclear magnetic resonance
NOESY	Nuclear Overhauser effect spectroscopy
NP	Natural product
NP-	Normal phase
NS	Number of scans (in NMR experiments)
OAc	Acetoxy group
O1P	Transmitter offset (in NMR experiments)
Pet	Petroleum ether (in CCS solvent system)
pH	$-\log_{10}[H^+]$
ppm	Parts per million
Pro	*n*-Propanol (in CCS solvent system)
qHNMR	Quantitative ^{1}H NMR
qCNMR	Quantitative ^{13}C NMR
R	Recovery yield
Rf	Retention factor: migration distance of an analyte as a fraction of distance of origin to solvent front in thin-layer chromatography
RG	Receiver gain (in NMR experiments)
RGA	Automatic receiver gain (in NMR experiments)
RP-	Reversed phase
rpm	Rotations per minute
Sf	Retention volume ratio (*syn.* Stationary phase fraction): volume of stationary phase as a fraction of total coil volume in countercurrent chromatography

SFE	Supercritical fluid extraction
So	Dimethyl sulfoxide (in CCS solvent system)
SP	Stationary phase
SS	Solvent system
SW	Spectral width (in NMR experiments)
TCM	Traditional Chinese Medicine
TRM	Traditional Medicine
TD	Number of time domain points (in NMR experiments)
ter	*tert*-butyl methyl ether (in CCS solvent system)
TLC	Thin-layer chromatography
UP	Upper phase
UV	Ultraviolet light
v	Volume
Vis	Visible light
Wat	Water (in CCS solvent system)
wt	Weight

SUMMARY

Recently, natural deep eutectic solvents (NADES) were found as natural media in living plants. This provided a clue that some "basic" metabolites, such as sugars, organic acids, and amino acids, may form NADES and, thus, act as important roles that serve unrecognized, important functions in traditional medicine (TRM) and botanical dietary supplements (BDSs).

To evaluate this hypothesis, the present work initially reviews NADES properties and applications in literatures. The present thorough chronological and statistical analysis of existing reports adds to the recognition of the distinctiveness of (NA)DES, involves a discussion of NADES-related observations in NP research, and reports applications of these eutectic mixtures.

In addition, this study investigates the interface of NADES liquid and lipophilic metabolites in botanical extracts, and their cooperative effects. Therefore, this study seeks (Aim 1) to develop methods for NADES analysis: (i) A reproducible ultrasound-vacuum NADES preparation method is developed; (ii) ^{1}H-^{1}H nuclear Overhauser effect (nOe) NMR spectroscopy is used to determine intermolecular interactions in NADES matrix, and to demonstrate the existence of NADES; (iii) A countercurrent separation is trialed to "fully" isolate lipophilic NPs from NADES matrix. In this way, it can provide a tool to investigate the potential roles of the NADES-forming metabolome in botanical extracts, which is the essential forms in botanical dietary supplements and traditional medicine. Meanwhile, countercurrent separation is also used to isolate some NADES components in botanical materials, e.g., citric acid and malic acid in *Schisandra chinensis*. (iv) Quantitative NMR and some reviewed data are used to discover new NADES species in a NP lab. The present work then (Aim 2)

studies the roles of NADES in solubilizing natural products. Except "hole theory", a "binding theory" is proposed to explain NADES extraordinary solubilizing ability for some lipophilic NPs. The nOe NMR experiment provides some specific evidence to support this hypothesis. To observe the NADES behavior in a hydrophilic environment, a hydrophilic hydrogel model is developed. The results show that either artificial NADES solution or botanical extract (e.g., crude extract of *S. chinensis*) can load lipophilic NPs in hydrogel. Interacting with hydrogel polymers, the NADES may act as a "shuttle" in this delivery mechanism, where NADES help to load some lipophilic NPs in polymer network, and then move out of the polymers driven by diffusion. At the end, this study (Aim 3) studies the NADES stability using sucrose-based NADES and the NADES influence on metabolic stability. As NADES involved, ligustilide stability in *Angelica sinensis*-related materials and isoflavone glucosides in *Trifolium pratense*-based hydrolysis model are investigated. The results suggest that herbal extracts or their mixture exhibit NADES properties, stabilizing NPs in study models.

Towards the understanding of the importance of NADES in biological systems, this study also discusses both NADES species and their phenomenon observed in NP research. This aims at rationalizing the applications and assisting future users of NADES by raising some critical NADES applications.

Keywords: natural deep eutectic solvent, countercurrent separation, NMR, *Glycyrrhiza glabra* Linnaeus. (Fabaceae), *Schisandra chinensis* Turczaninow (Schisandraceae), *Trifolium pratense* Linnaeus (Fabaceae), *Angelica sinensis* (Oliver) Diels (Apiaceae).

1. INTRODUCTION

(Previously published as Liu Y., Friesen J.B., McAlpine, Lankin, D.C., Chen, S.N., and Pauli, G.F. (2018) Natural Deep Eutectic Solvents: Properties, Applications, and Perspectives. J. Nat. Prod. 81 (3): 679–690.)

1.1. Eutectic Clues in Traditional and Alternative Medicine

In human history, traditional medicine (TRM) has been making an important therapeutic contribution, prior to the era of modern medicine as well as ongoing. The World Health Organization (WHO) defines TRM as "the sum of the knowledge, skills, and practices based on the theories, beliefs, and experiences indigenous to different cultures, whether explicable or not, used in the maintenance of health as well as in the prevention, diagnosis, improvement or treatment of physical and mental illness."(WHO Executive Board, 2013)

Commonly, TRM depends on the selectivity and availability of officinal herbs (Ekor 2013). Geographically, there are four major herbal healing traditions: Chinese, Ayurvedic (in India), European (including Egyptian), and American Indian (Azaizeh et al. 2010). Due to documented and pertinent efficacy of herbal healing, people continue to use these health care practices, and related knowledge for health improvement or maintenance (Firenzuoli and Gori 2007). Herbal medicines are an important form of TRM and include the application of herbs, herbal materials, herbal preparations, and finished herbal products. Their active ingredients are parts of a single herb or herbal mixture (Oreagba et al. 2011).

Botanical dietary supplements (BDSs) have been developed as an inter-changeable form of alternative medicine in modern society. Although alternative medicine is not integrated into dominant western health care systems, it is still

accepted widely worldwide.

One major goal of natural product research has been to provide direct evidence for the validation of traditional or alternative medicines. Major effects have been expanded to discover pharmaceutical molecules from herbs that can feed drug development work flows, and lead to commercial drugs. Avoiding a random selection of their study material, many NP researchers have been following the documented or proposed efficacy of traditional and alternative medicines. The screening for potential leads typically involves chromatographic technology, and many potential leads or even drugs have been discovered by this approach since 1900s, such as artemisinin (anti-malaria) from *Artemisia annua* Linnaeus (Asteraceae) (Elfawal et al. 2015), cocaine (local anesthesia) from *Erythroxylum coca* Lam (Erythroxylaceae) (Calatayud and González 2003), glycyrrhizic acid (chronic viral hepatitis) from *Glycyrrhiza glabra* Linnaeus (Glycyrrhiza) (Rossum et al. 1998), or salicylic acid that triggered the development of aspirin (anti-inflammatory and fevers) from *Salix cinerea* Linnaeus (Salicaceae) (Wilson 1915). However, this natural product research approach differs with the tenets of the preparation of traditional medical formulae in several ways: (1) TRMs are used in the form of crude extracts rather than single compounds; (2) due to the absence of non-polar organic solvents and chromatographic procedures, it is unclear that traditional or alternative medicines can achieve high yields of these potential hits or leads; (3) while lipophilic molecules require special formulation to achieve efficacy, TRM is short of such technological support or concepts. These collectively raise the interesting question of how TRM preparations can attain their activity by nature of their lipophilic metabolites and maintain their solubility and stability.

A closer examination of TRMs can give some clues regarding this question. For example, Traditional Chinese Medicine (TCM) almost always employs mixtures of herbs to form an efficacious and safe formula (Ekor 2013). Interestingly, some herbs in these mixtures do not contain any significantly active ingredients. Two possible explanations have been proposed. One suggests that auxiliary ingredients from different sources in the mixture may serve a poly-pharmacological function along with the lipophilic metabolites (Malongane et al. 2017), as has been shown for some specific cases (Gisi et al. 1985; Sanhueza et al. 2017). Another theory suggests that redundant ("mimic") metabolites from adjuvant herbs that enhance body's immune response may assist the function of lipophilic active constituents. However, studies have so far overlooked the highly abundant group of hydrophilic metabolites. Recently, some of these metabolites, such as sugars, organic acids, and amino acids, have been determined to function as constituents of eutectic mixtures in natural sources. These natural deep eutectic solvents (NADES) have extraordinary solubilizing and stabilizing abilities for a broad hydrophilicity/lipophilicity range of NPs. This prompted the present studies to explore the proposed and potential poly-pharmacological involvement of these metabolites in botanical extracts.

1.2. Eutectic Phenomenon

The term "eutectic" is derived from the Greek word for low melting and applies to either an alloy or liquid medium. In general terms, a eutectic system represents a mixture of components that by virtue of specific proportions have the lower melting point than any individual component. This study focuses on NP research related eutectics and, thus, only covers eutectic solvents. As evident from the phase diagram shown in Figure 1, temperature and component ratio are two major

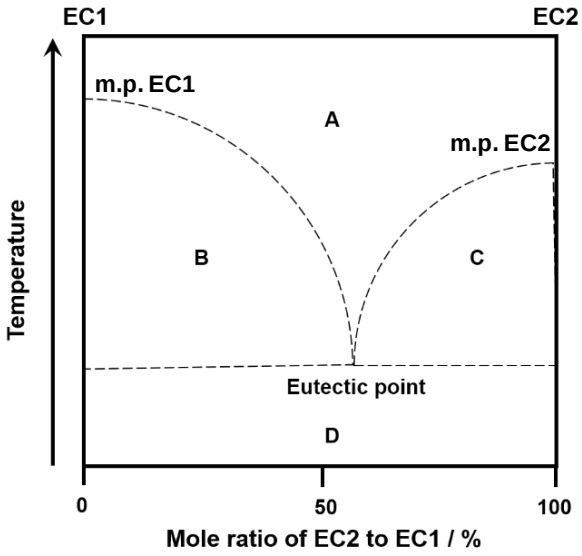

Figure 1. Schematic diagram of the eutectic point in a binary system. A two-component (eutectic component, EC1 and EC2) phase, where m.p. represents melting point. (A) represents the liquid state. (B) and (C) represent "refining zones" that correspond to mixed medium of crystal and liquid. (D) represents the mixture of two solids, EC1 and EC2.

determinants in a binary eutectic system. The components interact via intermolecular forces, but not through covalent or ionic bonds (Pandey et al. 2017). Theoretically, the involvement of other component molecules delocalizes the component molecular lattice units, causing a melting point depression of the corresponding eutectic mixture (Abbott et al. 2003). Compared to the covalent or ionic bonding in a chemical entity, e.g., in ionic liquids (Table I), a eutectic mixture with a low thermodynamic stability tends to be influenced by geometry and chemical environment (Okuniewski et al. 2016), and can dissociate into the individual substances. Owing to this thermodynamic transition, the existence of a eutectic state is not readily recognized in natural materials, which may explain why

TABLE I. COMPARISON OF IONIC LIQUIDS AND EUTECTICS

	Ionic liquids	Deep eutectic solvents
	Distinguishing characteristics	
Constituent	Salt	Salt, sugar, organic acid, amino acid, etc.
Composition	Single salt	Mixture
Intermolecular force	Ionic bonding	Hydrogen bonding
Molecular force	Strong	Weak
Free energy content		1 - 5 kcal/mol
Intermolecular distance	< 1.2 Å	2 - 5 Å
Conductivity	Often moderate	moderate to poor
Vapor pressure	Low	Low
Cytotoxicity	Positive for many	Hardly detectable
	Identical Characteristics	
Melting point	Some are liquid below a given temperature, e.g. 100°C, or some are liquid at or below room temperature.	
Viscosity	Positive correlation with temperature	
Solvating properties	A range of polar and non-polar compounds	
Mobility of solute	Dependent on the size of the mobile species and the availability of hole's appropriate dimensions	

it is a relatively under-represented topic in NP research. As shown by the following examples, eutectic phenomena are encountered in our daily life. Classical examples are honey or syrup, representing mixtures of sugars that are highly viscous media at ambient temperature. They have been used as ingredients for TRMs for hundreds of years (Jain et al. 2010). Another prominent example is the mixture of the two solids menthol and camphor, which can form a eutectic liquid that is used as a vehicle for dissolving drugs (Ribeiro et al. 2015).

1.2.1. Evolution of Eutectic to Natural Deep Eutectic Solvents

As a retrospective example illustrated in Figure 2, the eutectic precipitate of

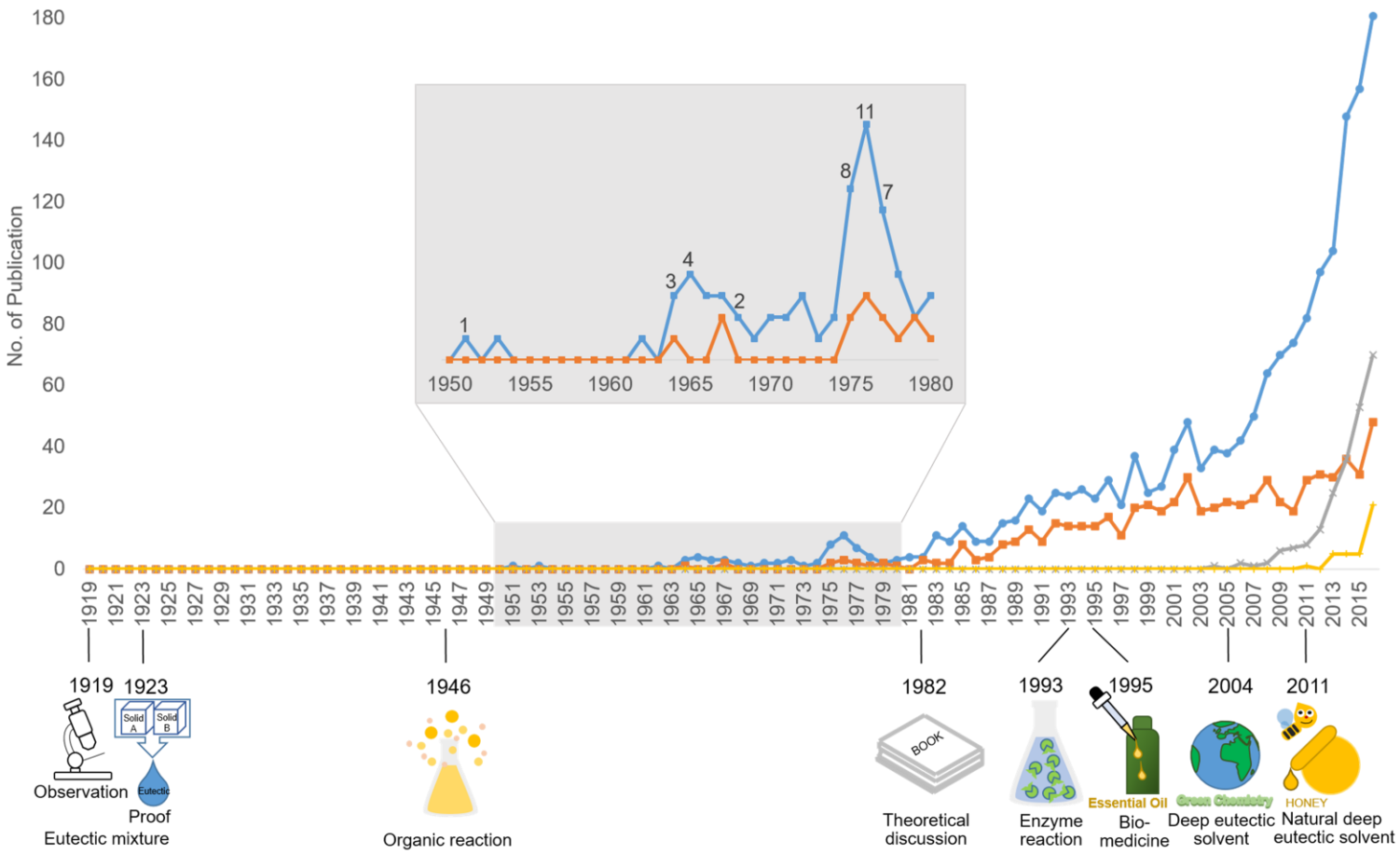

Figure 2. A thorough chronological analysis of the distinctiveness of (NA)DES
Number of publications on eutectic (● in blue, 1700 items), eutectic mixture (■ in orange, 652 items), deep eutectic solvent (- in gray, 224 items), and natural deep eutectic solvent (+ in yellow, 37 items) since 1950. The analysis data were retrieved through PubMed (National Center for Biotechnology Information, NCBI) on November 7, 2016. At the bottom, the chronology of milestones in the research of eutectic events is illustrated.

$NaNH_2$-KNH_2 (1:2, mol/mol) was initially observed as an entity in ammonia solution in 1918 (Franklin 1918). This eutectic phenomenon was studied by establishing a melting point curve of the $NaNH_2$-KNH_2 mixture, as modeled in Figure 1. The eutectic point of $NaNH_2$- KNH_2 was found to be at 97°C at the molar ratio of 1:2 (Kraus and Cuy 1923). Due to its chemical stability and nonvolatile properties at high temperatures, the eutectic mixture of sodium amide and potassium amide was first employed in organic synthesis in 1946 (Bergstrom et al. 1946). Since then, it took more than 30 years before studies of eutectic mixtures entered exponential growth (Figure 2). A series of eutectics and their properties have been uncovered, and the quantity of their relevant applications continues to grow. More examples can be summarized as follows: (i) to overcome the incompatibility issue between enzymes and organic solvents, eutectic media were used as alternatives to organic solvents in catalyze reactions (Gill and Vulfson 1993; 1994). (ii) Eutectic phenomena, e.g., two liquid-solid phase diagrams (often called refining zones, Figure 1B and C), have been used for producing a crystal by changing the temperature, e.g., a melt- or cold-crystallization procedure. This eutectic property has been utilized in a purification study (Davey et al. 1995). (iii) Lipophilic NPs have also been recognized as eutectic components. For instance, a mixture of ibuprofen and certain terpenes, such as 1,8-cineole, *p*-cymene, D-limonene, menthol, menthone, or thymol, can be developed into medical eutectic mixtures. Eventually, these eutectic mixtures were advanced into transdermal drug delivery systems (Stott et al. 1998). (iv) Due to its ecological friendliness and low toxicity, the concept of a deep eutectic solvent was proposed in 2004 to describe a group of eutectic mixtures (Abbott et al. 2004). As alternative candidates to ionic liquids (TABLE I), the deep eutectic solvents represent a group

of universally applied green media; (v) In a key contribution by Choi, Verpoorte, and co-workers on eutectic mixtures in Nature, the concept of a natural deep eutectic solvents (NADES; used as both singular and plural in this work) was advanced recently (Choi et al. 2011). As NADES components always refer to NPs, NADES media gradually have received attention of the NP scientific community.

1.2.2. Deep Eutectic Solvents in Nature

The NADES concept has been proposed via the observation of both the diversity of redundant metabolites in natural sources and the occurrence of certain natural eutectic mixtures (Choi et al. 2011). For example, many plant constituents that have been classified as hydrophilic metabolites are also recognized as being functionally overproduced in their producing organisms. This disproportionality seems to conflict with the natural roles of energy expenditures by living systems. Hence, it is only logical to hypothesize that these metabolites may also play other physiological roles, e.g., as NADES components in Nature. Moreover, certain NPs considered to be lipophilic metabolites may also be produced in copious quantities. For instance, quercetin, which recently has been recognized as a likely invalid metabolic panaceas (IMPs) (Bisson et al. 2016), is highly produced in several plant species, mainly in the form of its glycosides. Therefore, one might assume that it serves a useful purpose in the organisms that produce it. Although this does not imply that all IMPs are NADES components, some of such lipophilic metabolites can be part of NADES matrices. Considering the polarities of both hydrophilic and lipophilic metabolites, NADES media can achieve a broad application. Hence, the diversity of NADES components can enrich the properties and expand the pool of NADES applications.

1.2.3. Applications of Natural Deep Eutectic Solvent

1.2.3.1. NADES as Extraction Media

Any NADES extraction strategy includes two basic steps: (i) the separation of the target analytes from the source tissues or a chemically complex matrix. As NADES species exhibit a superior solubilizing ability for NPs, this provides a special advantage for NADES as the extraction media. Practitioners interested in extraction capabilities of NADES are referred to a pair of excellent recent reviews (Dai et al. 2013, Ruesgas-Ramón et al. 2017). TABLE II provides an update on some of the literature findings, covering 29 compounds belonging to nine different classes that were extracted using NADES media (Dai et al. 2013; Mariappan et al. 2015; Mulia et al. 2015; Zhao et al. 2015; Dai et al. 2016; Kumar et al. 2016; Paradiso et al. 2016). Chalcones, anthocyanins, and phenolic acids are the major target NP classes covered in this work. The most commonly used NADES components are lactic acid, choline chloride, and 1,2-propanediol (used in eight of the nine NADES systems). Compared to organic solvents, many NADES species are relatively viscous at ambient temperature (Duan et al. 2016). This may reduce the capability of target analytes to diffuse passively from the tissues, through relevant cell walls, into the NADES media and, thus, impede the recovery of the target compound from the NADES matrix. (ii) Recovery of target compounds from a NADES matrix. As extraction media, most NADES species are hydrophilic metabolite-based and, therefore, usually nonvolatile (Liu et al. 2015). NADES cannot be evaporated, thus requiring additional chromatographic treatment for neat analyte recovery. According to a previous study (Dai et al. 2016), NADES do not disrupt LC systems. Usually, the chromatographic step enables a separation of the target analytes from

the (NA)DES matrix (Dai et al. 2013). To overcome the absence of UV absorption in many hydrophilic constituents, a conductivity-based device (Liu et al. 2016) has been developed for chromatographic monitoring. Hence, NADES media can even be recycled. Compared to fresh NADES media, reconditioned systems have been shown to exhibit similar extraction yields for the target analytes (Martinez et al. 2016).

1.2.3.2. NADES as Chromatographic Media

In a chromatographic system, the ideal eluent can separate the target analytes into separate concentrated zones at an appropriate separation resolution. As NADES species are capable of selectively extracting NPs in high yields, they may also exhibit efficient chromatographic selectivity for the separation of NPs. In addition, a polarity gradient of NADES species can be designed using organic dyes (Reichardt 1994). Due to the development of hydrophobic NADES species (Ribeiro et al. 2015), the diversity of NADES candidates as chromatographic eluents is likely to increase over time. The compatibility of the thermodynamics also suggests that some NADES species may qualify as chromatographic media. Altogether, NADES media may function as proper mobile phases in different chromatographic strategies. For example, regarding a liquid-only countercurrent separation, one documented biphasic solvent system represents an individual column behavior. As with all solvents, the development of the biphasic solvent systems becomes a priority task for countercurrent separation (Liu et al. 2015), including for NADES. To extend differences in column behavior, a NADES-based solvent system has been demonstrated recently (Roehrer et al. 2016).

TABLE II. OVERVIEW OF NADES APPLICATIONS AS EXTRACTION MEDIA

NADES systems	Class	Analytes	Resource
1,2-Propanediol-choline chloride-	Xanthonoid	α-Mangostin	*Garcinia mangostana*
Lactic acid–glucose 1,2-Propanediol–choline chloride	Anthocyanins	Delphinidin, cyanidin, peonidin, pelargonidin, petunidin and malvidin	*Catharanthus roseus*
Proline-malic acid-water Sucrose-choline chloride-water Lactic acid-glucose	Chalconoid	Carthamin, cartormin, hydroxysafflor yellow A, N1,N10,N5-(*Z*)-tri-pcoumaroylspermidine, N1-(E)-N5,N10-(*Z*)-tri-p-coumaroylspermidine, N1,N10-(*E*)-N5-(*Z*)-tri-p-coumaroylspermidine, stereoisomer of tri-pcoumaroylspermidine, N1,N10,N5-(E)-tri-p-coumaroylspermidine	*Carthamus tinctorius*
Lactic acid-glucose-water	Phenolic acid	Hydroxybenzoic acid, protocatechuic acid, vanillic acid; *p*-coumaric acid; caffeic acid	Olive oil
	Phenethyl alcohol	Tyrosol	
	Flavone	Apigenin	
	Lignan	Pinoresinol	
Lactic acid-choline chloride	Biopolymer	Lignin, cellulose, hemicellulose, holocellulose	Rice straw
Proline-lactic acid	Zingerone	Gingerol, shogaol	*Zingiber officinale*

1.2.3.3. Biomedical Applications of NADES

Investigations of the biocompatibility of NADES have shown that NADES species can replace organic solvents, such as DMSO as dissolving media in biological assays. In the reported applications, the NADES solutions of the test samples were diluted during the biological studies, typically to the point where the NADES matrix was disrupted, meaning that the NADES species eventually lost their solubilizing and/or stabilizing abilities. Therefore, reported protocols have been carrying the inherent risk of not determining the true bioactivity of the target analyte, because disruption of the NADES matrix may cause the loaded NPs to precipitate and/or change their physiochemical stage. However, the disruption of NADES matrices together with the NADES duality (lipophilicity and hydrophilicity) feature suggests that NADES are capable of serving a helpful role in small-molecule formulation. For example, NADES can carry lipophilic bioactive ingredients for subsequent loading into an otherwise polymer such as a hydrogel. This is feasible, as spontaneous diffusion by movement along a concentration gradient removes NADES components from the polymer, whereas a sizable portion of the lipophilic molecules passively remains inside the biopolymer construct. This advantageous behavior indicates that NADES species may be structurally analogous to cyclodextrin, a commonly used excipient in hydrophobic drug delivery system.

In the context of biomedical applications, it is important to remember that lipophilic synthetic-based or metabolite-based NADES can form biomedical delivery systems by themselves. For example, lidocaine hydrochloride-acrylic acid and lidocaine hydrochloride-methacrylic acid can form polymerized eutectic systems (Sanchez-Leija et al. 2014). Considering the structural similarity between lidocaine

and the capsaicins, eutectic formation is likely a shared property of these types of amides. Other examples are the eutectic ibuprofen-menthone, ibuprofen-1,8-cineole, ibuprofen-D-limonene, and ibuprofen-*p*-cymene systems, which have been developed into transdermal delivery eutectic systems (Stott et al. 1998). Ibuprofen-menthol-poly-ϵ-caprolactone has even been developed to create eutectic controlled release systems (Aroso et al. 2015).

1.2.3.4. Basic Research on NADES

The electrochemical properties of NADES including their conductivity allow their Ohm-metric monitoring. For example, when studying the recovery of NPs from a NADES matrix, a phase metering apparatus could be employed to differentiate NADES (as a negative/dispersive signal) from the absorption signals of eluting analytes (Liu et al. 2016). With the assistance of a buffer solution, NADES as electrochemical reagents can also enhance the electrochemical detection of NPs (Gómez et al. 2016). Moreover, dipeptide-based eutectic solvents have been shown to catalyze organic reactions (Kumar et al. 2016). An unexpected property of some amine-based NADES species was their high solubility for CO_2, compared to aqueous amines (Sze et al. 2014; Uma Maheswari 2015; Trivedi et al. 2016). Amine-based NADES species can avoid elevated vapor pressure in the procedure of CO_2 dissolution. This suggests that NADES have the potential capability of capturing gaseous molecules from the air, and can possibly be developed into novel absorbent materials.

1.3. Statement of the Problems

As NADES species are not commercially available, their systematic preparation becomes the first step of this study. As shown in Figure 1, NADES preparation is

about the administration of a certain component ratio and the generation of a suitable entropy in the NADES matrix. It consists of a heating and/or homogenizing procedure. Notably, the simple mixing of NADES components together may or may not transfer the solid phase of NADES components into a liquid phase. Especially for the NADES research novice, this leads to the challenge of producing a proposed NADES. Although a vortex-vacuum evaporating method has been developed, this preparation is routinely laborious. For example, when glucose-choline chloride-water (2:5:5, mol/mol) was prepared, the glucose crystals greatly slowed down the dissolving procedure when using vortex. Thus, an alternative preparation strategy was in demand. Moreover, while ternary aqueous NADES species are empirically important for NP research, the preparation is an iterative process, where the practitioner must measure the water content in the NADES matrix several times until achieving an accurate result. Therefore, it was necessary to perform a systematic study for assessing the water loss process during the vacuum evaporation step.

Unlike for organic solvents or ionic liquids, the basic structural unit of NADES media primarily depends on the intermolecular interactions (e.g., hydrogen bonding) among the components. This makes NADES matrices sensitive to various factors, such as water content, temperature, and component ratio. For efficient NADES applications, the practitioner must consider such inherent properties of NADES species. For example, because of the weak intermolecular interactions, it is challenging to preserve an entire NADES matrix during dilution.

NADES media can dissolve natural or synthetic chemicals of low water solubility. However, it is still unclear how the NADES matrix structure achieves such a property. Thus, the intermolecular interactions of NADES components have to be

investigated, which requires development of a suitable protocol. To understand NADES's solubilizing and stabilizing abilities, the interactions between NADES components have to be examined.

As this study also hypothesizes that NADES exists as liquid in Nature, direct evidence is also sought in support of this hypothesis. For this, the NADES components in natural sources have to be characterized. Also, as the function of NADES in botanical extracts has rarely been investigated, the poly-pharmacological interaction mechanisms between NADES and some lipophilic metabolites need to be studied. Namely, newly discovered NADES functions can provide an improved perspective for the understanding of the NADES mechanism in NP extracts, BDSs, and TRMs.

Because of the inherently great hydrophilicity and low vapor pressure of some NADES, it is difficult to recover the lipophilic metabolites from a NADES solution. Hence, a separation or chromatography step has to be implemented. However, conventional solid-phase-based liquid chromatography is known to cause some sample loss, complicating the systematic explanation of the NADES' functions in botanical extracts. To overcome this deficiency, an alternative methodology needs to be developed. Being a liquid-only chromatography, countercurrent separation (CCS) minimizes analyte losses on the column, and thus, sample recovery is approximately 100%, practically depending on sample handling. Moreover, in CCS, achievable resolution depends on the partitioning coefficient of the analytes. Compared to most lipophilic metabolites, the hydrophobic NADES components usually are very polar, and thus, CCS can fully separate lipophilic metabolites from NADES matrix according to the theory. To evaluate this proposal, a CCS strategy

was designed as a study model. On another level of study, the key of successful CCS is the selection of a suitable solvent system. To alleviate an excessive workload, a TLC-based CCS solvent system strategy tends to be used and could be extended to NADES studies. For evaluation of feasibility, such a strategy should provide the theoretical support required to develop correlations between TLC R*f* and CCS K values.

New study models also have to be developed to reveal whether cooperative mechanisms exist in natural sources, BDSs, and TRM formulas. Such study models would also be helpful for better understanding of the NADES phenomenon and the development of new NADES applications.

Most NADES components are abundant metabolites that predominate quantitatively in many natural sources. At the same time, NADES composition differs from plant to plant, and sometimes even between different parts of the same plant. This suggests that NADES components could be suitable marker compounds for quality control of botanical products, a possibility that will also be investigated in this study.

Finally, the known special role of the water molecules in NADES triggers a reasonable hypothesis that some liquid/gaseous ingredients may also be able to serve as (NA)DES components. However, this type of NADES components is rarely reported. Therefore, this study will also examine some unique NADES species to discuss the possibility of NADES component extension.

1.4. General Hypothesis and Aims

General hypothesis: In NP research, fractionation often causes the loss of bioactivity. Therefore, TRM formulae and BDSs are still applied in the form of crude

extracts. Moreover, NADES media show distinctly solubilizing or stabilizing abilities on purified lipophilic materials. This suggests that NADES metabolites as components of a liquid phase may have important functions in botanical extracts, including a poly-pharmacological influence that is often referred to as "cooperative". The present work is driven by the hypothesis that NADES existing in a botanical extract can interact with the lipophilic metabolites and, thus, impact the corresponding pharmacological activities. Accordingly, NADES may play important roles in BDS and/or TRM formulae. To validate this hypothesis, three specific aims have been proposed.

Aim 1: Methods for NADES analysis

Aim 1a) Development of a NADES preparation protocol

In order to prepare NADES in a reproducible and efficient manner, an ultrasound-vacuum centrifugal evaporation method was developed. The use of ultrasound permitted the efficient dissolution of solid particles, while vacuum centrifugation led to the reproducible removal of extra infused water. Moreover, the NADES (e.g., glucose-choline chloride-water and mannose-dimethylurea-water) can be used to perform water loss studies. By means of observed correlations of water loss data points, the corresponding NADES preparation time can be estimated individually.

Aim 1b) Intermolecular interactions of NADES components

To understand the mechanism of NADES solubilizing and/or stabilizing power, the molecular interactions among NADES components have to be investigated. As the intermolecular interactions mainly involve hydrogen bonding, ^{1}H-^{1}H nuclear Overhauser effect NMR spectroscopy can be used to determine 2 - 5 Å distance interactions. A further aim was to increase resolution of the ^{1}H NMR spectra through

dilution of NMR samples to an optimal concentration. For this purpose, the NADES species can be diluted with solvents under control conditions (see water loss study in **Section 2.1.1**), as the NADES NMR samples are prepared.

Aim 1c) NADES behavior in countercurrent separation (CCS)

One important prerequisite for studying the potential function of the NADES-forming metabolome in botanical extracts is the ability to separate cleanly these polar hydrophilic molecules from the lipophilic NPs. To achieve this goal, a recovery study model was developed using CCS. The advantage of CCS can be found in **Section 2.4.1**. In brief, compared to other chromatographic methods, CCS minimizes and theoretically eliminates sample loss on the column. The recovery study aims to develop a technology for future pharmacological studies.

Aim 1d) Standardization of NADES components in herbal preparations

One challenge related to this aim relates to the polar nature of NADES: many of the NADES metabolites show unfavorable solid-support chromatography characteristics, particularly in isolation procedures that are key to the characterization of the NADES components. As a liquid-only chromatographic method, CCS exhibits the potential to solve this issue. As its column behavior depends on the corresponding solvent systems, some highly polar solvent systems (e.g., EtOAc-BuOH-Water and MeCN-Water) can be selected and be used for the standardization or characterization of NADES components in herbal preparations.

Aim 2: NADES's role in solubilizing natural products

Aim 2a) The role of NADES in solubilizing other metabolites

Although many studies have shown that NADES exhibit an extraordinary solubilizing ability for NPs with a broad hydrophilicity/lipophilicity range, the

corresponding mechanisms are still not fully uncovered. So far, the "hole theory" has been used to explain the capability of NADES's extraordinary solubilizing ability. As the NADES matrix is formed via intermolecular interactions (e.g., hydrogen bonding) of different components, any extra hydrogen bonding among the NADES components may contribute to the solubility of target analytes. To uncover the NADES solubilizing ability for lipophilic metabolites, some studies must be implemented, e.g., using quantitative NMR method.

Aim 2b) Establishment and evaluation of a hydrogel model

NADES species have great solubilizing power for some lipophilic molecules despite their simple composition of hydrophilic organic molecules and water. At the same time, a NADES matrix can be readily disrupted into individual NADES component via dilution with water. The unique properties of NADES species can be applied to a model polymer system: a hydrophilic chitosan/alginate-based hydrogel. On one hand, NADES behavior in (bio)polymers can be observed using this system. On the other hand, the possibility of NADES as dissolving solvent used in a formulation can be evaluated.

Aim 2c) Interaction between *Schisandra chinensis* fruit extract and a hydrogel model. NADES species occur ubiquitously in natural sources. Thus, a crude extract from a natural source is usually a mixture of the NADES species and other lipophilic metabolites. This suggests that a botanical extract may bode a similar mechanism as put forward in Aim 2b. With the assistance of a hydrogel, the behavior of botanical NADES in biopolymer can be simulated. This may also provide insight on the molecule-loading selectivity of a (bio)polymer.

Aim 3: NADES influence on metabolic stability

Aim 3a) NADES stability

In Nature, the NADES state can be considered as being a dynamic equilibrium. The stability of NADES can be influenced by the water content (see water loss study in **Section 2.1.1**). This change may influence solubility of dissolved molecules. On another level of concern, NADES preparation (heating or dissolving with water) may influence the stability of NADES components. This study will investigate whether NADES experience instability during preparation or storage. This finding may be helpful for the development of future NADES applications.

Aim 3b) NADES and stability of NPs

Due to the difficulty of recognizing NADES in natural sources, artificial combination of presumptive NADES components becomes a lead strategy for NADES discovery. NADES have already exhibited a stabilizing ability for many NPs. However, the stabilizing capability of NADES matrices from natural sources is still unclear. Thus, this study focuses the stability of NPs in natural sources such as *Angelica sinensis* to help clarify the stabilizing properties of NADES. This may provide additional evidence for the hypothesis that TRMs and BDSs are best administrated in the form of crude extracts, rather than purified compounds.

Aim 3c) NADES's influence on stability of the metabolites

Insight is growing that the abundance and importance of NADES in natural sources get important, but neglected factors to consider. However, TRMs and BDSs consider the entire crude extract as a complex of active pharmaceutical ingredients, assuming that the therapeutic function could be established on a potential poly-pharmacology mechanism, but may not only depend on one or a few major lipophilic compounds. Therefore, the NADES metabolites may play a vital role in the

therapeutic formulae. Specifically, NADES may influence stability of the metabolites (or metabolic stability). To uncover this possibility, *S. chinensis* fruits and their extract was used to explore the botanical NADES effect on a hydrolysis model based on *Trifolium pratense* in this work.

2. BACKGROUND

(Previously published as Liu Y., Friesen J.B., McAlpine J.B., Lankin, D.C., Chen, S.N., and Pauli, G.F. (2018) Natural Deep Eutectic Solvents: Properties, Applications, and Perspectives. J. Nat. Prod. 81 (3): 679–690.; Liu, Y., Friesen, J.B., McAlpine, J.B., and Pauli, G.F. (2015) Solvent System Selection Strategies in Countercurrent Separation, Planta Med. 81: 1-10.; Liu Y., Zhang Y., Chen, S.N., Friesen J.B., Nikolić D., Choules M.P., McAlpine J.B., Lankin, D.C., Gemeinhart R.A., and Pauli, G.F. (2018) The influence of natural deep eutectic solvents on bioactive natural products: studying interactions between a hydrogel model and *Schisandra chinensis* metabolites. Fitoterapia. In Press.)

2.1. Natural Deep Eutectic Solvent (NADES)

2.1.1. Chemical Constituents of NADES

Due to the difficulty of recognizing NADES in natural sources, artificial combinations of presumptive NADES components became a leading strategy for NADES discovery (Choi et al. 2011, Dai et al. 2013). Regarding binary eutectic systems, once a mixture of natural metabolites under a certain molar ratio (usually close to 1:1) turns into a unified and transparent liquid at ambient temperature, these NPs are, *a priori*, NADES components. The corresponding NADES species may coexist in Nature. It is noted that this NADES discovery strategy may somehow distract from the actual discovery of truly multicomponent NADES species in natural sources. Nonetheless, the sets of possible NADES components are reviewed, as follows.

The most understudied NADES components are hydrophilic metabolites. This group of NADES components is characterized by their high hydrophilicity and comprises sugars, organic acids, amino acids, and choline salts (Liu et al. 2016). Over 135 hydrophilic metabolite-based binary NADES species have been found (Choi, et al. 2011 and 2013; Ru and König 2012). Working combinations of binary eutectic mixtures can almost always be developed into multicomponent eutectic

systems. Accordingly, the hydrophilic metabolite-based NADES species have a rather sizable group of systems. Until now, most NADES studies or applications have been developed via this relatively simplistic group of NADES species.

Whereas many NADES constituents are organic molecules with relatively simple structures, it is important to realize that some other formulations consisting of more complex lipophilic NPs, plus sometimes including designated NPs, are also capable of forming eutectic systems at ambient temperature. Examples are: (i) some essential oil ingredients with low melting points, such as 1,8-cineole, *p*-cymene, D-limonene, menthol, menthone, or thymol, which tend to form NADES (Stott et al. 1998). (ii) A eutectic solvent can also consist of a hydrophilic metabolite and a lipophilic metabolite. For example, a mixture of menthol (lipophilic metabolite) and an organic acid (hydrophilic metabolite) is known to form a hydrophobic NADES system (Ribeiro et al. 2015). In addition, nuclear Overhauser effect (nOe) NMR experiments have indicated strong dipole-dipole interactions between the hydroxy groups of quercetin and the components of the NADES consisting of xylitol-choline chloride-water (1:2:3, mol/mol) (Dai et al. 2013). Thus, the designated lipophilic metabolite, quercetin, could well form part of a NADES matrix. (iii) Glycosidic NPs are characterized by the abundance of functional groups (OH) that are common in both hydrophilic and lipophilic metabolites. For example, rutin is often found in vascular plants, and although no reports have been found yet, it is likely that rutin will be recognized as a NADES component.

Water is one of most abundant and smallest chemical entities on earth and universally present in living organisms. Thus, it is not surprising that water is a NADES component. Until now, at least 39 aqueous NADES species have been

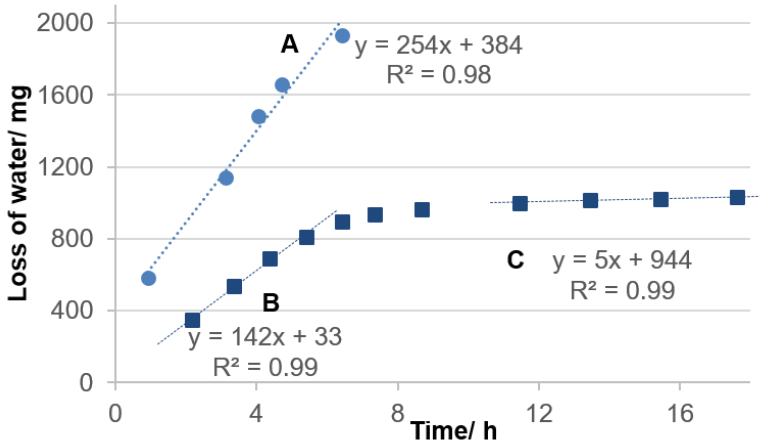

Figure 3. Water loss study shows the transition from a NADES solution to the NADES state. For curve A, (●) distilled water was dried by a vacuum centrifugal evaporation. For B and C (■) a NADES composed of mannose (0.01 mol), dimethyl urea (0.025 mol) and distilled water (2 mL) was used. After dissolving the constituents in the water, the resulting solution was treated by vacuum centrifugal evaporation. The drying curve of the mannose-dimethyl urea-water mixture was split into two time zones: a rapid drying zone (B) during the first 7 h and a subsequent stage, (C) that reflects the asymptotic loss of water from 12 to 18 h. During both stages, a linear correlation can be established between the time and the quantity of water loss.

described in the literature (Dai et al. 2015; Zhao et al. 2015; Craveiro et al. 2016), and all of them are ternary NADES systems. The intermolecular interactions between water and the other components can be recognized via nOe NMR measurements. For example, the intermolecular interactions between the components of 1,2-propanediol-choline chloride-water (1:1:1, mol/mol) could be distinguished using NOESY experiments (Choi et al. 2011). To better understand the role of water in a ternary aqueous NADES system, a water loss study was performed as shown in Figure 3. It demonstrates that two major hydrogen bonding zones, the NADES state and the NADES solution state, existed, where the data points have a linear

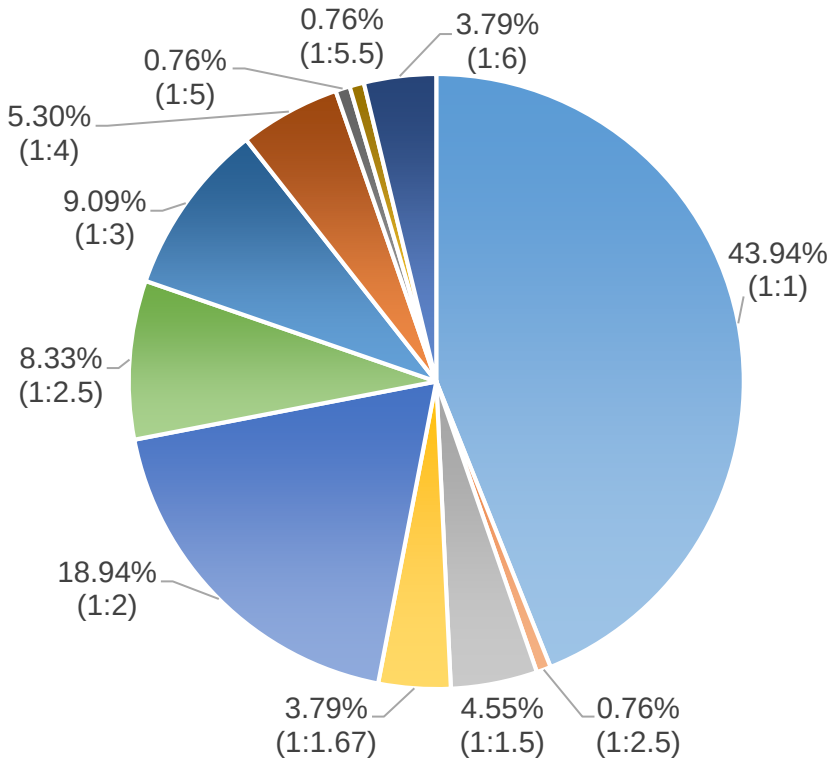

Figure 4. Distribution of the percentage of each component molar ratio of NADES.
The units were normalized to molar ratio (mol/mol) in this work. The data were from NADES publications (Choi et al. 2011 and 2013; Liu et al. 2016; Ribeiro et al. 2015).

correlation in either state. Compared to the solution state, the NADES state demands more energy to remove water from the NADES matrix. According to the Frank model (Frank and Wen 1957) for the structure of water around an ion, a closer intermolecular distance (or NADES state) means an ordered zone, and, thus, causes a stronger intermolecular force. The NADES state consists of an ordered hydrogen-bonding matrix. In the NADES state matrix, the minute quantities of water enable formation of a higher ordered hydrogen-bonding network. Here, water becomes an

integral NADES constituent, at molar proportions similar to those of the other constituents.

Inorganic salts are also universal in Nature in the form of aqueous solutions. Although they form a small group of NADES components, $AlCl_3$, NH_4Cl, NaCl, $ZnCl_2$, $ZnBr_2$, $FeCl_3$, $SnCl_2$, and $CaCl_2$ have been recognized as NADES components (Ru and König 2012; Dai et al. 2013). Regarding this type of NADES, the eutectic donor mates are usually organic alcohols, such as ethylene glycol, or amides, such as urea. They function as donors in nonmetal complexation and always coordinate to the cation (Ru and König 2012). As such, inorganic salts have become a less studied, but still important factor in NP research, e.g., when investigating the water fraction of a crude extract.

2.1.2. Ratios of NADES Components

Empirically, the molar ratio of the eutectic components in a binary system should be near unity, because the lattice binding of a single component depends on the involvement of the other components of the lattice (Abbott et al. 2003). Moreover, the ratio of hydrogen bonding donors and acceptors is another factor that implies unity ratio principles. However, the stoichiometry of hydrogen bonding donors of a certain NADES component can be inconsistent with that of the acceptor function from other components. This may introduce a deviation from the "theoretical" component ratio of 1:1 (mol/mol). Over 135 hydrophilic metabolite-based binary NADES were surveyed and facilitated in preparing this work. Among these NADES (Figure 4), those with a molar ratio of 1:1 constitute about 44%, whereas NADES with molar ratios no higher than 1:4 account for almost 95% of all assessed NADES

TABLE III. INTERMOLECULAR INTERACTIONS IN NADES AS DETERMINED BY FT-IR AND NMR

	NADES system	Functional groups	Reference
FT-IR			
	Proline-malic acid	C=O and O-H	(Dai et al. 2015)
	Trehalose-choline Cl	C=O, C-H, CH_3, and O-H	(Xin et al. 2017)
	Quercetin-glucose-choline chloride	C=O, O-H, and aromatic ring	(Dai et al. 2014)
	1,2-Propanediol-choline Cl	CH_3 and O-H	(Mulia et al. 2015)
NMR			
^{1}H NMR	Trehalose-choline Cl	Dilution effect (CH_2)	(Xin et al. 2017)
NOESY	Sucrose-malic acid	H, O-H and water	(Choi et al. 2011)
	1,2-Propanediol-choline Cl-water	H	(Dai et al. 2013)
	Xylitol-choline Cl-quercetin	O-H	(Dai et al. 2013)
	Glycerol-choline Cl-water)		(Hadj-Kali et al. 2015)
HOESY	1,2-Propanediol-choline chloride-water	C and H	(Dai et al. 2013)

Note: NOESY, nuclear Overhauser effect spectroscopy; nOe, nuclear Overhauser effect; HOESY, Heteronuclear nOe experiment; choline Cl, choline chloride

species. No binary NADES species has been found yet, where the ratio rises over 1:6. Regarding multicomponent NADES systems, the binary component-based rules continue to apply in principle.

2.1.3. Physicochemical Interactions of NADES Components

The most prominent functional groups of NADES are the carboxylic acids, hydroxy groups, and carbonyl groups (Dai et al. 2013). In a NADES matrix, these groups can form a hydrogen bonding network via intermolecular interactions that modify their physicochemical environment. At least two basic strategies can be used to determine the physicochemical interactions: one strategy involves referencing functional group properties. As shown in TABLE III, FT-IR spectrometry (Dai et al. 2014 and 2015; Mulia et al. 2015; Xin et al. 2017) and ^{1}H NMR spectroscopy (Xin et al. 2017) have been used to recognize functional group modifications by comparing them to the individual isolated components. The hydroxy and carbonyl groups are two major functional groups used in this strategy. The second method involves detection of nOe effects via ^{1}H,^{1}H dipole-dipole relaxation. An nOe between small molecules may be observed between hydrogen nuclei that are 2 - 5 Å apart. Typically, NOESY (Choi et al. 2011 and 2013; Hadj-Kali et al. 2015) and HOESY (Dai et al. 2013) experiments are applied to measure the intermolecular ^{1}H dipole-dipole interaction (TABLE III). In this strategy, the signals of interacting protons are the investigated subjects. However, as the high viscosity of some NADES species may lower the resolution of the ^{1}H NMR spectra, it becomes difficult to distinguish the ^{1}H signals of the corresponding functional groups, especially for the mixtures of sugars and/or amino acids. To overcome this disadvantage, two major approaches can be used, see also the proposed entropy models in Figure 5. (i) Temperature

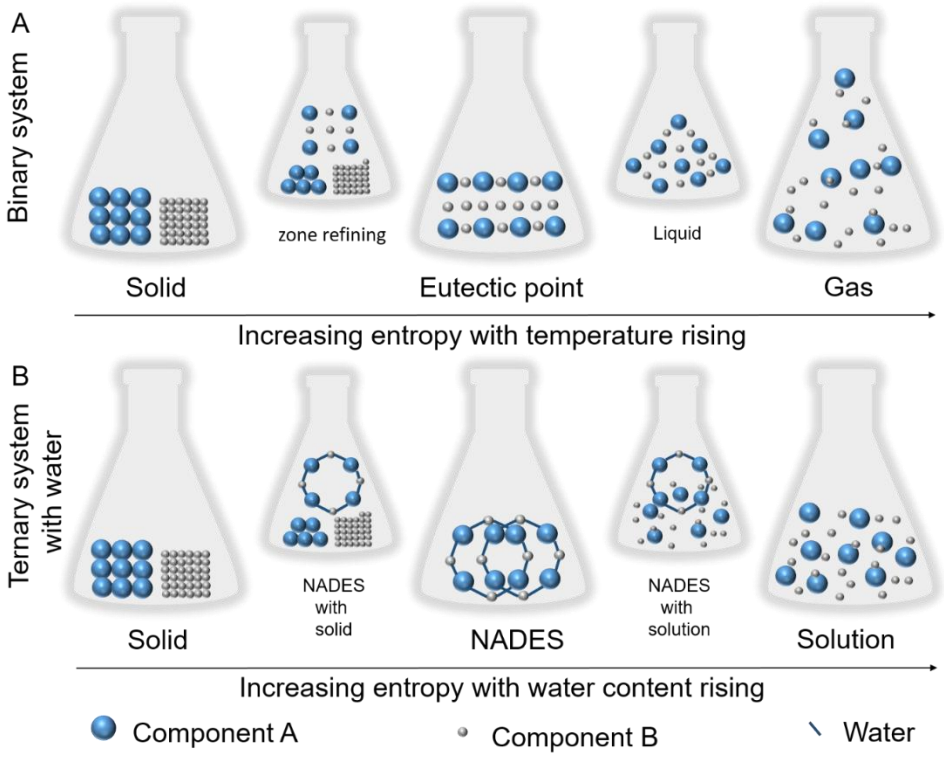

Figure 5. NADES kinetic energy model. (A) a binary NADES system (temperature administration); (B) a ternary aqueous system (water content administration). As entropy rises, the strength of intermolecular bonding decreases, and other relevant physical parameters, such as melting point, solubilizing and stabilizing abilities, polarity, and biomedical property, will be influenced.

administration: usually, a higher temperature increases the entropy level in the NADES matrix and, thereby, reduces the viscosity effects. Thus, NOESY experiments used in NADES studies should be acquired at a temperature ≥ 40°C (Choi et al. 2011). Depending on the capabilities of the NMR instruments, particularly the probe, temperatures up to 80°C are typically practical. However, the boiling point of the NMR solvent is another consideration. (ii) Water content administration or "diluting effect". As discussed in the water loss study (Figure 3), an appropriate dilution can reduce the viscosity of the NADES matrix. This entropy regulation

(Figure 5) can produce an increase in the NMR spectral resolution. However, because overdilution causes NADES disruption, the optimum degree of dilution has to be determined for each individual NADES when using this approach.

2.1.4. NADES Properties

Expanding both NADES applications and overall understanding of NADES in the future will depend on the observation, comprehension, and interpretation of observed NADES phenomena. The study of NADES properties lies mainly in the fields of physical chemistry and thermodynamics. Herein, several important properties are reviewed to summarize the current knowledge and provide guidance for NADES applications relevant to NP research.

2.1.4.1. Renewability and Biodegradability

One of the main attractive properties of NADES is that their components are all NPs. Thus, NADES can be biosynthesized as well as metabolized by many organisms, explaining why they are ultimately highly "biocompatible". Compared to organic solvents and ionic liquids, the biodegradability of NADES helps avoid potential environmental hazards. Therefore, NADES systems are generally considered to be environmentally friendly and function as green solvents (Paiva et al. 2014). For applications as functional solvents, NADES can be recycled and reused. So far, many recovery strategies, such as supercritical CO_2, anti-solvents, back extraction, chromatography (anion exchange resin and countercurrent separation) (Dai et al. 2013) have been used for this purpose. According to one study (Dai et al. 2016), dilution of a NADES will not influence its chromatographic behavior. This suggests that the separation of a target analyte and the recycling of a NADES can be achieved simultaneously. In order to maintain the quality of reconditioned

NADES, they can be analyzed quantitatively by MS, IR and/or NMR methods (Florindo et al. 2014; Liu et al. 2016). Sometimes, the composition needs readjustment by addition of precise amounts of certain individual components. This renewable cycle can reduce the total cost of NADES applications.

2.1.4.2. Conductivity and Viscosity

As the conductivity and viscosity of NADES are influenced by similar physiochemical factors, they can be discussed together. In an ionic (or electrolyte) solution model, temperature (Equation 1) is one major factor determining conductivity. As the kinetic energy rises, the conductivity of a binary NADES system can increase significantly (Zhao et al. 2015). On the other hand, the intermolecular cohesive forces contribute to liquid viscosity (Stefanovic et al. 2017). Because entropy energy can regulate the cohesive forces in a NADES matrix (Abbott et al. 2004), the viscosity of a NADES species is very sensitive to temperature (Zhao et al. 2015). High temperature will overcome the strength of intermolecular forces and, thus, lessen the matrix viscosity. These indicate that conductivity is directly proportional to viscosity, consistent with the results of a study on a group of the choline chloride-based NADES species (Ru and König 2012; Zhao et al. 2015).

Equation 1: $\rho(T) = \rho_0[1 + \alpha(T - T_0)]$

where α is the temperature coefficient of resistivity, T_0 is a fixed reference temperature (usually ambient temperature), and ρ_0 is the resistivity at temperature T_0. The parameter α is an empirical parameter deduced from measured data. α differs as the reference temperature changes.

For a ternary aqueous NADES species, the water content is another determining factor of conductivity and viscosity. As only a relatively small quantity of water is

involved in a binary NADES matrix, conductivity will increase with addition of more water. However, as the water content increases, resistance may also rise (Dai et al. 2015). Thus, the correlation between conductivity and water content in NADES (solutions) follows a near Gaussian distribution. Parallel to the effect of temperature, NADES viscosity decreases as the amount of water increases (Zhao et al. 2015). Within the range of typical experimental temperatures, conductivity and viscosity exhibit a positive linear correlation (Craveiro et al. 2016).

2.1.4.3. Polarity

Generally, the greater the intermolecular attractions, the larger the polarity. Thus, polarity is generally a solubilization determinant. To study NADES polarity, solvatochromic studies have been performed using Reichardt's organic dyes (Osterby and McKelvey 1996; Machado and Machado 2001) (Equation 2) as well as Nile red dye (Fowler and Greenspan 1985) (Equation 3). Although the solvatochromism in organic solvents covers almost the entire visual spectrum (Reichardt 1994), solvatochromic effects of the hydrophilic metabolite-based NADES species are limited to parts of the visual spectrum. The parameter $E_T{}^{\mathrm{N}}$ (Equation 4) (Hernández-Perni et al. 2005) can be quantitatively applied for a polarity assessment. Polarity intervals can be identified by referencing against a standard.

Equation 2 $E_T{}^{(30)}(30)/Kcal \cdot mol^{-1} = hc\nu_{max}N_A = 28591/\lambda_{max,30}$

where $^{(30)}$ means the standard solvatochromic betaine dye No. 30 (Reichardt's dye), h is Planck's constant, c is the speed of light in vacuum, and $\lambda_{\mathrm{max}\,=}$ wavelength of a maximum UV absorbance.

Equation 3 $E_T{}^{(NR)}(NR)/Kcal \cdot mol^{-1} = hc\nu_{max}N_A = 28591/\lambda_{max,NR}$

where NR represents Nile red dye, *h* is Planck's constant, *c* is the speed of light in vacuum, and λ_{max} = wavelength of a maximum UV absorbance.

Equation 4 $E_T{}^N = \frac{E_T(Solvent) - E_T(TMS)}{E_T(Water) - E_T(TMS)}$

where $E_T{}^N$ is a normalized parameter. Both water and tetramethylsilane (TMS) are reference solvents. For water, E_T(Water) is defined as 1, whereas for TMS, E_T(TMS) is defined as 0.

For a ternary aqueous NADES matrix, a water loss study can reflect the strength of intermolecular forces and, thus, provide a measure of polarity. In the linear equation of the NADES state (Figure 3), the corresponding slope displays intermolecular forces and their arrangement in the NADES matrix (Liu et al. 2016). When comparing NADES with different components, the slopes can be used to compare polarities. When the slope is high, it indicates that the intermolecular forces are comparatively low. In a ternary aqueous NADES family, the water quantity can be used to estimate the corresponding polarity (Craveiro et al. 2016). As less water content means that a greatly ordered arrangement can be formed in the matrix, this corresponds to a higher polarity of the NADES.

2.1.4.4. Hydrophilicity and Hydrophobicity

Assessment of the hydrophilicity/hydrophobicity balance of NADES can be divided into two layers: the state of its mostly hydrophilic components and a consideration of extraordinary solubilities of the more hydrophilic NADES species for lipophilic metabolites. NADES components include hydrophilic and lipophilic molecules. Hydrophilic components with highly electronegative groups can form hydrogen bonding via special cases of dipole-dipole interactions. This explains the

tendency of hydrophilic NADES species to be miscible with polar solvents such as water and MeOH (Abbott et al. 2004). Conversely, due to difference in their capability of hydrogen bonding through the electrostatic forces, lipophilic compounds remain relatively passive participants in the hydrophilicity/lipophilicity balance phenomenon. Some NADES species, such as menthol- or fatty acid-based NADES (Ribeiro et al. 2015; van Osch et al. 2015), hold the components with the electronegative groups and, thus, mainly induce electrostatic interactions between different components. These NADES species are immiscible with water (Abbott et al. 2003; Li et al. 2013), a behavior that appears to be counterintuitive at first. Examples for these (perceived) exceptions are eutectic mixture of citric acid-menthol (Ribeiro et al. 2015) that contain a hydrophilic and a hydrophobic component to create a lipophilic NADES species. The hydrophilicity/lipophilicity balance of such eutectic mixtures has to be measured individually. Interestingly, the hydrophilic, aqueous NADES species can exhibit a remarkable solubilizing ability for some lipophilic NPs (Dai et al. 2013). Compared to conventional neat polar solvents such as water, the lipophilic net effect reflects the observed tendency of nonpolar substances to aggregate in aqueous solution, and exclude water molecules. In this way, the segregation maximizes hydrogen bonding between water molecules, and minimizes the area of contact between water and the nonpolar molecules. However, hydrophilic NADES species differ from water properties, and show an intriguing duality of lipophilicity and hydrophilicity.

2.1.4.5. Solubilizing and Stabilizing Abilities

Solvents can have an effect on solubility and stability of a solute by inducing or preventing certain molecular associations. The unique intermolecular interactions

or arrangements of a NADES matrix generate its special solubilizing (Dai et al. 2013) and stabilizing (Dai et al. 2014; 2016) properties. Two main theories have been proposed to explain the extraordinary features of NADES: (i) the hole or liquid crystal theory (Choi et al. 2011) and (ii) the binding theory. According to (i), the hole theory, the inner structure of a NADES forms a polymer-like matrix, and the solute can dissolve into the space (or holes) of this molecular network. As the component ratio changes, the inner arrangement such as the size and shape of the matrix holes of the NADES may be modified significantly. For example, as the water content in a NADES matrix changes, the matrix hole size can alter from micrometer to nanometer levels (Ma et al. 2016; Hammond et al. 2017). Following (ii), the binding theory, the target solutes actually become segments/parts of the NADES matrix through intermolecular interactions. For example, xylitol-choline chloride-water (XChWat) exhibits an extraordinary solubilizing ability for quercetin (Dai et al. 2013). According to nOe measurements, the components of XChWat have a significant intermolecular correlation with the solute, quercetin. Moreover, due to the influence of the intermolecular bonding, some properties of the target analyte may be greatly changed. For example, while proline is only sparingly soluble in DMSO, a proline-based multiple-component NADES can be fully miscible with this organic solvent.

2.1.4.6. Biocompatibility

Researchers working on eutectics generally consider NADES as nontoxic media (Hayyan et al. 2013; Zhao et al. 2015; Faggian et al. 2016). The collective experience of research on NPs over the past decades has repeatedly led to the observation that NADES-enriched water fractions are most often devoid of pharmacological activity (Liu 2008). While being a general indicator of lack of (cyto)toxicity, this observation

TABLE IV. SUMMARY OF NADES TEST METHODS, STUDY MODELS, AND SAMPLE TREATMENTS

Methodology	Study model	Sample treatment	Reference
Cytotoxic MTT cell viability (IC50)[a]	A375, B16F10, CaOV3, H413, HelaS3, HepG2, HT29, MCF-7, OKF6, and PC3 (cell line)	A two-fold dilution series of six concentrations of the solvents	(Hayyan et al. 2015 and 2016)
Cytotoxic others	*Artemia salina* (Brine shrimp)	-	(Hayyan et al. 2013)
	Differentiated T37i brown adipocytes	0.01%-10% of culture medium	(Rozema et al. 2015)
Bacterial phototoxicity[b]	*E. coli*, *E. faecalis*, *S. aureus*	0-200 times in PBS or water of dilution	(Wikene et al. 2015 and 2016)
Bacterial inhibition[b]	*E. coli*, *S. aureus*, *P. aeruginosa* and *B. subtilis*	-	(Hayyan et al. 2013)
Microtox toxicity (luminescence inhibition)	*Vibrio fischeri*	Diluted aqueous solution of tested compound (from 0 to 81.9%)	(de Morais et al. 2015)
Fungal toxicity	*Aspergillus niger*	0-4500 mM (or 0-650 mg/mL)	(Juneidi et al. 2015)
Acute toxicity	*Cyprinus carpio* (Common carp)	25-14000 mg/L	(Juneidi et al. 2015)
(toxicological symptoms)	Imprinting Control Region mice	Vehicle (dH_2O), 20 g/kg, 10 g/kg and 5 g/kg doses	(Hayyan et al. 2015)

[a] Mouse: B16F10, skin cell line; Human: A375, malignant melanoma cell line; CaOV3, ovarian cell line; H413, carcinoma-derived oral keratinocyte cell; HelaS3, cervical cell line; HepG2, liver hepatocellular cell line; HT29, colon adenocarcinoma cell line; MCF-7, breast cell line; OKF6, oral keratinocyte cell line; PC3, prostate cell line.; [b]*B. subtilis, Bacillus subtilis; E. coli, Escherichia coli; E. faecalis, Enterococcus faecalis; P. aeruginosa, Pseudomonas aeruginosa; S. aureus, Staphylococcus aureus.* – no data available.

may also require a more critical interpretation due to the extremely shifted relative concentrations of solutes in these polar materials. However, hydrophilic metabolites are usually dietary, food additives, or drug excipients. Still, many hydrophilic metabolite-based NADES species can exhibit side-effects in biological tests. TABLE IV provides the details on the test models, including cell line (Hayyan et al. 2015, Rozema et al. 2015, Hayyan et al. 2016), bacterial (Hayyan et al. 2013; de Morais et al. 2015; Wikene et al. 2015 and 2016), fungal (Hayyan et al. 2013; Juneidi et al. 2015) shrimp (Hayyan et al. 2013), carp (Juneidi et al. 2015), and murine (Hayyan et al. 2015) models. These two general observations are not necessarily in conflict. For example, honey is a widely used food. On the other hand, it is also capable of inhibiting bacterial growth and serves as an important ingredient in preparations used for human health services.

Notwithstanding their general biocompatibility, unexplained molecular interactions with NADES during sample treatment can be a potential cause of concern for some assays. For example, it is known that by diluting NADES species such as mannose-dimethylurea-water (2:5:5, mol/mol) over five times, no intermolecular interactions among the components can be detected by an nOe NMR experiment. However, for some test studies, the samples were diluted over 100-fold (TABLE IV). Theoretically, this overdilution leads to matrix disruption into the individual components (Figure 5) and, thus, will cease to function as a NADES species. Accordingly, the observed outcomes of tested NADES primarily depend on the individual components of NADES and related cooperative effects (Zhao et al. 2015).

TABLE V. THE COST OF NMR USING EXISTING INSTRUMENTATION

	Corporate lab	Academic lab
Standard ^{1}H NMR	$45/analysis	$5-$10/h
Standard ^{13}C NMR	$45/analysis	$5-$10/h
Quantitative ^{13}C NMR	$65/analysis	$5-$10/h

2.2. Nuclear Magnetic Resonance (NMR) in Botanical Analysis

2.2.1. Cost of NMR Spectroscopy

According to common sense in analytical chemistry, the minimal initial hardware for NMR analysis render this as the "most" costly instrument, compared to other detectors. Unbiased cost calculations are very heterogenous or unavailable. Based on the laboratory experience, a high-performance NMR, e.g., 400 MHz, has a price, around $500K. In addition, the amortization of the investment in the instrum--ent depends heavily on the use of the instrument time (max. 8,760 h/year). For example, when used fully for automated NMR (90% time = 7,900 h/year, the rest for maintenance), a 400 MHz 5mm N2CP ($500k and 100k maintenance/service) over 10 years provides 79,000 h of service, at $7.60/h – regardless of its environment. This matches with the hourly rate generally charged in academic laboratories (TABLE V). In pharmaceutical industry, the major cost of NMR experiments is the labor involved in the operation, which accounts for over 80% of the total NMR operation cost and excludes data interpretation. (Webster and Kumar 2014). This is the reason why the costs of ^{1}H NMR and ^{13}C NMR in corporate labs are same, at $45/analysis (TABLE V).

Although a longer acquisition time for ^{13}C NMR is needed, the final cost of ^{1}H NMR and ^{13}C NMR would not be very different. According to TABLE V, in an academic laboratory, the shared equipment (hourly fee based) costs of qCNMR (D1 10s, NS ~12,000, ~10 h of acquisition time) are in the range of $50 to $80 per analysis, similar to the cost in a corporate laboratory. As labor cost of NMR and other analytical methods should be similar in different specific environments, NMR should not be an extraordinarily costly analytical means either in corporate or academic labs. In addition, as low field NMR can be used in laboratories, the cost of NMR application can be greatly reduced. For example, a benchtop 60 MHz NMR is less than $100K (the quotes were recieved from Magritek, Oxford, and Nanalysis), including shipment and general maintenance. The above information should benefit potential users who wish to perform (qualitative/quantitative) NMR analyses.

2.2.2. Quantitative NMR Spectroscopy of NADES

NMR spectroscopy is a nondestructive and nearly-universal detection method that can simultaneously perform both qualitative and quantitative analyses (Pauli et al. 2005 and 2012; Qiu et al. 2012). NMR is an analytical method with great specificity, predominantly involving two nuclei, ^{1}H and ^{13}C that occur ubiquitously in NPs and are of major importance in BDSs and marker characterization: ^{1}H, because it offers the high sensitivity in NMR, and ^{13}C, because of its large chemical shift dispersion. Moreover, NMR is receiving increasing attention as a primary analytical method due to its intrinsic advantage of allowing a strictly mole-based quantitative determination. However, in the ^{1}H NMR of more complex samples such as BDS extracts, signal overlap due to spin-spin coupling and limited chemical shift dispersion creates challenges. As a result, ^{1}H NMR marker signals are often

confounded and sometimes even hardly identifiable in 1D ^{1}H NMR spectra. For ^{13}C NMR, the major challenge is extended experiment time that results from low natural abundance and reduced gyromagnetic nuclei sensitivity of the ^{13}C. Historically, this has prevented a more prolific development of this method for pharmacopoeia analysis. To partially overcome this limitation, relaxation reagents such as $Cr(acac)_3$ can reduce the D1 requirement in ^{13}C NMR. Analysis of the integrals of all signals of a given analyte showed that each individual component exhibited a low standard deviation, indicating that the use of the relaxation reagent permits quantitative analysis with very reasonable precision. In addition, chemical shift dispersion of ^{13}C NMR is ~200 ppm and, thus, certainly 20× greater than that for ^{1}H. Due to the lack of signal splitting when applying broad-band ^{1}H decoupling, ^{13}C spectra are highly distinct as signal clusters that arises from different carbon types that are located in specific spectral regions. Profiles are generated that are unique to each molecule. For a preliminary study, when schisandrol A (29 mg) was dissolved in a multicomponent NADES, citric acid-choline chloride-proline-sucrose-water (CChPSuWat, 3:2:1:1:4, mol/mol, 135.68 mg, equivalent to 100 μL, the assignments in Figure 6B), qCNMR can provide a nearly full spectral analysis of schisandrol A (S/N ~ 15, Figure 6C) and even other "major" ingredients in the target sample. As shown in Figure 6B, the molar ratio of citric acid : choline chloride : proline : sucrose was 3:2:1:1. Quantitatively, proline was 0.098 mmole (or 11.28 mg). Integral ratio of proline to schisandrol A was 1.46:1, which showed that schisandrol A was 29 mg. Accordingly, ^{13}C NMR analysis is shown to be generally feasible for either qualitative or quantitative purposes. Although the exact NMR acquisition parameters, such as relaxation delay, acquisition time, pulse width, and the qualitative or quantitative

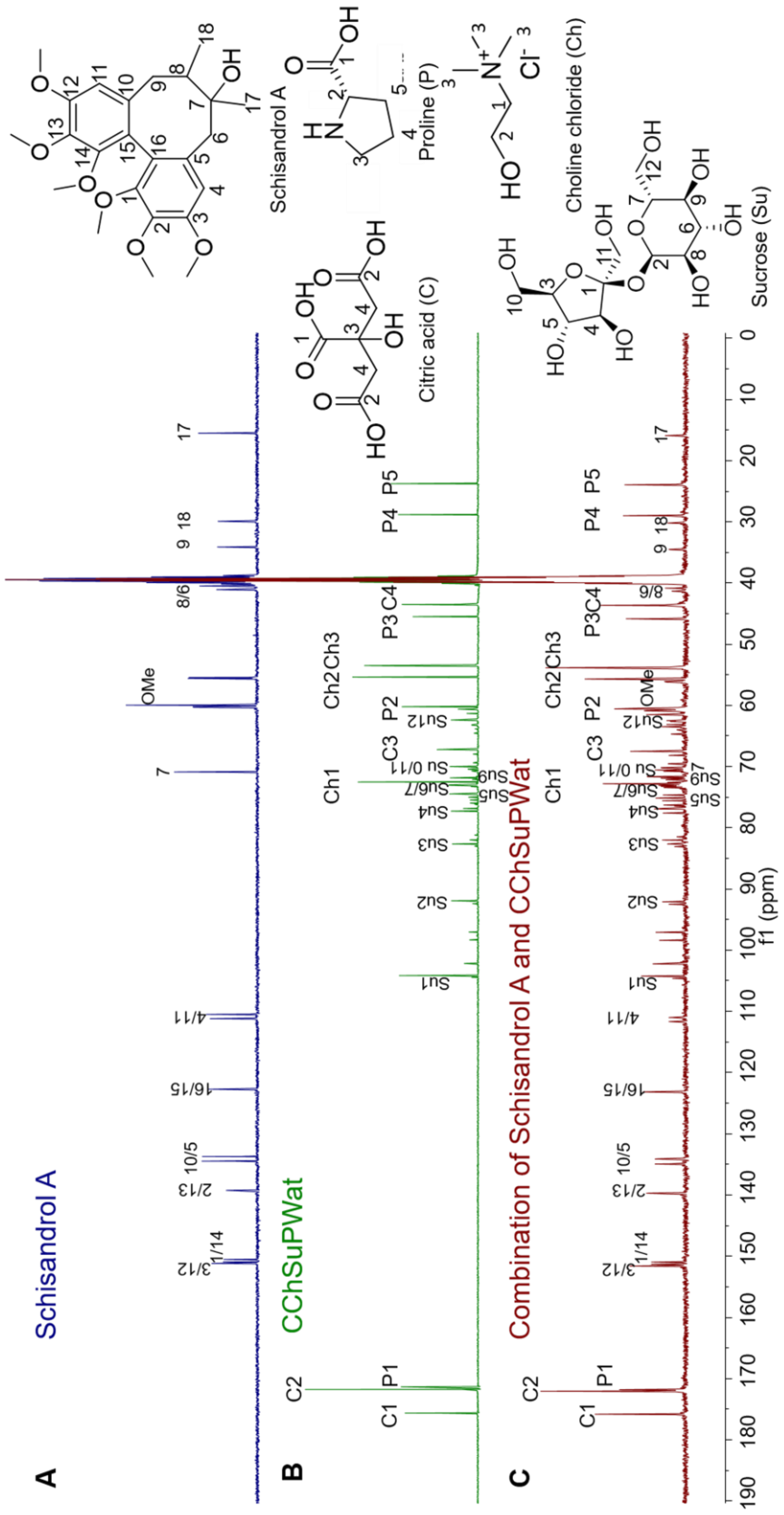

Figure 6. The qCNMR spectra of schisandrol A in NADES of citric acid-choline Cl-proline-sucrose-water, citric acid-choline chloride-proline-sucrose-water (CChPSuWat). The qCNMR can easily recognize target analyte, schisandrol A in the mixture (C) of schisandrol A (A) and CChPSuWat (B). For the acquisition of C, the mixture was dissolved in 200 µL of DMSO-d_6 with 35 mM of Cr(acac)$_3$

method need further optimization for different analytes, ^{13}C NMR is capable of characterizing and quantifying (BDS) markers and can serve as an alternative form of mass balance analysis.

The present study uses qNMR, which has shown to be a valuable, orthogonal quantification method as it represents an alternative to the widespread use of LC-based techniques: the quantitative ^{1}H and ^{13}C NMR (qHNMR and qCNMR) approach does not rely on the availability of high purity standard as identical, external or internal calibrants (EC and IC, respectively) (Gödecke et al. 2013) as would be the case for LC-based quantification methods. The absence of a requirement for identical calibrants is a major advantage for NPs and other rare chemical entities. A molarity-based metabolite quantification can be achieved using an EC (e.g., caffeine) and/or via the residual solvent signal ($CHCl_3$ in $CDCl_3$ or DMSO-d_5 in DMSO-d_6) for a combined ECIC, see (Gödecke et al. 2013) for details about qNMR calibration. Quantitative evaluation was based on NMR signal area achieved by integration. The target metabolites (lipophilic ingredients) and the NADES components were quantified, using methods that are equally suitable for botanical extracts. Notably, quantification of the hydrophilic metabolites by qNMR avoids the cumbersome requirement of special liquid chromatography columns that can accommodate the analysis of the highly polar metabolites.

The qNMR approach can be used more generally not only to detect and establish threshold assays for botanical negative markers, but also to quantify major and minor desired components as well as unwanted additives in plant extracts, herbal medicines, and food and other complex nature-derived commercial preparations. In addition, a high-resolution NMR spectrum can be converted into an electronic data

(e-data or simulated spectrum), which is not influenced by S/N issues and can be stored in a digital database for a further application. These e-data can be used for quantitative NMR, and, thus some e-data were developed (see Appendix A), and used in the present work as a preliminary test.

2.2.3. ^{1}H-^{1}H Nuclear Overhauser Effect Spectroscopy of NADES

The nuclear Overhauser effect (nOe) is the transfer of nuclear spin polarization from one spin vector to another via cross-relaxation. ^{1}H-^{1}H Nuclear Overhauser Effect Spectroscopy (NOESY) can be used to determine the intra- and inter-molecular dipole-dipole interaction between hydrogens. Determining nOe effects from is helpful for understanding the mechanism of NADES unexpected solubilizing abilities for lipophilic molecules.

However, due to high viscosity of most NADES species at ambient temperature, the ^{1}H spectral window should be optimized for an nOe experiment. Until now, as NADES viscosity changes with temperature, elevated temperatures (40 – 80 °C) have been used when acquiring NOESY experiments. Considering the insight gained about the intermolecular interactions among NADES components from the water loss study, a dilution strategy was followed in this work. It aims to provide an additional means for NADES researchers to study intermolecular interactions in NADES matrix.

2.3. Countercurrent Separation in Botanical Analysis

2.3.1. Countercurrent Separation

Nature creates abundant molecular structures with diverse pharmacological activities. Active lipophilic molecules of particular interest are often present at low abundance levels, down to parts per million in the raw plant material.

Countercurrent separation (CCS) includes both centrifugal and gravitational methods of stationary phase retention (Friesen et al. 2015). Centrifugal CCS as a modern liquid-only chromatography technique was introduced in the 1970s (Ito and Bowman 1970). It can be divided into hydrodynamic mode, generally termed countercurrent chromatography, and hydrostatic mode, generally described as centrifugal partition chromatography (Friesen et al. 2015). Being a liquid-only technique, CCS avoids analyte loss by degradation or absorption as observed often on a solid support chromatography. It is characterized by high recovery and reproducibility, and also has demonstrated its usefulness in the NP laboratory (Ito 1987; Hopmann et al. 2011; Choi et al. 2012). Because the stationary phase is a liquid in CCS, resolution depends on the relative partition coefficients (K values) of analytes, i.e., their relative distribution between the mobile and the stationary phases of the solvent system. Thus, K is an invariant parameter of any analyte in a given solvent system and a highly characteristic parameter in any CCS experiment. If the analyte greatly prefers the mobile phase, it will be eluted along with, or close to the solvent front, whereas, if it strongly favors the stationary phase, the analyte will stay in the column and may be extruded, a mechanism unavailable to solid phase-based LC. However, neither of these extreme K values ($K \backsimeq 0$ or $K \backsimeq \infty$) are likely to provide efficient analyte separation. Therefore, an ideal solvent system should deliver an analyte into a distinctive K value range, referred to as the "sweet spot". This range generally spans the interval from $K = 0.25$ to $K = 16$ (Friesen and Pauli 2007). Because of the consistency of a K value in a given solvent system (SS) and the reproducibility of CCS column behavior, centrifugal CCS provides orthogonal and scalable separation capabilities (Liu et al. 2015). Thus, CCS has been

widely used for NP research (Inui et al. 2007; Friesen and Pauli 2008; Pauli et al. 2008; Qiu et al. 2012; Liu et al. 2014; Ramos et al. 2014; Simmler et al. 2014). SS selection is the key step to achieve a successful CCS, but it can be the most time consuming and labor-intensive step in the entire process. Here, the Generally Useful Estimate of Solvent Systems (GUESS) method (Friesen and Pauli 2005) was employed or advanced to accelerate SS selection. The great hydrophilicity of individual NADES components introduces a challenge into the ability of conventional solid-support based chromatography to recover potential active lipophilic metabolites. This complicates the systematic explanation of the NADES' functions in botanical extracts. The present study establishes CCS methodology that can overcome this recovery challenge and advance bioactivity studies of NADES using crude extracts. Differently designed mixtures or extracts can be prepared, and then tested in bioactivity assays. As most SS families used in CCS are composed of ternary or quaternary SSs, the regular names of these multicomponent mixtures can quickly become cumbersome. Therefore, an abbreviated and universal naming system for CCS solvent systems (TABLE VI) was developed which allows for the assembly of pronounceable names that rapidly identify the system. Such naming scheme has commonly been used in CCS studies for the past 12 years (Friesen and Pauli 2005). Following the same logic, a NADES naming scheme was also developed. For example, the NADES of glucose-choline chloride-water can be abbreviated by GCWat. More detailed discussions on NADES naming can be found in Appendix B.

In CCS practice, SS selection may occupy 90% of the time taken in an entire CCS operation (Ito 2005). Thus, in the past decade, CCS researchers have sought new methods or models to reduce the effort of determining the appropriate SS and have

TABLE VI. THE CCS SOLVENT SYSTEM NAMING SYSTEM

Multi-component naming system	Abbreviated naming system	Pronunciation of abbreviated naming system
n-Butanol-Water	BuWat	*buwat*
Chloroform-Methanol-Isopropanol-Water	ChMIsoWat	*chemisowat*
Chloroform-Methanol-Water	ChMWat	*chemwat*
Dichloromethane-Methanol-Water	DiMWat	*dimwat*
Ethyl acetate-*n*-Butanol-Water	EBuWat	*ebuwat*
Ethyl acetate-Ethanol -Water	EEtWat	*e' etwat*
Ethyl acetate-Methanol-Water	EMWat	*emwat*
n-Hexane-Acetone- Ethyl acetate-Isopropanol-Ethanol-Water	HAtEIsoEtWat	*hate' iso' etwat*
n-Hexane-Butanol-Water	HBuWat	*hæ' buwat*
n-Hexane-Chloroform-Methanol-Water	HChMWat	*hæ' chemwat*
n-Hexane-Dichloromethane-Acetonitrile	HDiAc	*hæ' diac*
n-Hexane-Dichloromethane-Methanol-Water	HDiMWat	*hæ' dimwat*
n-Hexane-Ethyl acetate-Methanol-Water	HEMWat	*hemwat*
n-Hexane-Ethyl acetate-Methanol- DMSO -Water	HEMSoWat	*hemsowat*
n-Hexane-Ethanol-Water	HEtWat	*hetwat*
n-Hexane-Methanol-Water	HMWat	*hemwat*
n-Hexane-Methyl *tert*-butyl ether-Water	H*ter*Wat	*hæ' terwat*
n-Heptane-Acetonitrile-Dichloromethane	HepAcDi	*hepacdi*
n-Heptane-Ethyl acetate-Methanol-Water	HepEMWat	*hepemwat*
n-Heptane-Methanol-Water	HepMWat	*hepmewat*
Methyl acetate-Water	MaWat	*mawat*
Petroleum ether -Ethyl acetate-Ethanol-Water	PetEEtWat	*pete' etwat*
n-Propanol-Acetonitrile-Water	ProAcWat	*pro acwat*
Methyl *tert*-butylether-Acetonitrile-Water	*ter*AcWat	*teracwat*
Methyl *tert*-butylether-*n*-Butanol-Acetonitrile-Water	*ter*BuAcWat	*terbu acwat*

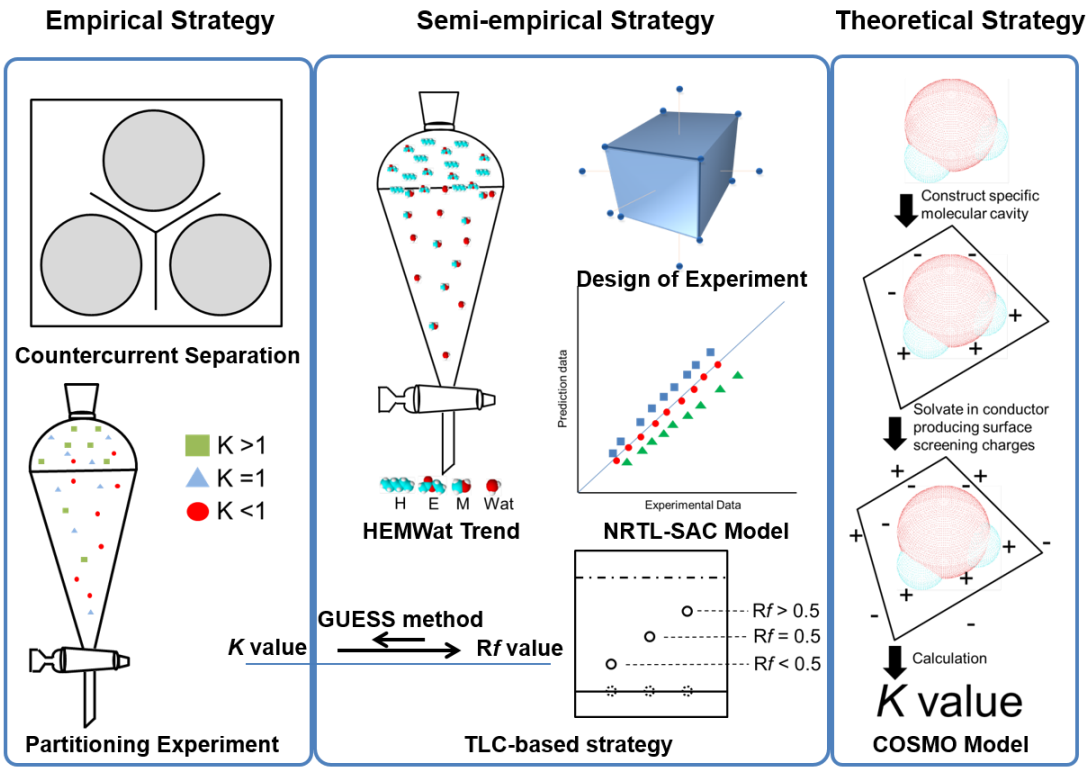

Figure 7. A diagrammatic sketch of solvent system (SS) selection strategies in countercurrent separations (CCS).
The empirical strategies are comprised of an analytical CCS and a partitioning experiment. The semi-empirical strategies involve a TLC-based method, the general HEMWat family trend, three dimensional-K value maps, and the Non-Random Two-Liquid Segment Activity Coefficient (NRTL-SAC) model. One representative theoretical strategy is the Conductor-like Screening Model for Real Solvents (COSMO-RS) model.

introduced several selection strategies. In the following, these strategies are classified into, and presented as, three main classes: empirical, semi-empirical, and theoretical. Figure 7 offers a comparison of the primary features of the three different approaches to SS selection.

2.3.2. Empirical Solvent System Selection Strategy

Empirical methods require the practitioner to choose the SS composition, the SS

family, and the constituent proportions of the initial SS(s). Typical applications may be divided into three categories: 1) the isolation of a single target analyte; 2) the separation and isolation of a group of analytes; and 3) the distribution of a complex mixture, in which the target analytes are not explicitly known. As the desired outcomes vary accordingly, researchers attempt to discover a SS where: 1) the target analyte has a K value near unity; 2) the target compounds have K values in the sweet spot with a desirable resolution; and 3) an optimal distribution of mass and/or biological activity is observed. Empirical SS selection is an iterative process. Once the results are known for the first set of trials, the second set of trials is planned. Sometimes the optimal solvent may be discovered by adjusting the solvent ratio within a SS family (a group of SSs that are mixtures of the same components). For example, if the target analyte has a high affinity for the organic upper phase of a *n*-hexane-ethyl acetate-methanol-water (HEMWat) SS, the proportions of *n*-hexane and/or methanol relative to ethyl acetate and/or water may be increased in the next set of trials. On the other hand, an SS with a different composition than the original may be attempted if a) there is not a good polarity and/or solubility match between the original SS and the target analytes, b) the target analytes are poorly resolved in several formulations of the original SS family, c) emulsions form with the extract that may result in poor CCS behavior. Overall, this approach requires skill and experience on the part of the practitioner to determine what the next steps of the iterative process should be, as well as knowing when the desired objective has been sufficiently attained.

The use of partitioning experiments (also known as “shake flask” experiments) relies on the fact that the partition coefficient (K) obtained by the static equilibrium

of an analyte between two phases of a biphasic solvent system will coincide with the K of the analyte in the same solvent system produced in a dynamic CCS experiment. The K value is, therefore, a constant parameter to describe the distribution of a given analyte in a specific SS. In the partitioning experiment, the K value is calculated by the following Equation 5:

Equation 5: $K = [C]_{upper\ phase}/[C]_{lower\ phase}$

where $[C]_{upper\ phase}$ is the concentration of the analyte in the upper phase and $[C]_{lower\ phase}$ is the concentration of the analyte in the lower phase. This distribution corresponds to the dynamic K value obtained from a CCS experiment run with the upper phase stationary (in practice, the CCS-based determination of K values has to be done manually, and automatic determination is unsupported by most CCS laboratories). If the lower phase is the stationary phase in the CCS experiment, the ratio must be inverted.

Analytes with different K values in a SS may be separated by CCS with that SS (Ito 2005). The loading material may be a standard sample (Shibusawa et al. 2001; Yanagida et al. 2006; Inoue et al. 2010) or a crude material (Chen et al. 2007; Luo et al. 2008; Ye et al. 2008; Yuan et al. 2008; Cicek et al. 2010; Luo et al. 2010; Yao et al. 2010; Zhang et al. 2011). Such experiments have been described in detail (Ye et al. 2008; Inoue et al. 2010). Simply, the material is distributed to equilibrium, by vigorous shaking, between the two phases of a small amount of the SS. This may be done in a separatory funnel or in a vial. Samples of each phase are drawn off and assayed to quantitate the concentration of the desired analyte(s) in the upper and lower phases. The quantitative method is most often HPLC with UV-vis detection

(Garrard 2005; Inoue et al. 2008; Wagenaar et al. 2009). However, a wide range of analytical methods have been reported, such as thin-layer chromatography (TLC) with chemical revelation (Leitao et al. 2005), TLC coupled with fluorimetry (He et al. 2012), GC-MS (Dang et al. 2010), LC-MS (Inoue et al. 2010), and quantitative ^{1}H NMR (qHNMR) (Qiu et al. 2012, Liu et al. 2014). The choice of quantitation method often reflects the properties of the NP(s) being targeted, the complexity of the sample, and/or targeting of single vs. multiple analytes, as well as the preferences of the researcher. If the analyte is unknown in an experiment to discover the lipophilic component in a crude mixture, K-by-bioactivity is a practical method to correlate the distribution of the target principle(s) to the sweet spot of a CCS chromatogram (Yeh et al. 2012). TABLE VII describes 73 compounds belonging to ten different classes that were isolated and purified using SSs selected by partitioning experiments. Terpenoids, flavonoids, and alkaloids are the major target. The most commonly selected solvent system is HEMWat (used for 18 of the 73 natural products), because this SS provides two-phase systems over a wide polarity range (Sutherland and Fisher 2009). Although predetermination of K before a CCS instrument operation avoids solvent waste, an examination of several SSs takes a large amount of extra experimental effort. In one study, as many as 47 candidate SSs have been examined (Inoue et al. 2008). Automation, with a liquid handling robot, may ease the burden (Garrard 2005), but most laboratories do not have this capability.

CCS chromatograms are linearly scalable from 20 mL to multi-liter capacity instruments (Sutherland et al. 2001; Ignatova et al. 2007; Wood et al. 2007). Empirically, a large-scale CCS would provide greater separation efficiency. Furthermore, with the development of CCS instruments and control system (TABLE

TABLE VII. OVERVIEW OF ANALYTES AND THEIR RESPECTIVE SOLVENT SYSTEMS (SS) THAT WERE SELECTED THROUGH EXTENSIVE PARTITIONING EXPERIMENTS

Class	Analytes	Selected SS (v/v)	References
Terpenoids	Bilobalide, ginkgolides A, B, C, and J	ChMWat (10:7:3) and HEMWatSo (4:6:4:6:0.5%)	(Peng et al. 2008; Cicek et al. 2010; Han et al. 2010; Qiu et al. 2012)
	2,3-*O*-Acetylshengmanol-3-*O*-β-D-xylopyranoside, cimiracemoside D, 2,5-*O*-acetylcimigenol-3-*O*-β-D-xylopyranoside, and aglycone cimigenol	HAtEIsoEtWat (3.5:1:2:1:0.5:2)	
	Triptonide, isoneotriptophenolide, hypolide, triptophenolide, and triptonoterpene methyl ether VI	HEMWat (3:2:3:2)	
	Eriocalyxin B	HEMWat (1:1:1:1)	
Flavonoids	Tephrosin, 4',5'-dimethoxy-6,6-dimethylpyranoisoflavone, deguelin, and dehydrodeguelin	HEMWat (5:4:5:3)	(Shibusaw et al. 2001; Yanagida et al. 2006; Ye et al. 2008; Yuan et al. 2008; Inoue et al. 2012)
	Amentoflavone, robustaflavone, bilobetin, hinokiflavone, isocryptomerin and apigenin-diglucoside	HepEMWat (2:3:2:3)	
	Procyanidins	Methyl Acetate-Water (1:1)	
	Anthocyanins	BuWat (1:1)	
	Catechins	*ter*AcWat(TFA) (2:2:3:0.1%)	
Alkaloids	Daurisolin, dauricine, daurinoline, and dauricicoline	PetEEtWat (1:2:1:2)	(Yao et al. 2010; Liu et al. 2014)
	Ansamitocin P-3	HEMWat (3:5:3:5)	
	Ginkgotoxin	ChMWat (10:5:5)	
Lignans	3'-Formylhonokiol, 5-formylhonokiol, and 3',5-diformylhonokiol	HEMWat (5:2:5:2)	(Wang et al. 2004; Chen et al. 2007; Luo et al. 2008)
	Honokiol and magnolol	HEMWat (5:2:5:2)	
Quinones	Tanshinone IIA	HDiMWat (16:3:16:4) and HEtWat (4:2:2)	(Zhang et al. 2011)
Organic acids	(+/-)-Cyclohexylmandelic acid	H*ter*Wat (9:1:10) with chiral selectors	(Maier et al. 2006; Tong et al. 2010; Hammann et al. 2013)
	Caftaric acid, coutaric acid, and fertaric acid	*ter*AcBuWat(TFA) (2:2:1:5:0.5%)	
	20 Fatty acids	HMWat (350:175:2)	
Cholesterol	Sitostanol and β-sitosterol	HM(aqueous silver nitrate solution) (34:24:1)	(Schroder and Vetter 2011)
Coumarins	Notoptol and divaricatol	HEMWat (1:1:1:1)	(Skalicka-Wozniak et al. 2012)
Peptides	Enramycin A and B	HBuWat(TFA) (43:7:50:0.05%)	(Inoue et al. 2010; Dai et al. 2013)
Curcuminoids	Curcumin, desmethoxycurcumin, and bisdemethoxycurcumin	HChMWat (5:10:7.5:2.5)	(Inou et al. 2008)

TABLE VIII. OVERVIEW OF CONTEMPORARY CCS INSTRUMENTS (< 100 ML COLUMN CAPCITY) AND CONTROL SYSTEMS

Instrument	Source/Manufacturer	Sample loop capactiy	Coil column capacity	Flow rate
Mini HPCCC	Dynamic Extractions (Slough, UK)	1.0 mL	17.2 mL	0.5-2.0 mL/min
Spectrum/Midi	Dynamic Extractions (Slough, UK)	150 mg	22.0 mL	0.5-2.0 mL/min
Mini-DECCC	Dynamic Extractions (Slough, UK)	-	18.0 mL	1.0 mL/min
FCPC A 50	Kromaton (Sainte Gemmes Sur Loire, France)	up to 1 g	50.0 mL	≤ 10 mL/min
TBE CCC-20	Shanghai Tauto Biotech Co., Ltd (Shanghai, China)	20-500 µL	16.0 mL	0.5-1.5 mL/min
Model GS-20	Beijing Institute of New Tech Application (Beijing, China)	1.0 mL	30.0 mL	1.0 mL/min
The type-J coil planet centrifuge	Renesas Eastern Japan Semiconductor Inc (Tokyo, Japan)	0.5 mL	40.0 mL	0.5 mL/min
HPCPC™ CPC 80	Everseiko Corporation (Tokyo, Japan)	-	80.0 mL	5 mL/min
Cherry Instrument*	Wrightwood Technologies (Chicago, USA)	Alternative	-	Alternative

- : Variable, no specific information provided; *:Cherry Instrument is a control system for CCS instruments and is separate from the actual coil/column; the Cherry Instrument includes a monitor, a data processing system, pumps, replaceable sample loops, a UV detector, a PMA detector, and a sample collector. The data processing system controls the flow rate, pumps, and injection of sample. It also monitors the real-time parameters, such as the stationary phase volume retention ratio (S_f value), the partition coefficient (K value), and the eluting phase using a phase metering apparatus (PMA value).

TABLE IX. OVERVIEW OF THE ANALYTES AND THEIR RESPECTIVE SOLVENT SYSTEMS THAT WERE SELECTED AND/OR ISOLATED, RESPECTIVELY BY ANALYTICAL SCALE CCS INSTRUMENTS

Class	Analyte	Selected SS (v/v)	References
Terpenoids	Linalool, terpinen-4-ol, α-terpineol, and *p*-anisaldehyde	HEMWat (5:5:2:2)	(Wei et al. 2001; Skalicka-Wozniak et al. 2013)
	Anethole and foeniculin	HM (1:1)	
	Lycopene	HDiAc (10:3.5:6.5)	
Flavonoids	Hispidulin, nepetin, homoplantaginin and nepetin-7-glucoside	HChMWat (0.5:4:3:2) and ChMWat (4:3:2)	(Chen et al. 2005; Wei et al. 2009 and 2011; Li et al. 2014)
	Patuletin-3-*O*-glucoside, hyperoside, 6-methoxykaempferol-3-*O*-galactoside, and astragalin	EMWat (10:1:10)	
	Quercetin, kaempferol, and isorhamnetin	DiMWat (5:3:2)	
	Amygdalin	EBuWat (5:2:5), (5:1:5), (10:1:10), (50:1:50) and BuWat (1:1)	
	Axifolin-3-glucoside and hyperoside	EMWat (25:1:25), (10:1:10) and (5:1:5)	
	Baicalein-7-*O*-diglucoside, baicalein-7-*O*-glucoside, baicalein and chrysin	HEMWat (1:1.2:1:1)	
	Isoflavan glycoside and pterocarpan glycoside	EEtWatAa (4:1:5:0.25)	
Alkaloids	Betalain	ProAcWat-$(NH_4)_2SO_4$ (1:0.5:1:1.2) and *ter*BuAcWat(HFBA) (2:2:1:5:0.7)	(Yang and Ito 2002; Deng et al. 2009; Sporna-Kucab et al. 2013; Jerz et al. 2014)
	Betacyanin	*ter*BuAcWat(HFBA) (1:3:1:5:0.7)	
	Dehydrocavidine	ChMWat(0.3 M HCl) (4:0.5:2)	
	Lappaconitine, ranaconitine, *N*-deacetyllappaconitine and *N*-deacetylranaconitine	ChMWat(0.3 M or 0.2 M HCl) (4:1.5:2)	
Phenylpropanoids	Salvianolic acid B	HEMWatAa (1:5:1.5:5:0.6%)	(Wei et al. 2002; Zhang et al. 2009)
	Eleutheroside E	ChMIsoWat (5:6:1:4)	
Coumarins	Imperatorin, oxypeucedanin and isoimperatorin	HEMWat (1:1:1:1) and (5:5:4.5:5.5)	(Ma et al. 2004; Wei and Ito 2006)
	Osthol and xanthotoxol	HEMWat (1:1:1:1) and (5:5:6:4)	
Iridoids	Geniposide	EBuWat (2:1.5:3)	(Zhou et al. 2005)
Anthraquinones	Rhein	HEMWat (3:7:5:5)	(Wei et al. 2003)
Benzoquinones	Coenzyme Q10	HepAcDi (12:7:3.5)	(Cao et al. 2006)

TABLE X. THE SURVEYED HEMWat SS AND POLARITIES

The polarity gradient may be obtained by experimental methods (e.g., the GUESS method (Friesen and Pauli 2005) or by calculation of the average of polarity (Zhang et al. 2008).

Defined HEMWat SSs		HEMWat SSs vs. average polarities	
HEMWat No.	HEMWat ratios (v/v)	HEMWat ratios (v/v)	Polarity
HEMWat -7	HEMWat (9:1:9:1)	-	-
HEMWat -6.5	-	HEMWat (5:1:5:1)	3.38
HEMWat -6	HEMWat (4:1:4:1)	-	-
HEMWat -5	HEMWat (7:3:7:3)	-	-
HEMWat -4	HEMWat (7:3:6:4)	-	-
HEMWat -3.5	-	HEMWat (6:4:5:3)	4.13
HEMWat -3	HEMWat (3:2:3:2)		
HEMWat -2.5	-	HEMWat (5:4:5:4)	4.69
HEMWat -2	HEMWat (7:3:5:5)	-	-
HEMWat -1	HEMWat (6:4:5:5)		4.74
HEMWat 0	HEMWat (1:1:1:1)		4.95
HEMWat +1	HEMWat (4:6:5:5)		5.16
HEMWat +2	HEMWat (3:7:5:5)		5.38
HEMWat +3	HEMWat (2:3:2:3)	-	-
HEMWat +3.5	-	HEMWat (3:5:3:5)	5.54
HEMWat +4	HEMWat (3:7:4:6)	-	-
HEMWat +4.5	-	HEMWat (1:2:1:2)	5.73
HEMWat +5	HEMWat (3:7:3:7)	-	-
HEMWat+5.51	-	HEMWat (2:5:2:5)	5.96
HEMWat+5.52	-	HEMWat (3:10:3:10)	6.22
HEMWat +6	HEMWat (1:4:1:4)	-	-
HEMWat +6.5	-	HEMWat (1:5:1:5)	6.52
HEMWat +7	HEMWat (1:9:1:9)	-	-
EWat	EWat (1:1)	-	-

VIII), the runtime has been shortened from days or hours to minutes. Thus, analytical CCS may be used to test different SSs and directly observe K values, separation resolution, and stationary phase retention. TABLE IX provides details of the use of analytical CCS for the separation of 44 NPs from eight classes. HEMWat and chloroform-methanol-water (ChMWat) systems are the main selected SSs used for 15 and 9 of the 44 compounds, respectively. Empirical SS selection strategies have a reputation of being labor intensive and tedious. However, they have several advantages, such as flexibility in the source material used for SS selection. Any source material may be employed for these experiments from commercial standards to crude extracts. Depending on the method of analysis, the K values of many different analytes in a SS may be determined simultaneously. In addition, the flexibility of analytical methods to quantitate the composition of upper and lower phases includes the assessment of biological activity (Yeh et al. 2012) and the acquisition of structural data by NMR (Qiu et al. 2012). Finally, the results from empirical methods transfer well into the larger scale separations in terms of K value, resolution, and SS suitability for the dynamic CCS process.

2.3.3. Semiempirical Solvent System Selection Strategies

Semiempirical SS selection strategies attempt to reduce the number of partitioning experiments. They can identify a suitable SS by replacing some or all of the partitioning experiments with a simple method of predicting K values and/or using mathematical relationships to minimize the number of experimentally determined K values needed to predict additional data points.

TLC separation depends on two mechanisms, principally absorption and, to a lesser extent, partitioning. Although the CCS mechanism is only based on

partitioning, both systems provide separations coordinated with analyte polarities. This is demonstrated by the commonly used TLC analysis of CCS fractions, which shows the distribution of analytes as strongly polarity related (Hostettmann et al. 1979). This general observation inspired the development of a TLC-based SS selection methodology. Marston and Hostettmann proposed that the upper and lower phases of samples from a partitioning experiment be developed on silica gel TLC with the organic phase as the mobile phase (Marston and Hostettmann 2006). In this way, both the partitioning and the suitability of the compound for a SS may be assessed.

The Generally Useful Estimate of Solvent Systems (GUESS) method (Friesen and Pauli 2005) established the relationship between the TLC Rf value and the CCS K value. A mixture of 21 NPs with widely varying polarities (termed the GUESSmix) was prepared (Friesen and Pauli 2005 and 2007). The K values were determined by partitioning experiments in both HEMWat and ChMWat SSs. These were compared with Rf values from TLC plates developed with the organic phase of that SS and/or a simplified formulation of the organic phase (Friesen and Pauli 2005). This study demonstrated a relationship between Rf values and K values such that Rf values between 0.29 and 0.71 (optimal value 0.5) could be correlated with K values from 0.4 to 2.5 (with a perceived optimal value 1).

Representing an exemplary application of the GUESS method, the present work enriched ginkgotoxin, present at the parts per million level from *Ginkgo biloba* Linnaeus (Ginkgoaceae) seeds using GUESS-based CCS combined with qHNMR (Liu et al. 2014). In work by another group, the EBuWat (2:1:6, v/v) solvent system, predicted by TLC, led to the separation of isorhamnetin-3-*O*-gentiobioside, rutin, and

narcissin (Yang et al. 2012). Thus, it becomes evident that mobility on TLC may be used as an indicator of CCS selectivity, and that the TLC-based GUESS method provides a convenient means of estimating the K value in an SS. TLC-based methodology has the added advantage that it may be combined with a bioautography-based evaluation of bioactivity (Chen and Schwack 2014). While the GUESS method simplifies the empirical methodology, its establishment and extension still requires the same iterative process of partitioning experiments. Wagenaar et al. described the correlation of synthetic compound groups (from compound libraries) with RP-HPLC (acetonitrile with 0.1% TFA and water gradient) and CCS retention times in select HEMWat SSs (Wagenaar et al. 2009) and found a nearly linear correlation between closely related compounds. However, the methodology has not been extended to NPs or beyond the HEMWat SS.

K value prediction within the HEMWat family: one outcome of the previously mentioned GUESS article (Friesen and Pauli 2005) was the observation that the logarithmic K value of an analyte, such as umbelliferone, has a linear relationship in 16 predefined HEMWat SSs This creates the scenario where, if the K value in one HEMWat SS is known, the corresponding K value in a different HEMWat SS may be predicted. Ignatova et al. also observed a nearly linear correlation between the LogK values of pharmaceuticals and the respective HEMWat SS number (Ignatova et al. 2011). The use of the HEMWat solvent system as a test case for SS selection methodologies arises, in part, because of the predominance of HEMWat in reported CCS applications (Friesen et al. 2015). For example, TABLEs VII and IX include a total of 33 compounds from eight different classes that were separated by CCS with a HEMWat SS. A significant feature of the HEMWat SS is that a wide range of

polarities may be covered by the systematic modification of the *n*-hexane and ethyl acetate relative to the methanol and water proportions between HM 1:1 on the nonpolar extremity and EWat 1:1 on the polar extremity.

Han et al. described a method for predicting K values for a series of HMWat and HEMWat SSs by methodically modifying a pair of parameters. For example, the K value of an analyte may be mapped in the HMWat SS family by following the formula 5:x:10-x, where "x" is the volume ratio of methanol in the range from 0 to 10. The K values of four formulas created a map that may be described by a mathematical equation ($y = a \cdot b$) that may be used to predict K values. The authors also investigated the families created by HEMWat 5: 5:x:10-x ("x" again being the volume of methanol) and HEMWat x:10-x:5:5 ("x" being the volume of hexane). The method was applied to determine that HEMWat 1:1:1:1 was the optimal two-phase solvent system for the CCS preparation of pseudolaric acid from *Pseudolarix kaempferi* (Lindl.) Gordon (Pinaceae) (Han et al. 2008). Zhang et al. reported a SS selection method that was guided by the calculation of the average polarity (P′) of 36 SS (TABLE X). The calculations were based on the solvent proportions and their Rohrschneider P′ solvent polarity values. The method was employed to isolate racemic tetrahydropalmatine from *Corydalis yanhusuo* W.T. Wang. (Papaveraceae) with HEMWat (4:6:5:5) (Zhang et al. 2008). TABLE X lists the defined HEMWat SSs and those used for the calculation of average polarity.

Three-dimensional K value maps: Dubant et al. described a SS screening method that created a three-dimensional map correlating the composition of the upper and lower phases with the partition coefficient of a target analyte (Dubant et al. 2008). Creating the map required performing partitioning experiments to determine the

partition coefficients of the target analyte in at least nine carefully selected SSs. Proof of principle was done with a mixture of seven chemicals: reserpine, ninhydrin, chloropropamide, dipropyl phthalate, methyl prednisolone, cortisone, and lidocaine. Further applications have not been reported, and future work will be needed to demonstrate that the primary screening of the K values with single factor experiments can be applied more generally.

Predictive models using empirical data to define descriptors: Renon et al. developed a K value prediction process employing a Non Random Two-Liquid Segment Activity Coefficient (NRTL-SAC) model (Renon and Prausnitz 1968) for representing liquid-liquid equilibria. NRTL-SAC relies on solvent and analyte descriptors that define the liquid "nonideality" of analytes and solvent molecules in terms of interactions among three pairwise interacting conceptual segments: the hydrophobic segment (molecular surface area that is adverse to hydrogen bonding), the polar segment (molecular surface area with interactions characteristic of an electron donor or acceptor), and the hydrophilic segment (molecular surface area with interactions characteristic of a hydrogen-bond donor or acceptor). The descriptors for the most common solvents are already known (Chen and Song 2004). The K value of an analyte may be calculated as follows (Equation 6) (Chen and Crafts 2006):

Equation 6: $K = f(X, Y-, Y+, Z, PE)$

where X = hydrophobic segment, Y− = polar-attractive segment, Y+ = polar-repulsive segment, and Z = hydrophilic segment. The liquid phase equilibrium composition of a selected SS is represented by PE.

It was previously shown that NRTL provided the best thermodynamic equation for the investigation of the K value of an analyte (Chen et al. 2005). The NRTL-SAC model has been developed for solvent prediction based on a few partitioning experiment results. In order to evaluate the precision of the NRTL-SAC model, acetaminophen, sulfadiazine, cimetidine, sulfamerazine; magnolol, honokiol, 3-hydrophloridzin, and phloridzin were selected as standard analytes (Chen and Crafts 2006; Ren et al. 2013 and 2014).

Another application of using descriptors to predict partition coefficients was reported by Qian and Poole. They determined the partition coefficients for 86 analytes in ChMWat (8:4:3, v/v), representing the SS for the Folch partition. The empirical data was used to determine the coefficients for a series of five solute descriptors based on excess molar refraction, polarizability, hydrogen-bond acidity, hydrogen-bond basicity, and McGowan' s characteristic volume (Qian and Poole 2007).

Other semiempirical strategies: both step gradients (Leitao et al. 2005) and continuous gradients (Ignatova et al. 2011) have been successfully employed for the isolation of selected analytes by CCS. However, the use of gradient CCS chromatography as a SS selection technique is still in its infancy. More likely, the SS selection approach may introduce the researcher to attempt a gradient as the best means of achieving a particular separation goal.

Semiempirical strategies reduce, but do not entirely replace, the need for multiple partitioning experiments for SS selection. This reduces not only the workload but also the required expertise of the researcher. The iterative process of partitioning experiments is replaced by allowing the researcher to evaluate K values

from many different SSs simultaneously. The choice of SS composition must still be determined by the researcher. However, the exploration of suitability of a formulation within the chosen SS family is facilitated by semiempirical methods. It may still be necessary to verify the resulting SS choice by either an equilibrium partitioning ("shake flask") experiment or by CCS before committing the experimental sample to the appropriate CCS scale. In addition, the general applicability of semiempirical methods outside of the common solvent SS has not been explored in most cases.

2.3.4. Theoretical Strategies

Theoretical strategies attempt to preclude the need for partitioning experiments altogether by combining solvent descriptors with similar properties attributed to an analyte to predict relative solubility. Predictive methods to determine the partition coefficient of a given analyte in the octanol/water solvent system are examples of theoretical strategies (Moriguchi et al. 1992; Ghose et al. 1998). The main concept is that the solubility of an analyte in the upper and lower phases of a biphasic SS may be calculated independently given the structure of the analyte, the structures of the solvents, and the solvent composition of the phase.

The Conductor-like Screening Model (COSMO) calculates the dielectric screening charges and energies on a van der Waals' surface like a conductor and optimizes the analyte molecular geometry within a SS (Stewart 1990). COSMO focuses on evaluating the analyte's interaction with a few solvent molecules to predict the influence of the rest of the solvent on the analyte by an effective solvent continuum. COSMO for Real Solvents (COSMO-RS) has been developed as a quantum chemical and thermodynamic model (Klamt 1995). It combines both

solvent and analyte descriptors to calculate K values based on the structural information of analytes and solvents along with the SS phase composition. Two steps of the process include the optimization of the analyte's molecular geometry as well as the generation of charge density of the analyte's molecular surface. At this point, the COSMO-RS model is not applicable to ionized analytes. The details on K value calculations by COSMO-RS are described by Hopmann et al. (Hopmann et al. 2011 and 2012). Several case studies have been offered including *n*-alkylbenzenes in HepMWat SSs, steroids in HepEMWat, benzyl alcohol in HepEMWat, phenols in HepEMWat, and selected GUESSmix analytes in HEMWat. Furthermore, coumarin, piperine, capsaicin, and dihydrocapsaicin were isolated by SSs selected with the COSMO-RS model (Hopmann et al. 2012, Goll et al. 2013).

A recent article employs both the COSMO-RS and the UNIversal quasi-chemical Functional-group Activity Coefficients (UNIFAC) predictive thermodynamic models in calculating K values. Both COSMO-RS and UNIFAC predictions may be calculated with or without partitioning experiment data to inform the descriptor values. Various combinations of UNIFAC, experimental, and COSMO-RS generated data were compared with the goal of predicting K values that coincide with experimental values. It was concluded that, in most cases, the values obtained from semiempirical and even theoretical methods was sufficient to recommend one or more SSs for further analysis with partitioning experiments. It was proposed that these theoretical predictive models may be employed to explore the suitability of a wide variety of SS families for CCS (Frey et al. 2014).

Analyte solubility behavior in SSs may be evaluated by software programs. This shifts the iterative solvent system selection process from the laboratory bench to

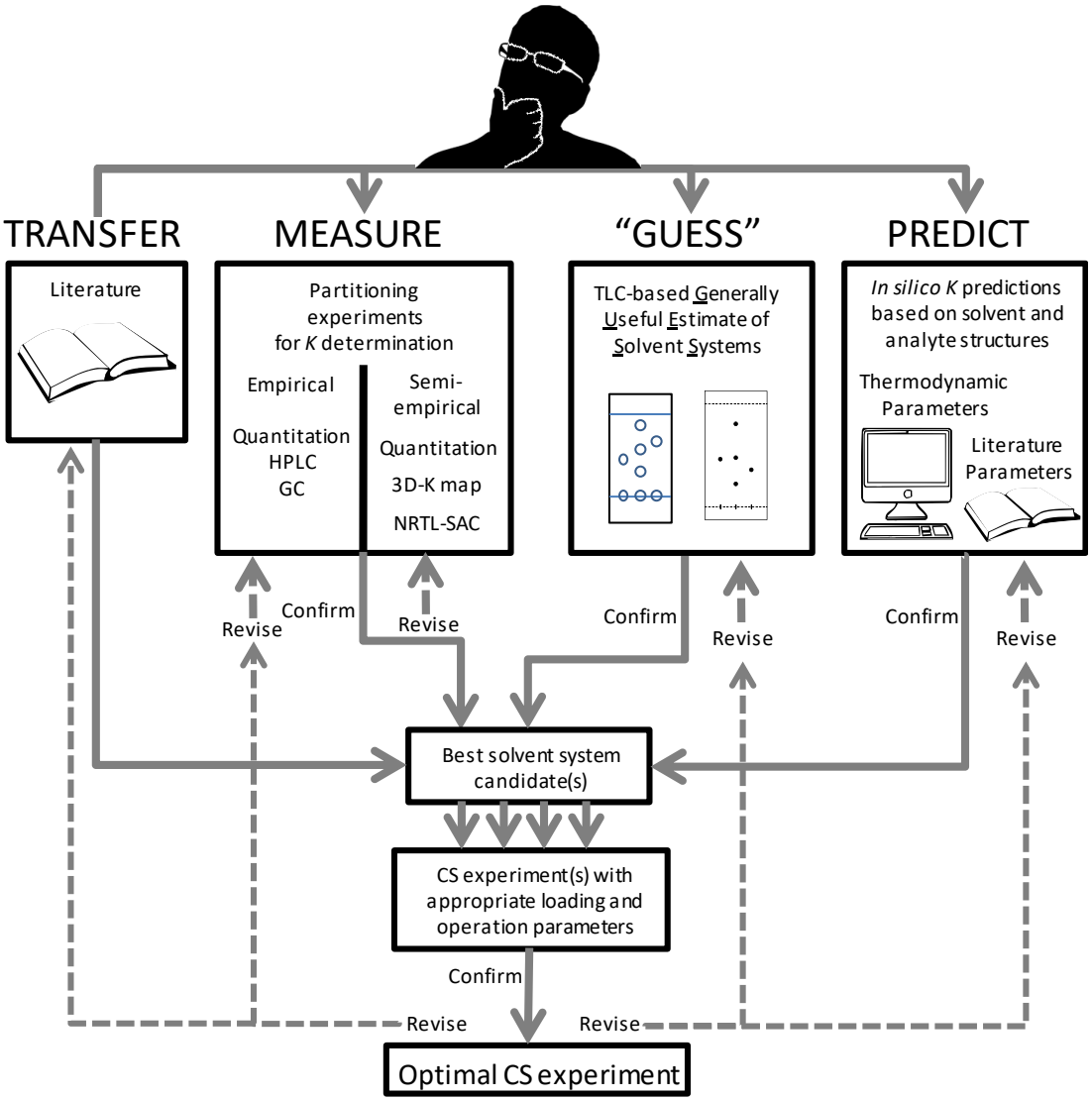

Figure 8. Workflow highlighting the four principal methods of solvent system selection.

At the top, the chromatographer must decide which SS(s) will be tested. On the first level, the researcher may TRANSFER SSs from the CS literature directly to second level best SS testing. The researcher may MEASURE the K values of target analytes by a series of partitioning experiments. Partitioning experiments may be performed independently in an empirical manner or they can be organized in a semi-empirical fashion to maximize the information generated. The researcher may employ the GUESS method which relies on TLC Rf values to predict the best SS(s) for separation. Finally, the researcher may PREDICT the best solvent system(s) through theoretical modelling of solubility parameters generated from structural information or gleaned from the literature. The workflow highlights the iterative nature of the SS selection process by showing that each SS must be evaluated and either confirmed or revised.

the computer screen. Many solvent system formulations may be investigated systematically with minimal effort once the geometric and thermodynamic characteristics of both solvents and analytes have been established. The complete process from molecular structure to K calculation requires at least three different commercial software platforms, which may somewhat limit the overall applicability of the approach. As with the previous methods, the ability of the researcher to input SS families and to intelligently guide an iterative selection process is still needed. Because analyte structural information must be provided, application in NP discovery is limited in instances of unknown molecules.

2.3.5. Navigating the Maze of Solvent System Selection Strategies

Figure 8 represents the workflow divisions that belong to different methods of SS selection and how they interrelate to each other. The workflow in Figure 8 emphasizes the iterative nature of the SS selection process. There are several decision points which will indicate whether or not the tested SS should be carried forward (confirmed) or reformulated (revised) and retested.

In the beginning, the researcher must decide which SS(s) will be attempted. Often, the CCS literature, such as the references in TABLEs VII and IX, are helpful to reveal SSs that have been successfully employed to isolate certain types of compounds. Another approach is to start with well-known "portal" SSs that have established usefulness such as HEMWat 1:1:1:1 (v/v)) and ChMWat 10:3:7 (v/v) (Marston and Hostettmann 2006). In addition, a skilled CCS practitioner may be able to propose a feasible starting point based on the structural characteristics or TLC polarity of the target compound(s).

The SS selection method may take four different pathways: "TRANSFER" - the

researcher has a high degree of confidence that a literature SS will be effective. "MEASURE" – the researcher has high-throughput quantitative analysis method (chemical or biological) that may analyze partitioning experiments. Measuring can be approached by testing a large number of SSs or a "smart" methodology that uses a limited number of partitioning experiments to predict the analyte(s) K value(s) in other solvent systems. "GUESS" – the compound(s) are readily identifiable by TLC (chemically or biologically) and the researcher prefers to work with TLC data for preliminary testing. "PREDICT" - the structure(s) of the target compound(s) are known and the research team has the hardware as well as software expertise to analyze a large number of potential SSs in silico. Once the preliminary testing has finished, a second level of SS testing is warranted. A primary SS should be tried on a CCS instrument. This will reveal the performance characteristics of the SS and extract combination. Adjustments may need to be made at this level to improve the stationary phase retention volume or reduce column overloading. The optimal CCS experimental procedure is a combination of sample extraction method, preliminary purification, SS selection, and appropriate operating conditions which will lead to a desirable separation.

2.4. Study Models

Due to the limited number of NADES observed that have been in Nature, study models still have to be developed to assist studying and understanding the NADES phenomenon better. In the present study, several models such as hydrogel and hydrolysis models have been developed, aiming to reveal if they may potentially function in natural sources, BDSs, and TRM formulae. Although this work only demonstrated one additional possible NADES function, it provides evidence that

NADES may play the role of functional solvents in Nature.

2.4.1. Hydrogel Model

Alginate is a linear unbranched polysaccharide with (1-4) links, and varying residue amounts of α-L-guluronic and β-D-mannuronic acids. It is a natural water-soluble polymer extracted from brown algae (Torelli-Souza et al. 2012). Alginate is widely used in pharmaceutical applications as a drug carrier due to good biocompatibility and biodegradability. It is challenging to load lipophilic metabolites into alginate hydrogels due to the high water content of these drug carriers (Hoare and Kohane 2008). However, the hydrogen bonding capabilities of alginates could provide a welcoming environment for NADES, which are composed of hydrophilic components. In order to confirm this hypothesis, a NADES solution and an alginate solution were introduced dropwise into a stirred chitosan/Ca^{2+} solution using an insulin syringe. Subsequently, the test molecule, curcumin (as component of curcuminoids), was loaded into the negatively charged alginate hydrogel core, for which Ca^{2+} acts as a crosslinker. The cationic chitosan also interacts with the anionic alginate on the hydrogel to form polyelectrolyte complexes, which solidify the hydrogel beads.

The aim of the hydrogel model development was to simulate biopolymers *in vitro*. Through a series of tests about interactions between NADES solutions and the hydrogel, this approach may provide some clues that NADES in botanical extracts may utilize a similar mechanism to deliver lipophilic metabolites into biopolymers. Studying the controlled release of the hydrogel model also uncovered a possible functional pathway for target metabolites in TRMs or BDSs.

The disruption of NADES matrices together with the NADES duality feature

(lipophilicity and hydrophilicity) suggests a potentially unique role in small molecule formulation. NADES can carry lipophilic ingredients and load them into a hydrophilic polymer such as a hydrogel. NADES components were removed from the formulation via spontaneous diffusion by movement down a concentration gradient, whereas a part of lipophilic molecules passively remained in the biopolymer. The inherent advantage indicates that NADES species may be structurally analogous to cyclodextrin, a commonly used excipient in hydrophobic drug delivery systems.

2.4.2. Hydrolysis Study

Trifolium pratense from the Fabaceae family, commonly known as red clover, is a medicinal herb used for the treatment of menopause symptoms, premenstrual syndrome, mastalgia, high cholesterol, and even sexual transmitted diseases (Booth et al. 2006). Some isoflavones occurring in *T. pratense* may account for these therapeutic effects and have been ascribed to their positive thermodynamic interactions with estrogen receptors (Beck et al. 2005; Booth et al. 2006). However, considering potential side-effects of phytoestrogen consumption, especially for breast cancer patients (Dunlap et al. 2017), serious concern should be taken with the dose of these isoflavones (Jargin 2014). For example, biochanin A and formononetin can induce cytochrome P450 metabolism (Dunlap et al. 2017). But when cytochrome P450 inducers, e.g., biochanin A and formononetin, are accumulated, they may cause an adverse therapeutic effect. Accordingly, appropriate levels of isoflavones in crude extracts become a key factor for the quality control of *T. pratense* products. Equally important, compared to other organic solvents, *T. pratense* can yield a higher total isoflavone content when using water as the extraction solvent (Klejdus

et al. 2001). This may be due to aqueous hydrolytic cleavage of isoflavone glucosides into corresponding isoflavones during extraction (Hösel and Barz 1975).

Regarding the hydrolysis, an enzyme family, β-glucosidases, may be responsible for cleaving the sugar moiety from the isoflavone glucosides (Booth et al. 2006; Kusaikin et al. 2011) and, thereby, liberating the aglycones spontaneously (Vuong and Wilson 2010). The hydrolysis model aims to uncover another potential NADES regulation mechanism. The higher isoflavone content change in aqueous hydrolysis could be helpful to monitor the influence of NADES interactions with some specific isoflavone glycoside. Moreover, to form a therapeutic formula, TRMs and BDSs are usually applied as crude extracts of herbal mixtures. However, the highly abundant NADES molecules in the extract are considered to be devoid of pharmacological activity and, thus, insight is growing that some potential poly-pharmacological function may be derived from their relative abundance. From this perspective, TRMs and BDSs consider the entire crude extract as a complex of active pharmaceutical and cooperative ingredients, supposed that the therapeutic function could be established on a potential poly-pharmacological mechanism. Tracing back to the source of the crude extract, hydrophilic molecules tend to occur in larger quantities. Meanwhile, NADES metabolite-based media were proposed and identified in natural sources.

3. RESEARCH AIM 1: METHODS FOR NADES ANALYSIS

(Previously published as Liu Y., Friesen J.B., McAlpine, Lankin, D.C., Chen, S.N., and Pauli, G.F. (2018) Natural Deep Eutectic Solvents: Properties, Applications, and Perspectives. J. Nat. Prod. 81 (3): 679–690.; Liu Y., Friesen J.B., Grzelak, E.M., Fan, Q., Tang, T., Durić, K., Jaki, B.U., McAlpine, J.B., Franzblau, S.G., Chen, S.N., and Pauli, G.F. (2017) Sweet Spot Matching: A TLC-based Countercurrent Solvent System Selection Strategy. J. Chromatogr. A 1504: 46-54.; Liu Y., Garzon, J., Friesen, J.B., Zhang, Y., McAlpine, J.B., Lankin, D.C., Chen, S.N., Pauli, G.F. (2016) Countercurrent assisted quantitative recovery of metabolites from plant-associated natural deep eutectic solvents. Fitoterapia. 112:30-37.)

3.1. NADES Preparation

Most NADES components are commercially available and usually should be treated under vacuum and/or at high temperature for water removal before use (Radošević et al. 2016). As shown in Figure 1, NADES preparation is about administration of both the proper component ratio and the entropy in the matrix via heating and/or agitating treatments (TABLE XI). Nevertheless, documented NADES preparation methods are not uniform. The neat mixing of NADES components may inefficiently transfer the solid state of NADES components into a liquid state. Hence new practitioners can find the production of a proposed NADES challenging.

This problem is overcome by entropy regulation (Figure 5) during NADES preparation, for which heating and vacuum evaporation are the two major strategies (TABLE XI). In the heating strategy, the NADES components are mixed at the designated component ratio and then stirred at a certain temperature from 50 to100°C (Dai et al. 2013; Jablonský et al. 2015; Zhao et al. 2015). The increased entropy enables the eutectic matrix to assemble rapidly. Depending on the NADES' properties, a homogeneous transparent liquid can be formed. After the mixture has cooled to ambient temperature, maintenance of transparent unified mixture

TABLE XI. SUMMARY OF STANDARDIZED PREPARATION STRATEGIES FOR NADES SPECIES

Methods		Procedure	Reference
Heating		Agitation (50-100 °C)	(Dai et al. 2013, Hayyan et al. 2015, Jablonský et al. 2015, Zhao et al. 2015)
Vacuum evaporation	Dissolution	Evaporation	
	Heat (50°C)	Rotatory evaporator (45°C)	(Wikene et al. 2015 and 2016)
	Vortex (25°C)	Rotatory evaporator (50°C)	(Dai et al. 2013)
	Ultrasound (25°C)	Speed vacuum concentrator (37-40°C)	(Liu et al. 2016)

indicates that the designated NADES has indeed been obtained. The vacuum evaporation strategy (Dai et al. 2013; Wikene et al. 2015 and 2016) includes two basic steps. (i) Dissolution of NADES components in water: heat, vortex, and/or ultrasound are used to accelerate dissolution. (ii) Water removal via evaporation: a centrifugal vacuum evaporator or a rotatory evaporator are the most used apparatus in this step. A centrifugal vacuum evaporator provides comparatively low power and, thus, is appropriate for a small scale preparation (milligram level); A rotatory vacuum evaporator tends to be practical for a medium scale preparation (gram level) (Choi et al. 2011). The relevant water removal procedure can be explored by the water loss study. Due to the linear correlation of data points in the NADES state (shown in Figure 3), a water loss equation can be followed to obtain the corresponding NADES preparation time.

The component ratio unit is usually specified as a molar ratio (or mol/mol), which can reflect directly the contribution of either the donor or the acceptor of hydrogen bonds. A weight ratio (wt/wt) (Ru and König 2012) can be more practical for component measurement. When probing for a new NADES, it is best to start with a component molar ratio of 1:1 and adjust this ratio in subsequent steps according to the number of hydrogen acceptors and donors present in individual component of the matrix.

Most NADES in the literature are hydrophilic metabolite-based and, characterized by high hydrophilicity, but they can dissolve analytes with a broad hydrophilic/lipophilic range. This indicates that the solubilizing ability of NADES does not follow the "like dissolves like" principle. Screening of NADES species as promising solvents is still an empirical procedure. According to the Flory-Huggins equation (Huggins 1971 and 1976), the NADES' viscosity delays the penetration of analyte molecules into the NADES matrix. Compared to conventional organic solvents, some NADES with high viscosity will dissolve an analyte slowly. However, speed of dissolution is not equivalent to solubility. Heating together with stirring commonly increases the rate of dissolution.

In order to prepare the NADES in a reproducible manner, an ultrasound-vacuum centrifugal evaporation method was developed. The use of ultrasound permitted the efficient dissolution of solid particles, and vacuum centrifugation led to the removal of extra water. Compared to the reported vortex-vacuum evaporation method (Dai et al. 2013), the ultrasound-vacuum centrifugal evaporation method avoids the laborious vortex step. Importantly, the present procedure optimizes the reproducibility of the water removal. A systematic investigation of water loss during

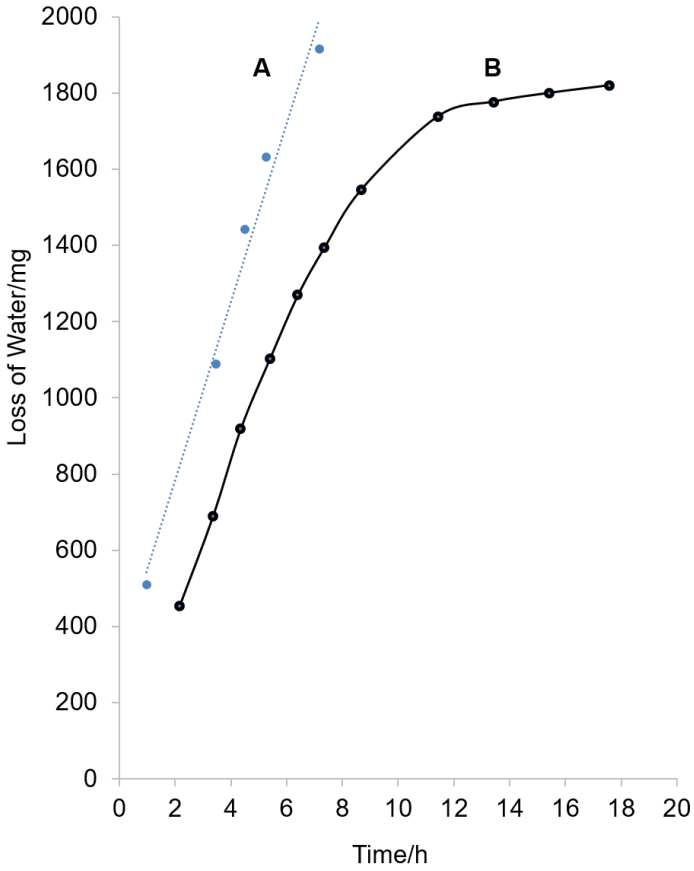

Figure 9. Water loss study of the glucose-choline chloride-water (GCWat).
(A) Distilled water was dried by a vacuum centrifugal evaporation. (B) Glucose (0.01 mol) and choline chloride (0.025 mol) were dissolved in distilled water (2 mL). After total dissolution, the resulting solution was treated by a vacuum centrifugal evaporation.

the evaporation stage helped to understand how long the drying step lasts. Furthermore, it provided indications as to how the intermolecular forces change during NADES preparation. Figure 9 compares NADES solution drying (B) with the drying of free water (A). While water showed the expected linear drying loss ($y = 253x + 384$, $R^2 = 0.982$), the drying curve of the GCWat NADES exhibited two distinct

zones: a rapid drying zone (i) during the first 8 h, which was linear, following the equation: $y = 169x + 140$, $R^2 = 0.986$; and a much slower zone (ii) reflecting the asymptotic loss of residual water from 12 to 18 h, which was partially linear following equation: $y = 10x + 1640$, $R^2 = 0.996$.

The slope of equation (i) from 2 to 8 h was 169. With reference to the observed slope of 253 for free water, the removal of water molecules is likely influenced by the molecules of the NADES components. According to the Frank model for structure of water around an ion (Frank and Wen 1957), water molecules removed from 2 to 8 h may originate from the disordered zone. The much lower slope of 10 observed for the linear portion of the slower drying period (ii) from 12 to 18 h indicated the much higher resistance of removing additional residual water from the NADES. This indicated that the hydrogen bond strength had increased in the NADES matrix. The water molecules being removed at this stage likely stay in the ordered zone, i.e., they are surrounded by NADES ions, and, thus, stronger (more highly ordered) hydrogen bonds are formed in the NADES matrix. This indicates that the hydrogen bonding network reaches a maximum strength during the final stage (iii) of the ultrasound-vacuum centrifugal evaporation procedure, leading to a defined amount of retained water. Therefore, hydrogen bonding is likely one of the most important molecular forces in GCWat. Moreover, this confirms results demonstrated by FT-IR spectral analysis (Dai et al. 2014). The formation of hydrogen bonding is an important factor affecting analyte solubility and stability in NADES. Thus, the water content of NADES may be highly correlated with their solubilizing and stabilizing ability for NPs.

Reproducibility is another important aspect for a NADES preparation method.

Based on the zone (ii) equation y = 10x + 1640, the preparation time can be calculated as 14.4 h. In this manner, the ultrasound vacuum centrifugal evaporation method can provide highly consistent GCWat solutions. To evaluate the ultrasound-vacuum centrifugal evaporation method further, the solubility of rutin was assessed in a range of NADES. An optimum solubility step was performed via changing water content in NADES matrix. GCWat, 5% GCWat (GCWat:water, 95:5, v/v), and 10% GCWat (GCWat:water, 90:10, v/v) were investigated, and the solubilities were found to be 0.26 M, 0.40 M, and 0.18 M, respectively. These findings are consistent with previous results (Dai et al. 2013).

3.2. Intermolecular Interactions of NADES Components

Mannose-dimethylurea-water (MDWat, 2:5:5, mol/mol) was used as a NADES model system to study the NADES solubility mechanisms. To understand the mechanism of MDWat's solubilizing power for lipophilic metabolites, the molecular interaction among the intermolecular components in the MDWat matrix was investigated via the intermolecular nuclear Overhauser effect (nOe). To optimize the spectral window, different volume ratios of MDWat to DMSO-d_6, including 1:1, 1:2, 1:5, and 1:10 (v/v) were used to perform 2D nOe spectroscopy (NOESY) NMR experiments. The ratio of 1:5 exhibited the desired spectral window, where 1D ^{1}H NMR spectra could be acquired in high resolution and dipole-dipole interactions be determined as well (Figure 10). The data indicated that the three components of MDWat interact with one another through a complex hydrogen bonding network. Herein, due to the minimization of thermodynamic effects, the dimethylurea (DMU) configuration (Figure 10) can be assigned to represent the major population. Thus, because of hydrogen bonding between the carbonyl group of DMU and exogenous

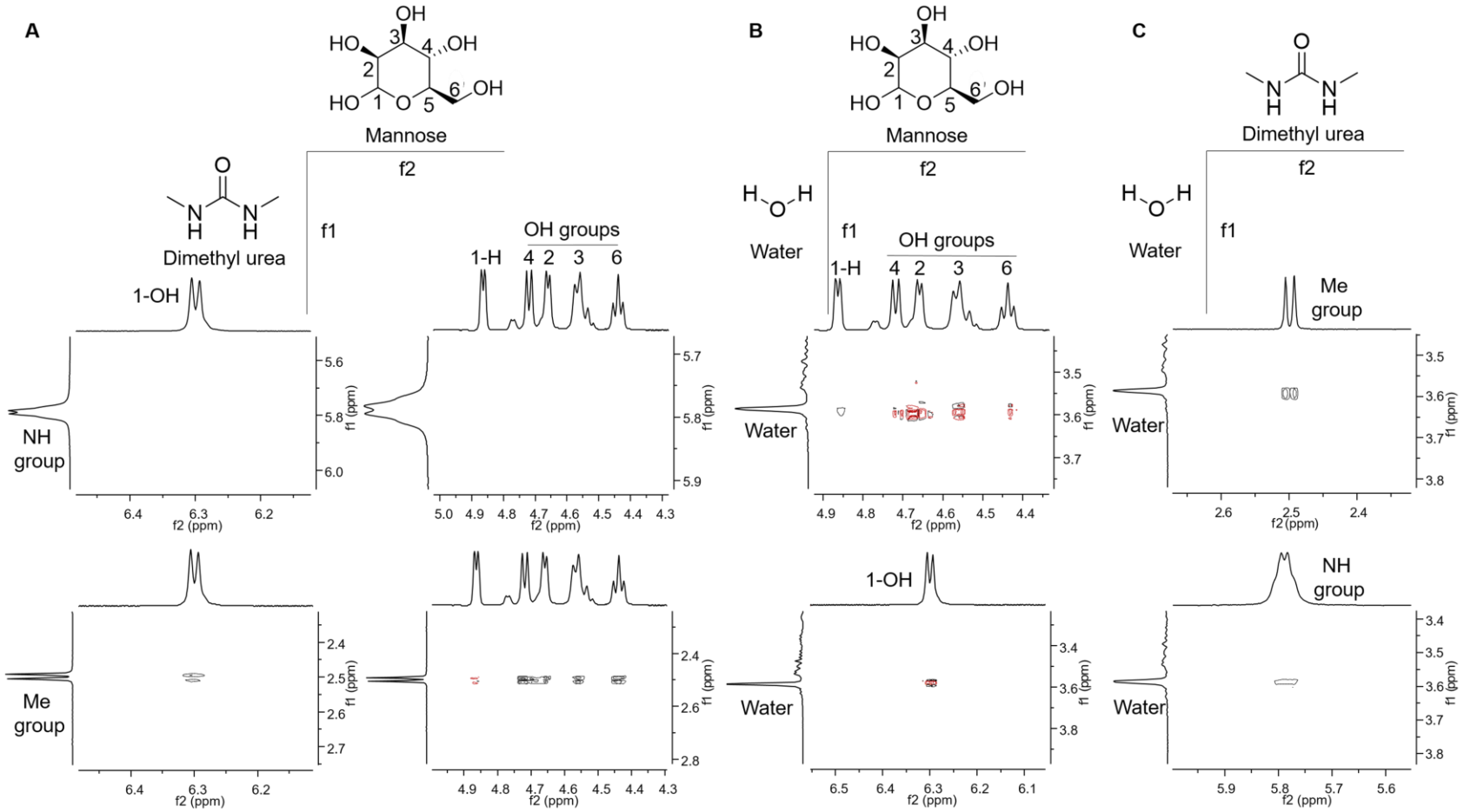

Figure 10. Nuclear Overhauser effect spectroscopy of MDWat in DMSO-d_6. An 8 s relaxation delay (D1) and a 0.4 s of mixing time (D8) were used. The dipole-dipole interaction between (A) mannose and DMU; (B) mannose and water; (C) DMU and water are shown.

OH groups (C=O···H-O), the methyl (Me) groups of DMU exhibited interactions with OH groups of mannose. However, the NH groups in DMU exhibited no interaction with mannose (Figure 10a). In Figure 10b, dispersive peaks occurred between the signals of water and OH groups of mannose. This is consistent with hydrogen bonding between water and the OH groups of mannose. As a result, the nOe signals were partially suppressed. The dispersion signals also show that water may bind primarily with two endogenous OH groups of mannose. Figure 10c demonstrates that water also hydrogen bonds to the NH groups. All of these results suggest that the water molecules behave as linkers between the other two NADES components. This also suggests that NADES may be structurally analogous to cyclodextrin, a commonly used excipient in lipophilic drug formulation. The three MDWat components, i.e., mannose, dimethylurea, and water, may orient themselves forming a complex microstructural hydrophilic outside, as well as a lipophilic niche inside of MDWat matrix to accommodate lipophilic compounds, resulting in their superior solubilizing power for lipophilic molecules. This occurs despite the fact all the components comprising this NADES are strongly hydrophilic in Nature.

3.3. NADES Behavior in Countercurrent Separation (CCS)

3.3.1. TLC-based CCS Solvent System Prediction

Numerous studies have used the GUESSmix selection of commercially available natural products, but few applications of the TLC-based SS selection scheme have been reported (Liu et al. 2015). Another anomaly is the observation that CCS selectivity, which depends only on liquid–liquid partitioning, cannot always be predicted from the TLC behavior. This raises the question whether the defined matching of Rf and K value ranges are appropriate. To answer this question, both

theoretical hypotheses and case studies were developed.

3.3.1.1. Theoretical discussion

Normal-phase TLC uses silica gel as a stationary phase and predominantly various organic solvents as a mobile phase. The migration rate of an analyte is affected by both its solubility in the mobile phase and its affinity for the silica gel. In a normal-phase CCS, an aqueous alcohol phase approximates the hydrophilic and selectivity characteristics of the TLC silica gel stationary phase. Normal-phase CCS holds the aqueous phase in the column, while the mobile phase carries the analytes which partition between the two liquid phases by a series of mixing and settling stages. In both TLC and CCS, the eluotropic series of solvent "eluting strengths" is generally followed. The similarities of action in TLC and CCS are the theoretical foundation of the TLC-based CCS solvent system (SS) prediction strategy.

At the same time, differences between the two methods exist. One basic distinction between TLC and CCS is the nature of the mobile and stationary phase interactions. The rate of analyte migration in TLC is largely influenced by low surface area adsorption and desorption interactions. In contrast, the rate of analyte elution in CCS is governed almost completely by high surface area liquid–liquid partitioning. The phase interactions with the tubing (countercurrent chromatography) or cell (centrifugal partition chromatography) walls may also be a supposedly neglectable factor. Another difference between CCS and TLC is that the nature of the silica gel stationary phase is rather static, whereas in CCS the composition of the stationary phase may be highly variable depending on the composition of the chosen SS.

In the GUESS method, the mobile phase in both chromatography systems has

approximately the same contribution. Indeed, it was proposed that a simplified, hydrophilicity/lipophilicity matched organic phase composition could be substituted for the equilibrated organic phase in TLC (Friesen and Pauli 2005). The rationale for this simplification is that equilibration requires mixing the solvents of the biphasic SS, agitation, settling, and physically separating the two layers in order to prepare the TLC mobile phase. The simplified TLC eluting solution in the GUESS method was found to give approximately the same results as those with equilibrated organic phases. The aim of the original GUESS method was not to calculate K values based on TLC Rf values, but simply to determine which SS may provide a good starting point for the SS selection process, where K values are calculated based on observed partitioning. There has always been some concern that the simplified approach may not be adequate for SSs where one or more organic solvents is/are found in significant quantities in both phases of the equilibrated SS. This potential limitation led to the proposal that, e.g., ethyl acetate-containing SSs such as *n*-hexane-ethyl acetate (3:7, v/v) (SSE 7) corresponded to three HEMWat CCS SSs: 3:7:5:5, 3:7:4:6, and 3:7:3:7 (v/v).

In order to devise a system of comparing Rf and K values, the nature of these values should be understood better. Rf values in TLC result from the experimental measurement of two distances. Rf values are rarely recorded for analytes in the literature due to their relatively variable nature and the limitations of the most widely used simplistic experimental conditions. In contrast, in CCS, the K value is a partition coefficient, a physicochemical constant that can be measured from the appropriate CCS experimental values and by partitioning experiments (Pauli et al. 2015). A practical consideration is that lipophilic analytes in normal-phase TLC receive higher

Rf values (near 1), while the same analytes in normal-phase CCS receive low K values. This can be compensated for by using the reversed-phase K values for CCS, which are simply (and remarkably) the reciprocal of the normal-phase K values (Friesen and Pauli 2008). This strict, mathematical reversibility cannot be achieved with TLC (or by solid phase based LC) even though both normal-phase and reversed-phase media are available.

A much more serious consideration is the scale used for each value. TLC Rf values are calculated as ratios between zero and unity. On the other hand, K values are calculated as ratios between zero and infinity. There are at least two methods of reconciling these values so that their scales have the same range. (i) The CCS elution scale may be placed in the zero to unity range by defining a partition retention factor (Pf) as the concentration of the analyte in the stationary phase, divided by the sum of the concentrations in the mobile and stationary phases (Pf=K/(K+1)) (Friesen and Pauli 2005). (ii) Another approach is to compare Rf values with logK values. This is also a reciprocal scale, as logK and log(1/K) are equidistant from unity. In this case, however, the resulting logK values are between negative and positive infinity with log0 being undefined.

For the second method, the possible range of Rf and logK values are not the same. Therefore, a factor must be introduced to correlate Rf and logK. A linear correlation (m) between Rf and logK, where Rf ∝ logK, may be created by proposing that any three SSs (a, b, and c) with respective TLC Rf and CCS K values will create a straight line with a slope that follows Equation 7.

Equation 7. $m = \frac{\mathrm{R}f\mathrm{b}-\mathrm{R}f\mathrm{a}}{\log K\mathrm{b}-\log K\mathrm{a}} = \frac{\mathrm{R}f\mathrm{c}-\mathrm{R}f\mathrm{b}}{\log K\mathrm{c}-\log K\mathrm{b}}$

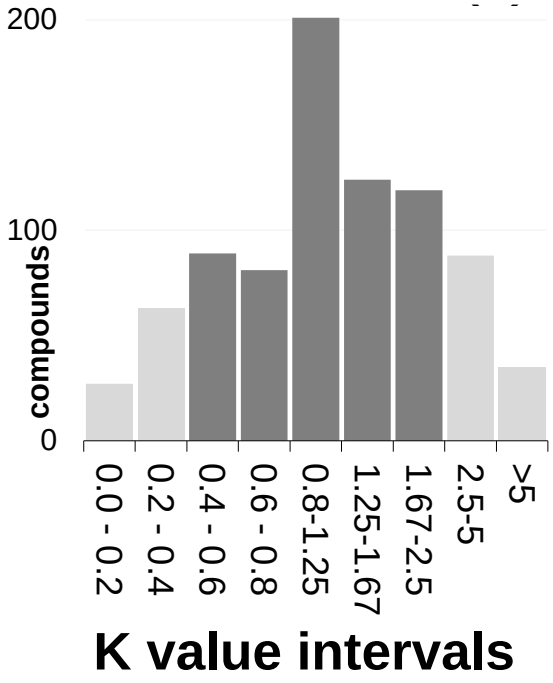

Figure 11. Literature analysis of the K value distribution of NPs isolated or purified by CCS

where the assumptions are that $R_f_c > R_f_b > R_f_a$ and $\log K_c > \log K_b > \log K_a$.

"Sweet spot" is a term used in bat and racket sports to denote the area on a hitting implement that makes the optimal contact with the ball. Sweet spot was, therefore, used to describe the region of optimum separation in CCS (Friesen and Pauli 2005). There is evidence that the great majority of NPs isolated with CCS have a K value in the range of 0.4 to 2.5 in the solvent system used in their isolation. The information in Figure 11 was gathered from reports of NP separations where the K values of the analytes were calculated based on partitioning or CCS experiments (Friesen et al. 2015).

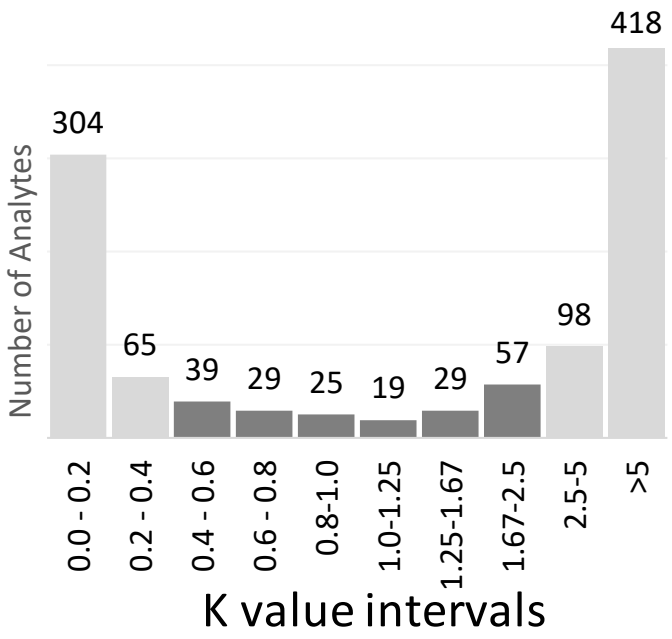

Figure 12. K value distribution of 19 GUESSmix compounds (excluding 0 and ∞ markers) in 57 solvent systems (1083 data points).

There are practical reasons, why the sweet spot paradigm is widely practiced in CCS (Pauli et al. 2008; Friesen et al. 2015). Analytes with low partition constants ($0 \leq K < 0.4$) are held in the column a short time, therefore, they undergo an insufficient number of mixing and settling stages that are required for adequate chromatographic separation (resolution). In addition, there is a practical lower limit to peak width for rapidly eluting compounds. Analytes with longer retention times ($2.5 < K \leq \infty$), on the other hand, are held in the column during many mixing and settling stages, so that they are better resolved. However, the practical limitation of high K value compounds is the increased time and solvent consumption associated with eluting high K value and the concomitant peak broadening. Indeed, several

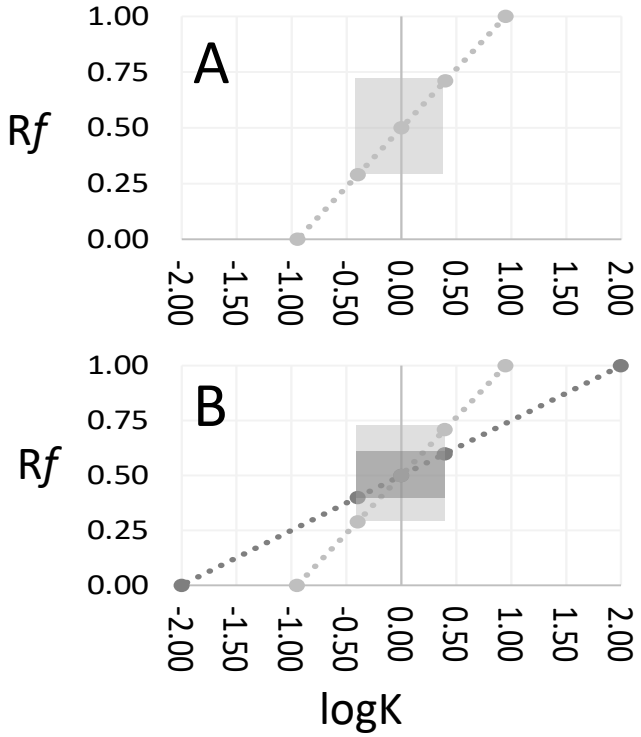

Figure 13. Models correlating Rf and K sweet spots by comparison of Rf and logK values with a K sweet spot 0.4 ≤ K ≤ 2.5. (A) logK working interval -1.0 ≤ logK ≤ 1.0. (B) logK working interval -2.0 ≤ logK ≤ 2.0. The results of larger logK working intervals are found in Table XI and Figure 16

methods have been devised to hasten the elution of highly retained compounds such as gradient, elution-extrusion, dual, and cocurrrent modes in CCS. It is interesting to note that experimental duration plays such an important role in the SS selection process, which is in itself prolonged and labor intensive. Finding the best balance between both continues to be an analytical challenge.

There is an attraction to specifying K = 1 as the epicenter of CCS that goes beyond simple practical considerations. At unity, the concentration of the analyte is the same in both phases and it will elute at one column volume in both normal-

phase and reversed-phase modes. This eliminates potential error in the selection of experimental and instrument conditions, which are known to pose binary challenges that can lead to experiment failure (Friesen and Pauli 2009).

In order to ascertain the probability of discovering a particular analyte in the sweet spot of particular SS we asked the question "How often is an analyte found to be in the sweet spot of a solvent system?" To answer this question, K values from 19 GUESSmix compounds (excluding 0 and ∞ markers) in 57 solvent systems were plotted in frequency bins, with reciprocal intervals centered at unity (Figure 12) (Friesen et al. 2015). The resulting convex curve shows a minimum in the middle of the sweet spot. Out of 1053 data points, 198, or 18%, are in the sweet spot, which shows the rarity of finding a specific analyte in the sweet spot of a specific SS. Each analyte was found, on average, in the sweet spot of 10 out of 57 SSs. Combined with Figure 11, this graphic illustrates why SS selection is a challenging, and at the same time a desirable process. Figure 11 shows the distribution of all the K values of a set of compounds in a SS panel. This is in sharp contrast to the widely used gradient method in liquid chromatography that tends to place a large number of analytes within a solvent composition range to facilitate their purification.

The GUESS method proposes a correlation between the TLC Rf value in a certain region (Rf sweet spot) with the region of optimal separation (K sweet spot) in CCS. The optimum separation region in CCS has been proposed: $0.5 \leq K \leq 2$ (Ito 2005), $0.4 \leq K \leq 2.5$ or $0.25 < K < 16$ (Friesen and Pauli 2005). Interestingly, both sweet spot boundaries, described by different groups, are represented in terms of reciprocal values ($2/5 \leq K \leq 5/2$ or $½ \leq K \leq 2$ respectively), which illustrates the importance of K

TABLE XII. THE CALCULATED RF SWEET SPOTS BASED ON DIFFERENT K WORKING INTERVALs

K	logK	R*f*	K	R*f*	K	R*f*	K	R*f*	K	R*f*
max	Log_{max}	1.00	100		1000		10000		10^{25}	
4.00	0.60	x		0.65		0.6		0.58		0.5012
1.00	0.00	0.50								
0.25	-0.60	y		0.35		0.4		0.43		0.4988
min	Log_{min}	0.00	0.01		0.001		0.0001		10^{-25}	

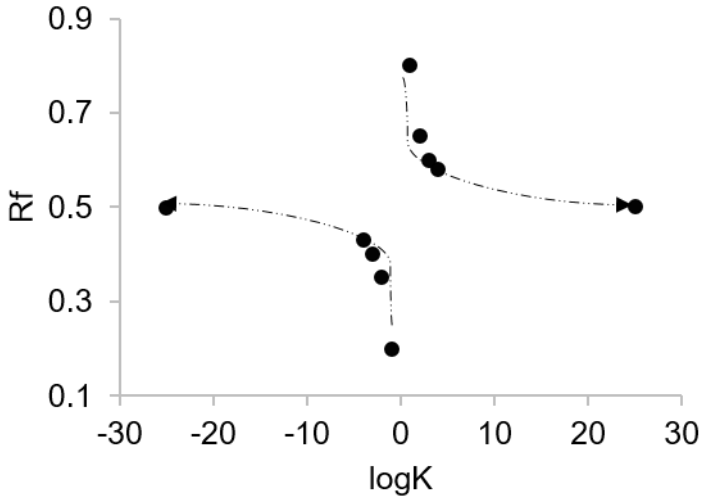

Figure 14. Simulated correlation model of Rf and logK

= 1 in CCS. The TLC vs. CCS sweet spot correlation strategy (ii) may be used to illustrate the challenges in correlating Rf and K values. The potential correlation between Rf and K or Rf and logK is proposed. Because log0 is undefined, the previously proposed two-dimensional sweet spots $0.4 \leq K \leq 2.5$ and $0.29 \leq Rf \leq 0.71$ may be used to calculate the logK working interval that corresponds this 2D sweet spot. The resulting calculations define the logK working interval to be $-0.95 \leq logK \leq$

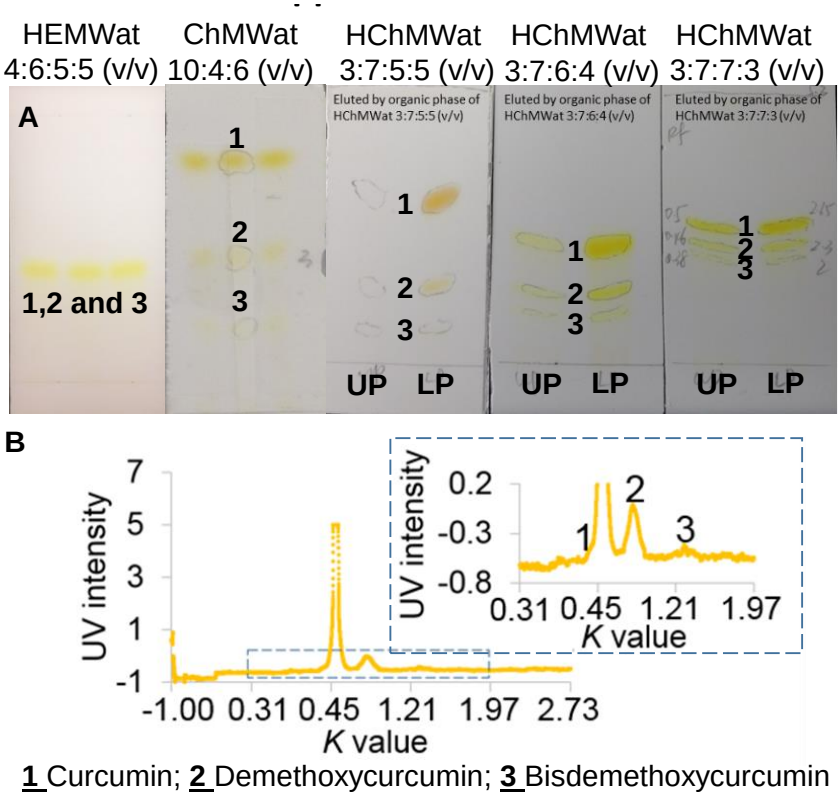

Figure 15. GUESS method applied to the separation of three curcuminoids. (A) shows TLC results of a screening procedure. The SS candidates were taken from the HEMWat, ChMWat, and HChMWat families. The predicted SSs and their corresponding K values are HEMWat (6:4:5:5, v/v), 0.94 (1), 1.02 (2), and 1.07 (3); ChMWat (10:4:6, v/v), <0.02 (1), <0.02 (2), and <0.02 (3); HChMWat (3:7:7:3, v/v), 0.67 (1), 1.09 (2), and 1.76 (3). (B) CCS result using HChMWat 3:7:7:3. The order of elution in CCS is the same as in the normal phase TLC as the CCS experiment was performed with the organic (lower) phase mobile.

0.95 which corresponds to 0.11 ≤ K ≤ 8.9 (Figure 13A). This is a rather narrow windowconsidering the full range of possible K values of zero to infinity. The logK working interval may be expanded by adjusting the Rf sweet spot. In this case, the K sweet spot remains 0.4 ≤ K ≤ 2.5, and the logK working interval is set at -2.0 ≤ logK ≤ 2.0. The resulting Rf sweet spot (on the y-axis) narrows to 0.4 ≤ Rf ≤ 0.6 (Figure 13B). The results of larger logK working intervals may be found in TABLE XII and

Figure 14. These data show that, as the K working interval widens, the slope of the line tends towards 0, and the Rf sweet spot becomes extremely narrow and narrows down to 0.5. This demonstrates the challenge of defining the two-dimensional Rf × K sweet spot in a universal way. Proposing a one-to-one correlation with adjusted Rf or K values is very likely an oversimplification. In order to make such a correlation universal, a correlation factor would need to be created to account for differences in SSs and methodology (e.g., following the basic form of Rf = a logK + b).

The following example with curcuminoids illustrates the challenges of matching both hydrophilicity/lipophilicity and selectivity between TLC and CCS. Initially, HEMWat and ChMWat organic phases and the GUESS method were used for the separation of curcumin, desmethoxycurcumin, and bisdemethoxycurcumin. Preliminary results indicated that HEMWat (6:4:5:5, v/v) and ChMWat (10:4:6, v/v) were good SS candidates (Figure 15A). After the partitioning experiments, it was discovered that HEMWat (6:4:5:5, v/v) provided reasonable K values for the curcuminoids (0.94 for curcumin, 1.02 for desmethoxycurcumin, and 1.07 for bisdemethoxycurcumin), but with separation factors less than 1.2. However, ChMWat (10:4:6, v/v) partitioning experiments showed that all K values were in fact lower than 0.02. When *n*-hexane was added to the ChMWat system to produce the HChMWat SSs 3:7:5:5, 3:7:6:4, and 3:7:7:3 (Figure 15A), the curcuminoids were more tightly grouped in the TLC sweet spot for the organic phase of HChMWat 3:7:7:3. When a CCS experiment was then performed with this SS (Figure 15B), the three analytes showed baseline separation with experimentally determined K values of 0.67 (curcumin), 1.09 (desmethoxycurcumin), and 1.76 (bisdemethoxycurcumin).

Notably, even though the three curcuminoids do not appear to be well separated in the GUESS method TLC, they were resolved in the corresponding CCS experiment. The outcome of this experiment suggests that the TLC method is a good indicator of overall hydrophilicity/lipophilicity match, but a poor indicator of CCS selectivity. However, if the analytes of interest can be placed in the sweet spot of the SS, the selectivity might be satisfactory; but this will not be revealed until an actual CCS run has been performed.

3.3.1.2. Validation and Practice of Rf Sweet Spots

The ability to match both hydrophilicity/lipophilicity and selectivity remains a challenge for correlating TLC and CCS. Thus, it was useful to validate the feasibility of the proposed Rf sweet spots with an expanded range of analytes and SSs. Two basic strategies were utilized: (i) "normal prediction," where Rf value sweet spots (TLC) were used to predict the K value sweet spots (CCS), and (ii) "reversed prediction" for an analyte that had a K value in the sweet spot range for a particular biphasic SS, the organic phase of that SS was used to develop the analyte in TLC.

In order to explore the correlation between Rf and K value sweet spots, a sufficient diversity of both analytes and SSs must be considered. *n*-Hexane-ethyl acetate-methanol-water (HEMWat), chloroform-methanol-water (ChMWat), and ethyl acetate-*n*-butanol-water (EBuWat) SS families were studied (Liu et al. 2015). These three SS families were used initially along with 29 commercially available NPs to validate the proposed Rf sweet spots in the "normal prediction" strategy.

The GUESSmix, as originally formulated, includes 22 NPs with a broad hydrophilicity/lipophilicity range (Friesen and Pauli 2005). The initial purpose of the

TABLE XIII. TLC RF VALUES AND CORRESPONDING CCS K VALUES OF GUESSMIX COMPOUNDS IN HEMWat AND CHMWat SOLVENT SYSTEMS

GUESSmix	TLC solvent system/R*f* value			Predicted CCS solvent system/K value
				HEMWat+1/0.77
Aspirin	SSE5/0.36	SSE6/0.51	SSE7/0.63	HEMWat+3/1.44
Caffeine	SSC3/0.14	SSC4/0.42	SSC5/0.66	ChMWat 0 /6.25
Carvone	SSE1/0.45	SSE2/0.54	SSE3/0.66	HEMWat-6/1.19
				HEMWat-3/1.03
Cholesterol	SSE3/0.25	SSE4/0.48	SSE5/0.77	HEMWat-1/1.63
	SSC2/0.20	SSC3/0.42	SSC4/0.67	ChMWat-1/10.9
				HEMWat-3/0.55
Coumarin	SSE3/0.29	SSE4/0.43	SSE5/0.64	HEMWat-1/1.05
Estradiol	SSE4/0.20	SSE5/0.45	SSE6/0.67	HEMWat 0/1.40
				HEMWat+1/0.40
Ferulic acid	SSE5/0.27	SSE6/0.46	SSE7/0.63	HEMWat+3/0.82
β-Ionone	SSE1/0.44	SSE2/0.53	SSE3/0.65	HEMWat-6/2.44
				HEMWat+1/1.46
Naringenin	SSE5/0.37	SSE6/0.66	SSE7/0.82	HEMWat+3/4.40
Nicotinic acid	SSC6/0.41	SSC7/0.48	SSC8/0.58	ChMWat+3/0.71
				HEMWat+1/0.58
Quercetin	SSE5/0.19	SSE6/0.47	SSE7/0.70	HEMWat+3/1.90
				HEMWat+2/0.73
				HEMWat+4/1.30
Reserpine	SSE6/0.37	SSE7/0.59	SSE8/0.70	HEMWat+5/2.88
				HEMWat+1/0.58
Umbelliferone	SSE5/0.39	SSE6/0.63	SSE7/0.77	HEMWat+3/1.15
Vanillin	SSE4/0.29	SSE5/0.52	SSE6/0.71	HEMWat 0/0.49
				HEMWat+1/2.91
Salicylic acid	SSE5/0.41	SSE6/0.49	SSE7/0.59	HEMWat+3/5.67

* All data were extracted from original GUESS method research. The equivalent organic-only SS based on HEMWat and ChMWat families (solvent systems based on ethyl acetate, SSE or solvent systems based on chloroform, SSC)

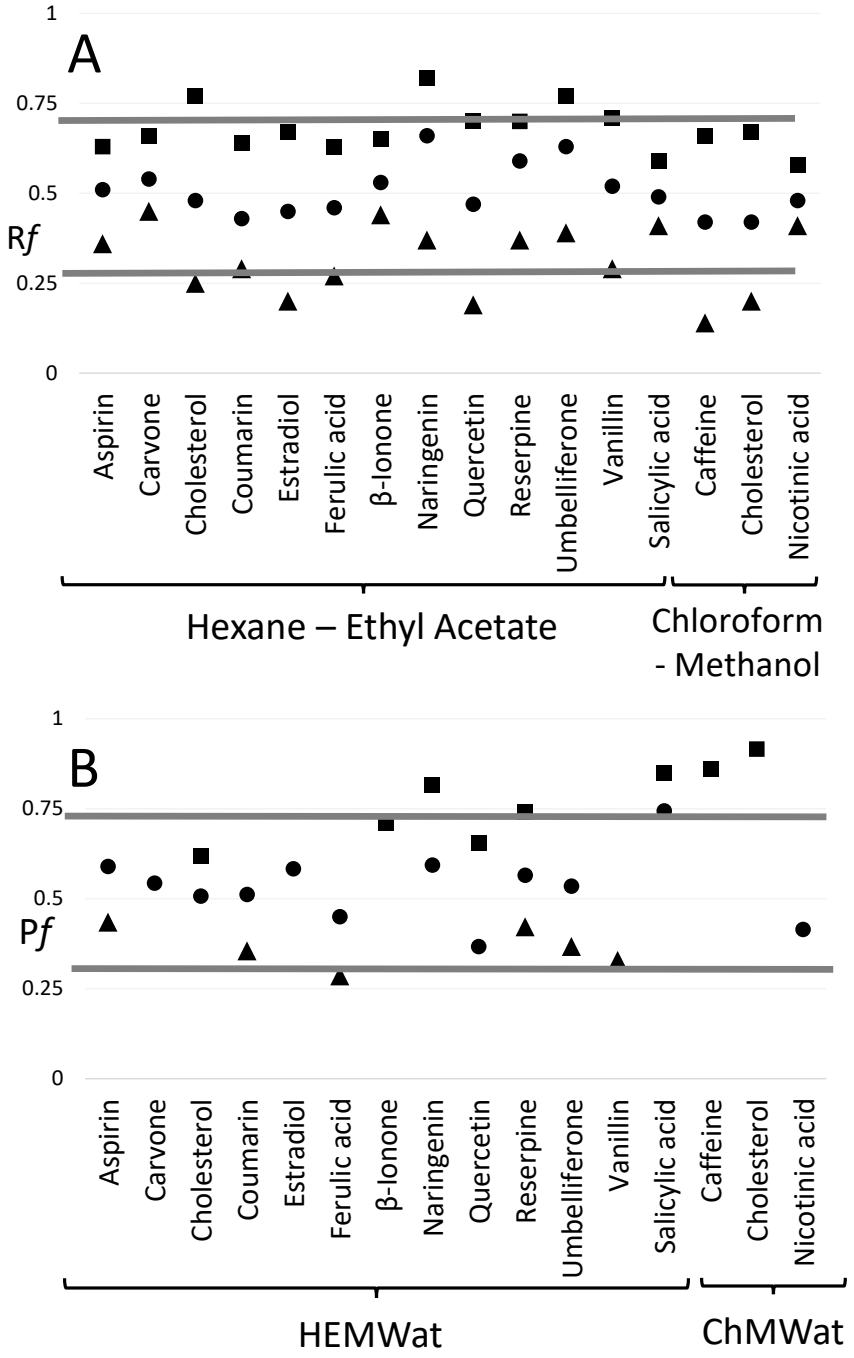

Figure 16. The relation between Rf or Pf values and two solvent system families via the GUESSmix method. (A)The three Rf values closest to 0.5 for each of 15 GUESSmix analytes were screened in both hexane-ethyl acetate and chloroform-methanol based TLC SSs. The values for data points and SSs are given in Table XIII. (B) K values (expressed in Pf) for the GUESSmix compounds in A in the SS(s) as predicted by the Rf values closest to 0.5. In some case, one TLC SS is used to predict more than one CCS SS. The $0.4 < K < 2.5$ interval corresponds to $0.29 < Pf < 0.71$. The K values for data points and SSs are given in TABLE XIII.

TABLE XIV. TLC RF VALUES AND CORRESPONDED CCS K VALUES OF GUESSMIX COMPOUNDS IN EBuWAT

GUESSmix	EBuWat (v/v)	K value	R*f* value
Arbutin	6:4:10	From 0.25 to 0.5	> 0.70
	4:6:10	From 0.5 to 1	> 0.70
	2:8:10	From 0.5 to 1	> 0.70
Caffeine	4:6:10	From 2 to 4	0.50
Chlorogenic acid	2:8:10	From 4 to 8	0.27
Nicotinic acid	6:4:10	From 1 to 2	0.42
Tryptophan	2:8:10	From 0.5 to 1	0.37
Salicin	0:10:10	From 0.5 to 1	0.65

GUESSmix was to investigate the correlation among Rf, K, and SSs. Accordingly, the GUESS method was established and applied to HEMWat and ChMWat SS families. For the present work, a database with the three-dimension correlation of Rf, K, and SS was available from that study. The results showed that, in the HEMWat family, these three factors exhibited significant correlation for most of the analytes. However, for the ChMWat family, the same potential correlations were not as obvious. According to TABLE XII, Figures 13 and 14, conditions between Rf sweet spots and K values function differently in the HEMWat family, compared to the ChMWat SSs.

The GUESS database of SS and K values was mined to identify three Rf values closest to 0.5 for 15 analytes (TABLE XIII and Figure 16). Applying the prediction strategy, the corresponding K values in their respective SSs were extracted (Figure 16B). According to the GUESS method, some TLC SSs may correspond to two or three CCS SSs. Therefore, all corresponding K values were obtained for the Rf value closest to 0.5, e.g., the TLC SS for reserpine, SSE7, corresponded to HEMWat 3:7:5:5,

3:7:4:6, and 3:7:3:7. Three of the 15 analytes achieved Rf sweet spots using chloroform-based SSs. Cholesterol had TLC sweet spot values in both HEMWat and ChMWat families. Rf values of 0.48 in the *n*-hexane-ethyl acetate SSs and 0.42 in chloroform-methanol based SSs corresponded to K values of 1.03 in HEMWat 6:4:6:4, 1.63 in HEMWat 6:4:5:5, and 10.9 in ChMWat 10:2:8. To display the results in Figure 16B, the K values were converted to their Pf values, i.e., the $0.4 < K < 2.5$ sweet spot interval corresponds to $0.29 < Pf < 0.71$.

The HEMWat correlation results show that 19 out of 23 times, the GUESSmix method predicted a suitable SS for the targeted separation of the analyte. Interestingly, all the misses were on the high side, which arguably still represents a viable SS for targeted separation or at least a reasonable starting point. Chloroform-methanol based TLC SSs predicted one match and two misses with their corresponding ChMWat CCS SSs. Therefore, the general feasibility of this TLC and CCS correlation scheme needs to be further discussed, as follows: TLC-based prediction methodology is based on correspondence of polarities. In contrast, selectivity decides the resolution on TLC and in CCS. Although hydrophilicity/lipophilicity and selectivity are linked to each other, they are still distinct. Accordingly, a 100% rate in TLC-based CCS SS prediction is unlikely to be feasible. However, for a given analyte, if hydrophilicity/lipophilicity and selectivity stay constant, the hydrophilicity/lipophilicity prediction will hit a target SS which is at least suitable for an initial CCS trial.

When performing TLC screening for Rf values close to 0.5 using different CCS SSs, some analytes with extreme hydrophilicity/lipophilicity are unlikely to exhibit an Rf value close to 0.5, which makes prediction impossible. The ratio of analytes

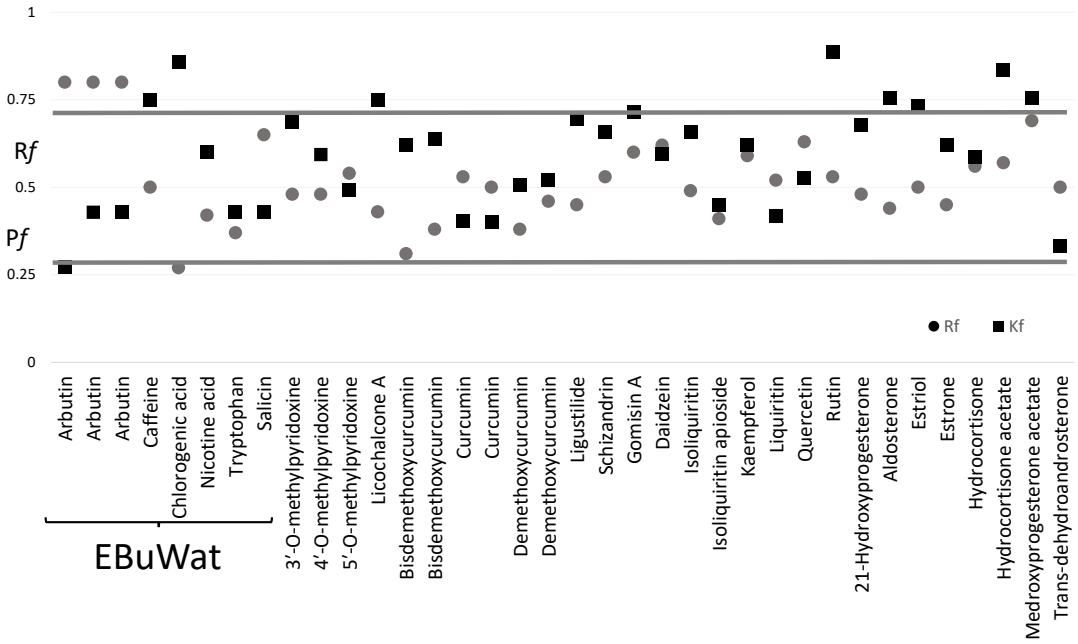

Figure 17. Rf (●) and K values (expressed as Pf values ■) for selected GUESSmix compounds in the SS(s) predicted by the GUESS method.
The 0.4 < K < 2.5 interval corresponds to 0.29 < Pf < 0.71. The actual values of the data points and SSs are given in TABLEs XII and XIII.

with Rf values near 0.5 to the total investigated can be defined as the prediction hit ratio. The hit ratio will reflect how many SSs need to be selected for any candidates. Once there is one SS matching the criterion, it can be considered as a candidate. The selected candidate SS should be used to determine K value using a partitioning experiment. If the K value is then located within the sweet spot range, a positive prediction can be obtained. If not, additional attempts with other SS families are required until a positive prediction can be achieved. The ratio of positive predictions to total candidates can be defined as the predictive rate. *The predictive rate is a suitable measure for the feasibility of TLC-based SS selection strategies*.

The ethyl acetate-*n*-butanol-water (EBuWat) SS family was investigated using

TABLE XV. TLC RF VALUES AND CORRESPONDING CCS K VALUES OF ADDITIONAL NATURAL PRODUCTS

Class	Analyte	Solvent system (v/v)	R*f*	K
Alkaloid[a]	3′ -*O*-methylpyridoxine	ChMWat 10:5:5	0.48	2.19
	4′ -*O*-methylpyridoxine	ChMWat 10:5:5	0.48	1.46
	5′ -*O*-methylpyridoxine	ChMWat 10:5:5	0.54	0.97
Chalcone[b]	Licocalcone A	HEMWat 4:6:5:5	0.43	3.00
Curcuminoid[b]	Bisdemethoxycurcumin	HChMWat 5:10:7.5:2.5	0.31	1.64
		HChMWat 3:7:7:3	0.38	1.76
	Curcumin	HChMWat 5:10:7.5:2.5	0.53	0.68
		HChMWat 3:7:7:3	0.50	0.67
	Desmethoxycurcumin	HChMWat 5:10:7.5:2.5	0.38	1.03
		HChMWat 3:7:7:3	0.46	1.09
Phthalide[b]	Ligustilide	HEMWat 9:1:9:1	0.45	2.27
Lignan[b]	Schizandrin	HEEtWat 5:5:5:5	0.53	1.92
	Gomisin A	HEEtWat 5:5:5:5	0.60	2.52
Flavonoid[b]	Daidzein	HEMWat 3:7:5:5	0.62	1.47
	Isoliquiritin	EAcWat 5:4:7	0.49	1.93
	Isoliquiritin apioside	EAcWat 5:6:9	0.41	0.82
	Kaempferol	HEMWat 4:6:5:5	0.59	1.63
	Liquiritin	EAcWat 5:6:9	0.52	0.72
	Quercetin	HEMWat 3:7:5:5		1.11
	Rutin	EBuWat 6:4:10	0.53	7.75
Steriod[a]	21-Hydroxyprogesterone	HEMWat 3:7:5:5	0.48	2.10
	Aldosterone	HEMWat 3:7:5:5	0.44	3.06
	Estriol	HEMWat 5:5:5:5	0.50	2.72
	Estrone	HEMWat 3:7:5:5	0.45	1.63
	Hydrocortisone	HEMWat 5:5:5:5	0.56	1.42
	Hydrocortisone acetate	HEMWat 4:6:5:5	0.57	5.11
	Medroxyprogesterone acetate	HEMWat 5:5:5:5	0.69	3.06
	Trans-dehydroandrosterone	HEMWat 5:5:5:5	0.50	0.50

[a] Represents the TLC eluent that was the equivalent organic-only SS based on HEMWat and ChMWat families, i.e. SSE or SSC; [b] means the TLC eluent that was the organic phase of the candidate biphasic SS.

the reversed prediction strategy. Although K values of polar GUESSmix components (Friesen and Pauli 2007) have been investigated using the EBuWat family (TABLE XIV), the TLC Rf information was absent. The polar GUESSmix components: caffeine, chlorogenic acid, nicotine acid, tryptophan, arbutin, and salicin had K values in the sweet spot for the EBuWat family SSs. The results shown in Figure 16 indicate that three of the eight SS and analyte pairs had both Rf and K values in the defined sweet spots. SS pairs for chlorogenic acid and arbutin had either Rf or K values outside of the sweet spot. The investigation of the GUESSmix compounds in three popular SS families, HEMWat, ChMWat, EBuWat, showed that the GUESS method is most effective for compounds in HEMWat SSs. Generally, HEMWat covers a range of compounds with lower hydrophilicity than ChMWat and EBuWat. Accordingly, the proposed Rf sweet spots may be applied to a broad range of SS polarities. In order to test different SSs with the GUESS method, we employed the "reversed prediction" strategy, which involved determining Rf values from compounds in SSs that had already been assigned K values as a result of partitioning studies and/or an actual CCS run. As a result, *n*-hexane-chloroform-methanol-water (HChMWat), ethyl acetate-acetonitrile-water (EAcWat), and *n*-hexane-ethyl acetate-ethanol-water (HEEtWat) were added to the previously investigated HEMWat, ChMWat, and EBuWat SS families. A cohort of 25 NPs representing seven NP classes (alkaloids, lactones, curcuminoids, lignans, chalcones, flavonoids, and steroids) were tested in 28 SSs representing six SS families (Figure 17 and TABLE XV). TLC plates were eluted with the organic phase of preequilibrated biphasic SS in which the K value of the analytes had already been determined.

The alkaloids 3′-*O*-methylpyridoxine, 4′-*O*-methylpyridoxine (ginkgotoxin), and 5′-*O*-methylpyridoxine are structural isomers. Ginkgotoxin was used to perform the prediction for this set of compounds by screening in both HEMWat and ChMWat SS families (Liu et al. 2014). ChMWat (10:5:5, v/v) placed all three isomers in both the TLC and CCS sweet spots and afforded a baseline separation (Liu et al. 2015). This is an example similar to the case of curcuminoids where placing the analytes of interest into the sweet spot also gave a reasonable separation. Ligustilide has been successfully purified in HEMWat 9:1:9:1 (Schinkovitz et al. 2008). The organic phase of this SS gives ligustilide an Rf value of 0.45 in silica gel TLC, indicating a good predictive match. Curcumin, desmethoxycurcumin, and bisdemethoxycurcumin were tested in a variety of HChMWat SSs (Inoue et al. 2008). These systems also showed matches between Rf and K sweet spots for these compounds. Schisandrin and gomisin were tested in HEEtWat SSs, and again gave matches between Rf and K sweet spots. This was the first time that this particular SS family has been used to separate these NPs. The chalcone, licochalcone A, was screened using the HEMWat family, and the organic phase of HEMWat 4:6:5:5 was found to give a 0.43 Rf value. Its K value in this SS was 3.00. Using the predicted SS in an actual CCS run yielded licochalcone A in a purity of > 95% when evaluated by qNMR. Collectively, these cases demonstrate the predictive power of the TLC/CCS sweet spot approach for this compound. The flavonoids, daidzein, kaempferol, and quercetin, were screened using HEMWat SSs as well. According to the results, the rutin separation was approached with EBuWat. The selected SS gave an Rf value a little above 0.5 and a K value above 7. Higher K values can be deemed superior to lower K values for effective separations of flavonoids (Liu et al. 2016) and other compounds. The

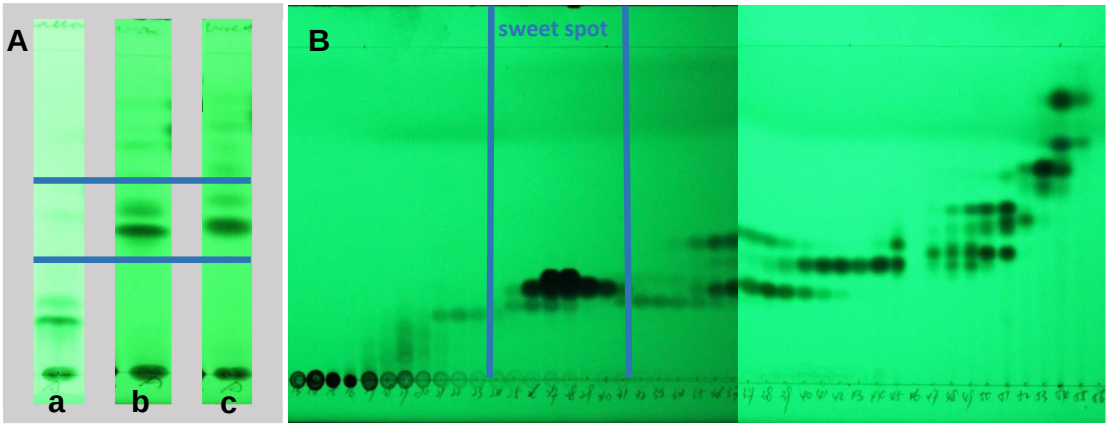

Figure 18. CCS results of a natural chemical matrix using TLC-based SS predict. (A) shows the screening procedure, in which the SS candidates are HEMWat (a) 6:4:6:4, (b) 5:5:5:5, and (c) 4:6:4:6 (v/v). (B) TLC monitoring results of a CCS run in HEMWat 5:5:5:5. Analytes with a K value of ~1 reside in fraction 28 (F28), representing one column volume. The test sample was 150 mg of an open HP-20 column methanol fraction from *Schisandra chinensis* extract. The TLC was developed with the organic phase of the HEMWat (5:5:5:5, v/v) SS.

flavonoids, isoliquiritin, isoliquiritin apioside, and liquiritin performed well in EAcWat SSs (Simmler et al. 2014). It is noteworthy that flavonoids are a class of compounds which has shown to be particularly amenable to CCS (Neves Costa and Leitão 2010).

Finally, a group of eight commercially available steroids were screened with HEMWat SSs. For all but one, the K values correlated with Rf values near 0.5 were matches with K sweet spots. This further supported the utility of the sweet spot validation. Interestingly 22 out of 28 Rf and K pairs had both values in the sweet spot. Notably, in all 6 "misses," the sweet spot Rf values correlated to K values above the upper limit of the accepted sweet spot (see Appendix C) and, therefore, still represented a viable CCS SS.

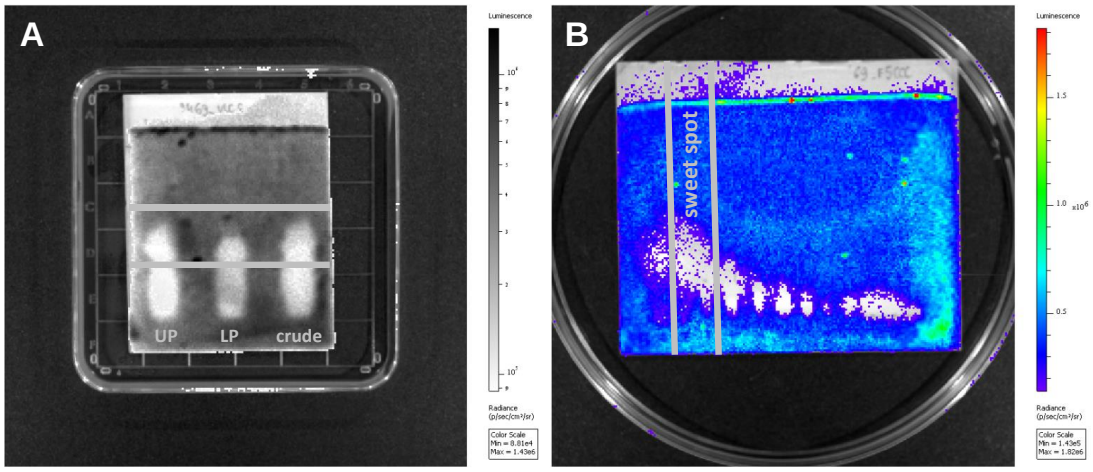

Figure 19. Exemplary bioautography application for TLC-based CCS SS prediction using *Mycobacterium tuberculosis* (Mtb) inhibition zone analysis. (A). This led to the resolution demonstrated in the bioautography of the CCS fractionation, B. UP designates the upper phase of the partitioning experiment; LP is the lower phase; and crude is crude extract.

In summary, six SS families, i.e., HEMWat, HEEtWat, HChMWat, ChMWat, EAcWat, and EBuWat, and 25 natural products (Appendix D) were investigated for the Rf sweet spot evaluation. Of 28 Rf and K pairs, TLC can predict a usable CCS SS for 22 compounds. In terms of hydrophilicity/lipophilicity, the great majority of these analytes would be considered as having moderately lipophilic range, which may also be a factor in their applicability to the GUESS method.

In NP research, analytes in extracts may be either known compounds or unknown entities. Targeted isolation of important known compounds from metabolic mixtures with CCS has been widely practiced for decades. For the known analytes, their spectral and/or chromatographic properties can be exploited to measure K values by partitioning experiments as well as via the GUESS method. Indeed, analytical methods such as HPLC-UV, fluorimetry, UV-vis, GC-MS, and NMR

have been used to quantitate compounds in partitioning experiments (Liu et al. 2015). The GUESS "normal prediction" method usually relies on the availability of reference standards. In addition, the GUESS method can also be performed with mixtures by tracking easily distinguishable TLC bands (Fan et al. 2016).

A chemistry focused approach, which attempts the targeted isolation of a particular analyte, is clearly insufficient for bioactivity-guided fractionation studies, because chemistry guidance does not correlate with biological guidance, meaning that the most easily identifiable analytes are likely not to be the ingredient of interest. In fact, restricting the search for target molecules to easily identifiable, most likely known compounds, defeats the actual purpose of a bioactivity-guided search. Moreover, using chemical methods to pursue biological targets creates incoherency between the methodology and the desired outcome. To overcome this disadvantage, a TLC-based bioautography method was introduced. The (HP)TLC-direct bioautography method was specifically developed in-house for the extremely slow-growing Mycobacterium tuberculosis, using the mc2 7000 lux ABCDE strain. This avirulent BSL-2 level strain contains a luminescence reporter as highly sensitive indicator of bacterial viability and does not require addition of reagents or further processing (Grzelak et al. 2016). The use of TLC both in the GUESS method and in bioautography to visualize bioactivity creates a seamless transition from chemical based fractionation to biological targeting. Bioautography linked with CCS provides for a bioactivity-guided fractionation methodology in which bioactivity is the main driving force of the overall strategies. The fact that CCS is essentially a loss-free separation technique further enhances its suitability for bioactivity-guided fractionation.

An example of the usefulness of the GUESS method for targeted isolation of analytes can be found in our recent work with *Schisandra chinensis* metabolites. Figure 18A shows the initial GUESS method exploration of a crude extract sample. A dark band occupies the Rf sweet spot for these TLC plates that were developed in the upper phase of the equilibrated HEMWat SSs 6:4:6:4, 5:5:5:5, and 4:6:4:6 (v/v), as seen by UV inspection at 254 nm. The subsequent HEMWat (5:5:5:5, v/v) CCS of the sample shows a likely major compound in the K value sweet spot shown on the TLC fractogram, along with other analytes closely related by hydrophilicity/lipophilicity (Figure 18B). Interestingly, the CCS reveals a greater sample complexity than the preceding TLC analysis, especially concerning analytes with lower hydrophilicity than the targeted region.

In the next step, the GUESS method was extended by adding the bioactivity evaluation using bioautography, a TLC-based bioactivity determination method. Bioautography can be used to directly screen for potential lead compounds, e.g., by revealing target analytes on the developed TLC plate that inhibit the bacterial growth and show inhibition zones. The combined GUESS plus bioautography method provides information regarding the optimal CCS SS needed for further chromatographic purification of the active principle(s). Sometimes, a more globalized search is required, i.e., more SS families need to be considered. Combined with bioautography, the TLC-based SS selection (GUESS) strategy can be applied without a predetermined reference or target compound. This establishes a chemically untargeted but biologically fully targeted approach. Thus, GUESS-based bioautography exhibits two major advantages: (i) the target prediction can be achieved without chemical reference and/or bias; (ii) CCS can be performed more

TABLE XVI. THE SCREENED CCS SOLVENT SYSTEMS FOR ANALYTES IN NADES AND THEIR RELATED TLC RESULTS

Rutin			Quercetin	Kaempferol	Daidzein
EBuWat	R*f*	HEMWat		R*f*	
5:5:10	0.59	3:7:5:5	0.63	0.73	0.62
6:4:10	0.53	4:6:5:5	0.36	0.59	0.37
7:3:10	0.41	5:5:5:5	0.20	0.37	0.21

readily, avoiding multiple partitioning experiments and *in vitro* assays. Figure 19A show the TLC plate of a crude Streptomycetes' sample along with its upper and lower phases after partitioning in the same SS. In the "crude" TLC, one part of the inhibition zone occupies the Rf sweet spot of the TLC plate developed in the upper phase of the SS. In a partitioning experiment (Figure 19A "LP" and "UP" lanes), the majority of activity around the Rf sweet spot was present in both the LP and the UP. According to the intensities of the inhibition zones, the corresponding K value(s) of the target analyte(s) should be close to 1. While the majority of activity tends to be present in the organic lower phase (sweet spot part in Figure 19B), the range of Rf values for target analytes suggests that the SS may be suitable for CCS. The TLC monitoring of the CCS fractionation in Figure 19B demonstrates the affinity of the activity for the organic phase, along with a reasonable separation of active components into discrete fractions. While further results from this ongoing anti-tuberculosis drug discovery project will be reported in due course, the present results demonstrate already the utility and feasibility of GUESS-guided bioautography.

Overall, 43 natural products and six SS families were involved in this study,

providing coverage for a substantial range of natural product hydrophilicity/lipophilicity and CCS application space. The results showed that out of 62 correlations, 45 (predictive ratio, 73%) had both Rf and K values in their respective sweet spots. This confirms the fitness of the GUESS method as a semi-empirical methodology with good predictive potential for the combinations of analytes and solvent systems investigated. While the determination of the K value(s) of each target analyte prior to a preparative CCS run is desirable especially in cases of the targeted isolation of known compounds, a TLC-based SS prediction methodology provides a straightforward technique to greatly accelerate CCS SS selection and to foster the usability of CCS for novice practitioners. In conclusion, the GUESS concept is capable of the rapid approximation ("GUESSing") of SSs and CCS experimental conditions for any separation problem that can be examined by TLC.

3.3.2. Practice of Rf Value Sweet Spots in NADES Studies

GUESS approach has been used for this practice (Schinkovitz et al. 2008). The equivalent organic-only SS is a variant of the organic phase of the solvent system, which facilitates preparation of the TLC eluent and conserves solvent. As no equivalent organic-only solvent has been developed for the EBuWat solvent system family, the organic phases of the candidate systems were used.

The Rf value of each target analyte was determined using each candidate solvent system, and the results are listed in TABLE XVI. Considering the high hydrophilicity of many NADES components, if a SS delivers the analyte in or near the K value sweet spot, the analyte will be recovered quantitatively from the NADES matrix. It should be noted that a better resolution can be achieved if the Rf value of the target

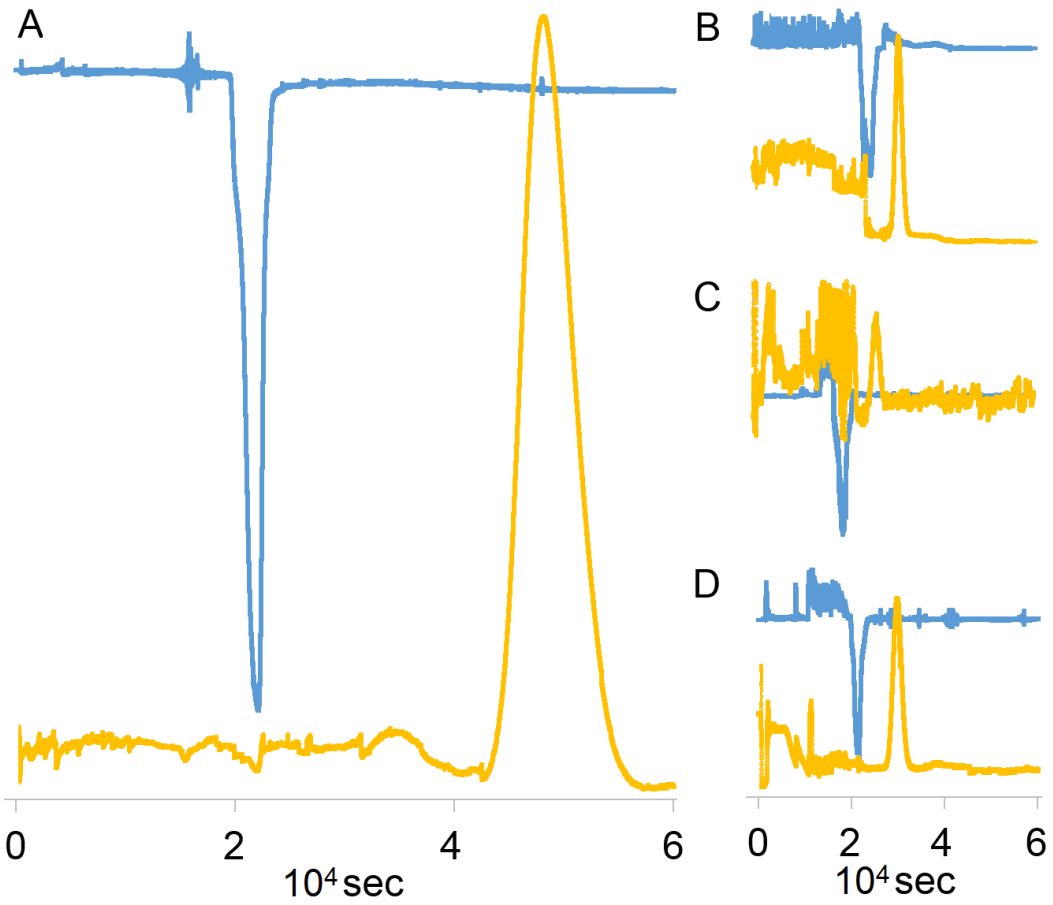

Figure 20. The Real time parameters (UV and PMA value) were determined by the CherryOne instrument.
The four plots (A, B, C and D) originate from different CCS operations. A shows the behavior of GCWat-rutin solution in EBuWat (6:4:10, v/v). B reflects the behavior of GCWat-quercetin solution in HEMWat (3:7:5:5, v/v). C that of GCWat-kaempferol solution in HEMWat (4:6:5:5, v/v) and D the behavior of GCWat-daidzein solution in HEMWat (3:7:5:5, v/v). The dispersion signals represented PMA detection in blue, and the absorption peaks represent UV absorption in yellow. The x-axis reflects the separation time.

analyte is > 0.5, with the target analyte favoring the organic phase. This approach was used for SS selection for all test compounds. According to TABLE XVI, the CCS SSs were selected as follows: EBuWat (6:4:10, v/v) for rutin, HEMWat (3:7:5:5, v/v) for quercetin and daidzein, and HEMWat (4:6:5:5, v/v) for kaempferol.

3.3.3. Compatibility Studies

Due to the high viscosity of the NADES, one of the main concerns was the potential blockage of the CCS column by a "NADES pulp" that could be potentially formed as a result of NADES enrichment. In order to assess this possibility, compatibility studies were performed prior to the actual CCS' fractionation of the target compounds. Partitioning experiments evaluated the fluidity of the solutions. GCWat was dissolved in the selected SSs HEMWat (4:6:5:5, v/v), HEMWat (3:7:5:5, v/v), and EBuWat (7:3:10, v/v), respectively. In all tests, 100 µL of GCWat was mixed with 200 µL of each upper and lower phase. No precipitation of particles from the partitioned solution occurred. The viscosity of the solution was clearly lower than that of GCWat alone. Due to the hydrophilicity of GCWat, the volume ratio of lower to upper phase was close to 3:2 after partitioning. This evidence matched what could be predicted from the K values of NADES components, which were close to 0 in all of the tested SSs. Next, a series of CCS trials were performed in a 16 mL high-speed countercurrent chromatography (HSCCC) instrument. GCWat (100 µL) was dissolved in equal volumes of upper and lower phase (200 µL of each), which yielded the trial sample that was loaded into the sample loop (2 mL). All three selected SSs were tested. The whole CCS operation worked, and the pressure remained at a low level (<18 psi). In all SSs, the K values of GCWat were close to 0 in a reversed phase (lower phase mobile) mode. Based on these results, a mixture of upper phase, lower phase, and a GCWat solution of the test sample (2:2:1, v/v) was used for sample loading in subsequent studies. The components of GCWat showed a characteristic dispersion signal (Figure 20) when monitored by the Phase Metering Apparatus (PMA) of the CherryOne instrument, thus allowing the targeted collection and

TABLE XVII. THE SOLVENT SYSTEMS SELECTED FOR THE CCS RECOVERY OF THE TARGET METABOLITES FROM NADES SOLUTIONS AND THEIR K VALUES

Target analyte	Solvent system	*K* value
Rutin	EBuWat 6:4:10	7.75
Quercetin	HEMWat 3:7:5:5	1.11
Kaempferol	HEMWat 4:6:5:5	1.63
Daidzein	HEMWat 3:7:5:5	1.47

TABLE XVIII. UHPLC CONDITIONS FOR THE TARGET METABOLITES

Sample	Water (%)	ACN (%)	Wavelength (nm)	Flow rate (mL/min)	Retention time (min)
Rutin	90	10	350/254	0.4	4.9
Quercetin	85	15	350/254	0.4	6.9
Kaempferol	80	20	350/254	0.4	5.4
Daidzein	85	15	300/254	0.4	4.6

recovery of GCWat. Furthermore, as the NADES components represent hydrophilic and/or ionic molecules, it was conceivable that they might break the equilibration of the biphasic CCS SSs. This was assessed by real time monitoring of the stationary phase volume retention ratio (Sf) using the CherryOne system (Pauli et al. 2015). The results showed that the Sf values were constant during the CCS operation (data not shown), indicating that NADES has no detrimental effect on CCS SS performance.

3.3.4. Recovery of Flavonoids from a NADES Matrix via HSCCC

Small-volume (16 mL) CCS was used for the recovery study. The K values of the

target analytes were all above 1 as predicted by the GUESS approach for the chosen SSs (TABLE XVII). This is consistent with the discussion in Section 3.2. Accordingly, CCS was successfully performed to individually recover the target analytes from the NADES-analyte matrix. As mentioned above, the CherryOne PMA can detect ions or polar NADES components during CCS elution. Additionally, as all target analytes showed UV absorption to this wavelength (TABLE XVIII), the UV detector in the CherryOne system (Pauli et al. 2015) was set at 254 nm. The whole CCS operation was monitored by both the PMA and the UV (Figure 20). The K values were also recorded by the CherryOne system (data not shown). Guided by the PMA and UV absorption values, GCWat and the target analytes were well separated (Figure 20). GCWat and the target metabolites were then collected into separate fractions. Furthermore, after drying of the fractions by vacuum centrifugal evaporation, the GCWat-containing fraction still retained the viscous liquid characteristics of NADES. The target-metabolite-containing fraction could also be recognized by the presence of a yellow-colored solid residue. Additional qualitative and quantitative analyses focusing on both fractions were also performed, as follows.

3.3.5. Recovery Determination

Two identical aliquots (100 µL) of each of the GCWat-test-sample solutions were used for the determination of analyte recovery. One aliquot (100 µL) was subject to CCS and the fractions were evaluated by quantitative ^{1}H NMR (qHNMR). The other aliquot was used as a quantitative (100%) reference control and directly analyzed by qHNMR, without CCS. When the aliquot from CCS and the control aliquot were dissolved in DMSO-d_6 (600 µL), the volume of each solution was measured precisely using a 1000 µL analytical syringe. Otherwise, sample preparation procedures and

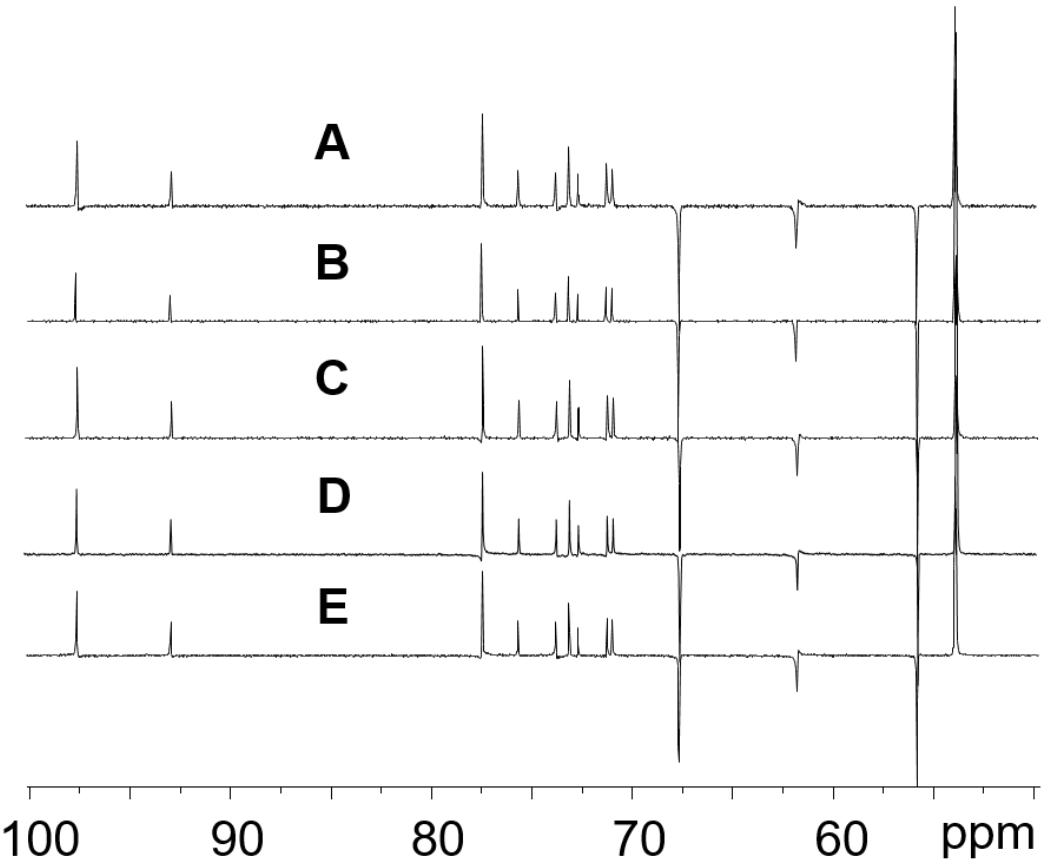

Figure 21. DEPT-135 NMR spectra of the GCWat containing fractions from different recovery studies.
A to D are the GCWat containing fractions from different NADES-test sample solutions. A was from the GCWat-rutin matrix, B from the GCWat-quercetin matrix, C from GCWat-kaempferol and D from the GCWat-daidzein matrix. E was the standard GCWat sample.

NMR instrumentation were the same as described above, including the parameters of the qHNMR analysis.

3.3.5.1. Characterization of the GCWat containing-fraction

The GCWat-containing fraction was dissolved in DMSO-d_6 for DEPT-135 NMR analysis (Figure 21). Compared to unprocessed GCWat, the data demonstrated that the NADES-containing fractions consist of both glucose and choline chloride. This

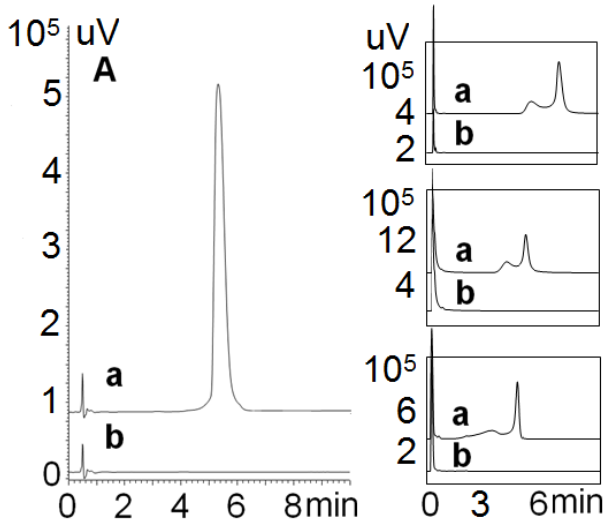

Figure 22. UHPLC results on GCWat containing fractions from different recovery studies. In the chromatograms, (a) represents the reference standard sample whereas (b) is the GCWat containing fraction. The GCWat containing fractions A, B, C, and D were recovered from the rutin-GCWat, quercetin-GCWat, kaempferol-GCWat, and daidzein-GCWat solutions, respectively.

is consistent with the high hydrophilicity of both glucose and choline chloride. Under the chosen CCS conditions, the K values of the two components are nearly identical, explaining why they are not separated and co-occurred in one fraction. The strong, highly ordered hydrogen bonding among the GCWat components (Figure 9) also explains why GCWat components consistently form a liquid. Moreover, this supports the hypothesis that NADES such as GCWat can form larger structures such as liquid crystals, which could affect the solubility and stabilizing ability of NADES species. Depending on the size and shape of the liquid crystals, NADES may also produce micro- or even nano-particles of the lipophilic constituents (Ma et al. 2016). This mechanism may increase further the solubility of

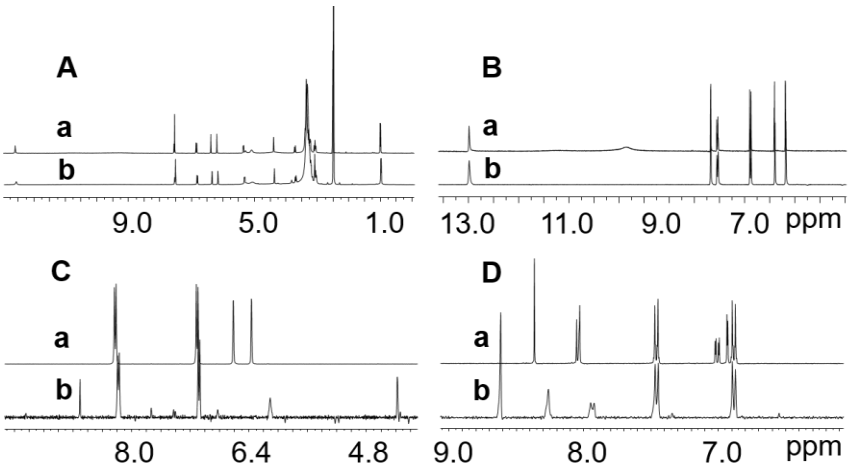

Figure 23. ^{1}H NMR spectra of target metabolite containing fractions from different recovery studies. In the spectra, (a) represents the standard reference sample, whereas (b) is the fraction containing the test sample. A, B, C and D represent the four investigated cases of rutin, quercetin, kaempferol and daidzein, each in GCWat, respectively.

lipophilic molecules in physiological and similar environments, such as *in vitro* assays. Furthermore, due to reduced aqueous solubility, any lipophilic lead compounds are transported from the lipophilic cellular membranes to hydrophilic extracellular fluids at a slower rate. Meanwhile, protein binding in extracellular submucosal tissue can cause lower compound permeability.

Collectively, these effects represent major challenges in small molecule absorption (Artursson et al. 2001; Lipinski et al. 2001). As NADES and NADES-like components are abundant in crude botanical extracts, lipophilic components can be loaded into a hydrophilic environment. It is very conceivable that this has a potential impact on the pharmacokinetic behavior of lipophilic metabolites. The unusual solubilizing power of NADES for a wide range of NPs and their lipophilicity/hydrophilicity duality suggest a unique role for NADES in small

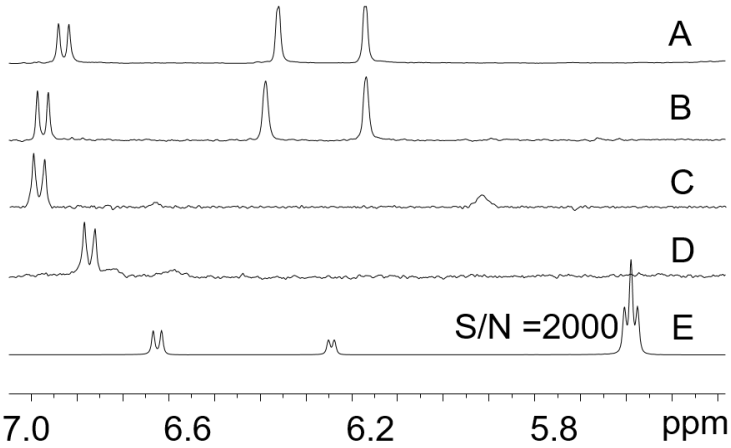

Figure 24. Target-compound-containing fractions from different recovery studies were detected by qHNMR. The recovered compounds were rutin (A), quercetin (B), kaempferol (C), and daidzein (D). E represents a reference sample of GCWat.

molecule formulation. This behavior may represent the desired property responsible for the inherent advantage of crude herbal BDSs and traditional medicinal preparations over modern single compound formulations.

UHPLC analyses (TABLE XVIII) showed that the GCWat containing fraction did not contain traces of the target analytes (Figure 22). This clearly demonstrated that CCS offered highly efficient separation of the target analytes and the NADES, and allows a quantitative (full) recovery of the target analyte from NADES matrices.

3.3.5.2. Characterization of the target-analyte-containing fraction

The target-analyte-containing fractions were further characterized by ^{1}H NMR (Figure 23) and compared with reference standards of the same analytes. The GCWat components were completely absent from the target analyte containing fractions (Figure 24). As shown in Figure 24E, the signal at 5.591 ppm (CH_2 of choline chloride) had a signal to noise ratio of 2000. In contrast, none of the recovered

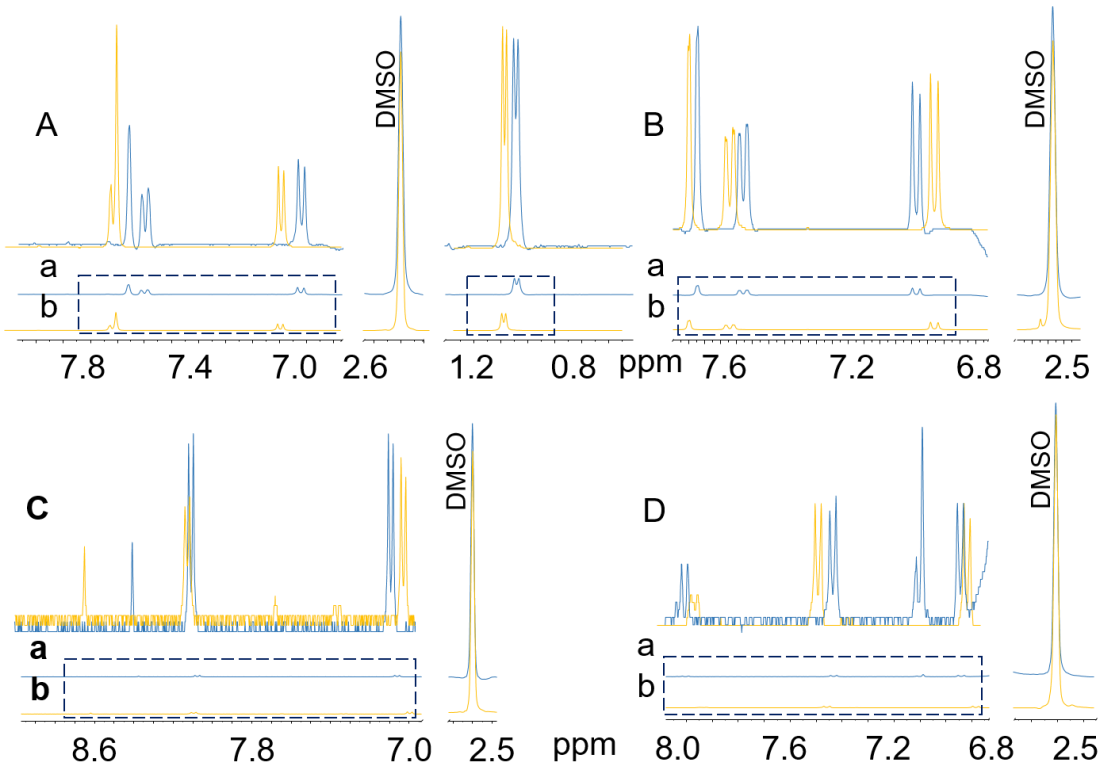

Figure 25. The qHNMR spectra used for calculation of the recovery rate (%) using the residual DMSO solvent signal (DMSO-d_5) area as internal calibrant.
(a) shows the aliquot positive control, in blue. (b) the recovered test sample, in yellow. A, B, C and D represent rutin, quercetin, kaempferol, and daidzein, respectively.

samples (Figure 24A, B, C, and D) showed such a signal. The recovery of NADES was > 99% in all CCS runs. The same result can be calculated based on the signals of glucose at 6.238 ppm and 6.625 ppm. The results from the CherryOne system (PMA and UV at 254 nm), UHPLC, ^{1}H NMR, qHNMR, and ^{13}C NMR combined with all signals of NADES components, indicated that the target analyte was recovered completely from the NADES-analyte matrix. As a nondestructive and near universal detection method, qHNMR is ideal for quantitative analysis. Because it is a mole-based determination, qHNMR does not need an identical, high purity, calibrant for

the establishment of a standard curve (Liu et al. 2014).

Additionally, based on the UHPLC results, there was a small peak with a close retention time and a major absorption (Figure 22B, C and D). This may be caused by a low flow rate or a high loading concentration. The potentially compromised specificity of UHPLC was avoided by the use of qHNMR, which was applied to quantify the recovery of each target analyte from the GCWat-analyte solution. The externally calibrated (EC) DMSO-d_5 residual solvent signal area was used as the internal calibrant (IC). The qHNMR sample preparation and acquisition parameters were identical for all samples. Because the GCWat-test analyte solution had a high GCWat concentration, the receiver gain was set to a low level (14.3). The resulting signal areas corresponding to the test sample were normalized to the internal calibrant area (Figure 25). Because qHNMR provides a molar ratio, the volumes of the solutions were also involved into the recovery calculation. The recovery of each target analyte was calculated by Equation 8, and the results were as follows: rutin, 95.7%; quercetin, 94.6%; kaempferol, 97.0%; daidzein, 96.7%.

Equation 8: $R = \frac{Int\ post-CCC \times Vr}{Int\ pre-CCC \times Vs} \times 100\%$

where $Int_{post\text{-}ccc}$ is the signal area of the recovered sample, $Int_{pre\text{-}ccc}$ is the signal area of the aliquot positive control, Vr is the volume of the dried recovered sample dissolution in 600 μL of NMR solvent, Vs is the volume of the aliquot positive control dissolution in 600 μL of NMR solvent, and R represents the recovery (%).

3.3.5.3. Evaluation of the Recovery Study

Performed in reverse phase mode, CCS showed a high separation resolution and was capable of recovering target analytes (95%-99%) from NADES matrices. The

TABLE XIX. THE RF VALUES OF LICOCHALCONE A ELUTED USING ORGANIC PHASE OF CCS SS

Countercurrent separation solvent system (v/v)				R*f* values
n-Hexane	EtOAc	MeOH	Water	
5	5	5	5	0.25
4	6	5	5	0.43
3	7	5	5	0.68

"sample loss" may be caused when the sample/NADES solution was prepared or where the NADES solution was injected into CCS instrument. The syringe used to transfer NADES solution is solid material that can absorb NADES solution to a certain degree. Thus, it may cause "sample loss". However, a solid-based chromatography would have such "sample loss" as well. Compared to solid-based chromatography, > 95% recovery yield from CCS indicates that liquid-only chromatography CCS is still a better option to implement a "full" recovery experiment in practice. While NADES cover a comparatively broad K value range (Figure 20), potentially causing a low separation resolution, this was not the limitation in the present study. In NP research, the extract matrix often contains metabolites that are dispersed in a very broad range of K values. The target compounds of interest are typically not expected to overlap in their K values with those of NADES. However, in reverse phase mode, a small-volume CCS may still not achieve the desired separation in some cases. There are two possible solutions to this issue. (i) A normal phase mode separation can be performed, using the organic phase as mobile phase. Under these conditions, NADES will stay in the tail

of the elution because of their high affinity for the aqueous stationary phase, which is far away from the desired K values of the target compounds. Once an appropriate SS is found for the target NPs, a highly sufficient K value range will be available for the target analytes. (ii) A larger scale of CCS can be employed. As a given analyte has a constant K value in a specific SS, CCS can be scaled up linearly and beyond the small-volume scale, based on the needs of a specific project. E.g., a medium

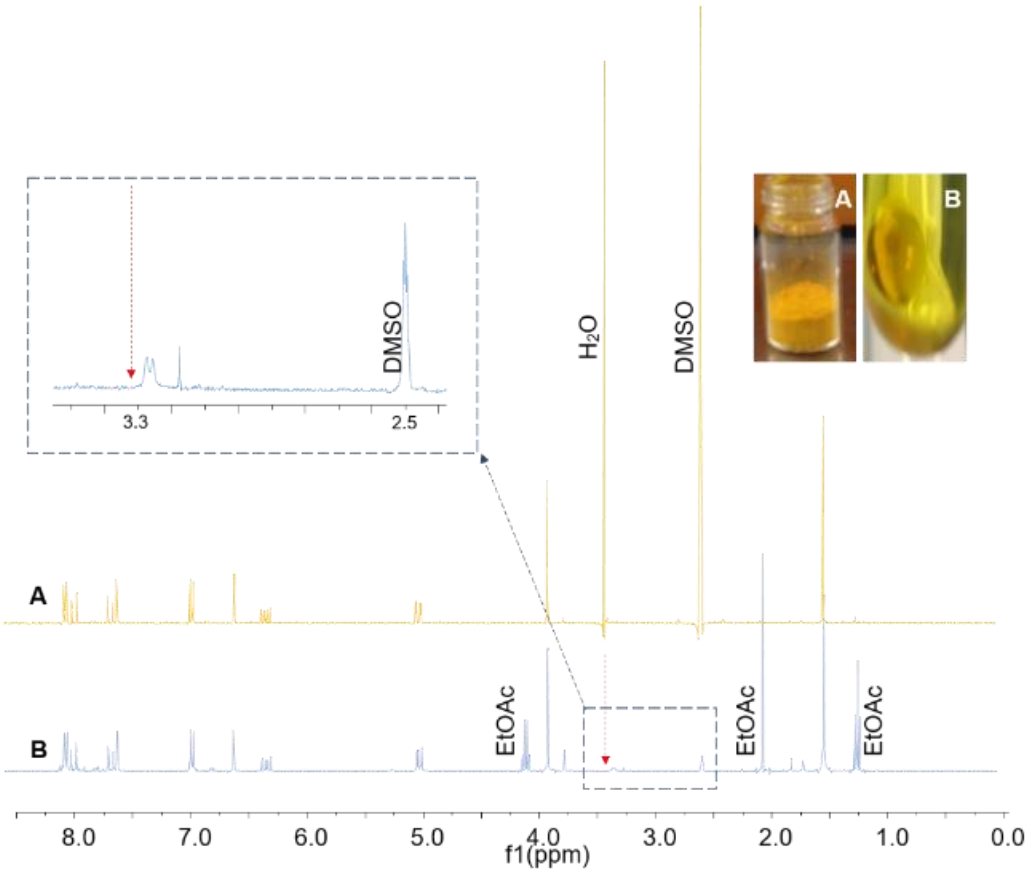

Figure 26. The qHNMR analyses of the licochalcone A samples. Highly pure licochalcone A (A) and licochalcone A purified using countercurrent separation (B) in DMSO-d_6 using a 60 s relaxation delay (D1). The insert images are the physical appearance of corresponding samples.

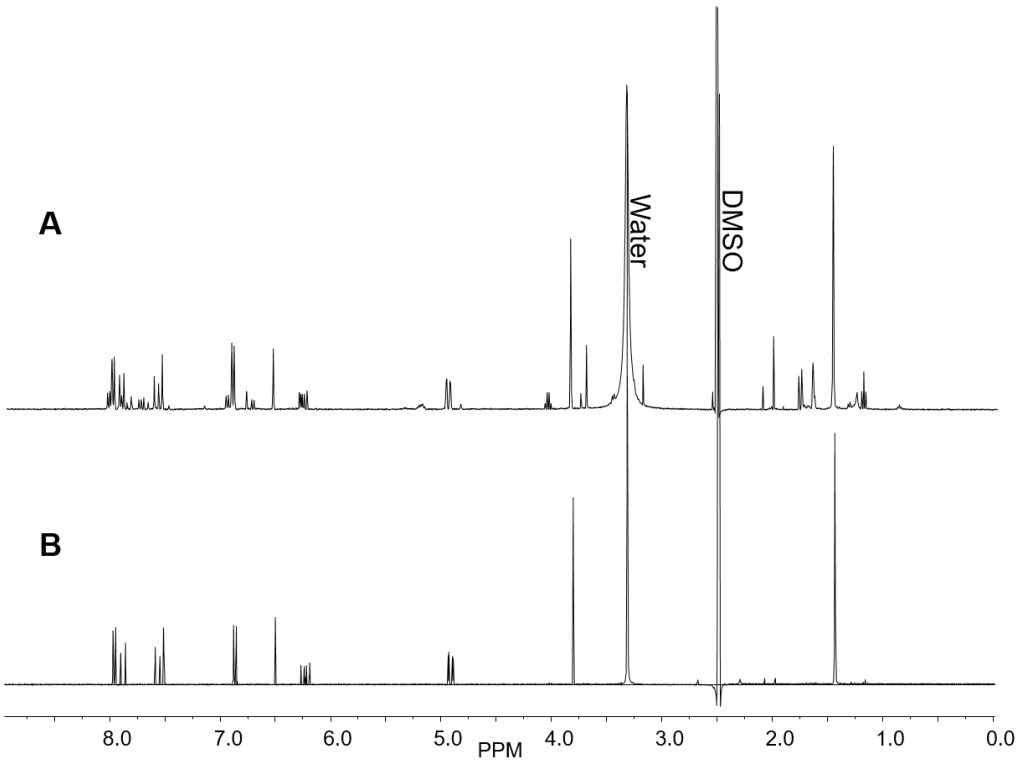

Figure 27. Comparison of achieved purity of licochalcone A when isolated via CCS using different SSs:
SSs (A) *n*-Hexane-chloroform-methanol-water (HChMWat, 5:6:3:2, v/v); (B) HEMWat (4:6:5:5, v/v) using the same small scale of CCS instrument (16 mL HSCCC).

capacity (~320 mL) CCS can increase the separation resolution beyond the small-volume scale, because the medium CCS provides more theoretical plates in practice (Liu et al. 2015). However, either normal phase mode using small-volume CCS or a medium capacity CCS will increase the amount of solvents consumed and the time of the separation cycle. Therefore, prior to a CCS operation, an appropriate operation mode and scale should be carefully selected.

3.4. Standardization of NADES Components in Herbal Sources

Glycyrrhiza glabra (DNA bar coding verified) and *Schisandra chinensis*, are

TRMs that are popularly adopted in the BDS market (Simmler et al. 2015). The NADES components in the two herbal sources were characterized in this study. Following USP protocols, crude extracts (200 mg) of *G. glabra* and *S. chinensis* were prepared in house.

G. glabra was authenticated in a previous study (Simmler et al. 2015). Licochalcone A is one of major compound markers in *G. glabra*, and the two most abundant metabolites (or NADES components in *G. glabra* extracts) are sucrose and proline, which can also be considered as marker compounds. On one hand, this presents a specific study about the purification of licochalcone A via CCS. Due to the essential absence of sample loss, CCS was implemented for the isolation of licochalcone A from the *G. glabra* extract, as follows: TLC-based solvent system strategy (Rf value ~ 0.5) was performed (TABLE XIX), with the result that the organic phase of *n*-hexane-ethyl acetate-methanol-water (HEMWat, 4:6:5:5, v/v) delivered licochalcone A to a TLC Rf value of 0.43. This suggested that the corresponding CCS SS may deliver the target analyte into a sweet spot range (K value from 0.25 to 4). Regarding evaluation of the selected SS, a small scale of CCS instrument (16 mL HSCCC, Tauto Biotech, China) was used. Compared to a reported SS (HEMWat, 5:6:3:2, v/v, Figure 26A), the selected SS (Figure 26B) achieved a higher purity, 95%. The K value of licochalcone A in the solvent system was 3.

Interestingly, the following phenomenon was recognized in a few CCS fractions: when the fractions were concentrated using vacuum evaporation (16 h, at 37°C and under vacuum in a centrifugal vacuum evaporator), as shown in Figure 27, the dried material showed that the sample held a physical eutectic appearance, and contained two major components: licochalcone A and EtOAc.

The molar ratio of licochalcone A to EtOAc as determined by qHNMR was close to 1:1. Although some minor impurities can be identified as well, the molar ratio of the licochalcone A (or EtOAc) to any impurity was over 7:1 (mol/mol) determined using qHNMR. When the licocalcone A signal (CH) integral of δ 7.5303 ppm was normalized as 1, impurity integrals of (CH) signals of δ 5.0000 to 8.0000 ppm were all < 0.13; those (CH_2 or OCH_3) of δ 3.0000 to 5.0000 ppm were all < 0.31; those (CH_3) of δ 0.0000 to 3.0000 ppm were all < 0.31. The low abundance of the impurities

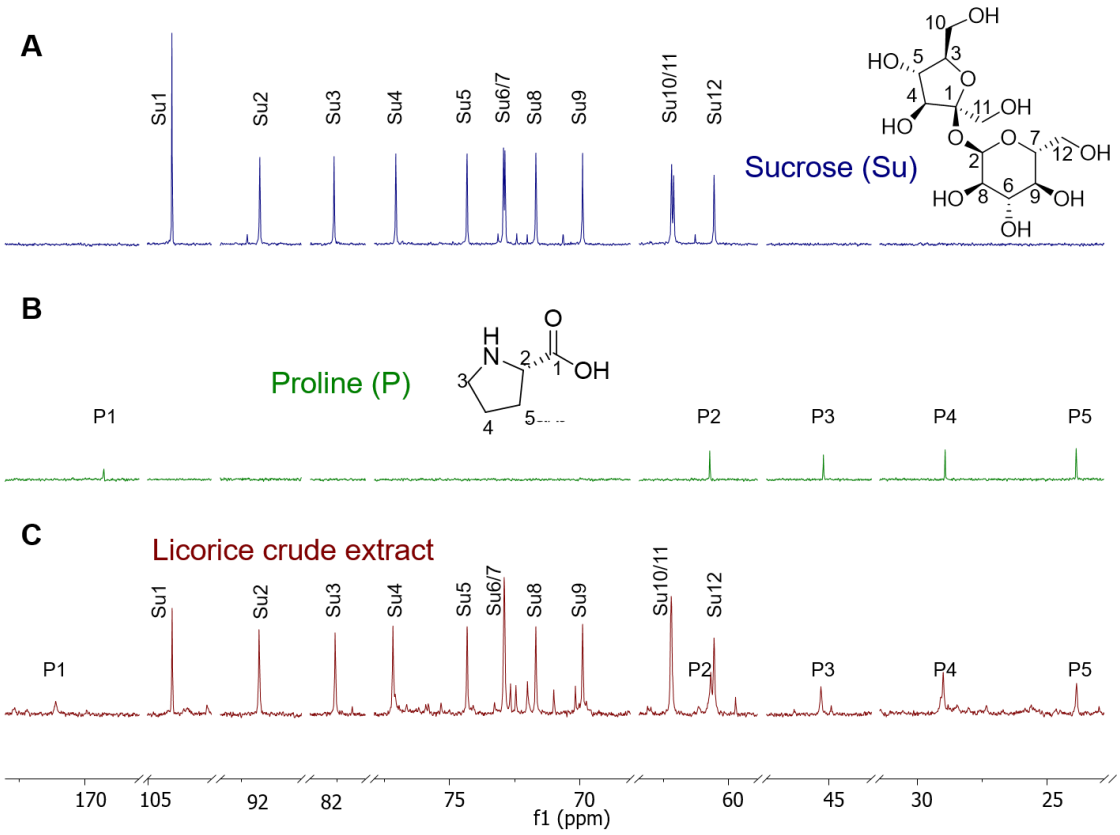

Figure 28. The ^{13}C NMR characterization of sucrose and proline in *G. glabra* crude extract. The comparison is of commercialized products, sucrose (A), proline (B), and *G. glabra* crude extract (C).

makes it unlikely that they serve as eutectic components (see also the section on Ratio of NADES Components). Prior to vacuum evaporation, the sample mainly contained licochalcone A, *n*-hexane, EtOAc, MeOH, and water. However, except for EtOAc, the other solvents including MeOH and the low volatile water were not observed in the concentrated sample. Considering that water has a higher evaporating point than EtOAc, this eutectic system may be caused by a similar hydrophilicity/lipophilicity (e.g., electrostatic force) between licochalcone A and EtOAc. This confirms that some organic solvents (such as 1,3-propanediol, EtOAc, and BuOH) used in NP studies may also serve as eutectic components (García, et al. 2014). Potentially, this behavior may influence the properties of the target analytes, such as solubility, stability, and pharmacokinetic properties. In the general practice of NP research, this phenomenon broadens more attentions.

In another study, sucrose and proline in *G. glabra* crude extract (52.4 mg) were also characterized via qCNMR with assistance of the relaxation reagent, 35 mM $Cr(acac)_3$ in 200 µL of $CDCl_3$ (Figure 28). The JEOL 400 instrument was used, and the parameters were as follows: D1, 2 s; NS, 12288; AQ, 1 s; and RG, 46. The qCNMR shows that sucrose and proline are marker compounds in licorice, consistent with the previous study (Simmler et al. 2015). Moreover, all signals of sucrose (Su 1-12 in Figure 28) and most signals of proline (P1-4 in Figure 28, except the P1 whose S/N is 7) can achieve a proper S/N ratio (> 10, e.g., S/N of Su2 was 38 and S/N of P5 was 14) for quality control analyses. The molar ratio of sucrose (average integral, 1.05 of Su 1-12 in Figure 28, normalized integral of Su1 signal as 1) to average integral (0.52) of proline (P1-4 in Figure 28) in licorice sample was 2:1 (mol/mol), i.e., 22.95 mg of sucrose and 3.82 mg of proline. Sucrose and proline accounted for 51% of the

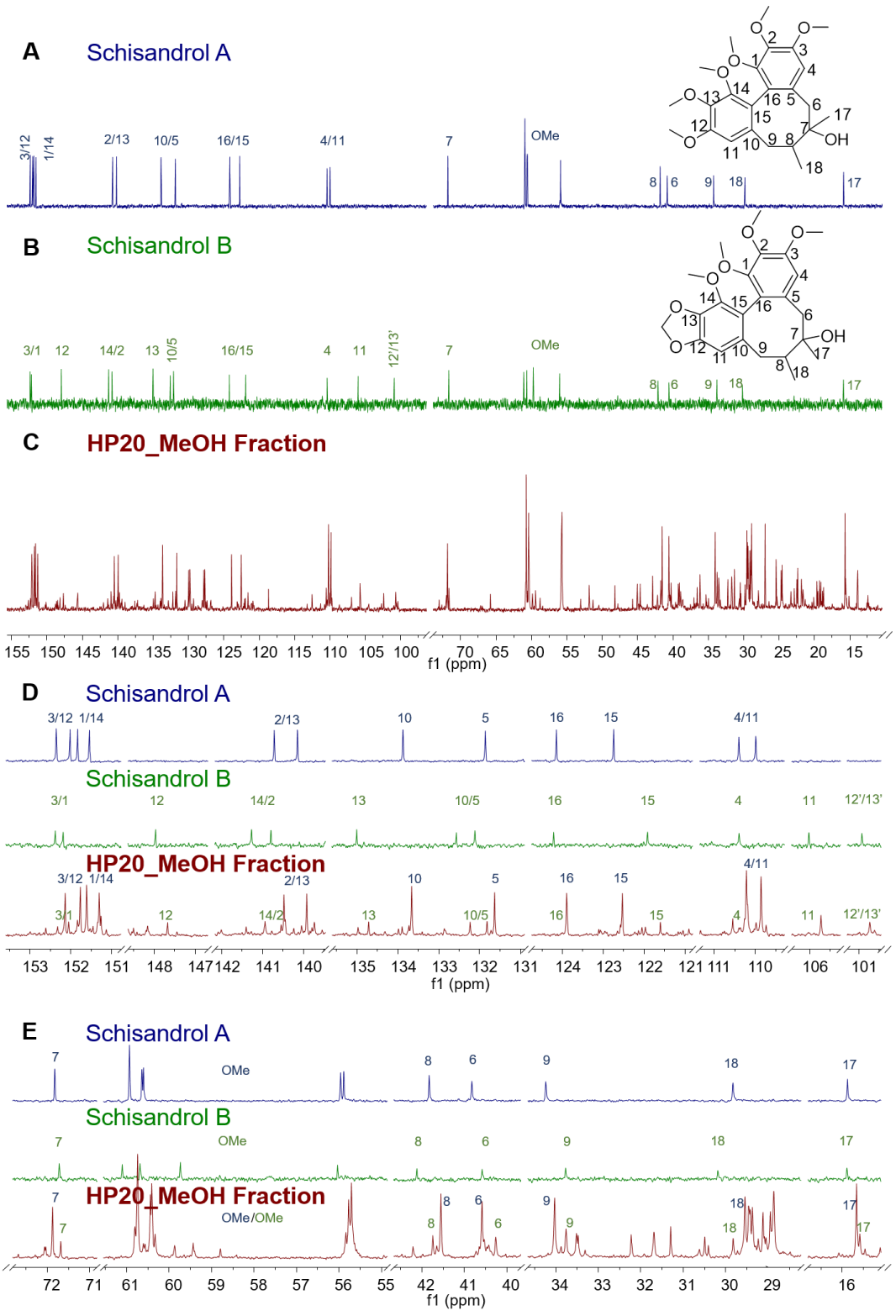

Figure 29. The ^{13}C NMR analyses of MeOH fraction of *S. chinensis* fruit extract via HP-20 resin column. (A) schisandrol A (B) schisandrol B (C) the HP-20 MeOH fraction, where the S/N of samples (A) and (B) were both over 10:1. (D) and (E) are expansions of (A), (B) and (C).

licorice crude extract.

As reported, *S. chinensis* fruits produce two major compound markers (schisandrol A and schisandrol B), as well as an abundance of organic acids (Bai et al. 2015). Thus, characterization of these marker compounds was performed initially. After concentrating the extract solution, the physical appearance of the obtained crude extract was highly viscous, suggesting that a NADES medium was present. Due to the hydrophilicity of organic acid-based NADES species, most of these NADES components should be very polar. Thus, the crude extract of *S. chinensis* fruits was fractionated using an HP-20 resin column. The bed volume (BV) of the resin column was measured as 1500 mL, and thus, the elution volume of each fraction was set to 10 L. 105 g of methanolic extract of *S. chinensis* was loaded on the HP-20 column. The order of elution was as follows: water, 25% MeOH, MeOH, and acetone. The flow rate was 20 mL/min during the day (12 h), and 4 mL/min during the night (12 h). All fractions were concentrated using a rotary evaporator at 37°C under vacuum. The total recovery yield was 95.3%, specifically as follows: water fraction (83 g, 79%); 25% MeOH fraction (4.71 g, 4.4%); MeOH fraction (11.73 g, 11.2%); acetone fraction (0.247 g, 0.2%). The MeOH fraction, a 38.7 mg sample, obtained from the HP-20 resin column, which was expected to contain the compound markers and was used directly for the characterization of schisandrols A and B via qCNMR with 35 mM $Cr(acac)_3$ in 200 µL of $CDCl_3$. Figure 29 shows that schisandrol A (1.12 mg) and schisandrol B (0.31 mg) are two major lipophilic metabolites (or compound markers) in *S. chinensis* fruits. The molar ratio of schisandrol A to schisandrol B was 3.63:1.00. The qCNMR analysis can be acquired in a reasonable amount of the time for a S/N ratio (> 10) for quality control analyses.

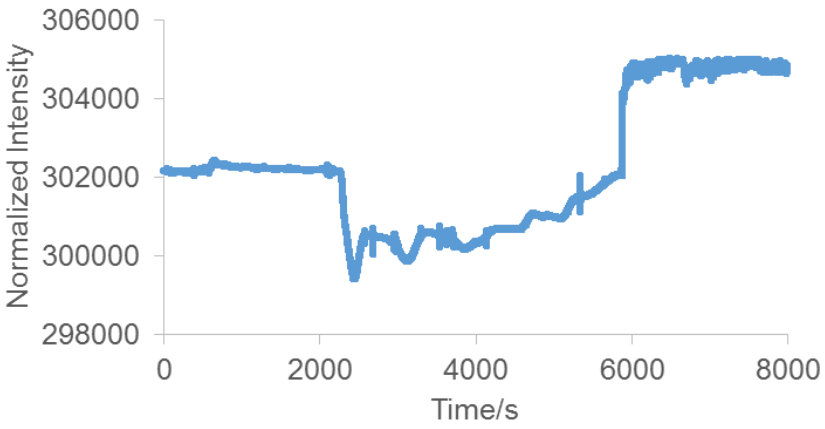

Figure 30. The real-time PMA chromatogram of the CherryOne instrument. It shows the behavior of HP-20 water fraction of *S. chinensis* fruit methanolic extract in EBuWat (6:4:10, v/v). The dispersion signals indicate the elution of NADES constituents which represented PMA values and the x-axis exhibited the operation time. The aim was to evaluate the potential CCS SS in a small volume HSCCC instrument (16 mL).

The parameters are D1, 2 s; NS, 12288; AQ, 1 s; and RG, 46. Thus, *S. chinensis* fruits were chemically analyzed.

The polar NADES ingredients were expected to be enriched in the HP-20 water fraction, so this sample was prepared for a further isolation and characterization by CCS. In a previous study (Liu et al. 2016), a CherryOne system within a phase metering apparatus was implemented to detect the NADES matrix constituents in real-time during the elution of CCS. Regarding the recovery of lipophilic molecules from the NADES matrix, a highly polar SS (EtOAc-*n*-BuOH-water, 7:3:10, v/v) was applied for pursuit of a higher separation resolution. In practice, a small scale (16 mL) HSCCC was performed for evaluation of the candidate SS. With assistance of the phase metering apparatus, significant negative signals were monitored in the

chromagraphic profile (Figure 30). This was used as an indication that the real-time elution may contain ionic NADES or NADES components. For preparative and characterization purposes, the CCS was scaled up using a larger scale (300 mL) HSCCC instrument (Pharmtech, USA), which in theory improved the separation resolution further. Specifically, the stationary phase volume retention ratio (Sf value) was 75%, and extrusion was applied after one total column of elution, i.e., reading a partition coefficient of K = 1. All CCS fractions were concentrated within a speed vacuum instrument and characterized by NMR. The results showed that at least two reported NADES components, i.e., malic acid and citric acid, were isolated have been recognized as NADES components (see Appendix E).

4. RESEARCH AIM 2: THE ROLE OF NADES IN SOLUBILIZING NATURAL PRODUCTS

(Previously published as Liu Y., Zhang Y., Chen, S.N., Friesen J.B., Nikolić D., Choules M.P., McAlpine J.B., Lankin, D.C., Gemeinhart R.A., and Pauli, G.F. (2018) The influence of natural deep eutectic solvents on bioactive natural products: studying interactions between a hydrogel model and *Schisandra chinensis* metabolites. Fitoterapia. In Press.)

4.1. NADES Role in Solubilizing NADES Metabolites

According to the binding theory, the interaction of a metabolite with the NADES matrix can increase its solubility. A NADES matrix consists of a hydrogen bonding network, where the basic units are the NADES components. In a previous study (Simmler et al. 2015), in which proline was identified as a marker compound of *G. glabra*, NMR analyses of *G. glabra* crude extract revealed that proline in the *G. glabra* crude extract is almost miscible with DMSO. In contrast, proline is insoluble in DMSO. These NMR analyses demonstrate that the physical property of proline

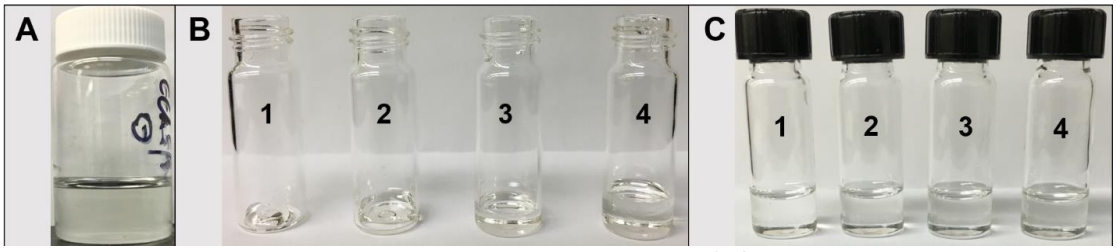

Figure 31. The CChPSuWat and its DMSO solutions. (A) Preparation of the NADES species CChPSuWat showing high viscosity. (B) Different quantities of CChPSuWat in vials 1-4. (C) The same vials. After addition of DMSO to achieve a total volume of 1 mL each. No precipitation occurred in each of the vials. This indicated that proline as a NADES component can achieve a high solubility in DMSO. Quantitatively, the vials contained, 13.3 mg/mL in **1**, 26.6 mg/mL in **2**, 53.2 mg/mL in **3**, and 106.4 mg/mL of proline in **4**, respectively.

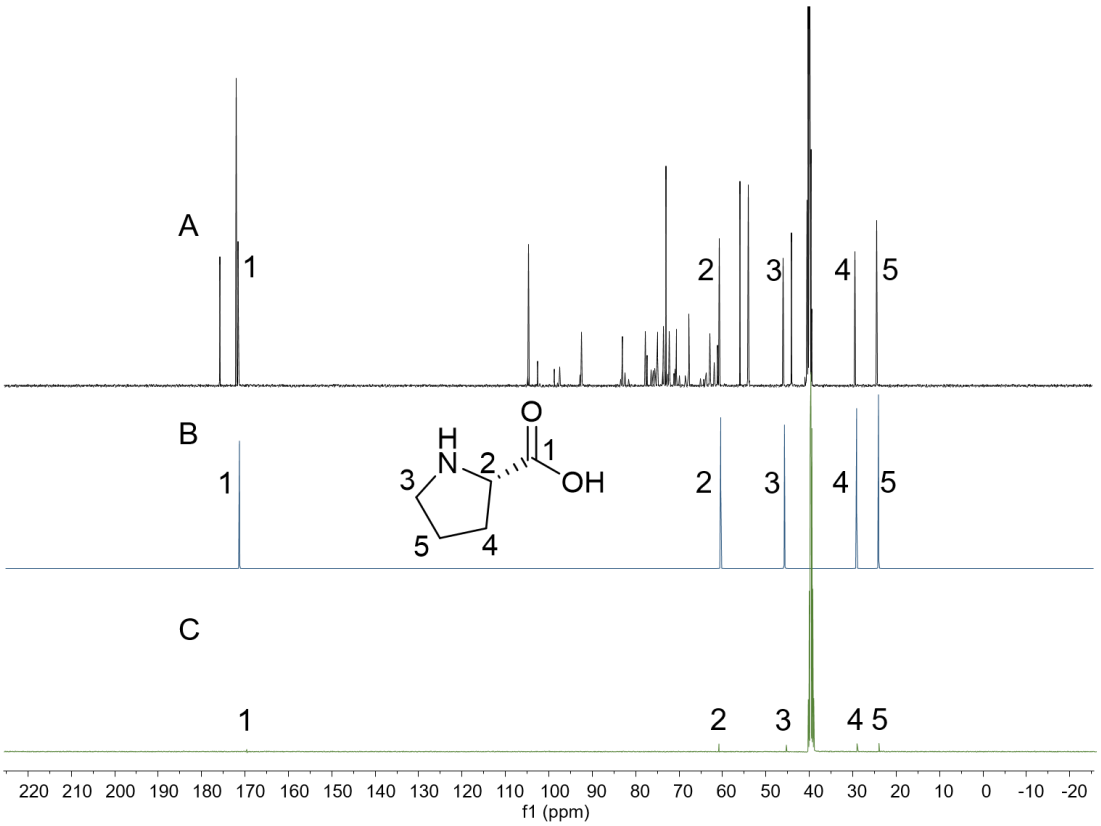

Figure 32. Investigation of proline in DMSO using ^{13}C NMR. (A) ^{13}C NMR spectrum of CChPSuWat (3:2:1:1:4, mol/mol), equal to 13.3 mg/mL of proline, in DMSO-d_6; (B) Deconvoluted/Extracted spectrum of proline using the deconvolution function; (C) ^{13}C NMR spectrum of saturated proline in DMSO-d_6.

changes greatly in a NADES component likely via binding with other NADES components. To evaluate this hypothesis that the formation of bonding network via hydrogen bonding can significantly influence the physical properties of corresponding NADES components, a multiple-component NADES, citric acid-choline chloride-sucrose-proline-water (3:2:1:1:4, mol/mol) was prepared. This experiment reinforced the observation as the proline in the form of the multiple-component NADES can be miscible with DMSO (Figure 31). Moreover, with

assistance of an external standard, caffeine, qNMR analyses (Figure 32) demonstrated that the solubility of proline in the multiple-component NADES (13.3 mg/mL) is 11.6 times greater than that of neat proline in DMSO (1.15 mg/mL). Equally important, this observation supports the "binding theory" and exemplified the co-solubilizing ability of NADES.

Collectively, these results combined with prior data from the licorice study (Simmler et al. 2015) and indicate that licorice roots as a BDS may contain a proline-based NADES species.

4.2. Establishment and Evaluation of Hydrogel Model

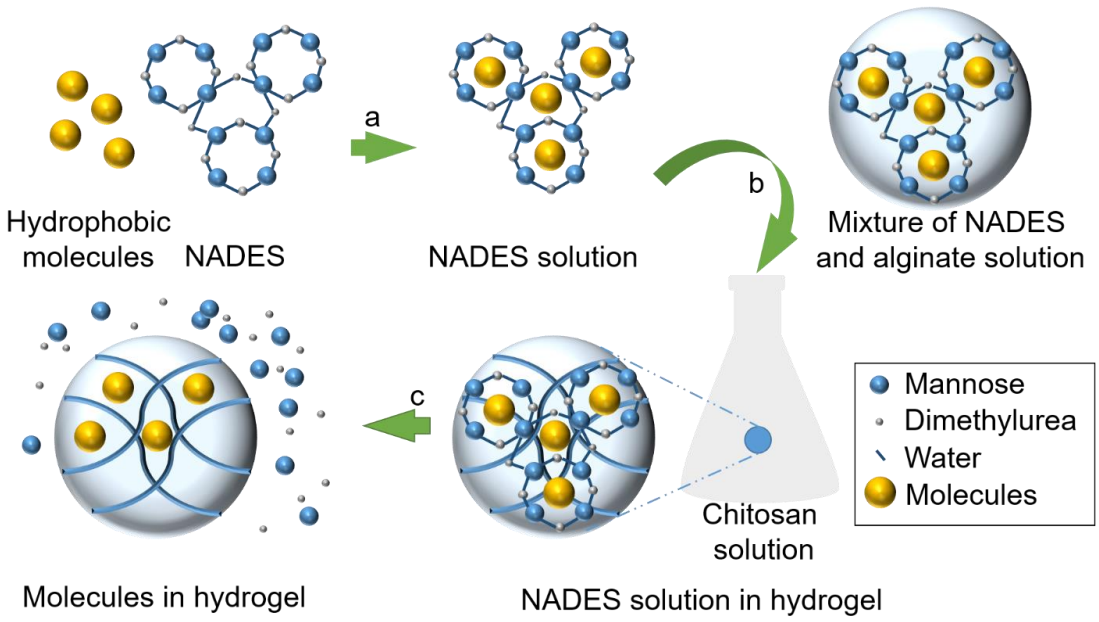

Figure 33. Model of the loading of hydrophobic molecules into a hydrogel using NADES as adjuvants. (a) NADES dissolves the hydrophobic molecules; (b) hydrogel-forming polymers are added to the NADES; (c) due to NADES' duality properties (hydrophilic components and capability of dissolving lipophilic molecules), most of NADES diffuse out of the hydrogel, leaving behind a certain amount of the hydrophobic molecule in the hydrogel.

The hydrogel system underlying this study can be summarized in the following three points (Figure 33). (a) NADES species are capable of dissolving relatively large amounts of hydrophobic molecules, such as shown for curcumin solubilized in MDWat (Figure 34). (b) The NADES solution was mixed with an alginate solution, and the mixture was introduced dropwise into the chitosan solution. Once the hydrogel network was formed, the NADES solution is trapped in the micro-environment. (c) Free water can migrate into and out of hydrogel and, thereby, disrupt the NADES matrix. Once the intermolecular interactions among different components in the NADES matrix are disrupted, free NADES components are released from the hydrogel. Because of their hydrophilic nature, NADES components spontaneously diffuse into the aqueous environment by movement down the concentration gradient. Meanwhile, lipophilic molecules are also released from the NADES matrix by passive diffusion. However, because of spontaneous emulsification (aka the "Ouzo Effect") (Lepeltier et al. 2014) and precipitation, a portion of the lipophilic metabolites may also be trapped in the hydrogel matrix. Therefore, a controlled released formulation system may be achieved in this model.

4.2.1. Selection of a Suitable NADES for a Given Marker Compound

To validate this hypothesis, a NADES formulation suitable for the selected marker compounds was developed. With the assistance of Reichardt's dye (Reichardt 1994), six NADES species from a broad hydrophilicity/lipophilicity range were tested, *viz*: Maleic acid-Choline chloride-Water (MaCWat), Mannose-Dimethyl urea-Water (MDWat), Choline chloride-Urea-Water (CUWat), Glucose-choline chloride-Water (GCWat), Glucose-Urea-Water (GUWat), and Fructose-Urea-Water (FUWat). The ratio of the components was 2:5:5 (mol/mol) in all cases.

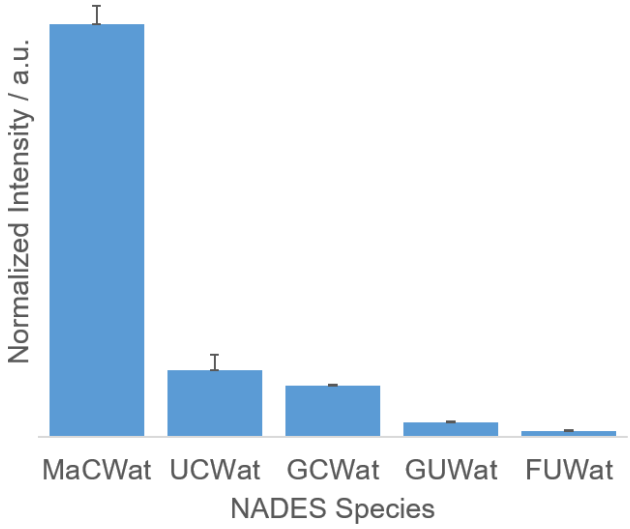

Figure 34. Solubility of curcumin in different NADES species.

The focus of this study was to determine if representative NADES species were capable of carrying and loading lipophilic molecules into the hydrogel system. Because of its strong fluorescence and distinctive yellow/orange color, curcumin was selected as a test molecule. Notably, the actual material used in this study was a curcuminoid mixture enriched in its primary phytochemical, curcumin, previously designated as curcumin-enriched material (CEM). This material represented the residual phytochemical complexity typically encountered in phytopharmaceutical practice. CEM is a refined form of crude curcuminoid-enriched turmeric extract (CTE). While CTE, CEM, and pure/isolated curcumin are often collectively referred to using the same term "curcumin" in the literature, it is important to differentiate these materials clearly. It is important to point out that only the most abundant constituent of the test materials, the single compound curcumin, was used as the

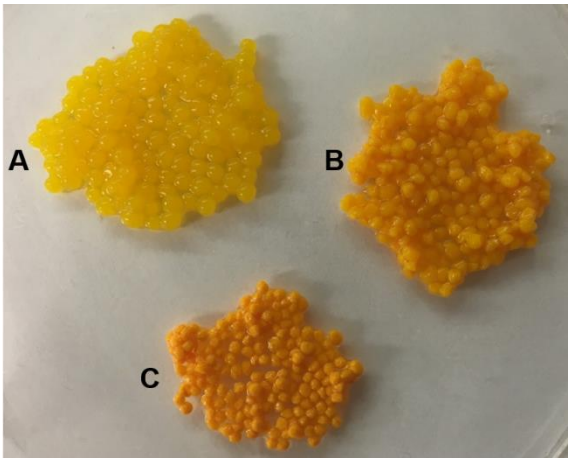

Figure 35. Curcumin-loaded hydrogel beads produced from different (concentration) ratios of MDWat solution to alginate solution (MDWat:Alginate, v/v): 3:1 in A, 1:1 in B, and 1:3 in C.

marker compound in this study. Accordingly, the term CEM/"curcumin" is used throughout the discussion.

The CEM/"curcumin" saturated NADES solutions were examined for curcumin using analytical HPLC. The highest curcumin concentration in the tested NADES was found in MDWat (Figure 34), with a solubility of 11 ± 1 mg/mL (n = 3, mean ± SD), which is close to the solubility of CEM/"curcumin" in DMSO (12 mg/mL).

To account for the potential water content increase from mixing with the alginate solution, the CEM/"curcumin" solubility in MDWat at higher water contents, 5% MDWat, (i.e., MDWat : water, 95:5, v/v) was determined (data not shown). The solubility of curcumin in 5% MDWat increased. Thus, when some water was added into NADES matrix during hydrogel preparation, CEM/"curcumin" did not precipitate. On the other hand, a saturated DMSO solution of CEM/"curcumin" could not be used for the hydrogel preparation because CEM/"curcumin" precipitated

from the DMSO once it was mixed with the alginate solution.

4.2.2. Feasibility of Loading Lipophilic Curcuminoids into a Hydrogel

To determine the optimal ratio between the CEM/"curcumin"-MDWat and the alginate solution, hydrogel beads were prepared at 1:3, 1:1, and 3:1 ratios of CEM/"curcumin"-MDWat/alginate (v/v) (Figure 35). No curcumin precipitated after vortex mixing, and uniform solutions could be formed at all three ratios. This indicated that the alginate solution did not significantly change or decrease the MDWat solubilizing ability, and that the entropy of diluted NADES solution was still in the NADES state. Visual inspection of the hydrogel beads suggests successful encapsulation of curcumin within the hydrogel, as evidenced by the bright orange color. The hydrogel beads successfully packaged the molecules at all of the tested CEM/"curcumin"-MDWat/alginate ratios (Figure 35). However, due to the fact that the alginate quantity determines its inner mesh size (Gillette et al. 2010), at the 1:3 ratio of alginate to MDWat solution, the hydrogel beads exhibited more irregular sizes and shapes, as well as more porous surfaces. These properties are less favorable for applications where diffusion is the release mechanism. On the other hand, the ratio of alginate to MDWat solution also determined the amount of CEM/"curcumin" loaded. At the 3:1 ratio, the hydrogel beads exhibited a lower quantity of loaded curcumin. Thus, the alginate to CEM/"curcumin"-MDWat solution ratio of 1:1 was selected for the subsequent release assays.

4.2.3. Dynamic Change of NADES Components

To understand the fate of the NADES components following hydrogel preparation, a ^{13}C NMR spectrum (Figure 36) of the chitosan solution was obtained immediately following removal of the hydrogel beads. Both DMU and mannose

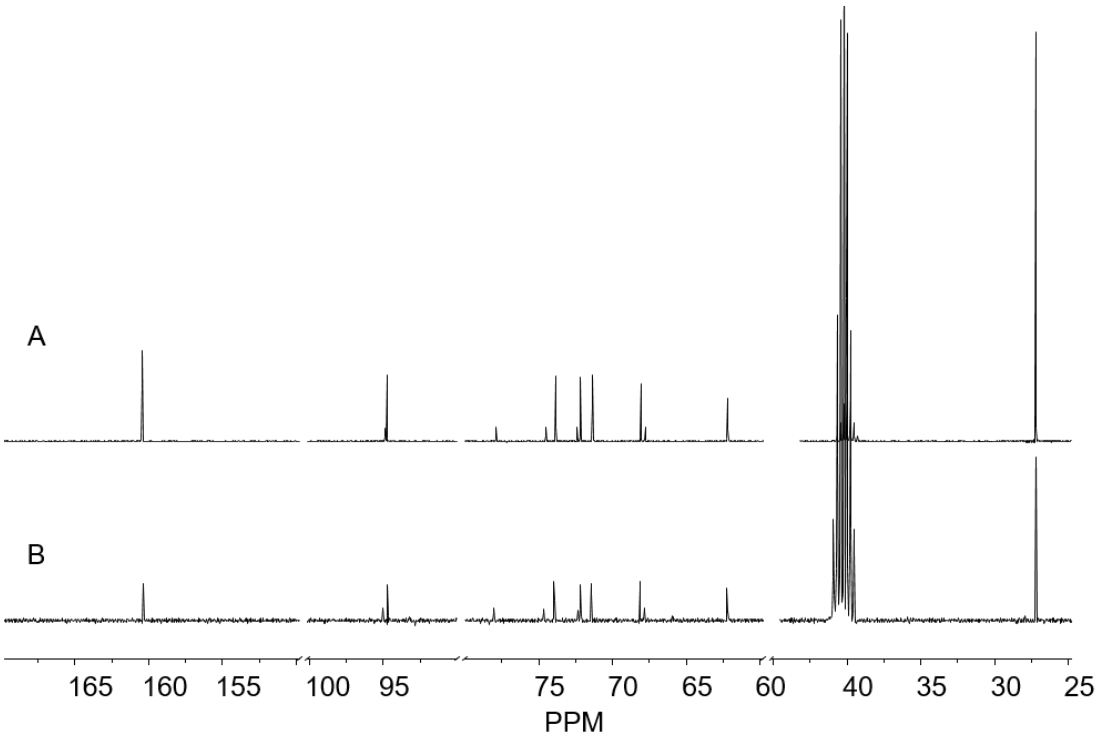

Figure 36. ^{13}C NMR of MDWat
^{13}C NMR of MDWat (A) and the unincorporated solution after hydrogel preparation (B). The unincorporated solution is composed of the used chitosan solution, solvent (water) and any molecules that were not incorporated into the hydrogel beads.

were detected in the chitosan solution when compared to the reference MDWat. The release of mannose and DMU from hydrogel beads was determined by qHNMR. As the DMSO solvent signal was superimposed by the methyl group of DMU (Figure 37), the solvent could not be used for calibration and caffeine was used as an internal calibrant (IC) instead. The qHNMR analysis also showed that 94.2% ± 3.9% of the mannose and 91.4% ± 2.8% of the DMU initially present in the exterior phase of the alginate formation media after hydrogel bead preparation. This suggests that, when the CEM/“curcumin”/NADES/alginate mixture was introduced dropwise into the

chitosan solution, mannose and DMU quickly diffused out into the chitosan solution as they are both very soluble in water. Finally, as the prepared beads were washed with fresh water five times, the mannose and DMU inside the prepared beads should be negligibly less than 0.01%. It is also plausible that the NADES microstructure may produce micro- or even nano-particles of lipophilic molecules (Hammond et al. 2017). Thus, the rapid removal of NADES components from the hydrogel indicated that the CEM/"curcumin"/NADES mixture may experience spontaneous emulsification during hydrogel preparation (Vitale and Katz 2003; Lepeltier et al. 2014). Accordingly, the microenvironment inside each alginate bead is capable of switching to non-solvent (water) for the loaded curcumin, and the system evolves towards phase separation, leading to the formation of particles. Flocculation of

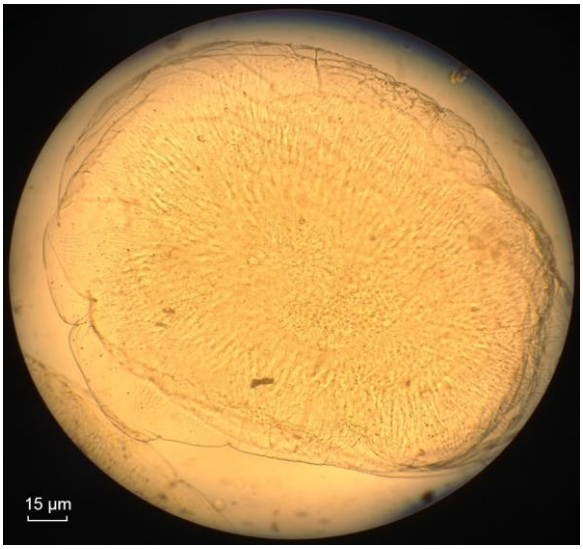

Figure 37. The light microscope (using a 10× lens, AmScope, Irvine, CA) image of a curcuminoid-loaded hydrogel.

particles and formation of large aggregates are a limitation for nanoprecipitation with spontaneous emulsification (Lepeltier et al. 2014). In order to determine if larger crystals or other aggregates were present inside the hydrogel beads, they were first stored at 4°C for 72 h, representing a condition that accelerates nucleation and aggregation. The beads were then sectioned and observed under a microscope. No crystal or large aggregates were observed (Figure 38). It is known that very low solubility of the hydrophobic solute in water and/or homogeneously sized particles opposes growth of larger particles (Ostwald ripening) (Lepeltier et al. 2014). Considering the outcomes, alginate polymer might also function as surface coating

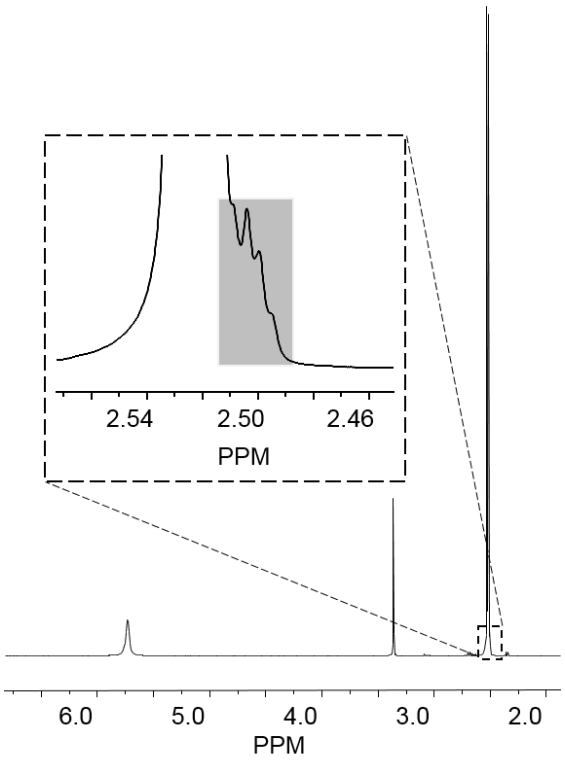

Figure 38. ^{1}H NMR of dimethyl urea in DMSO-d_6. The expansion shows that the methyl group of dimethyl urea overlaps with the DMSO residual solvent signal (gray area).

that prevents molecular agglomeration. This effect has been shown to stabilize the precipitation of β-carotene nanoparticles within poly(styrene)-β-poly(ethylene oxide) block copolymer (Liu et al. 2007).

4.2.4. Investigation of Loading Efficiency

The ability of the delivery systems to release curcumin was initially assessed using the biphasic solvent system of CH_2Cl_2 and water (Kim et al. 2009). Hydrogel beads (60 mg) loaded with CEM/"curcumin" were used, and the release occurred at the two-phase interface (Figure 39). The yellow color was only present in the CH_2Cl_2. The release occurred over 180 h in this biphasic system. This indicated that 60 mg of beads may maintain release for at least 180 h in aqueous media, considering the fact that CEM/"curcumin" has a higher solubility in CH_2Cl_2 than in water. The

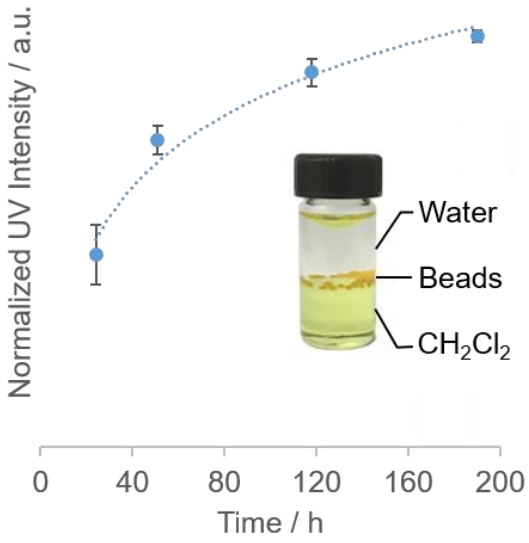

Figure 39. The release of curcumin from the hydrogel beads into the dichloromethane (or CH_2Cl_2). The release was observed from CDE/"curcumin"-loaded hydrogel beads, while suspended in a in a CH_2Cl_2/water solvent system (n=3, mean ± SD).

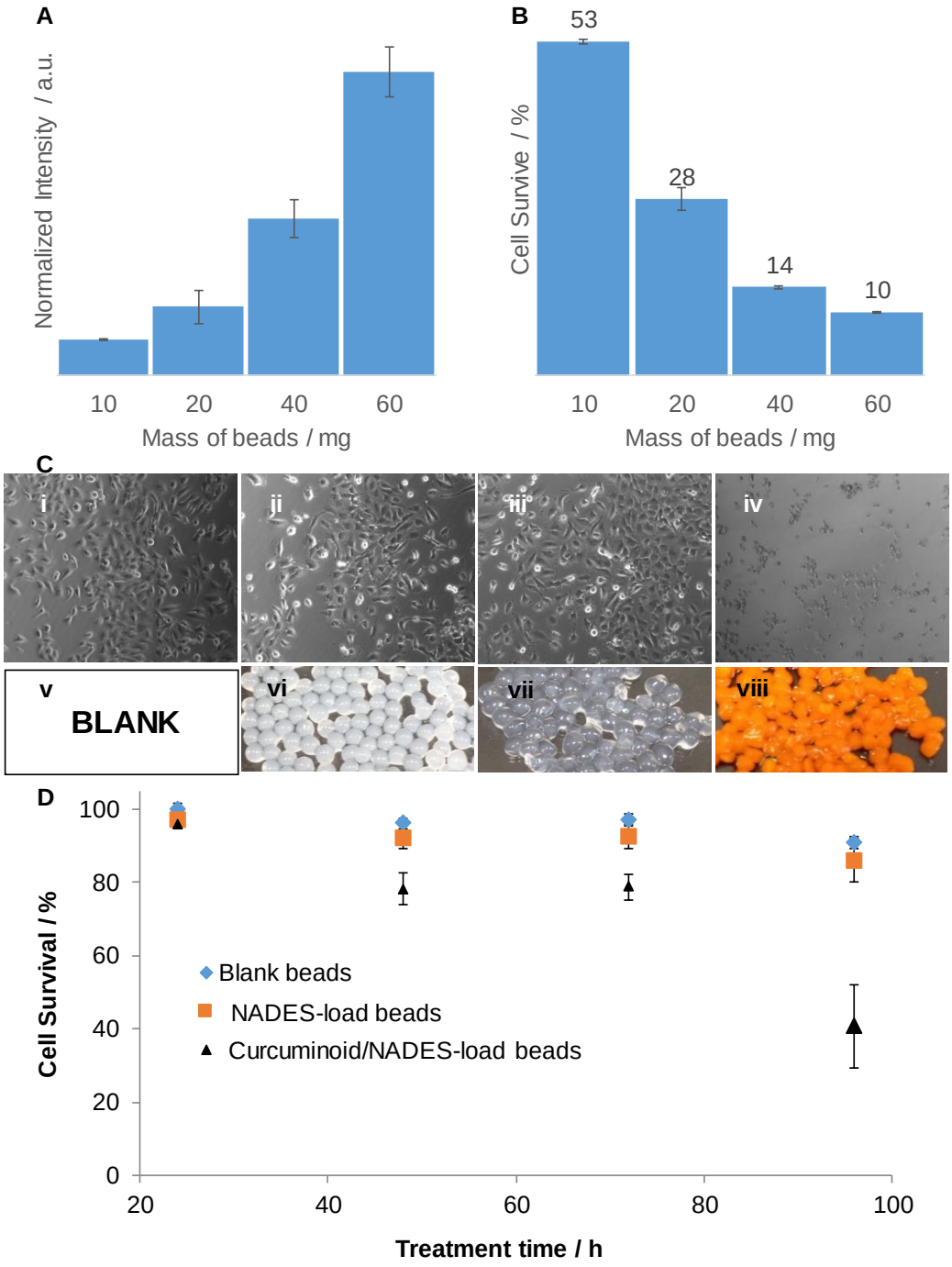

Figure 40. *In vitro* assays of curcumin loaded hydrogel beads.
Influence of the mass of beads on (A) a curcumin release assay in PBS buffer, and (B) on the cytotoxicity using U251 cell line. For (C), (i) cells cultured in wells, (ii) blank hydrogel beads in an insert, (iii) MDWat hydrogel beads in an insert, (iv) curcumin loaded hydrogel beads in an insert were used. C-i is control of C-ii; C-ii is control of C-iii; C-iii is control of C-iv. (D) A quantitative study of the curcumin loaded beads performed with U251 cells.

released CEM/"curcumin" was determined via qHNMR using internal calibration with caffeine. Compared to the original curcumin quantity in NADES solution, 13% ± 3% curcumin (n=3, mean ± SD) was collected in the released sample. The diffusion of similar species of similar size can be expected to have similar diffusion coefficients and, thus, will diffuse in a similar manner. Considering the different diffusion capabilities of NADES components and CEM/"curcumin", over 99% of the NADES components and near 87% of the CEM/"curcumin" were from the exterior phase of the alginate formation media removed after hydrogel bead preparation. Collectively, these results boded well for the feasibility of studying the potential interaction between the hydrogel model and lipophilic *S. chinensis* metabolites.

To determine whether the NADES is suitable for the loading of lipophilic drugs into the delivery formulation hydrogel, one of the critical factors is that the delivery system should be of negligible cytotoxicity while the released drug molecule maintains its bioactivity. Based on the analysis of the chitosan hydrogel preparation solution above, hydrogel beads are expected to be free of NADES components post production. The released CEM/"curcumin" from the hydrogel was investigated using the U251 brain cancer cell line. A CEM/"curcumin" release assay using different amount of beads was performed in PBS buffer for 72 h, and the released curcumin amount was determined by HPLC (Figure 40A). Meanwhile, the corresponding amount of beads were incubated with U251 cells for 72 h (Figure 40B). As the amount of hydrogel beads increased, the cell survival rate decreased (Figure 40A and B), indicating that the released curcumin did not saturate the release medium. CEM/"curcumin"/NADES beads (60 mg) were selected for a fully quantitative *in vitro* assay.

As shown in Figure 40C, compared to the control groups, the curcumin-loaded bead group showed poor morphological features compared to live and healthy cells. This indicated that the signs of cell death in this group (Figure 40C-iv) were independent of the hydrogel (Figure 40C-ii) and the NADES MDWat (Figure 40C-iii), but due to released curcumin. This suggests that the NADES, MDWat, was suitable as an alternative solvent for solubilizing lipophilic drugs and did not raise cytotoxicity concerns. The cancer cell viability inhibition by curcumin released from hydrogel was quantified at different time points (Figure 40D). Consistent with cell morphology observations, control groups (Figure 40C-i, ii, and iii) had minimal cell viability inhibition while curcumin hydrogel beads were associated with 60% inhibition.

4.3. Interaction between *S. chinensis* Fruit Extract and Hydrogels

4.3.1. Hydrogel loading with *S. chinensis* Fruit Extract

S. chinensis fruit extract itself exhibits the physical nature of a NADES, because the extract contains a significant amount of NADES components such as citric acid and malic acid (Appendix E) in addition to the more lipophilic lignan constituents. As such, *S. chinensis* fruit extract represents a similar situation to the modeled MDWat/curcumin matrix. In preliminary assays, the complexity of the crude *S. chinensis* extract prevented the formation of a homogeneous mixture with the alginate solution at a ratio of 1:1 (v/v, as Figure 41A). This may be due to the disruption of ionic interactions in *S. chinensis* fruit extract by the biopolymers or by other mechanisms that diminish the solubility of some components. Therefore, the

quantity of the alginate solution used in the formulation was increased. Several ratios of crude extract to alginate solution were examined: 1:1, 5:1, 10:1, 15:1, and 20:1 (v/v, Figure 41A). Homogeneous mixtures were obtained with ratios from 5:1 to 20:1 (v/v, Fig. 41B), and the hydrogel beads showed the best uniformity at ratios of 10:1, 15:1, and 20:1(v/v). Moreover, as discussed above, a high percentage of alginate solution in the homogeneous mixture resulted in a comparatively low loading efficiency in the hydrogel beads. Accordingly, the combination of 1 mL of *S.*

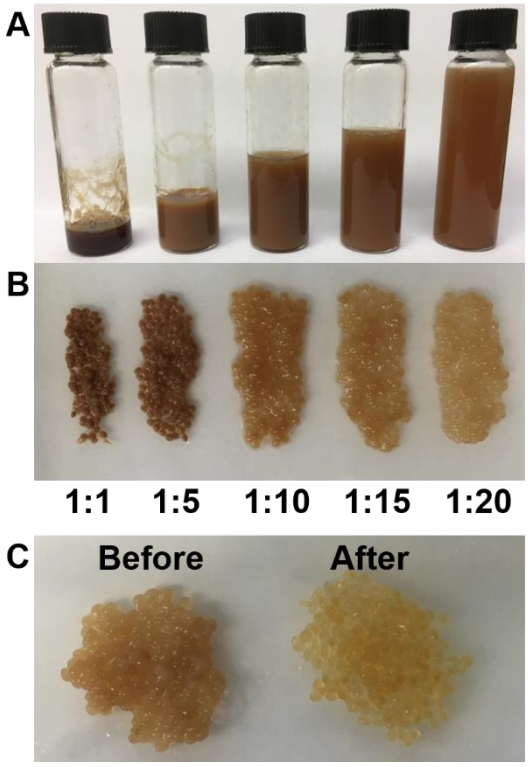

Figure 41. Crude extract of *S. chinensis* loaded hydrogel beads before and after releasing.
(A) Mixture of crude extract and alginate solution in different ratios were dropped into chitosan solution to obtain hydrogel (B). In (C), the extract loaded beads (Before, on the left) were extracted using MeOH to release the extract (After; on the right) and yield the unloaded hydrogel beads.

chinensis fruit extract (1.36 g) and 10 mL of alginate solution was used to investigate the potential interaction between the hydrogel model and *S. chinensis* metabolites. Once the *S. chinensis* metabolites were loaded successfully into the hydrogel beads, our hypothesis was that this pathway may be capable of introducing lipophilic metabolites into biopolymer matrices via NADES assistance.

Fractionation of *S. chinensis* fruit extract via chromatography on HP-20 resin mostly led to the elution of lipophilic compounds by 25% aqueous and 100% MeOH fractions. This indicated that MeOH could be an appropriate extraction solvent for loaded hydrogel beads. Accordingly, 50 mL of MeOH was used as the extraction solvent in a two-day release experiment. The extraction was performed three times, i.e., for a total of 144 h. The combined released metabolites had dry weight of 231 mg. This demonstrates that some lipophilic ingredients have been loaded in the hydrogel beads.

4.3.2. Analysis of Released *S. chinensis* Metabolites

Dibenzocyclooctadiene lignans are the major described lipophilic metabolites of *S. chinensis* fruits (Lu and Chen 2009). Detection of these lignans in the released metabolites indicated that the NADES species in the crude extract itself may function by the proposed "slow release" mechanism, i.e., that *S. chinensis* fruit extract contains both lipophilic constituents as well as NADES (species). NMR analyses of the released metabolites demonstrated that fatty acids (Figure 42) (San José et al. 2015) and some lignans (Figure 43) are among the major components of the released extract.

For a qualitative investigation of the released metabolites, one step of CCS was performed using centrifugal partition chromatography (CPC) (Ignatova et al. 2011).

The SS of *n*-Hexane-EtOAc-MeOH-Water (5:5:5:5, v/v) was selected using the GUESS TLC-based SS prediction strategy (Liu et al. 2015). The CPC system gave 0.76 as a stationary phase retention (Sf) value. The fractions were concentrated via a centrifugal vacuum evaporator and analyzed by NMR (Liu et al. 2014). The eluents were mainly located in two K ranges, i.e., K ≈ 3 identified as e.g., gomisin A, and K values close to infinity identified as fatty acids (see Figure 42B). NMR analyses of the fractions with K ≈ 3 led to the identification of three lignans (Figure 43A). The characteristic signals of the dibenzocyclooctadiene lignans bear an eight-membered ring, several methoxy groups, and one aromatic proton in each aromatic ring. Interestingly, both of the aromatic protons give rise to singlets. Based on their unique chemical shifts, these signals can be used for the lignan characterization and

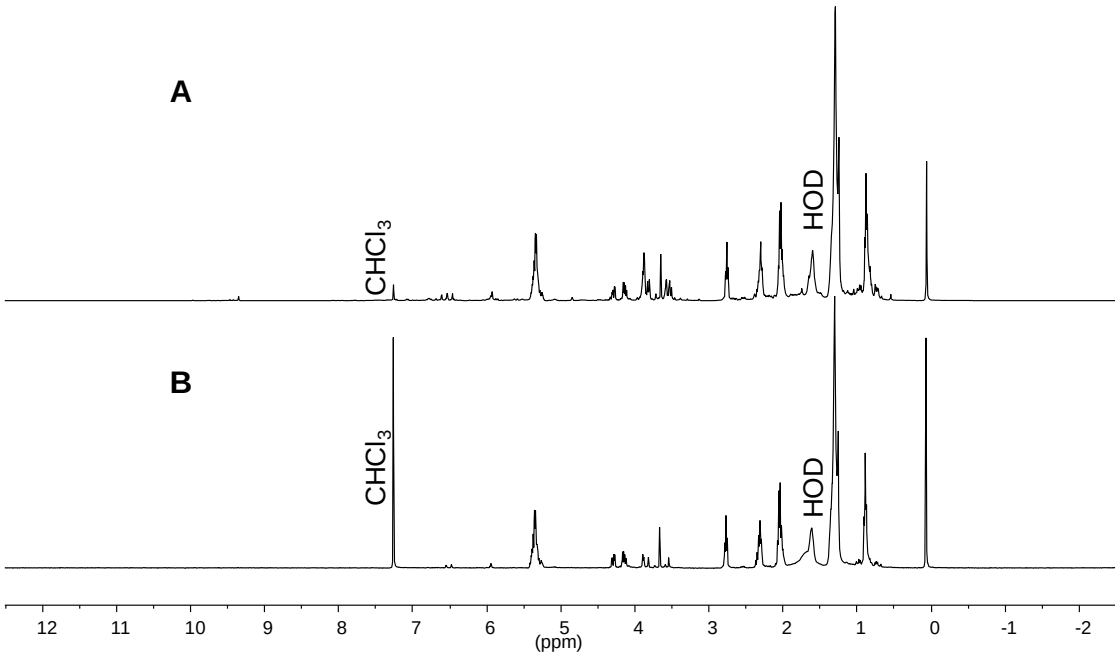

Figure 42. (A) Sample extracted from hydrogel using MeOH. (B) One CPC fraction as an example of released fatty acids. The NMR solvent was $CDCl_3$.

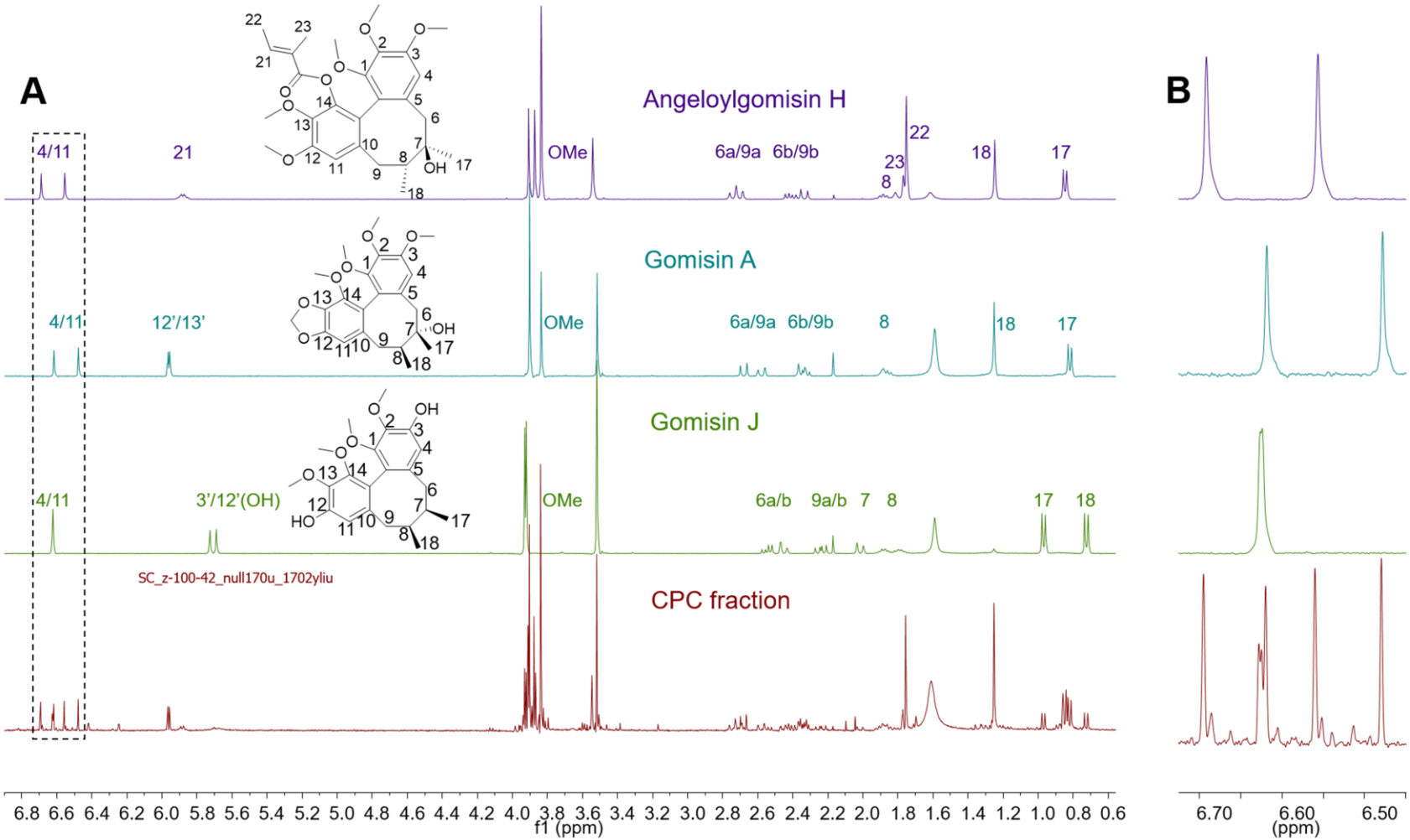

Figure 43. NMR analyses of the CPC fraction with 3 lignans released from the extract loaded hydrogel. (A) Comparison between the CPC fraction and lignan standards. B is expansion of one region indicated by boxes in A.

quantification. To evaluate this hypothesis further, a prep-HPLC fractionation was performed and yielded three lignans: gomisin J (retention time [t_R], 22.0 min), gomisin A (23.5 min), and angeloylgomisin H (26.5 min). Figure 42B demonstrates that the singlet aromatic hydrogen signals of dibenzocyclooctadiene lignans can be used for their identification. Integration of $CHCl_3$ solvent signal in each sample was normalized as 100, and the molar ratios of gomisin J to gomisin A to angeloylgomisin H was calculated using average integral of signals 1 and 4 (Figure 43), i.e., 1.00:1.93:2.16 (mol/mol).

These results indicate that the NADES present in crude *S. chinensis* extracts could potentially contribute to the delivery of lipophilic metabolites with the assistance of natural biopolymers. As shown with alginates, they can form a "slow release" delivery matrix that might assist with the pharmacological function of the lipophilic *S. chinensis* metabolites that otherwise show low aqueous solubilities. The documentation of the concept of a natural drug delivery mechanism shows that the NADES present in many crude herbal materials in the form of crude extracts might function as bioavailability enhancers.

5. RESEARCH AIM 3: NADES STABILITY AND ITS STABILIZING ABILITY

5.1. NADES Stability

NADES-family metabolites are stable compounds, and their mixtures, as they form NADES, can therefore be considered to pattern uniform matrices. According to observations in this study, although most of NADES species are very stable over time, some exceptions do exist. Potential reasons for the chemical change are: (i) the different conformations between natural eutectic metabolites and their corresponding commercial products; (ii) some organic acids contained in NADES

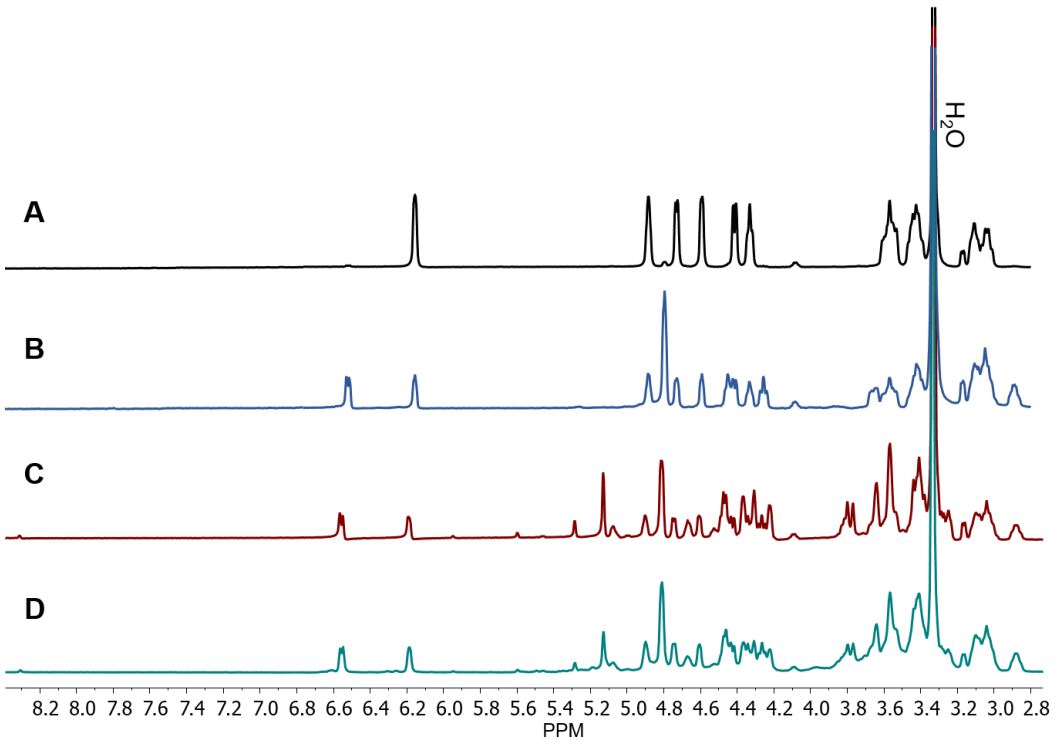

Figure 44. The qHNMR analyses of α-D-glucose and the NADES constituents of glucose and fructose (1:1, mol/mol). The test samples were α-D-glucose (A), α-D-glucose with 100°C heat treatment (B), the glucose-fructose NADES prepared using the heating strategy (C), and the glucose-fructose prepared using the vacuum evaporation strategy.

produce reactive conditions by lowering the pH value changes. Two specific examples are introduced, as follows.

The first example is about the stability of a commercial powder of α-D-glucose. NMR analyses of the α-D-glucose in DMSO-d_6 (Figure 44A) confirmed that the product only contained the α-isomer. However, in Nature, the glucose molecules are

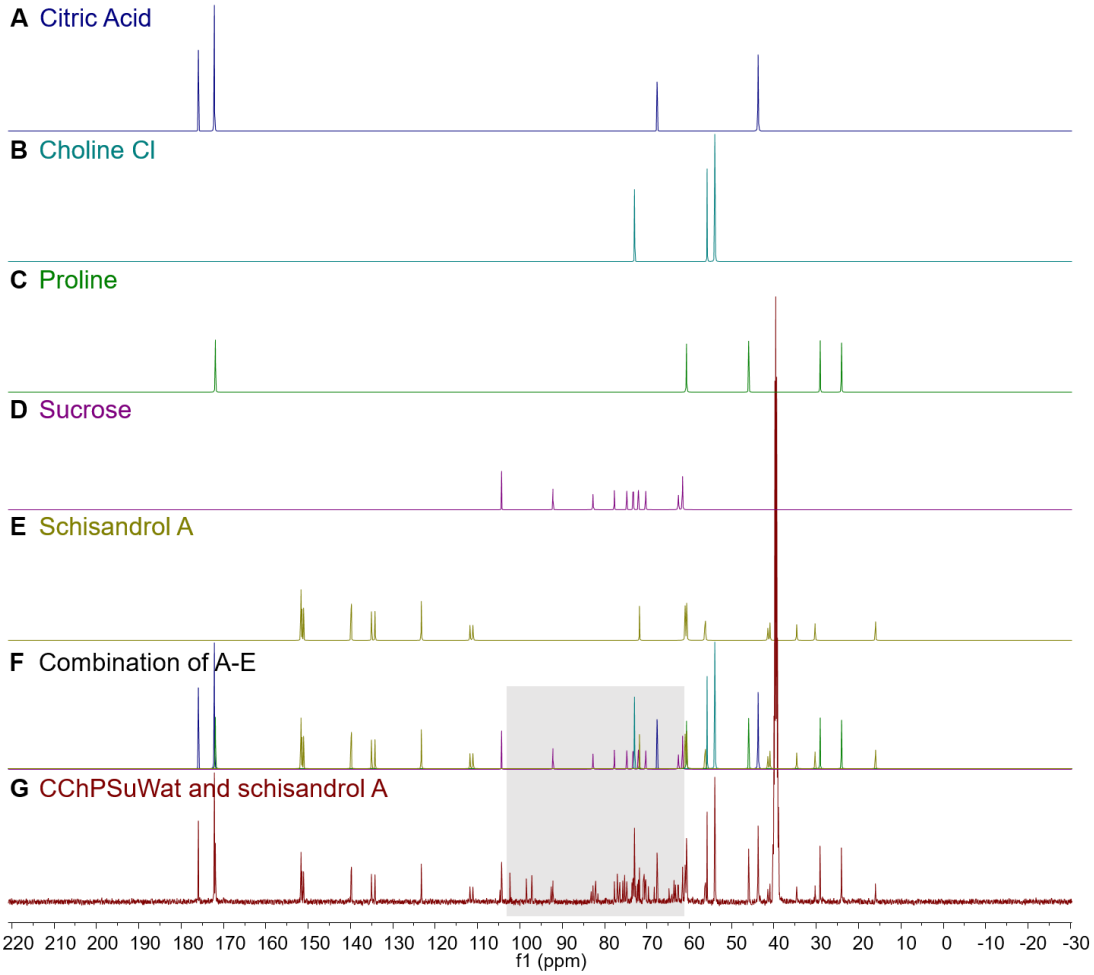

Figure 45. The ^{13}C NMR analyses of the mixture of schisandrol A and CChPSuWat. The spectra were e-data of sucrose (A), citric acid (B), choline chloride (C), proline (D), schisandrol A (E), stack A-E (F), and qCNMR spectrum of the mixture of schisandrol A and CChPSuWat.

always dissolved in water and, thus, muta-rotation occurs, generating an equilibrium mixture of both α- and β-anomers of glucose. In this work, it is proposed that entropy administration (such as water and heating involvements) is the key factor that influences this anomeric change. Thus, neat glucose was heated to increase the glucose crystal matrix entropy. Following the hypothesis, this should generate a mixture of α- and β-anomers of the glucose. The result (Figure 44B) matched with the hypothesis. Moreover, using α-D-glucose, a glucose-fructose NADES was prepared via the heating (Figure 44C) and the vacuum evaporation strategy (Figure 44D). Both the α- and β- anomers were involved in the NADES

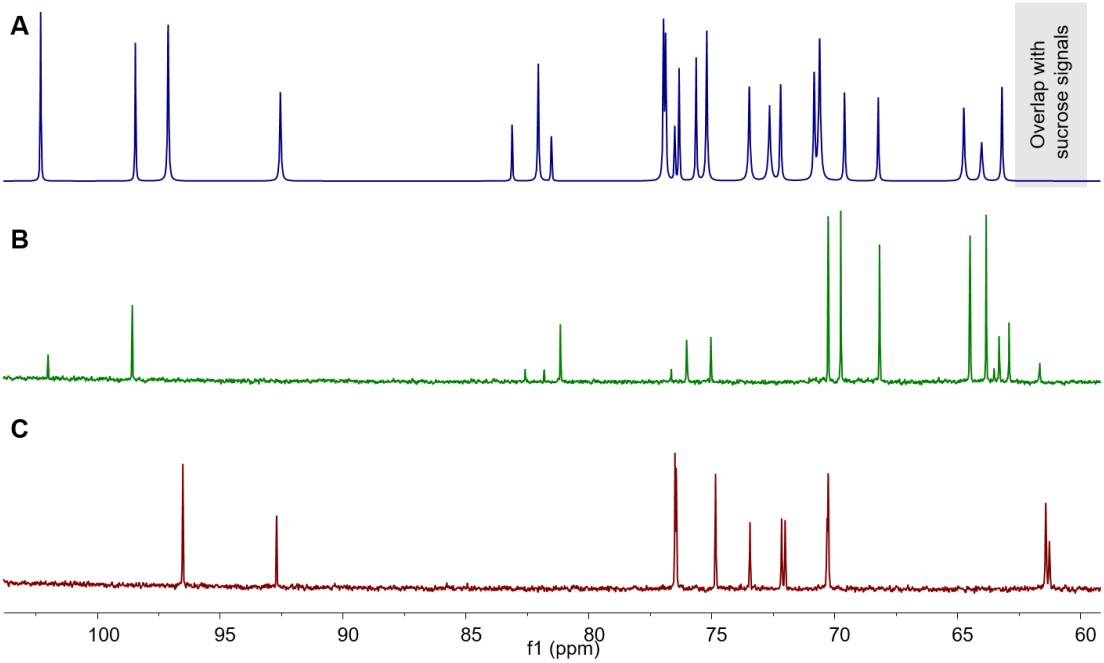

Figure 46. ^{13}C NMR analyses of the extra signals in CChPSuWat solution. (A) the (part of) deconvolution simulated spectrum from the CChPSuWat spectrum; reference spectra of glucose(B), and fructose (C), obtained from the Human Metabolome Database (HMDB).

formation. The ratio of both α- to β-anomers was nearly 4:6 (mol/mol). This suggests that the muta-rotation phenomenon can happen during NADES preparation.

The second example concerns a multiple component NADES, CChPSuWat. This work aimed to simulate whether ^{13}C NMR can identify lipophilic metabolites in complex (NADES) matrix. The result (Figure 45) showed that qCNMR exhibited a potential capability of characterizing the small molecules in a botanical extract. Interestingly, except signals of schisandrol A and CChPSuWat, some extra signals occurred over time (see Figure 32A and Figure 45G, where the two samples were from the same CChPSuWat stored at 37 ^{o}C). Using ^{13}C NMR, the sample in Figure 32A was analyzed 4 weeks before the sample shown in Figure 45G. The stored sample (Figure 46A) showed extra new signals that represent glucose and fructose, identified by comparison with reference spectra (Figure 46B and C) from the Human Metabolome Database (HMDB). This means that inverted sugar syrup was produced during storage, destroying the disaccharide sucrose into glucose and fructose. The occurrence of this reaction in CChPSuWat revealed that NADES matrices can degrade. This indicates that in an herbal formula, such as the mixture of licorice root (sucrose rich) and five flavor berry (citric acid rich), additional effects can occur including the hydrolysis of a honey-like BDS and that these matrices can be subject to dynamic change.

In addition, to facilitate NMR analyses, the electronic data (e-data, Figure 46 A and Appendix A) were extracted from the data in Figure 45G using the deconvolution function. The e-data can remove any noise from a ^{13}C NMR spectrum. This demonstrates the feasibility of electronically extracting signals of an individual compound via the deconvolution function for further qCNMR analyses. This

approach can also be developed for a quality control test.

5.2. NADES Induce Stability of Natural Products

Angelica sinensis is one of the most commonly used herb in Traditional Chinese Medicines (TCMs), predominantly in formulations for the treatment of irregular menstrual cycles and premenstrual syndrome (Wei et al. 2016). A compound marker in *A. sinensis* is the monomeric phthalide, ligustilide, which is known for its rapid chemical degradation (Schinkovitz et al. 2008), and susceptibility to the oxidation, dimerization, and isomerization (Deng et al. 2006). Therefore, *A. sinensis* TRM products are always used in the form of crude extract or essential oil (EO) solutions.

Considering that the root of the plant likely contains a NADES, either the EO or polar constituents, it is reasonable to hypothesize that the *A. sinensis* EO as a NADES matrix can protect otherwise labile ligustilide from the influence of environmental factors. To assess this hypothesis, the qHNMR analyses of ligustilide in different natural matrices were conducted. Specifically, this investigation elected to provide insights into the influence of temperature, light, and oxygen on ligustilide stability. For this purpose, plant material, EO, and high purity of ligustilide were assessed. The EO was obtained gently by supercritical CO_2 fluid extraction (SFE). High purity ligustilide was isolated from the EO by a two-step procedure involving CCS (Schinkovitz et al. 2008) and prep-HPLC, yielding 98% pure final product as determined by qHNMR analysis.

5.2.1. Stability of Ligustilide in Plant Material

Roots of *A. sinensis* was stored at 25°C, in aluminum bags placed in a dark and dry place. The material was extracted using SFE at month 1 and 12 of the study, and, the ligustilide content in both SFE extracts was analyzed using qHNMR. As an

TABLE XX. SFE OF *ANGELICA SINENSIS* ESSENTIAL OIL (EO): COMPARISON BETWEEN A STANDARD AND THE MODIFIED YIELD OPTIMIZED METHODS

Method	ETm (°C)	VTm (°C)	Pressure (Psi)	SET (min)	Flow rate (mL/min)	Modifier	EO Yield
Standard	50	120	250	20	2	No	10%
Modified	50	120	220	30	0.5	5%MeOH	14.8%

Note: ETm means extract temperature; VTm represents vessel temperature; SET is static extract time.

example, when integral of $CHCl_3$ signal was normalized as 100, integrals of H-7 were 1273.91 in Figure 47A and 188.54 in Figure 47B. Accordingly, the extraction yield was 14.8%. The results showed a consistent extraction yield of ligustilide SFE at month 1 and 12 of the study. They also demonstrated that ligustilide was stable in the plant material over a period of at least 1 year. Because ligustilide is the major constituent of the EO, and EO in the root of *A. sinensis* should be located in oil cavities and tubes situated in cellular parenchyma, ligustilide and the EO components are protected from environmental influence, such as temperature, light, and oxygen. Collectively, the raw plant material as well as the nature and location of the EO all may act as preservatives for ligustilide.

5.2.2. Stability Studies of Ligustilide in or Isolated from Essential Oil (EO)

Phthalides including ligustilide are relatively non-polar metabolites that occur in EOs. As discussed in Section 2.1.1, EO is one form of lipophilic NADES species in Nature. Therefore, it was hypothesized that the EO NADES matrix can protect ligustilide, thereby making it more stable when part of the EO is present in the plant

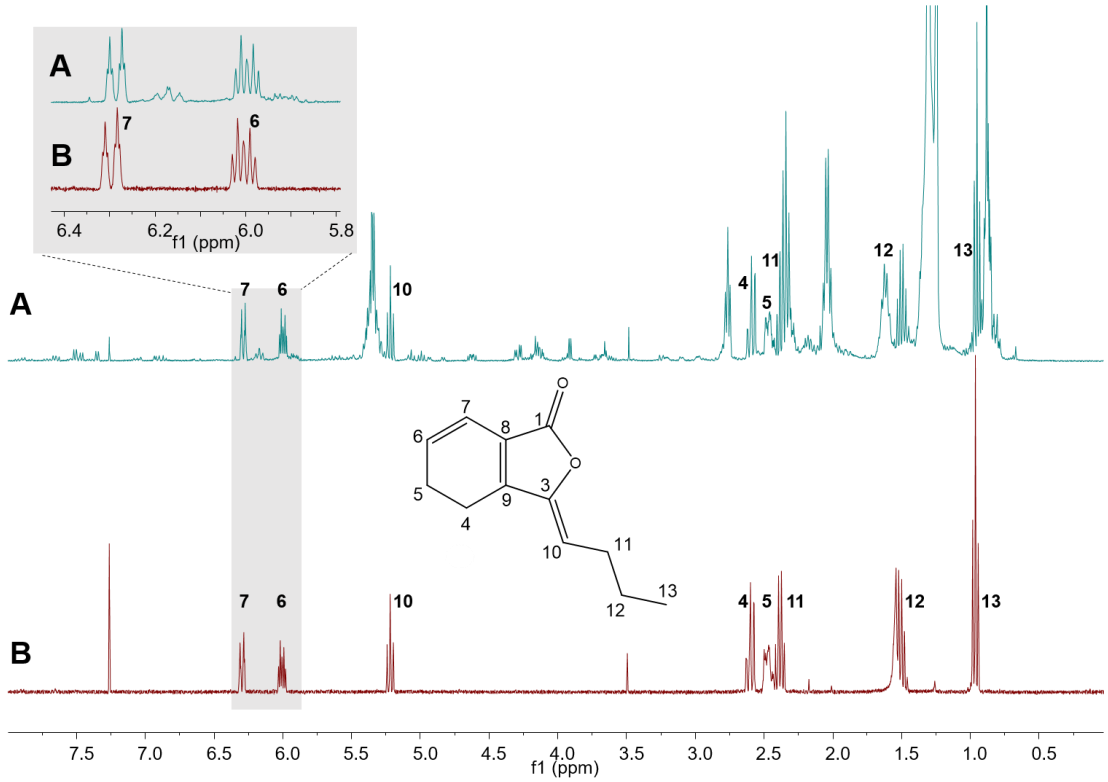

Figure 47. The ^{1}H NMR analyses of ligustilide samples.
(A) EO extracted from *A. sinensis* root material. (B) Purified ligustilide (98%) sample from prep-HPLC isolation.

material, compared to ligustilide as a pure chemical entity.

Viable EO extraction techniques include organic solvent extraction, steam distillation, and extraction with supercritical fluids. In this work, EO from *A. sinensis* root was extracted using the supercritical fluid extraction (SFE). To achieve a higher EO yield, the standard method was modified as shown in TABLE XX. The modified method obtained a yellowish EO at 1.5% (wt/wt) from the dry roots of *A. sinensis*. The ligustilide content was determined to be 14.8% (wt/wt) when quantified via qHNMR. Previous work using the standard SFE method achieved the ligustilide 10% in the EO. Although most regions of the ^{1}H NMR spectrum were complex and

overlapped, ligustilide quantification can be done via the characteristic signal of H-7 (δ 6.286, 1H, Figure 47), using the EC method (external calibrant, $DMSO_2$).

Ligustilide was isolated from the EO using HSCCC and the SS from a previous report (Schinkovitz et al. 2008) *n*-Hexane-EtOAc-MeOH-Water (HEMWat, 9:1:9:1, v/v) that gave a K value of 2.54 for ligustilide. Fractions with ligustilide were collected between 672 and 804 mL. Using NP-TLC, with the UP of the CCS SS as MP, a single spot at Rf 0.45 was clearly visible under UV at 356 nm and exhibited a blue-gray color after spraying with vanillin-H_2SO_4 reagent and heating. Using the advantage of qHNMR, i.e., a non-destructive method, fractions with ligustilide were combined, and then the purity (93.4 %) was determined using the EC method (external

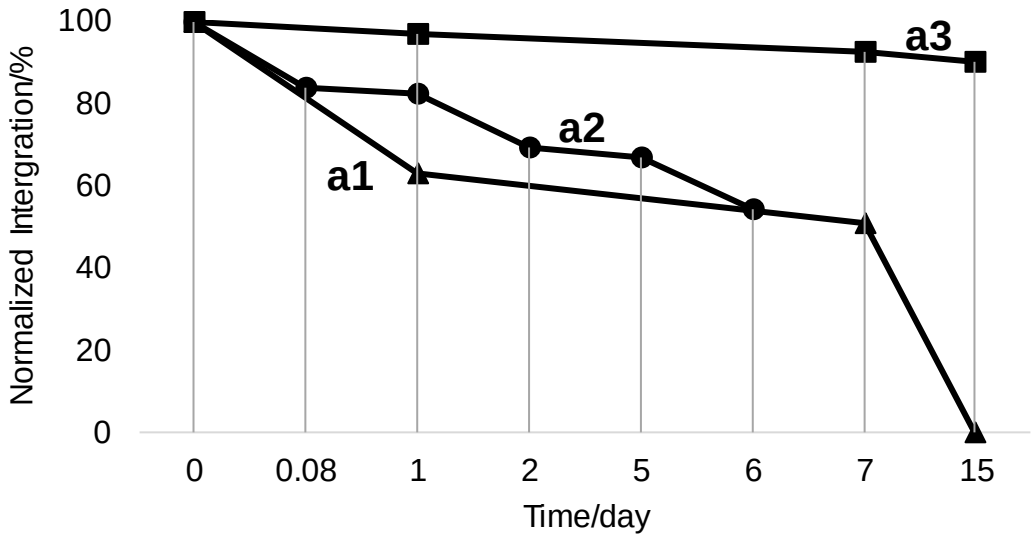

Figure 48. Influence of the light on ligustilide stability calculated from qHNMR data. For normalized NMR quantitation, ligustilide at the starting point (0 time point) represents 100% of the 93.4% purity value determined by qHNMR. Test samples: ▲a1, ligustilide exposed to natural light; ● a2, ligustilide exposed to UV wavelength (254 nm); ■ a3, ligustilide placed in a dark environment.

calibrant, $DMSO_2$).

Via CCS, ligustilide (18.66 mg, 93.4 % purity) was obtained from 150 mg of EO. Considering that the ligustilide content in SFE extract is 14.8%, the overall CCS yield was 85%. To achieve the highest possible purity for the ligustilide stability study, the combined HSCCC fractions were subjected to an additional prep-HPLC separation step. This final ligustilide product achieved 98% purity. Both samples (93.4% of HSCCC purity and 98.0% of prep-HPLC purity) were used for further stability studies.

Study of the influence of light. The purified ligustilide (5.4 mg, HSCCC purity, 93.4%) was dissolved in 1500 µL $CDCl_3$. The ligustilide solution was evenly distributed into three NMR tubes, which were flame sealed and kept at ambient temperature. As shown in Figure 48, the first NMR tube (a1) was exposed to daylight, the second (a2) to UV light (254 nm), and the third (a3) was kept in the dark. The a3 sample was degraded by 6.9% after day 15. Sample a1 showed nearly 100% degradation of ligustilide (below LOD) at the same time point. Sample a2 showed ligustilide degradation around 54.3% on the day 6, with a similar rate of degradation. The results indicated a pronounced influence of (day)light or UV on ligustilide stability and a relatively modest influence of ambient temperature.

Study of the influences temperature and argon. For the preparation of NMR sample A, ligustilide (1.80 mg; HPLC purity, 98%) was dissolved in $CDCl_3$ (500 µL) and flame sealed. For B, the same amount of the ligustilide was dissolved in $CDCl_3$, but argon was added to degas the NMR tube. It aimed to prevent the potential influence of air, in particular oxygen. Both samples were kept in the freezer (-20°C) for 30 days, after which they were transferred to ambient temperature and under daylight for the next 10 days. By sealing the NMR tubes with a flame, the potential

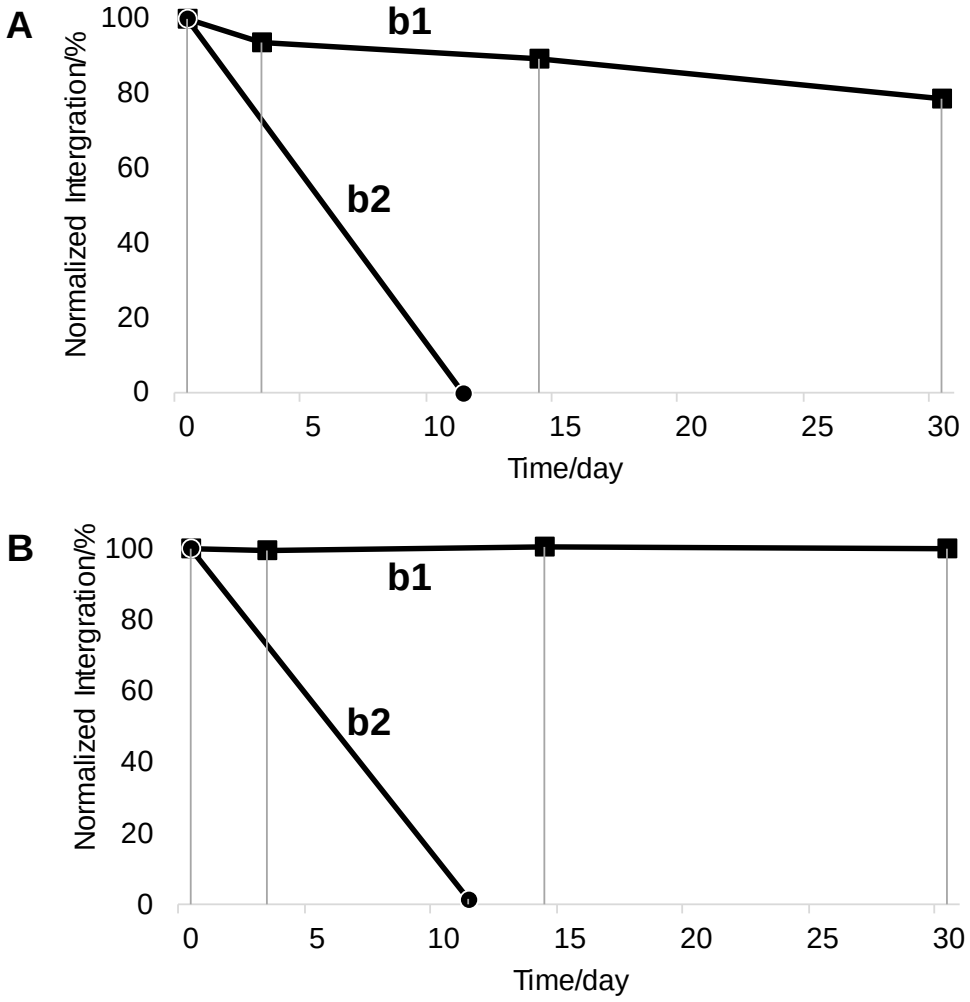

Figure 49 Ligustilide degradation in sealed NMR tubes in the presence (A) and absence of air, in particular oxygen (B, argon degassed sample). Test samples: ■ b1, ligustilide placed in a freezer; ● b2, ligustilide exposed to natural light at ambient temperature.

evaporation of solvent or volatile degradation products is prevented. The sealed tubes were weighted on the first and the last day of the experiment. No change in weight was measured, which confirms that no loss of solvent and degradation products had occurred, and, thus making this a true mass balance study.

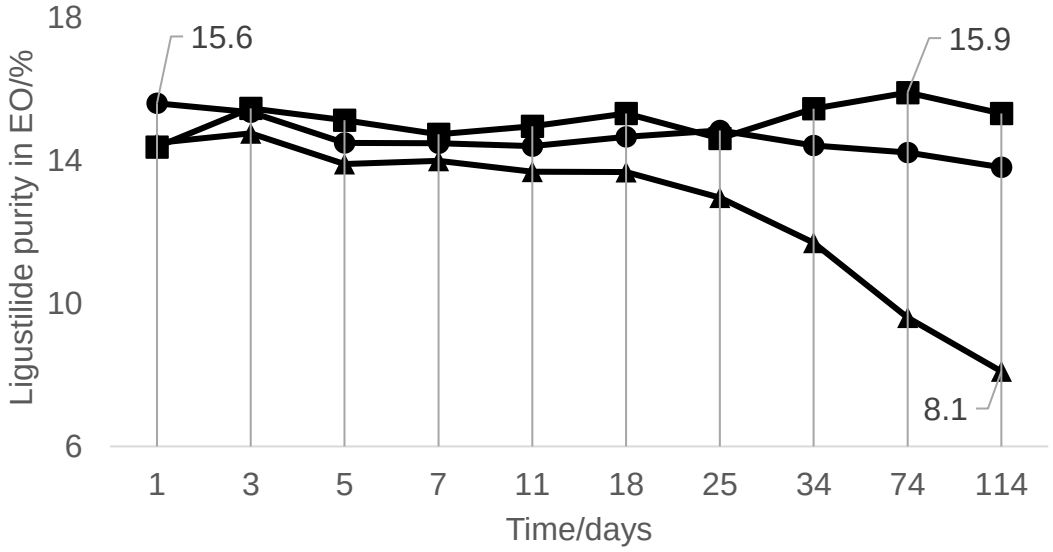

Figure 50. Stability study of ligustilide in *Angelica sinensis* essential oil. The ligustilide content (%) in EO was calculated from qHNMR data collected across 114 days. Test ligustilide samples: ■ c1, regular NMR sample preparation, stored in freezer; ● c2, NMR sample degassed using argon, then flame sealed, stored in freezer (-20 °C); ▲c3, NMR sample degassed using argon, then flame sealed, placed under natural light, at ambient temperature.

As shown in Figure 49, for the first 30 days, the ligustilides in samples (A) and (B) in freezer (b1) were hardly to recognize significant degradation. This suggests that air, most likely oxygen, is not the key factor, influencing ligustilide stability. Samples (A) and (B) were kept at ambient temperature and under daylight, nearly all the ligustilide decomposed within the next 10 days (Figure 49, b2). Combing with results from Figure 48, this indicates that photo-degradation is a key mechanism.

Ligustilide stability study in essential oil over 4 months. Three samples were used during the investigation. Each sample contained EO (20.0 mg) dissolved in 600 μL $CDCl_3$. Sample c1 was loaded in an NMR tube, a standard NMR tube cap was applied and sealed with parafilm, and the sealed tube placed in a freezer. The NMR

tubes loaded with samples c2 and c3 were degassed with argon and then flame sealed. Sample c2 was placed in a freezer, whereas sample c3 was placed at ambient temperature under daylight. During a four-month period, the ligustilide in each tube was quantified using qHNMR on day 1, 3, 5, 7, 11, 18, 25, 34, 74 and 114. As shown in Figure 50, the samples c1 and c2 which were stored in the freezer showed that ligustilide stability in the EO was regardless of the presence or absence of argon. On the last day (114), the samples c1 and c2 still maintained similar ligustilide levels, compared to the ligustilide in both samples on the day 1. However, in sample c3, 45.1% of the initial amount presence of ligustilide had degraded. This showed that daylight were both key factors for ligustilide stability. Interestingly, ligustilide degradation increased significantly after 18 days. Compared to highly pure ligustilide, which showed nearly 100% degradation within 10 days, the EO exhibited a remarkable capability of protecting ligustilide from daylight degradation.

In summary, as intermolecular interactions can be determined using NOESY NMR experiment, it suggests that some NADES species may exist in the *A. sinensis* EO. Meanwhile, ligustilide shows improved stability within both the normal *A. sinensis* EO and the original plant material, with less change in content after one year. In the EO, ligustilide stability was influenced mainly by temperature and light. This indicates that ligustilide may be protected by an EO NADES. Thus, the NADES may be involved in stabilizing mechanism of ligustilide in *A. sinensis* EO.

5.3. Study of the influence of NADES on Metabolic Stability

To form a therapeutic formula, TRMs or BDSs are usually used as crude extracts of an herbal mixture. The dominant content in the extract is mainly hydrophilic metabolites. This indicates that a potential relevant poly-pharmacological

mechanism may remain in practice of the TRMs or BDSs. Combining with NADES properties such as their solubilizing and stabilizing abilities for some natural products, these NADES metabolites in the form of NADES may play a vital role in the unexplored mechanism. Therefore, different NADES species were individually adopted for an investigation of their interaction with water soluble biomass in *Trifolium pratense* leaves using an aqueous hydrolysis model. Organic acid-based NADES exhibited a pronounced influence on the stability of isoflavone glycosides extracted from *T. pratense*. Altogether, the results revealed that NADES media can protect NPs (e.g., isoflavone glycosides) from hydrolytic degradation, and, thereby, may indirectly interfere with bioactivity mechanism of metabolites.

5.3.1. Establishment of a Hydrolysis Model for *T. pratense* Leaves

For the assessment of NADES function in a hydrolysis model, a single-factor optimization was performed initially. The three main impact factors, temperature (°C), hydrolysis time (h), and concentration in water (g/mL), were examined in preliminary experiments. Because the hydrolysis model was designed to investigate isoflavone glycoside degradation, a gradual degradation occurred in three days at 25°C, whereas only a small quantity of isoflavone aglycones (such as biochanin A and formononetin) can occur at 37°C. Thus, the model temperature was set as 25°C. To achieve adequate hydrolysis, a mixture of water and raw leaf material has to be completely suspended. Based on a series of observations (data not shown), a relatively large amount of water was required to suspend *T. pratense* leaf powder in the mixture media. Quantitatively, the ratio of the leaf powder to water should be equal to > 1:10 (g/mL). For a further optimum, hydrolysis time was screened with a ratio of 1:15 (g/mL) at 25°C. Normalized to the quantity of two target aglycones, i.e.,

TABLE XXI. ARTIFICIAL NADES SPECIES USED IN THE AQUEOUS HYDROLYSIS ASSAYS

NADES species	Abbr.	Component Ratio (mol/mol)	pH value
Maleic acid-Choline chloride-Water	MaCWat	2:5:5	< 4
Mannose-Dimethyl urea-Water	MDWat	2:5:5	5-6
Choline chloride-Urea-Water	CUWat	2:5:5	5-6
Glucose-Choline chloride-Water	GCWat	2:5:5	5-6
Glucose-Urea-Water	GUWat	2:5:5	5-6
Fructose-Urea-Water	FUWat	2:5:5	5-6
Citric acid-Choline Cl-Proline-Sucrose-Water	CChPSuWat	3:2:1:1:4	~ 4

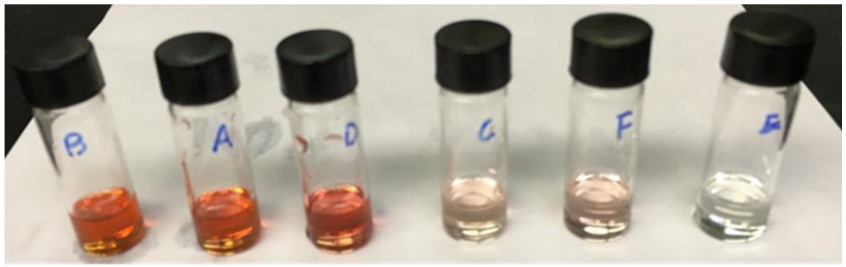

FUWat GUWat CUWat GCWat MDWat MaCWat

Figure 51. Reichardt's dye assay of the selected NADES species from Table XXI 0.5 mg of Reichardt's dye was dissolved in 1 mL of each of the NADES species.

biochanin A and formononetin, in the ethanolic extract of *T. pratense* leaves as unity, a 2.4-fold and 2.6-fold increase in these compounds was observed in a one-day aqueous hydrolysis, respectively. In a two-day assay, the yield was 2.6-fold for biochanin A, and stayed at 2.64-fold for formononetin. Accordingly, the hydrolysis model was subsequently operated using 1:15 (g/mL) ratio of material to water at 25°C, for 68 h.

5.3.2. Artificial NADES in the Hydrolysis Model

5.3.2.1. Investigation on Ternary NADES Species

Compared to other natural media, e.g., water and/or lipids, NADES species do not strictly follow the rule of like dissolves like: while NADES embody mostly highly polar constituents, they are still capable of dissolving hydrophobic molecules (Choi et al. 2011). Thus, NADES selection for experimental purposes is an empirical procedure.

To identify a most suitable NADES candidate(s) for this study, their polarity was studied using Reichardt's dye (Reichardt 1994). When dissolved in different solvents, the dye can absorb energy distinctly and, thus, yields different colors that reflect polarity intervals, which also indicates that the solvents may have other different properties such as solubilizing and stabilizing abilities. In this study, six NADES species, i.e. MaCWat, MDWat, CUWat, GCWat, GUWat, and FUWat (TABLE XXI), were chosen for screening their ability to inhibit the isoflavone hydrolysis. As shown in Figure 51, three major polarity intervals were covered. Expectedly, the NADES selection procedure can screen out a proper NADES for the experimental purpose.

Empirically, the kinetic energy in a NADES matrix may influence the matrix shape and size and, thus, potentially change the NADES solubilizing and stabilizing

abilities. At least two kinetic factors, water content and temperature, should be optimized in in hydrolysis model, because they may have directly influence on the isoflavone content after hydrolysis. A constant temperature (25°C) was adopted in all hydrolysis assays. Thus, the (volume) ratio of water to NADES in the hydrolysis system become the key factor in the evaluation of NADES function on hydrolysis. The (volume) ratio of water to NADES species was investigated, prior to determining the NADES function individually. For this purpose, a medium polarity NADES, GCWat, was selected, and four different ratios of water to NADES were investigated using optimized hydrolysis model. The absence of NADES was implemented as a control group (Figure 52). As a result, a GCWat to water ratio of 1:1 – 1:2.5 (v/v) exhibited the greatest inhibition for isoflavone hydrolysis: 74% biochanin A and 92% of formononetin (relative to the quantities of biochanin A and formononetin in the control group).

All selected ternary NADES species were evaluated using volume ratio of NADES to water content at 1:1 (v/v). As shown in Figure 53, MaCWat demonstrated the maximum inhibition of hydrolysis on the isoflavone glycosides, i.e. 93% inhibition of biochanin A and 94% of formononetin products. To assess the role of the pH value in the hydrolysis, all pH values of the selected NADES species were measured (TABLE XXI). While being among these nearly neutral NADES species, GCWat exhibited significant inhibition of isoflavone generation. In addition, the pH effects exhibited a contribution to the hydrolysis inhibition. Compared to the GCWat test group, MaCWat NADES exhibited a greater inhibitory effect. This indicated that organic acid-based NADES may be the potentially most promising NADES species, capable of protecting isoflavone glycosides from hydrolytic degradation.

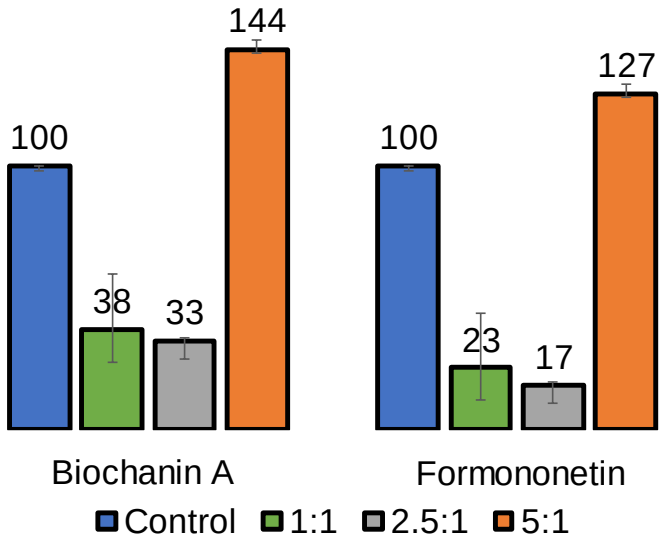

Figure 52. The hydrolysis assays with different water to GCWat ratios
Control represents a blank aqueous hydrolysis model; the volume ratios of water to GCWat in the hydrolysis model, 1:1, 2.5:1 and 5:1 (v/v), respectively. The y-axis was standardized to the content of biochanin A and formononetin in the control group, as unity. Compared to the control group, the volume ratio of water to GCWat at 1:1 (v/v) showed a significant inhibition of the hydrolysis of isoflavone glycosides to their aglycones.

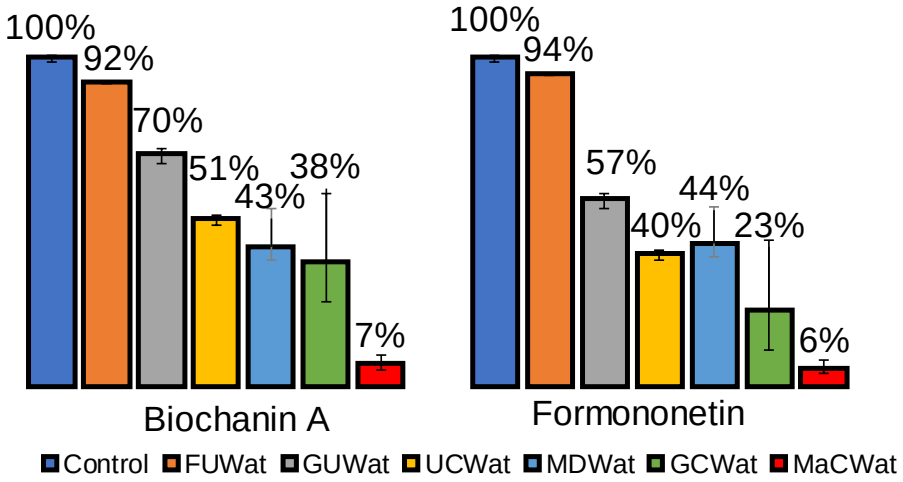

Figure 53. Study of hydrolysis inhibition of isoflavone glucosides using different artificial ternary NADES species
Control represents a blank aqueous hydrolysis model; the volume ratios of NADES to water used in the hydrolysis assay were 1:1, for all assays. The y-axis was standardized to the content of biochanin A and formononetin in the control group, as unity.

5.3.2.2. Investigation of multiple-component NADES species

To simulate the complexity of NADES matrices in natural sources, a multiple-component (organic acid-based) NADES, CChPSuWat as the test NADES (TABLE XXI) was evaluated. The CChPSuWat is a yellowish and highly viscous honey-like eutectic mixture). A ratio gradient (1:10, 1:5, 1:2.5, and 1:1, v/v) of CChPSuWat to water was tested in the hydrolysis model. Compared to the ternary NADES species, this multiple-component NADES medium had a higher inhibition capability (Figure 54). Quantitatively, over 90% inhibition of isoflavone aglycone formation can be achieved at a 1:5 (v/v) ratio of CChPSuWat to water. Apparently, ternary- and multiple-component NADES species display different behavior. Interestingly, although CChPSuWat provided a weaker acidic environment than MaCWat, it led to a greater inhibition. This indicates that pH is a less important factor, and that the chemical complexity and diversity of the NADES matrix also contributes to the NADES inhibitory function. These observations suggest that NADES matrices in botanical extracts may exhibit a similar or even more pronounced hydrolysis inhibition effect. Thus, raw plant sources or corresponding crude extracts may display efficiency in the protection of isoflavone glycosides and potentially other glycosidic NPs.

5.3.3. Interaction between of *S. chinensis* fruits and *T. pratense* leaves

5.3.3.1. Characterization of NADES components in *S. chinensis* fruits

S. chinensis as a traditional nutrient herb is popularly adopted as a BDS, and its crude extract was a highly viscous medium. As its fruits produce an abundance of organic acids, the fruit crude extract was similar to an organic acid-based NADES mixture/solution. To enrich such organic acid-based NADES solution, a HP-20 resin-

based fractionation was implemented using the MeOH crude extract of the *S. chinensis* fruit. All water fractions were combined together, and the recovery yield occupied 79%.

The preliminary studies (Figure 20 and 30) demonstrated that the real-time elution may contain ionic NADES or NADES components. For a preparative purpose, the CCS was scaled up into a large scale (300 mL) HSCCC instrument (Pharmtech, USA): the stationary phase volume retention ratio (Sf value) was 75%, and the extrusion mode was conducted after one total column elution, when the K value equals to 1. All CCS fractions were concentrated within a speed vacuum instrument, and then characterized using NMR, with the assistance of the online database

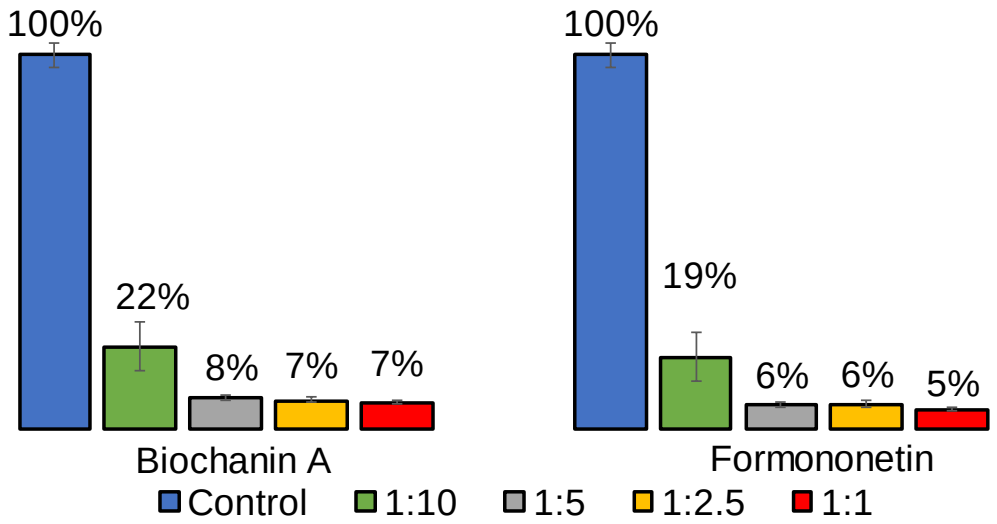

Figure 54. Study of isoflavone glycoside hydrolysis inhibition using a multiple component (citric acid-based) NADES, CChPSuWat. Control represents a blank aqueous hydrolysis model; the volume ratios of NADES to water used in hydrolysis assay were 1:10, 1:5, 1:2.5, and 1:1, respectively. The y-axis was standardized to the content of biochanin A and formononetin in the control group, as unity.

HMDB. The results showed that two organic acids, malic acid and citric acid, both being recognized as NADES components (Appendix E).

5.3.3.2. Investigation of *S. chinensis* fruit NADES matrix

To investigate the functional interaction between two botanicals, *S. chinensis* fruits and *T. pratense* leaves, two trial groups were examined using the hydrolysis model. To simulate the behavior formula used in the practice of TRM or BDSs, raw *S. chinensis* fruits were ground to particles, and then cocultured with powered of *T. pratense* leaves. Various ratios of *T. pratense* leaves to *S. chinensis* fruits (4:1, 2:1, 1:1, 1:3, and 1:6, wt/wt) were examined. As shown in Figure 55, it demonstrates that

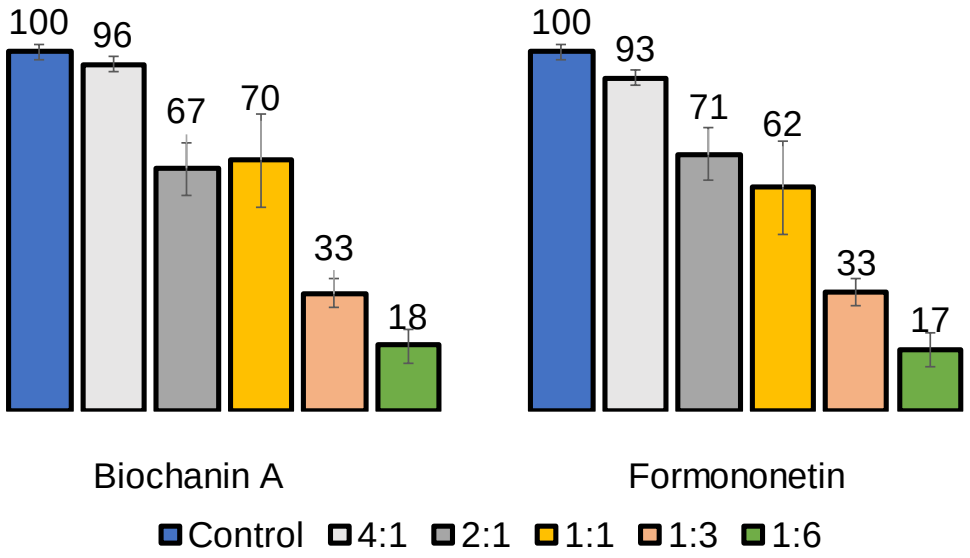

Figure 55. Study of the inhibition of the hydrolysis of isoflavone glycoside using the ground *S. chinensis* fruits. Control represents a blank aqueous hydrolysis model; the weight ratios of *S. chinensis* fruits to *T. pratense* leaves were 4:1, 2:1, 1:1, 1:3, and 1:6, respectively. The y-axis was standardized to the content of biochanin A and formononetin in the control group, as unity.

1.2 mg of *S. chinensis* fruit (equivalent to a ratio of *T. pratense* leaves to *S. chinensis* fruits, 1:6, wt/wt) can achieve over 80% hydrolysis inhibition. When the ratio was decreased to 4:1 (wt/wt), the inhibition becomes insignificant, like observed with the artificial NADES matrix (see Section 5.3.2.2), the inhibition was also concentration-dependent. Fundamentally, ingredients extracted from *S. chinensis* fruits were capable of regulating the hydrolysis of isoflavanone glycosides in *T. pratense* leaves. This suggests that, as the form of NADES matrix, crude herbal extracts from heterogeneous natural sources may provide a predominant poly-pharmacological effect in practice.

In order to validate the possible poly-pharmacological influence of NADES matrix in *S. chinensis* fruit on hydrolysis hydrolysis, the water fraction of *S.*

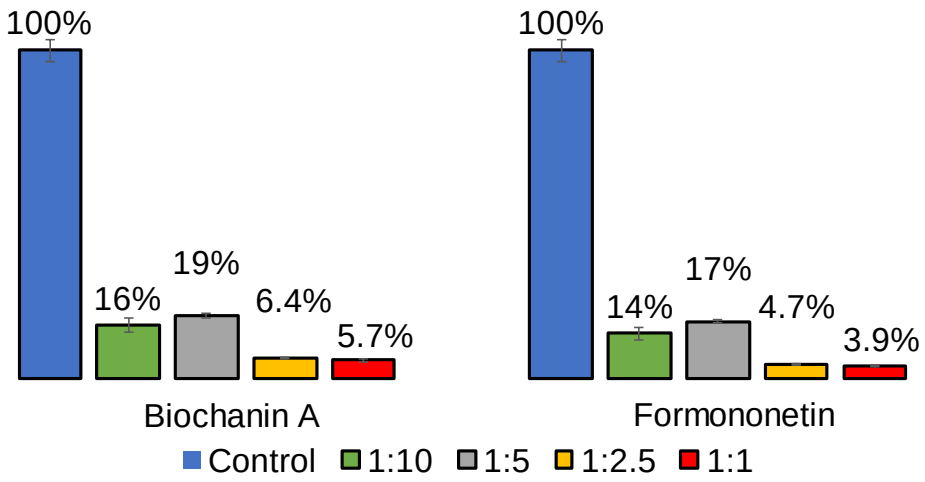

Figure 56. Study on hydrolysis inhibition of isoflavone glucosides using the water fraction of *S. chinensis* fruit methanolic extract. Control represents a blank aqueous hydrolysis model; the volume ratios of NADES to water used in hydrolysis assay were 1:10, 1:5, 1:2.5, and 1:1, respectively. The y-axis was standardized to the content of biochanin A and formononetin in the control group, as unity.

chinensis extract was independently evaluated as a test sample. As mentioned in section 3.2.1, an enriched organic acid-based NADES matrix was obtained through fractionation of a crude extract of *S. chinensis* fruits. The experimental design followed the described details in section 3.2.2. As shown in Figure 56, the results revealed that the NADES matrix in *S. chinensis* had a similar capability to inhibit hydrolysis, as the multi-component NADES species (CChPSuWat).

A quantitative analysis assessed the differences in the inhibition efficiency between raw fruits and their corresponding water fraction. The *S. chinensis* NADES matrix can be referenced in term of the quantity of *S. chinensis* fruits. For example, 1 mL of water fraction was measured as 2 g. Because the recovery yield of water fraction was 79%, it is equivalent to 2.53 g of crude *S. chinensis* fruit extract; because the extract yield of the crude extract was 62.7%, the corresponding raw fruits should be around 4 g. As shown in Figure 56, a ratio of *S. chinensis* NADES matrix (or water fraction) to water of 1:10 (v/v) caused inhibition of hydrolysis by about 80%. This effect was implied by 1.2 mL of the water fraction, equivalent to 2.4 g of raw fruits. In the meanwhile, at the level of 0.4 g of *T. pratense* leaves, the corresponding water content should be 6 mL in the hydrolysis model. Because the ratio of *S. chinensis* fruits to *T. pratense* leaves was 6:1 (wt/wt), hence, 2.4 g of *S. chinensis* fruit led to > 80% inhibition of the analyte hydrolysis. This demonstrated that the *S. chinensis* NADES matrix/water fraction is the main source and the primary contributor for the hydrolysis inhibition. Meanwhile, the inhibition capability of *S. chinensis* NADES was similar as that of the multi-component artificial NADES, CChPSuWat. This matches the hypothesis that *S. chinensis* fruits may contain a multi-component NADES species.

6. CONCLUSION AND GENERAL DISCUSSION

(Previously published as Liu Y., Friesen J.B., McAlpine J.B., Lankin, D.C., Chen, S.N., and Pauli, G.F. (2018) Natural Deep Eutectic Solvents: Properties, Applications, and Perspectives. J. Nat. Prod. 81 (3): 679–690.; Liu, Y., Friesen, J.B., McAlpine, J.B., and Pauli, G.F. (2015) Solvent System Selection Strategies in Countercurrent Separation, Planta Med. 81: 1-10.; Liu Y., Zhang Y., Chen, S.N., Friesen J.B., Nikolić D., Choules M.P., McAlpine J.B., Lankin, D.C., Gemeinhart R.A., and Pauli, G.F. (2018) The influence of natural deep eutectic solvents on bioactive natural products: studying interactions between a hydrogel model and Schisandra chinensis metabolites. Fitoterapia. In Press. Liu Y., Friesen J.B., Grzelak, E.M., Fan, Q., Tang, T., Durić, K., Jaki, B.U., McAlpine, J.B., Franzblau, S.G., Chen, S.N., and Pauli, G.F. (2017) Sweet Spot Matching: A TLC-based Countercurrent Solvent System Selection Strategy. J. Chromatogr. A 1504: 46-54.; Liu Y., Garzon, J., Friesen, J.B., Zhang, Y., McAlpine, J.B., Lankin, D.C., Chen, S.N., Pauli, G.F. (2016) Countercurrent assisted quantitative recovery of metabolites from plant-associated natural deep eutectic solvents. Fitoterapia. 112:30-37.)

Mainly due to demands for “green solvents”, NADES and related eutectic studies have rapidly gained attraction in the chemical and NP literature since 2011. Hence, this study reviews the reported basic NADES properties and applications. This benefits for further NADES investigation and even discovery. For example, a systematic analysis of designing binary NADES reveals that the component ratio is rarely over 1:6 (mol/mol) in a binary component system. This helps to modify the classic eutectic model (Figure 1), and to discover a eutectic mixture in NP lab, licochalcone A-EtOAc eutectic. Accordingly, the key aspects of NADES research can be successfully conducted, as follows.

(1) For NADES preparation, a reproducible ultrasound-vacuum centrifugal evaporation method was developed that was suitable for routine use in the NP laboratory. Over 20 NADES species were prepared using this strategy. Compared to the vortex dissolution method, the use of ultrasound reduced the dissolution time and the labor requirements, making it a more user-friendly approach. In addition, the water loss study was developed to measure the NADES preparation time via its

linear correlation equation in the NADES state.

(2) The water loss study also exhibited the change of intermolecular force among NADES components. Particularly, as diluting the NADES sample in a controlled fashion but, no more than five times, the intermolecular interaction (or nOe) of NADES components can be determined using a NOESY spectrum. In practice, the nOe determination became a very useful means to evaluate whether NADES have already been formed.

(3) Regarding the role of NADES in solubilizing NPs, a binding theory was proposed that complements the hole theory and enhances our understanding of the extraordinary solubilizing capabilities of NADES. Extra hydrogen bonding around lipophilic molecules may influence the solubility of both NADES components and lipophilic metabolites. For example, the solubility of proline in the formation of NADES was significantly improved in DMSO, demonstrating a potential co-solvent mechanism.

(4) CCS was shown to recover target lipophilic metabolites from NADES-containing botanical and other matrices. In more generalized terms, the CCS K-based approach can potentially be transferred to other low-level metabolites and be used to detect ppm levels of any target compound from natural or commercial products. The observed recovery efficiencies of targets ranged from 94.6% to 97%. As a proof of principle for the suitability of the GUESS prediction, the GUESS method was modified and applied to rapidly select the CCS solvent systems, thus, helping accelerate process development. The CherryOne instrument used in this study allowed an acquisition of UV and PMA signals of test samples or solvents. Because of a characteristic dispersion of PMA signal, the NADES components (e.g.,

glucose, choline chloride, citric acid and malic acid) could be detected during CCS elution.

The CCS recovery strategy overcomes the disadvantage of conventional LC methods. On one hand, CCS effectively solves the recovery challenge when using NADES as extraction media: regardless of whether NADES are contained in the extraction medium, are part of an experimental design, or occur as a natural phenomenon, the extracted target ingredients can be recovered, and the NADES components can be recycled as they remain nearly intact after CCS. This represents a potential contribution to the development of green chemistry. On the other hand, the hydrophilic metabolites in the botanical extract can be isolated from the crude extracts. This enables the investigation of the potential (poly-pharmacological) function of NADES in botanical extracts.

(5) NMR as a non-destructive detector was used for either qualitative (or identification) or quantitative analyses in this study. Quantification of the hydrophilic metabolites by quantitative NMR avoided the requirement of special liquid chromatography columns needed for analyses of hydrophilic compounds.

An off-line CCS-quantitative ^{1}H NMR (qHNMR) detection method was used for determining NPs. An authentic standard of each metabolite was isolated, characterized and quantified, e.g., ginkgotoxin, schisandrols A and B, and licochalcone A. Furthermore, quantitative ^{13}C NMR (qCNMR) was applied to NADES studies to analyze multiple-component NADES species, e.g., the multi-component NADES matrix, CChPSuWat. This strategy was equally suitable for quantitative analysis of the botanical extract, e.g., the quantities of sucrose and proline in licorice crude extract. Compared to qHNMR, qCNMR provides a broader spectral window

and, thus, the signals can easily be recognized. This avoiding potential overlap of NMR signals of highly hydrophilic metabolites, such as sugars, organic acids, and amino acids. On the other hand, for ^{13}C NMR, the extended experiment times resulting from low natural abundance and sensitivity of ^{13}C has historically prevented the further development of this method for pharmacopoeial analysis. Equally important, qNMR applied combined external/internal calibration (ECIC) with high-purity caffeine as EC and the residual solvent signal as IC.

(6) The special duality of NADES (lipophilicity and hydrophilicity) suggests their unique potential in small molecule formulation: NADES can carry lipophilic molecules and load them into a hydrophilic environment (e.g., hydrogels). Because of spontaneous diffusion by movement down a concentration gradient, NADES components can be removed gradually from the hydrophilic matrices. The observations in section **4.1** indicate that NADES may be structurally analogous to cyclodextrin, commonly used excipients in hydrophobic drug formulation. There was a demonstration with mannose-dimethylurea-water (MDWat, 2:5:5, mol/mol) as a model system that can behave as a "shuttle" by delivering the test marker compound (curcuminoid) into hydrogel beads and then spontaneously diffusing back into the chitosan solution during the preparation procedure. The marker ingredient exhibited a significant release efficiency. The crude extract (or NADES solution) of *S. chinensis* exhibited a similarity as MDWat-curcuminoid solution, which allowed lipophilic metabolites in NADES solution to be successfully loaded into the hydrogel polymer. This study validated the hydrogel model to be equivalent to a biopolymer, and capable of absorbing natural metabolites and allowing for their controlled release. Specifically, bioactive lignans (gomisin J, schisandrol B, and

angeloylgomisin H) were characterized in the released aliquots. This supports the broader hypothesis that NADES species (as natural solvents) related mechanism may improve the absorption of lipophilic molecules in TRM and BDSs. Thus, the established lignin-loaded model may display some related pharmacological activities, e.g., hepatic protective, anti-inflammatory, and anti-cancer effects (Lee et al. 2009; Na et al. 2010; Ryu et al. 2011; Kang et al. 2012; Wang et al. 2014; Jiang et al. 2015; Kim et al. 2015). Moreover, various alginate molecule weights determine the hole size of inner networks of a hydrogel and, thus, hydrogels derived from different alginate molecule weights may display a broad size selectivity for lipophilic metabolites and enable comparatively high loading efficiencies for specific compounds.

The hydrogels, composed of lipophilic metabolites loaded into chitosan-alginate beads, eliminates the use of organic solvents or surfactants to solubilize lipophilic components. It is composed of all-natural and biodegradable components and has potential for delivery formulation applications. Because it is still a challenge to load lipophilic drugs into an aqueous hydrogel, the solubility duality of NADES presents a viable option to overcome this hurdle. As an alternative solvent, the potential NADES effect on a whole organism (e.g., a bacterium) or a substructure of the organism (e.g., a cell) is still a major concern, which may limit its applications. This study presents NADES as a delivery “shuttle vector”. This avoids the potential impact, and also eliminates the solvent removal step that is needed when using organic solvents or chemical reactions in the preparation of delivery carriers.

(7) Some essential oil ingredients with low melting points, such as 1,8-cineole, p-cymene, D-limonene, menthol, menthone, or thymol, have been reported as

NADES components (Stott et al. 1998). In this study, intermolecular interactions between *A. sinensis* essential oil ingredients were determined using NOESY NMR experiment (data not shown). Meanwhile, ligustilide stability in EO was also investigated. The results showed that ligustilide was more stable in EO than in its purified form. Altogether, this suggests that NADES components may exist in *A. sinensis* EO, and probably influence on ligustilide stability. In future, fractionation will provide more evidence, and may find out NADES components from *A. sinensis* EO. By then, the influence of NADES on ligustilide stability will be completely clarified.

(8) Based on the NADES phenomenon, this work also investigated a potential interaction mechanism between herbal mixture. NADES matrix and raw *S. chinensis* fruits were involved into a hydrolysis model. The results revealed that the hydrolysis of isoflavone glucosidases may be regulated by NADES species. This implies that quantity regulation of NADES metabolites or administration of raw *S. chinensis* fruit extract is a means of controlling the yield of isoflavone aglycones in *T. pratense* leaf extract. Interestingly, as NP research often ignores the water fraction as "inactive" or irrelevant for bioactivity, the present study demonstrates that the NADES metabolites (e.g., citric acid and malic acid) in *S. chinensis* may stabilize NPs in *T. pratense* leaves. This provides direct evidence for the beneficial effects of exogenous sources of NADES, e.g., from other herbs. Multi-herbal preparations may regulate the occurrence of endogenous substances. This may represent a potential mechanism of complex TRM formulae and BDS products. Organic acid-based NADES exhibited an especially significant influence on the hydrolytic stability of

isoflavone glycosides extracted from *T. pratense*. Subsequently, an organic acid enriched herbal source, such as *S. chinensis* fruits warranted further assessment.

(9) This study also sheds light on the recent trends toward a series of NADES applications, which facilitates a discussion around the NADES functions in NP research and biological systems in general. The quest for determining their natural role and the appeal of finding novel applications create several major areas for future scientific inquiry regarding NADES research and applications: (i) NADES properties are directly associated with their components. Although 174 NADES species have already been described, the discovery of new NADES components and/or species will likely continue to be a major focus. Currently, NADES components are considered to be derived primarily from plant sources. Nevertheless, all metabolites produced by natural sources, including microorganisms and animals, have to be considered as potential NADES components. (ii) NADES species exhibit significant solubilizing selectivity for some natural products, which represents both opportunities and challenges in their applications. This partially explains how Nature formulates lipophilic ingredients without the assistance of organic solvents. However, this is also equivalent to the solubilizing exclusivity for others. Following this logic, although it is still unclear how such a mechanism works in Nature, it may be helpful for natural product enrichment in a specific tissue or organ in a living organism. For natural product research, such NADES species may not be good solvent candidates for a universal extraction purpose. (iii) In order to develop efficient NADES experiments and applications, practitioners must consider the inherent properties of NADES. For example, due to the relatively weak chemical force of intermolecular interactions

among NADES components, it is challenging to preserve an entire NADES matrix after a dilution. The ability of NADES to act as solubilizing agents or solvents in bioassays for the improvement of lipophilic analyte solubility will require validation of the impact of NADES in any given experiment/application. (iv) Documented observations of NADES in Nature are still limited, in particular with regard to their chemical diversity. Accordingly, study models are still in high demand that can reveal the biologically relevant and/or "cooperative" functions of NADES in natural sources, dietary supplements, and traditional medicinal formulae and whether they are physical or biochemical in type, or both. Except hydrogel and hydrolysis models, new experimental designs will need to be developed to observe NADES behavior more directly, to further our understanding of the already known or to uncover new NADES phenomena and develop potential applications. (v) The intriguing role of water molecules in NADES triggers the reasonable hypothesis that some liquid/gaseous ingredients may serve as NADES components. However, this type of NADES components is reported only rarely. Interestingly, results from a study aimed at the purification of licochalcone A from a plant extract serve to validate the general feasibility of this hypothesis. This suggests that other organic solvents such as 1,3-propanediol, EtOAc, EtOH, and *n*-BuOH, which are used widely in NP studies, may also serve as eutectic components. This piece of evidence is in-line with the general experience in the NP chemistry laboratory with regard to two broader observations: the frequent occurrence of (semi)liquids as isolation products of compounds that should form solids at ambient temperature and the frequent occurrence of EtOAc as residual solvent in purified NPs and commercial reference materials, which can be readily detected by quantitative ^{1}H NMR spectroscopy. The

potential broader impact of such phenomena on NP research makes it an important consideration for future work. (vi) NADES components are very common in organisms (most studied in plants) and their extracts. They frequently are major constituents in crude NP-derived materials, and, thus, NADES could be a dominant form of biomass in Nature. Considering the validity of the mass balance approach to the analytical description of biomedical intervention materials, in particular drugs, this suggests that NADES components should be considered more widely as candidate marker compounds for NP-derived materials. For example, extending botanical quality control to NADES will be a means of capturing the chemistry of these complex materials with a much-expanded latitude.

In summary, there is growing evidence that the NADES phenomenon has broadly impacts NP research, in particular TRMs and BDSs. This is expected to prompt the studies of the potential functions of the NADES in either the natural source or products derived from these sources.

7. EXPERIMENTAL SECTION

(Previously published as Liu Y., Friesen J.B., McAlpine J.B., Lankin, D.C., Chen, S.N., and Pauli, G.F. (2018) Natural Deep Eutectic Solvents: Properties, Applications, and Perspectives. J. Nat. Prod. 81 (3): 679–690.; Liu, Y., Friesen, J.B., McAlpine, J.B., and Pauli, G.F. (2015) Solvent System Selection Strategies in Countercurrent Separation, Planta Med. 81: 1-10.; Liu Y., Zhang Y., Chen, S.N., Friesen J.B., Nikolić D., Choules M.P., McAlpine J.B., Lankin, D.C., Gemeinhart R.A., and Pauli, G.F. (2018) The influence of natural deep eutectic solvents on bioactive natural products: studying interactions between a hydrogel model and *Schisandra chinensis* metabolites. Fitoterapia. In Press. Liu Y., Friesen J.B., Grzelak, E.M., Fan, Q., Tang, T., Durić, K., Jaki, B.U., McAlpine, J.B., Franzblau, S.G., Chen, S.N., and Pauli, G.F. (2017) Sweet Spot Matching: A TLC-based Countercurrent Solvent System Selection Strategy. J. Chromatogr. A 1504: 46-54.; Liu Y., Garzon, J., Friesen, J.B., Zhang, Y., McAlpine, J.B., Lankin, D.C., Chen, S.N., Pauli, G.F. (2016) Countercurrent assisted quantitative recovery of metabolites from plant-associated natural deep eutectic solvents. Fitoterapia. 112:30-37.; Liu, Y., Chen, S.N., McAlpine, J.B., Klein, L.L., Friesen, J.B., Lankin, D.C., and Pauli, G.F. (2014) Quantification of a botanical negative marker without an identical standard: ginkgotoxin in *Ginkgo biloba*, J. Nat. Prod. 77(3):611-617.)

7.1. Materials and Reagents

Choline chloride, chitosan, dimethylurea, D-(+)-fructose, D-(+)-glucose, D-(+)-mannose, maleic acid, sodium alginate, urea, curcumin (from *Curcuma longa*), rutin, all HPLC or UHPLC grade solvents, DMSO-d_6 (99.9 atom % D) and polyester membrane cell culture inserts were purchased from Sigma-Aldrich Inc. (St. Louis, MO, USA). Acetic acid and calcium chloride were obtained from Fisher Scientific (Hampton, NH, USA). The isoflavone standards were purchased from Indofine Chemical Co. (Hillsborough, NJ). Quercetin, kaempferol, and daidzein were obtained from the UIC/NIH Center for Botanical BDSs Research. All analytical grade solvents were purchased from Pharmco-AAPER (Crookfield, CT, USA) and redistilled before use.

Whole *G. biloba* seeds (commercial name: White Nut, Hongchanglong, China) were purchased at a local grocery store in Chinatown, Chicago. Powdered *G. biloba*

leaves were sourced from Mountain Rose Herbs (Lot No.: M10579, Eugene, OR, USA). Both samples were stored at -20°C until analyzed. Pyridoxine hydrochloride, caffeine (>99%) and $CDCl_3$ (99.9 atom % D) were obtained from Sigma-Aldrich Inc. (St. Louis, MO, USA). The leaves of *T. pratense* (BC 719) were collected in Illinois, USA. The dried fruits of *S. chinensis* (BC 805) were purchased at a local grocery store in Chinatown, Chicago. Voucher specimens (*T. pratense* leaf, BC 719 and *S. chinensis* fruit, BC 805) was deposited in the storage room of the UIC Botanical center, Chicago, IL. All herbal samples were stored at –20°C.

7.2. Countercurrent Separation (CCS)

7.2.1. CCS Solvent Systems Selection

Empirically, the HEMWat family was used for the non-polar targets, the (H)ChMWat family was applied to the medium-polar targets, and the EBuWat family was adopted for the polar targets. Biphasic solvent systems (SSs) from the CCS SS families were assayed using the TLC-based Generally Useful Estimate of Solvent Systems (GUESS) strategy or solvent partition ("shake-flask") trials. (i) The GUESS method was used for the selection of the biphasic SSs. Target analytes were dissolved in MeOH (1 mg/mL) and spotted individually on silica gel TLC plates (Macherey-Nagel, USA). All TLC plates were developed with the organic phase of the candidate SS, and the resulting chromatograms were screened for ones in which the Rf value of the test sample was close to 0.5. (ii) For the solvent partition trials, the following procedure was used: in a separatory funnel, 1 to 5 mg of the target analyte was added to 10 mL of a mixture containing equal volumes of the upper and lower phases of the two-phase SS, and the mixture was shaken adequately to equilibrate the sample. Equal volumes of each phase, UP and LP, were separated

and evaporated. Then the K value can be calculated using quantitative NMR, following Equation 5.

7.2.2. High-Speed Counter-Current Chromatography (HSCCC)

HSCCC was performed using a TBE-20A HSCCC (20 mL, Tauto Biotech, China), equipped with a 500 μL sample coil, pump, UV detector, thermostatic circulator, and data processing system (Cherry One, Cherry Instruments, Chicago, IL). The procedure was as follows: a certain amount (mg) of test sample were dissolved in 500 μL of CCS SS made-up from equal parts of the two phases. The solution was loaded into the injection loop. Then, the column was rotated at 800 rpm and filled with UP as the stationary phase. The LP was pumped as the mobile phase in a head-to-tail direction at a flow-rate of 0.5 mL/min, and the column was rotated at 2000 rpm. After the hydrodynamic equilibrium between the two phases was reached, i.e., the eluate had changed from stationary to mobile phase, the sample solution was injected through the six-port valve. Throughout the CCS operation, the stationary phase volume retention ratio (Sf), the partition coefficient (K), and the eluting phase (phase metering apparatus, PMA) were monitored and recorded by the CherryOne data system. Outflow was collected by a Foxy Jr. Fraction Collector (Teledyne Isco, Lincoln, NE, USA) and matched to the recorded K values.

Once a proper CCS SS was obtained. A large scale HSCCC was performed using Pharmtech-1000 HSCCC instrument (320 mL, Pharmtech, USA). The quantity of sample loading was limited to 300 mg, and the flow rate was 1.0 mL/min. The fractions were concentrated using vacuum centrifugal evaporation (a Speedvac system, Thermo Scientific, Waltham, MA, USA) at 37°C under vacuum, and subject to NMR analyses.

7.2.3. Centrifugal Partitioning Chromatography (CPC)

An FCPC instrument (185 mL, Kromaton Technologies, France) was applied for the CCS in this study. The hydrogel released samples were diluted with both upper and lower phase (2 mL of each), then loaded into the sample loop (10 mL). Reversed phase mode (equivalent to lower phase mobile) was used in all FCPC operations. An elution mode of lower phase as mobile phase was conducted at 1100 rpm rotation speed and in 8.0 mL/min of flow rate. The fractions were dried by vacuum centrifugal evaporation and subject to NMR analyses.

7.3. NMR Analyses

7.3.1. NMR Sample Preparation

Each sample was dried under vacuum (<1 mbar) in a desiccator overnight. Samples of each were dissolved in deuterated solvents (e.g., $CDCl_3$, DMSO-d_6, and D_2O) delivered with a 1000 µL analytical syringe (Valco Instruments, Baton Rouge, LA). NMR spectra were acquired on a BRUKER DPX-360 NMR spectrometer in 5 mm tubes with 500 µL of test samples or on a JEOL 400 MHz NMR spectrometer in 3 mm tubes with 200 µL of test samples at 25°C.

7.3.2. NMR Acquisition Parameters

Acquisition of quantitative ^{1}H NMR was as follows: acquiring a total of 64 scans (NS), 4 dummy scans (DS), and 4 s of acquisition time (AQ), collecting 32k of time domain (TD) data, and using a 90 degree excitation pulse and a relaxation delay (D1) of 60 s. Acquisition of ^{13}C NMR was as follows: acquiring a total of 2048 scans (NS), collecting 32k of time domain (TD) data, and using a relaxation delay (D1) of 2 s. Acquisition of ^{1}H-^{13}C Heteronuclear Single-Quantum Correlation (HSQC) NMR was as follows: setting the spectral width (SW) F2 in ppm for ^{1}H, transmitter frequency

offset for channel F2 in Hz (O2P) in ppm – middle of the ^{1}H spectrum, spectral width (SW) F1 in ppm for ^{13}C, transmitter frequency offset for channel F2 in Hz (O1P) in ppm – middle of the ^{13}C spectrum, ^{1}H T2 value (CNST2) at 150 Hz by default, and acquiring a total of 16 scans (NS). Acquisition of ^{1}H-^{1}H nuclear Overhauser effect spectroscopy (NOESY) NMR was as follows: setting the spectral width (SW) F2 equal to the spectral width (SW) F1, transmitter frequency offset for channel F1 in Hz (O1P) in ppm – middle of the ^{1}H spectrum, acquiring a total of 16 scans (NS), and using 8 s of the relaxation delay (D1) and 400 ms or 600 ms as mixing time (D8). Receiver gain (RG) in 2D experiments was set automatically by RGA.

7.3.3. NMR Data Processing

The spectra were processed using MestReNova v10.0.1 (Mestrelab Research, Santiago de Compostela, Spain) software. For 1D NMR, the line resolution was improved by applying a Gaussian-Lorentzian window functions (GB 0.05 and LB -0.3) and four times zero-filling prior to Fourier transformation of the FID. Baseline correction used a 5th order polynomial function, and phase correction was performed manually.

7.3.4. Quantitative NMR calculation with ECIC method

$CDCl_3$ or DMSO-d_6 was selected as the solvent for all qNMR analyses. Due to the NMR is a molarity-based quantification, this work mainly used caffeine as external calibrant (EC) and the residual solvent signal ($CHCl_3$ in $CDCl_3$ or DMSO-d_5 in DMSO-d_6) for a combined external/internal calibration (ECIC, also see examples of qCNMR in Figure 57 and TABLE XXI or of qHNMR in article) (Liu, et al. 2014).

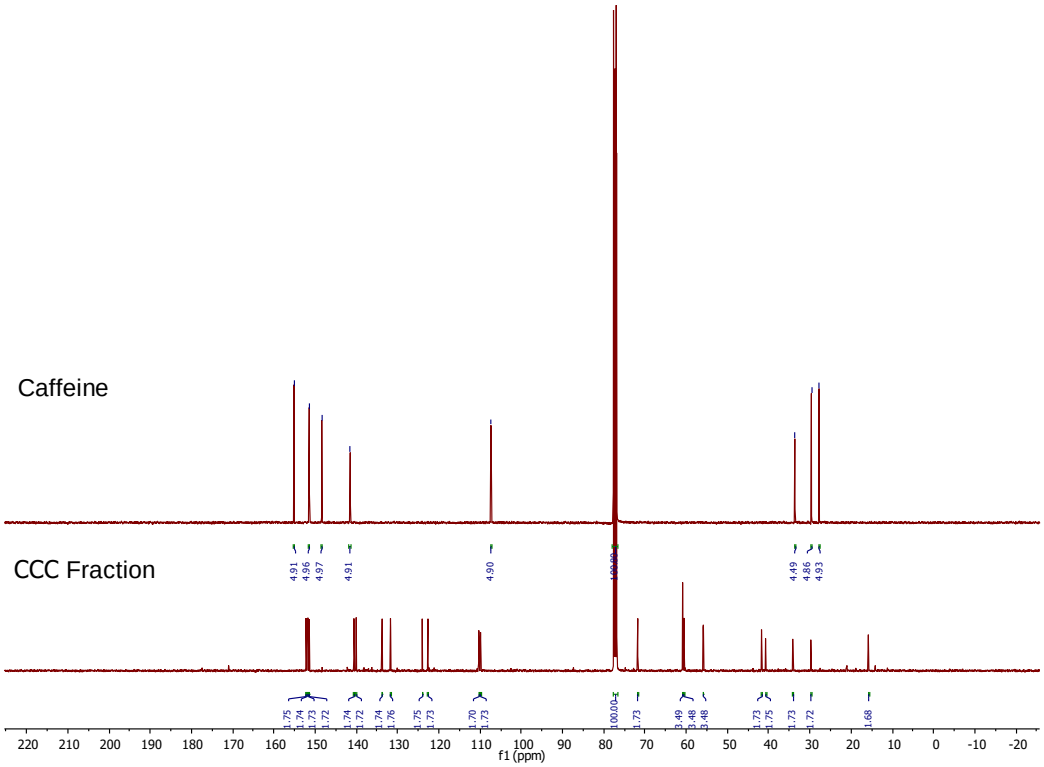

Figure 57 Purity determination of schisandrol A using qCNMR, ECIC strategy

Using the qCNMR results as an example, all data were obtained based on NMR peak area (integration). From the NMR and LC-MS analysis, the method specificity for schisandrol A is clearly confirmed, and CCS fraction was weighted as 21.8 mg. As spectra in Figure 57, the signal to noise ratio should be > 10, corresponding to LOQ. It normalized integral average of schisandrol A (molecular weight/M.W., 432.51 g/mol) was 1.73, and that of caffeine (25.0 mg, M.W., 194.19) was 4.92. the content of schisandrol A contained in the investigated CCS fraction can be calculated using the following equation $\frac{M.W.(RS)}{M.W.(Cal.)} = \frac{Wt(RS)}{Int(RS)} \times \frac{Int(Cal.)}{Wt(Cal.)}$. The schisandrol A was shown to be 19.61 mg, and its purity in CCS fraction was 90%. All qNMR analysis in this work followed the same quantitative procedure. In some special cases, alternative

external standard was used to replace caffeine.

7.4. (U)HPLC Analyses

7.4.1. HPLC Analyses

Prior to HPLC analyses, all concentrated samples were dissolved in equal volumes of acetonitrile-water (1:1, v/v). Analytical HPLC was performed on Waters 2695 system using Agilent ZORBAX SB-C18 analytical column (4.6 × 250 mm, Santa Clara, CA). For curcumin study, the sample was 100 μL of curcuminoid saturated NADES solution in 400 μL of MeOH. 10 μL of sample was injected. A Waters 996 PDA detector was used to monitor the absorbance of the eluent at 390 nm. For the NADES recovery study, the mobile phase consisted of MeOH/Water with a gradient run initiated with 30:70 and linearly increased to 95:5 under 0.8 mL/min, in 15 min, and at 25°C.

Regarding the *T. pratense* hydrolysis investigation, the binary mobile phase consisted of solvent A (water with 0.1% formic acid, v/v) and B (acetonitrile with 0.1% formic acid, v/v). A method with a flow rate of 1.0 mL/min and the gradient elution was performed, as follows: A/B (v/v) 100/0 to 60/40 from 0 - 20 min, hold at 60/40 from 20 - 22 min, 60%/40% to 10%/90% from 22 - 60 min, followed by a 24-min post-run for column reconditioning with solvent B (10 min) and solvent A (14 min). The detection wavelength was set from 210 to 400 nm. Injections of each sample (10 μL) were analyzed.

For the investigation of *S. chinensis* metabolites, preparative HPLC was performed on a Waters 600 controller with a Delta 600 pump and 717plus autosampler, using a YMC-pack ODS-AQ column (10 × 250 mmI.D., YMC, South Korea). The sample was dissolved in MeOH. 100 μL of sample solution was injected

per run. A Waters 2996 PDA detector was used to monitor the absorbance of the eluent at 254 nm. The mobile phase consisted of ACN/Water with a gradient run initiated with 60:40 and increased linearly to 95:5 under 1.5 mL/min, in 65 min, and at 25°C. Empower™ software (Waters Corporation, Milford, MA) was used to acquire, process, and analyze the chromatographic data. Areas under the curve from experimental peaks in the chromatogram were determined, and the percent weight of each compound present was calculated based on calibrated standard curves, considering the quantities of the injected test samples. Each HPLC analyses were calibrated using standard samples.

7.4.2. UHPLC Analyses

These were performed on a Shimadzu's Nexera ultra high-performance liquid chromatography system (UHPLC, Shimadzu Corporation, Kyoto, Japan) equipped with a Waters Acquity UPLC BEH C18 (2.1 × 5.0 mm, 1.7 µm) column and a diode array detector (DAD, Shimadzu SPD-M20-A). The autosampler temperature was set to 4°C, and the column oven temperature was set to 40°C. Post-run data analyses were performed using the Shimadzu LabSolution software package. Analytes were dissolved in MeOH (1 mg/mL, HPLC grade, Fisher Co. Ltd.) and filtered (Acrodisc CR 13 mm, 0.20 µm PTFE membrane) prior to injection (10 µL).

7.5. Preparation of Natural Deep Eutectic Solvent and Related Solutions

The ultrasound-centrifuge evaporation method was applied (see section 3.1). According to the desired molar ratio, the mass of each NADES component was calculated initially. The two solid components were weighed into a vial and excess water was added. For example, glucose-choline chloride-water (GCWat, 2:5:5, mol/mol) was prepared as follows: glucose (0.01 mol) and choline chloride (0.025

mol) were dissolved in distilled water (2 mL) and treated in an FS140 ultrasonic bath (Fisher Scientific, Loughborough, UK) until particles were completely dissolved. Then, the solution was placed in a Speedvac system (Thermo Scientific, Waltham, MA, USA) to remove water for 14.4 h. The Speedvac system consisted of an SC250 Express SpeedVac Concentrator (37°C and 4.7 torr), a RVT4104 Refrigerated Vapor Trap (4 L and -104°C) and an OFP 400 Vacuum Pump. After centrifugal evaporation, the NADES liquid was weighed. If water loss was more than the target amount of water, a certain amount of water was added into the liquid. Then, for equilibration, the liquid in a vial was placed into an ISOTEMP 110 water bath (Fisher Scientific, Loughborough, UK) at 37°C for over 1 h until a uniform solution was obtained.

NADES-analyte solutions were prepared as follows: the analytes were mixed with the appropriate volume of NADES in a vial. The vial was then placed into an ISOTEMP 110 water bath (Fisher Scientific, Loughborough, UK) at 37°C for 24 h. The mixture was then filtered, and the filtered solution was used as NADES test solution and stored at 25°C. As the NADES test solutions were in saturated. They were placed into a water bath at 37°C for 30 min prior to use.

7.6. Preparation of Hydrogel Beads

A sodium alginate solution (0.2 g/mL) was prepared by dissolving 6 g of sodium alginate in 30 mL of distilled water under constant stirring (Hotplate-Stirrer, Fisher Scientific, Hampton, NH). A chitosan solution (5 mg/mL) was prepared by dissolving 450 mg of chitosan and 5.4 g of $CaCl_2$ in 90 mL of distilled water, and 1 mL of acetic acid was added to facilitate chitosan dissolution under constant stirring and heating at 50°C until the solid was dissolved. To prepare curcuminoid loaded hydrogel beads, 500 µL of alginate solution and 500 µL of NADES solution were combined in

a 5 mL test tube using a 1 mL syringe. The alginate/NADES mixture was then vortexed (Vortexer 59, Labnet International Inc., Woodbridge, NJ) to obtain a uniform solution, and then transferred into the insulin syringe (0.5 mL, 100 U BD ultra-fine™, EXEL International Medical Products, Redondo Beach, CA). The alginate/NADES solution was added dropwise by using an insulin syringe into 20 mL of a chitosan solution placed in a 50 mL of round flask under constant stirring at 5 cm above the chitosan solution surface. After all beads were formed, the beads were hardened by keeping the solution stirring for another 15 min. A new chitosan solution was used for each experimental group. Beads were collected and washed with distilled water 5 times, then 60 mg of beads were weighed into vials and stored at 4°C before further use.

7.7. Crude Extract Preparation of *Ginkgo biloba* Seeds

The outer shells of the seeds were peeled off, and the meat was dried at 37°C, then powdered by trituration and stored at -20°C. Extraction was performed, briefly as follows: 100 g of the powder were transferred to a 1 L flask, 500 mL of freshly distilled MeOH were added, and the mixture was shaken at low speed for 1 h. The extract was filtered, and each extraction was performed three times. The combined extract solutions were concentrated on a rotary evaporator at 30°C under vacuum. The concentrated sample was stored at -20°C.

7.8. Preparation and Hydrolysis of *T. pratense* Leaves

The leaves of *T. pratense* were dried at 25°C and then powdered using a grinder (KitchenAid - St. Joseph, Michagan USA; Made in China). When the particles tended to form a uniform size, the powdered leaves were collected and then stored at 25°C. Hydrolysis was performed as follows: the designed quantity of the powder was

placed into a 25 mL capped vial. Distilled water was added to reach the material to water ratio (usually 1:12 or 1:15 g/mL). Then the vial was placed into a Hybridizition Incubator (Lab-Line Instruments) for the hydrolysis assays at 25°C for 68 h. After the hydrolysis, an equal volume of EtOH was added to aid the extraction of the isoflavone aglycones produced by hydrolysis. The solution was then filtered through filter paper, and all solvents removed using a rotary evaporator at 25°C under vacuum. The concentrated sample was stored at -20°C until HPLC analysis.

7.9. Crude Extract Preparation of *S. chinensis* Fruits

The raw fruits of *S. chinensis* were dried at 25°C, and then ground into small particles. These particles were store at 4°C until use. The ground raw fruits were subjected to a methanolic extraction (800 mL/time, four times totally). A concentrated crude MeOH extract was obtained after evaporation using a rotary evaporator at 37°C under vacuum.

To enrich the hydrophilic NADES mixture of *S. chinensis* fruits, 105 g of the crude extract was placed onto a 300 g HP-20 column (Diaion® HP-20, particle size: 250-850 μm; pore size: ~1.30 mL/g pore volume and 260 Å mean pore size; surface area: ~500 m^2/g, and density: 1.01 g/mL) at 25°C. The order of elution was as follows: water, 25% MeOH, MeOH, and Acetone. Distilled water was used as the first eluting solvent. The bed volume (BV) was measured as 1500 mL, and elution volume of each fraction was 10 L. The flow rate was 20 mL/min in a day, and 4 mL/min in a night. All fractions were concentrated using a Rotovap at 37°C under vacuum.

9. REFERENCES

Abbott, A. P., D. Boothby, G. Capper, D. L. Davies and R. K. Rasheed (2004). "Deep eutectic solvents formed between choline chloride and carboxylic acids: versatile alternatives to ionic liquids." Journal of the American Chemical Society **126**(29): 9142-9147.

Abbott, A. P., G. Capper, D. L. Davies, R. K. Rasheed and V. Tambyrajah (2003). "Novel solvent properties of choline chloride/urea mixtures." Chemical Communications (1): 70-71.

Aroso, I. M., R. Craveiro, Â. Rocha, M. Dionísio, S. Barreiros, R. L. Reis, A. Paiva and A. R. C. Duarte (2015). "Design of controlled release systems for THEDES—Therapeutic deep eutectic solvents, using supercritical fluid technology." International Journal of Pharmaceutics **492**(1): 73-79.

Artursson, P., K. Palm and K. Luthman (2001). "Caco-2 monolayers in experimental and theoretical predictions of drug transport1PII" Advanced Drug Delivery Reviews **46**(1): 27-43.

Azaizeh, H., B. Saad, E. Cooper and O. Said (2010). "Traditional arabic and islamic medicine, a re-emerging health aid." Evidence-based Complementary and Alternative Medicine **7**(4): 419-424.

Bai, X., I. B. Park, H.-J. Hwang and J.-H. Mah (2015). "The ability of *Schisandra chinensis* fruit to inhibit the growth of foodborne pathogenic bacteria and the viability and heat resistance of Bacillus cereus spores." International Journal of Food Science and Technology **50**(10): 2193-2200.

Beck, V., U. Rohr and A. Jungbauer (2005). "Phytoestrogens derived from red clover: An alternative to estrogen replacement therapy?" The Journal of Steroid Biochemistry and Molecular Biology **94**(5): 499-518.

Bergstrom, F. W., H. G. Sturz and H. W. Tracy (1946). "The use of the fused eutectic of sodium amide and potassium amide in organic syntheses." The Journal of Organic Chemistry **11**(3): 239-246.

Bisson, J., J. B. McAlpine, J. B. Friesen, S.-N. Chen, J. Graham and G. F. Pauli (2016). "Can invalid bioactives undermine natural product-based drug discovery?" Journal of Medicinal Chemistry **59**(5): 1671-1690.

Booth, N. L., C. R. Overk, P. Yao, J. E. Burdette, D. Nikolic, S.-N. Chen, J. L. Bolton, R. B. van Breemen, G. F. Pauli and N. R. Farnsworth (2006). "The chemical and biological profile of a red clover (*Trifolium pratense*) phase II clinical extract." Journal of Alternative and Complementary Medicine **12**(2): 133-139.

Booth, N. L., C. R. Overk, P. Yao, S. Totura, Y. Deng, A. S. Hedayat, J. L. Bolton, G. F. Pauli and N. R. Farnsworth (2006). "Seasonal variation of red clover (*Trifolium*

pratense L., Fabaceae) isoflavones and estrogenic activity." Journal of Agricultural and Food Chemistry **54**(4): 1277-1282.

Calatayud, J. and Á. González (2003). "History of the development and evolution of local Anesthesia Since the coca leaf." Anesthesiology **98**(6): 1503-1508.

Cao, X. L., Y. T. Xu, G. M. Zhang, S. M. Xie, Y. M. Dong and Y. Ito (2006). "Purification of coenzyme Q10 from fermentation extract: high-speed counter-current chromatography versus silica gel column chromatography." Journal of Chromatography A **1127**(1-2): 92-96.

Chen, C.-C. and P. A. Crafts (2006). "Correlation and prediction of drug molecule solubility in mixed solvent systems with the nonrandom two-liquid segment activity coefficient (NRTL–SAC) model." Industrial and Engineering Chemistry Research **45**(13): 4816-4824.

Chen, C.-C. and Y. Song (2004). "Solubility modeling with a nonrandom two-liquid segment activity coefficient model." Industrial and Engineering Chemistry Research **43**(26): 8354-8362.

Chen, J., Y. Yu and Z. Li (2005). "Accurate calculation for liquid–liquid equilibria of typical solvent systems used in CCC." Journal of Liquid Chromatography and Related Technologies **28**(12-13): 1937-1946.

Chen, L., Q. Zhang, G. Yang, L. Fan, J. Tang, I. Garrard, S. Ignatova, D. Fisher and I. A. Sutherland (2007). "Rapid purification and scale-up of honokiol and magnolol using high-capacity high-speed counter-current chromatography." Journal of Chromatography A **1142**(2): 115-122.

Chen, L., Q. Zhang, G. Yang, L. Fan, J. Tang, I. Garrard, S. Ignatova, D. Fisher and I. A. Sutherland (2007). "Rapid purification and scale-up of honokiol and magnolol using high-capacity high-speed counter-current chromatography." Journal of Chromatography A **1142**(2): 115-122.

Chen, L. J., H. Song, X. Q. Lan, D. E. Games and I. A. Sutherland (2005). "Comparison of high-speed counter-current chromatography instruments for the separation of the extracts of the seeds of *Oroxylum indicum*." Journal of Chromatography A **1063**(1-2): 241-245.

Chen, Y. and W. Schwack (2014). "High-performance thin-layer chromatography screening of multi class antibiotics in animal food by bioluminescent bioautography and electrospray ionization mass spectrometry." Journal of Chromatography A **1356**: 249-257.

Choi, S. J., M. Y. Lee, H. Jo, S. S. Lim and S. H. Jung (2012). "Preparative isolation and purification of neuroprotective compounds from *Rhus verniciflua* by high Speed

counter-current chromatography." Biological and Pharmaceutical Bulletin **35**(4): 559-567.

Choi, Y. H., J. van Spronsen, Y. Dai, M. Verberne, F. Hollmann, I. W. Arends, G. J. Witkamp and R. Verpoorte (2011). "Are natural deep eutectic solvents the missing link in understanding cellular metabolism and physiology?" Plant Physiology **156**(4): 1701-1705.

Cicek, S. S., S. Schwaiger, E. P. Ellmerer and H. Stuppner (2010). "Development of a fast and convenient method for the isolation of triterpene saponins from *Actaea racemosa* by high-speed countercurrent chromatography coupled with evaporative light scattering detection." Planta Medica **76**(05): 467-473.

Craveiro, R., I. Aroso, V. Flammia, T. Carvalho, M. T. Viciosa, M. Dionísio, S. Barreiros, R. L. Reis, A. R. C. Duarte and A. Paiva (2016). "Properties and thermal behavior of natural deep eutectic solvents." Journal of Molecular Liquids **215**: 534-540.

Dai, Y., E. Rozema, R. Verpoorte and Y. H. Choi (2016). "Application of natural deep eutectic solvents to the extraction of anthocyanins from *Catharanthus roseus* with high extractability and stability replacing conventional organic solvents." Journal of Chromatography A **1434**: 50-56.

Dai, Y., J. van Spronsen, G.-J. Witkamp, R. Verpoorte and Y. H. Choi (2013). "Ionic liquids and deep eutectic solvents in natural products research: mixtures of solids as extraction solvents." Journal of Natural Products **76**(11): 2162-2173.

Dai, Y., J. van Spronsen, G.-J. Witkamp, R. Verpoorte and Y. H. Choi (2013). "Natural deep eutectic solvents as new potential media for green technology." Analytica Chimica Acta **766**: 61-68.

Dai, Y., R. Verpoorte and Y. H. Choi (2014). "Natural deep eutectic solvents providing enhanced stability of natural colorants from safflower (*Carthamus tinctorius*)." Food Chemistry **159**: 116-121.

Dai, Y., G.-J. Witkamp, R. Verpoorte and Y. H. Choi (2013). "Natural deep eutectic solvents as a new extraction media for phenolic metabolites in *Carthamus tinctorius* L." Analytical Chemistry **85**(13): 6272-6278.

Dai, Y., G.-J. Witkamp, R. Verpoorte and Y. H. Choi (2015). "Tailoring properties of natural deep eutectic solvents with water to facilitate their applications." Food Chemistry **187**: 14-19.

Dang, Y.-Y., X.-C. Li, Q.-W. Zhang, S.-P. Li and Y.-T. Wang (2010). "Preparative isolation and purification of six volatile compounds from essential oil of *Curcuma wenyujin* using high-performance centrifugal partition chromatography." Journal of Separation Science **33**(11): 1658-1664.

Davey, R. J., J. Garside, A. M. Hilton, D. McEwan and J. W. Morrison (1995). "Purification of molecular mixtures below the eutectic by emulsion crystallization." Nature **375**(6533): 664-666.

de Morais, P., F. Gonçalves, J. A. P. Coutinho and S. P. M. Ventura (2015). "Ecotoxicity of cholinium-based deep eutectic solvents." ACS Sustainable Chemistry and Engineering **3**(12): 3398-3404.

Deng, J., X. Xiao, G. Li and G. Ruan (2009). "Application of microwave-assisted extraction coupled with high-speed counter-current chromatography for separation and purification of dehydrocavidine from *Corydalis saxicola* Bunting." Phytochemical Analysis **20**(6): 498-502.

Deng, S., S.-N. Chen, P. Yao, D. Nikolic, R. B. van Breemen, J. L. Bolton, H. H. S. Fong, N. R. Farnsworth and G. F. Pauli (2006). "Serotonergic activity-guided phytochemical investigation of the roots of *Angelica sinensis*." Journal of Natural Products **69**(4): 536-541.

Duan, L., L.-L. Dou, L. Guo, P. Li and E. H. Liu (2016). "Comprehensive evaluation of deep eutectic solvents in extraction of bioactive natural products." ACS Sustainable Chemistry and Engineering **4**(4): 2405-2411.

Dubant, S., B. Mathews, P. Higginson, R. Crook, M. Snowden and J. Mitchell (2008). "Practical solvent system selection for counter-current separation of pharmaceutical compounds." Journal of Chromatography A **1207**(1): 190-192.

Ekor, M. (2013). "The growing use of herbal medicines: issues relating to adverse reactions and challenges in monitoring safety." Frontiers in Pharmacology **4**: 177.

Elfawal, M. A., M. J. Towler, N. G. Reich, P. J. Weathers and S. M. Rich (2015). "Dried whole-plant *Artemisia annua* slows evolution of malaria drug resistance and overcomes resistance to artemisinin." Proceedings of the National Academy of Sciences of the United States of America **112**(3): 821-826.

Faggian, M., S. Sut, B. Perissutti, V. Baldan, I. Grabnar and S. Dall'Acqua (2016). "Natural deep eutectic solvents (NADES) as a tool for bioavailability improvement: pharmacokinetics of rutin dissolved in proline/glycine after oral administration in rats: possible application in nutraceuticals." Molecules **21**(11): 1531.

Fan, Q., H. Zhang, H. Hu, Y. Xu and Q. Song (2016). "Quick method for separating target compounds from the bark of Maqian (*Zanthoxylum myriacanthum* var. pubescens) by high-performance countercurrent chromatography." Journal of Separation Science **39**(20): 4049-4052.

Firenzuoli, F. and L. Gori (2007). "Herbal medicine today: Clinical and research issues." Evidence-based Complementary and Alternative Medicine **4**(Suppl 1): 37-40.

Florindo, C., F. S. Oliveira, L. P. N. Rebelo, A. M. Fernandes and I. M. Marrucho (2014). "Insights into the synthesis and properties of deep eutectic solvents based on cholinium chloride and carboxylic acids." ACS Sustainable Chemistry and Engineering **2**(10): 2416-2425.

Fowler, S. D. and P. Greenspan (1985). "Application of Nile red, a fluorescent hydrophobic probe, for the detection of neutral lipid deposits in tissue sections: comparison with oil red O." Journal of Histochemistry and Cytochemistry **33**(8): 833-836.

Frank, H. S. and W.-Y. Wen (1957). "Ion-solvent interaction. Structural aspects of ion-solvent interaction in aqueous solutions: a suggested picture of water structure." Discussions of the Faraday Society **24**: 133-140.

Franklin, E. C. (1918). "Potassium ammonosodiate, potassium ammonolithiate, and rubidium ammonosodiate, and rubidium ammonolithiate." The Journal of Physical Chemistry **23**(1): 36-53.

Frey, A., E. Hopmann and M. Minceva (2014). "Selection of biphasic liquid systems in liquid-liquid chromatography using predictive thermodynamic models." Chemical Engineering and Technology **37**(10): 1663-1674.

Friesen, J. B., S. Ahmed and G. F. Pauli (2015). "Qualitative and quantitative evaluation of solvent systems for countercurrent separation." Journal of Chromatography A **1377**: 55-63.

Friesen, J. B., J. B. McAlpine, S.-N. Chen and G. F. Pauli (2015). "Countercurrent separation of natural products: An update." Journal of Natural Products **78**(7): 1765-1796.

Friesen, J. B. and G. F. Pauli (2005). "G.U.E.S.S.—a generally useful estimate of solvent systems for CCC." Journal of Liquid Chromatography and Related Technologies **28**(17): 2777-2806.

Friesen, J. B. and G. F. Pauli (2007). "Rational development of solvent system families in counter-current chromatography." Journal of Chromatography A **1151**(1): 51-59.

Friesen, J. B. and G. F. Pauli (2008). "Performance characteristics of countercurrent separation in analysis of natural products of agricultural significance." Journal of Agricultural and Food Chemistry **56**(1): 19-28.

Friesen, J. B. and G. F. Pauli (2009). "Binary concepts and standardization in counter-current separation technology." Journal of Chromatography A **1216**(19): 4237-4244.

Garcia, J. I., H. Garcia-Marin and E. Pires (2014). "Glycerol based solvents: synthesis, properties and applications." Green Chemistry **16**(3): 1007-1033.

Garrard, I. J. (2005). "Simple approach to the development of a CCC solvent selection protocol suitable for automation." Journal of Liquid Chromatography and Related Technologies **28**(12-13): 1923-1935.

Ghose, A. K., V. N. Viswanadhan and J. J. Wendoloski (1998). "Prediction of hydrophobic (Lipophilic) properties of small organic molecules using fragmental methods: An analysis of ALOGP and CLOGP methods." The Journal of Physical Chemistry A **102**(21): 3762-3772.

Gill, I. and E. N. Vulfson (1993). "Enzymic synthesis of short peptides in heterogeneous mixtures of substrates." Journal of the American Chemical Society **115**(8): 3348-3349.

Gill, I. and E. N. Vulfson (1994). "Enzymic catalysis in heterogeneous eutectic mixtures of substrates." Trends in Biotechnology **12**(4): 118-122.

Gillette, B. M., J. A. Jensen, M. Wang, J. Tchao and S. K. Sia (2010). "Dynamic hydrogels: switching of 3D microenvironments using two-component naturally derived extracellular matrices." Advanced Materials **22**(6): 686-691.

Gisi, U., H. Binder and E. Rimbach (1985). "Synergistic interactions of fungicides with different modes of action." Transactions of the British Mycological Society **85**(2): 299-306.

Gödecke, T., J. G. Napolitano, M. F. Rodríguez-Brasco, S.-N. Chen, B. U. Jaki, D. C. Lankin and G. F. Pauli (2013). "Validation of a generic quantitative ^{1}H NMR method for natural products analysis." Phytochemical Analysis **24**(6): 581-597.

Goll, J., A. Frey and M. Minceva (2013). "Study of the separation limits of continuous solid support free liquid–liquid chromatography: Separation of capsaicin and dihydrocapsaicin by centrifugal partition chromatography." Journal of Chromatography A **1284**: 59-68.

Gómez, F. J. V., M. Espino, M. de los Angeles Fernández, J. Raba and M. F. Silva (2016). "Enhanced electrochemical detection of quercetin by natural deep eutectic solvents." Analytica Chimica Acta **936**: 91-96.

Grzelak, E. M., C. Hwang, G. Cai, J.-W. Nam, M. P. Choules, W. Gao, D. C. Lankin, J. B. McAlpine, S. G. Mulugeta, J. G. Napolitano, J.-W. Suh, S. H. Yang, J. Cheng, H. Lee, J.-Y. Kim, S.-H. Cho, G. F. Pauli, S. G. Franzblau and B. U. Jaki (2016). "Bioautography with TLC-MS/NMR for rapid discovery of anti-tuberculosis lead compounds from natural Sources." ACS Infectious Diseases **2**(4): 294-301.

Hadj-Kali, M. K., K. E. Al-khidir, I. Wazeer, L. El-blidi, S. Mulyono and I. M. AlNashef (2015). "Application of deep eutectic solvents and their individual constituents as surfactants for enhanced oil recovery." Colloids and Surfaces A: Physicochemical and Engineering Aspects **487**: 221-231.

Hammann, S., U. Tillmann, M. Schröder and W. Vetter (2013). "Profiling the fatty acids from a strain of the microalgae *Alexandrium tamarense* by means of high-speed counter-current chromatography and gas chromatography coupled with mass spectrometry." Journal of Chromatography A **1312**: 93-103.

Hammond, O. S., D. T. Bowron and K. J. Edler (2017). "The effect of water upon deep eutectic solvent nanostructure: An unusual transition from ionic mixture to aqueous solution." Angewandte Chemie International Edition **56**(33): 9782-9785.

Han, Q.-B., L. Wong, N.-Y. Yang, J.-Z. Song, C.-F. Qiao, H. Yiu, Y. Ito and H.-X. Xu (2008). "A simple method to optimize the HSCCC two-phase solvent system by predicting the partition coefficient for target compound." Journal of Separation Science **31**(6-7): 1189-1194.

Han, Q. B., T. Yu, F. Lai, Y. Zhou, C. Feng, W. N. Wang, X. H. Fu, C. B. Lau, K. Q. Luo, H. X. Xu, H. D. Sun, K. P. Fung and P. C. Leung (2010). "Quick identification of apoptosis inducer from *Isodon eriocalyx* by a drug discovery platform composed of analytical high-speed counter-current chromatography and the fluorescence-based caspase-3 biosensor detection." Talanta **82**(4): 1521-1527.

Hayyan, M., M. A. Hashim, M. A. Al-Saadi, A. Hayyan, I. M. AlNashef and M. E. S. Mirghani (2013). "Assessment of cytotoxicity and toxicity for phosphonium-based deep eutectic solvents." Chemosphere **93**(2): 455-459.

Hayyan, M., M. A. Hashim, A. Hayyan, M. A. Al-Saadi, I. M. AlNashef, M. E. S. Mirghani and O. K. Saheed (2013). "Are deep eutectic solvents benign or toxic?" Chemosphere **90**(7): 2193-2195.

Hayyan, M., C. Y. Looi, A. Hayyan, W. F. Wong and M. A. Hashim (2015). "*In vitro* and *in vivo* toxicity profiling of ammonium-based deep eutectic solvents." PLoS One **10**(2): e0117934.

Hayyan, M., Y. P. Mbous, C. Y. Looi, W. F. Wong, A. Hayyan, Z. Salleh and O. Mohd-Ali (2016). "Natural deep eutectic solvents: cytotoxic profile." SpringerPlus **5**(1): 913.

He, K., X. Ye, X. Li, H. Chen, L. Yuan, Y. Deng, X. Chen and X. Li (2012). "Separation of two constituents from purple sweet potato by combination of silica gel column and high-speed counter-current chromatography." Journal of Chromatography B **881**: 49-54.

Hernandez-Perni, G., A. Stengele and H. Leuenberger (2005). "Towards a better understanding of the parameter Ei/E in the characterization of polar liquids." International Journal of Pharmaceutics **291**(1): 189-195.

Hoare, T. R. and D. S. Kohane (2008). "Hydrogels in drug delivery: Progress and challenges." Polymer **49**(8): 1993-2007.

Hopmann, E., W. Arlt and M. Minceva (2011). "Solvent system selection in counter-

current chromatography using conductor-like screening model for real solvents." Journal of Chromatography A **1218**(2): 242-250.

Hopmann, E., A. Frey and M. Minceva (2012). "A priori selection of the mobile and stationary phase in centrifugal partition chromatography and counter-current chromatography." Journal of Chromatography A **1238**: 68-76.

Hösel, W. and W. Barz (1975). "β-Glucosidases from *Cicer arietinum* L." European Journal of Biochemistry **57**(2): 607-616.

Hostettmann, K., M. Hostettmann-Kaldas and O. Sticher (1979). "Application of droplet counter-current chromatography to the isolation of natural products." Journal of Chromatography A **186**: 529-534.

Huggins, M. L. (1971). "Thermodynamic properties of liquids, including solutions. IV. Entropy of mixing." The Journal of Physical Chemistry **75**(9): 1255-1259.

Huggins, M. L. (1976). "Thermodynamic properties of liquids, including solutions. 13. Molecular and intermolecular properties from excess enthalpies." The Journal of Physical Chemistry **80**(25): 2732-2734.

Ignatova, S., N. Sumner, N. Colclough and I. Sutherland (2011). "Gradient elution in counter-current chromatography: a new layout for an old path." Journal of Chromatography A **1218**(36): 6053-6060.

Ignatova, S., P. Wood, D. Hawes, L. Janaway, D. Keay and I. Sutherland (2007). "Feasibility of scaling from pilot to process scale." Journal of Chromatography A **1151**(1): 20-24.

Inoue, K., E. Baba, T. Hino and H. Oka (2012). "A strategy for high-speed countercurrent chromatography purification of specific antioxidants from natural products based on on-line HPLC method with radical scavenging assay." Food Chemistry **134**(4): 2276-2282.

Inoue, K., Y. Hattori, T. Hino and H. Oka (2010). "An approach to on-line electrospray mass spectrometric detection of polypeptide antibiotics of enramycin for high-speed counter-current chromatographic separation." Journal of Pharmaceutical and Biomedical Analysis **51**(5): 1154-1160.

Inoue, K., C. Nomura, S. Ito, A. Nagatsu, T. Hino and H. Oka (2008). "Purification of curcumin, demethoxycurcumin, and bisdemethoxycurcumin by high-speed countercurrent chromatography." Journal of Agricultural and Food Chemistry **56**(20): 9328-9336.

Inui, T., Y. Wang, S. Deng, D. C. Smith, S. G. Franzblau and G. F. Pauli (2007). "Counter-current chromatography based analysis of synergy in an anti-tuberculosis ethnobotanical." Journal of Chromatography A **1151**(1): 211-215.

Ito, Y. (1987). "High-speed countercurrent chromatography." Nature **326**(6111): 419-420.

Ito, Y. (2005). "Golden rules and pitfalls in selecting optimum conditions for high-speed counter-current chromatography." Journal of Chromatography A **1065**(2): 145-168.

Ito, Y. and R. L. Bowman (1970). "Countercurrent chromatography: liquid-liquid partition chromatography without solid support." Science **167**(3916): 281-283.

Jablonský, M., A. Škulcová, L. Kamenská, M. Vrška and J. Šíma (2015). Deep Eutectic Solvents: Fractionation of Wheat Straw, **10**(4): 8039-8047.

Jain, K., B. Ghai, A. K. Saxena, D. Saini and N. Khandelwal (2010). "Efficacy of two oral premedicants: midazolam or a low-dose combination of midazolam-ketamine for reducing stress during intravenous cannulation in children undergoing CT imaging." Pediatric Anesthesia **20**(4): 330-337.

Jargin, S. V. (2014). "Soy and phytoestrogens: possible side effects." German Medical Science **12**: 1-5.

Jerz, G., N. Gebers, D. Szot, M. Szaleniec, P. Winterhalter and S. Wybraniec (2014). "Separation of amaranthine-type betacyanins by ion-pair high-speed countercurrent chromatography." Journal of Chromatography A **1344**: 42-50.

Jiang, Y., X. Fan, Y. Wang, H. Tan, P. Chen, H. Zeng, M. Huang and H. Bi (2015). "Hepato-protective effects of six schisandra lignans on acetaminophen-induced liver injury are partially associated with the inhibition of CYP-mediated bioactivation." Chemico-Biological Interactions **231**: 83-89.

Juneidi, I., M. Hayyan and M. A. Hashim (2015). "Evaluation of toxicity and biodegradability for cholinium-based deep eutectic solvents." RSC Advances **5**(102): 83636-83647.

Kang, K., K.-M. Lee, J.-H. Yoo, H. J. Lee, C. Y. Kim and C. W. Nho (2012). "Dibenzocyclooctadiene lignans, gomisins J and N inhibit the Wnt/β-catenin signaling pathway in HCT116 cells." Biochemical and Biophysical Research Communications **428**(2): 285-291.

Kim, C. K., P. Ghosh, C. Pagliuca, Z.-J. Zhu, S. Menichetti and V. M. Rotello (2009). "Entrapment of hydrophobic drugs in nanoparticle monolayers with efficient release into cancer cells." Journal of the American Chemical Society **131**(4): 1360-1361.

Kim, M., S. J. Lim, H.-J. Lee, S. Y. Kim and C. W. Nho (2015). "Gomisin J inhibits oleic acid-induced hepatic lipogenesis by activation of the AMPK-dependent pathway and inhibition of the hepatokine fetuin-A in HepG2 cells." Journal of Agricultural and Food Chemistry **63**(44): 9729-9739.

Klamt, A. (1995). "Conductor-like screening model for real solvents: A new approach to the quantitative calculation of solvation phenomena." The Journal of Physical Chemistry **99**(7): 2224-2235.

Klejdus, B., D. Vitamvásová-Štěrbová and V. Kubáň (2001). "Identification of isoflavone conjugates in red clover (*Trifolium pratense*) by liquid chromatography–mass spectrometry after two-dimensional solid-phase extraction." Analytica Chimica Acta **450**(1): 81-97.

Kraus, C. A. and E. J. Cuy (1923). "Phase relations in the system, sodium amide-potassium amide, as determined from melting-point curves." Journal of the American Chemical Society **45**(3): 712-715.

Kumar, A. K., B. S. Parikh and M. Pravakar (2016). "Natural deep eutectic solvent mediated pretreatment of rice straw: bioanalytical characterization of lignin extract and enzymatic hydrolysis of pretreated biomass residue." Environmental Science and Pollution Research **23**(10): 9265-9275.

Kusaikin, M. I., A. M. Zakharenko, S. P. Ermakova, M. V. Veselova, E. V. Grigoruk, S. A. Fedoreev and T. N. Zvyagintseva (2011). "Deglycosylation of isoflavonoid glycosides from *Maackia amurensis* cell culture by β–D-glucosidase from *Littorina sitkana* hepatopancrease." Chemistry of Natural Compounds **47**(2): 197.

Lee, S. B., C. Y. Kim, H. J. Lee, J. H. Yun and C. W. Nho (2009). "Induction of the phase II detoxification enzyme NQO1 in hepatocarcinoma cells by lignans from the fruit of *Schisandra chinensis* through nuclear accumulation of Nrf2." Planta Medica **75**(12): 1314-1318.

Leitao, G. G., P. A. de Souza, A. A. Moraes and L. Brown (2005). "Step-gradient CCC separation of phenylpropanoid and iridoid glycosides from roots of *Stachytarpheta cayennensis* (Rich.) Vahl." Journal of Liquid Chromatography and Related Technologies **28**(12-13): 2053-2060.

Lepeltier, E., C. Bourgaux and P. Couvreur (2014). "Nanoprecipitation and the "Ouzo effect": Application to drug delivery devices." Advanced Drug Delivery Reviews **71**: 86-97.

Li, C., D. Li, S. Zou, Z. Li, J. Yin, A. Wang, Y. Cui, Z. Yao and Q. Zhao (2013). "Extraction desulfurization process of fuels with ammonium-based deep eutectic solvents." Green Chemistry **15**(10): 2793-2799.

Li, J., X. Zhang, Q. Yu, X. Fu and W. Wang (2014). "One-Step Separation of Four Flavonoids from *Herba Salviae Plbeiae* by HSCCC." Journal of Chromatographic Science **52**(10): 1288-1293.

Lipinski, C. A., F. Lombardo, B. W. Dominy and P. J. Feeney (2001). "Experimental and computational approaches to estimate solubility and permeability in drug discovery and development settings." Advanced Drug Delivery Reviews **46**(1): 3-26.

Liu, P., J.-W. Hao, L.-P. Mo and Z.-H. Zhang (2015). "Recent advances in the application of deep eutectic solvents as sustainable media as well as catalysts in organic reactions." RSC Advances **5**(60): 48675-48704.

Liu, Y., S. N. Chen, J. B. McAlpine, L. L. Klein, J. B. Friesen, D. C. Lankin and G. F. Pauli (2014). "Quantification of a botanical negative marker without an identical standard: ginkgotoxin in *Ginkgo biloba*." Journal of Natural Products **77**(3): 611-617.

Liu, Y., J. B. Friesen, L. L. Klein, J. B. McAlpine, D. C. Lankin, G. F. Pauli and S. N. Chen (2015). "The Generally Useful Estimate of Solvent Systems (GUESS) method enables the rapid purification of methylpyridoxine regioisomers by countercurrent chromatography." Journal of Chromatography A **1426**: 248-251.

Liu, Y., J. B. Friesen, J. B. McAlpine and G. F. Pauli (2015). "Solvent system selection strategies in countercurrent separation." Planta Medica **81**(17): 1582-1591.

Liu, Y., J. Garzon, J. B. Friesen, Y. Zhang, J. B. McAlpine, D. C. Lankin, S. N. Chen and G. F. Pauli (2016). "Countercurrent assisted quantitative recovery of metabolites from plant-associated natural deep eutectic solvents." Fitoterapia **112**: 30-37.

Liu, Y., K. Kathan, W. Saad and R. K. Prud'homme (2007). "Ostwald ripening of β-carotene nanoparticles." Physical Review Letters **98**(3): 036102.

Liu, Z. (2008). "Preparation of botanical samples for biomedical research." Endocrine, metabolic and immune disorders drug targets **8**(2): 112-121.

Lu, Y. and D. F. Chen (2009). "Analysis of *Schisandra chinensis* and *Schisandra sphenanthera*." Journal of Chromatography A **1216**(11): 1980-1990.

Luo, H., M. Peng, H. Ye, L. Chen, A. Peng, M. Tang, F. Zhang and J. Shi (2010). "Predictable and linear scale-up of four phenolic alkaloids separation from the roots of *Menispermum dauricum* using high-performance counter-current chromatography." Journal of Chromatography B **878**(22): 1929-1933.

Luo, Y., Y. Xu, L. Chen, H. Luo, C. Peng, J. Fu, H. Chen, A. Peng, H. Ye, D. Xie, A. Fu, J. Shi, S. Yang and Y. Wei (2008). "Preparative purification of anti-tumor derivatives of honokiol by high-speed counter-current chromatography." Journal of Chromatography A **1178**(1): 160-165.

Luo, Y., Y. Xu, L. Chen, H. Luo, C. Peng, J. Fu, H. Chen, A. Peng, H. Ye, D. Xie, A. Fu, J. Shi, S. Yang and Y. Wei (2008). "Preparative purification of anti-tumor derivatives of honokiol by high-speed counter-current chromatography." Journal of Chromatography A **1178**(1-2): 160-165.

Ma, B.-L., C. Yin, B.-K. Zhang, Y. Dai, Y.-Q. Jia, Y. Yang, Q. Li, R. Shi, T.-M. Wang, J.-S. Wu, Y.-Y. Li, G. Lin and Y.-M. Ma (2016). "Naturally occurring proteinaceous nanoparticles in *Coptidis Rhizoma* extract act as concentration-dependent carriers that facilitate berberine absorption." Scientific Reports **6** (20110): 1-11.

Ma, X., P. Tu, Y. Chen, T. Zhang, Y. Wei and Y. Ito (2004). "Preparative isolation and purification of isoflavan and pterocarpan glycosides from *Astragalus membranaceus* Bge. *var. mongholicus* (Bge.) Hsiao by high-speed counter-current chromatography." Journal of Chromatography A **1023**(2): 311-315.

Machado, V. G. and C. Machado (2001). "An easy and versatile experiment to demonstrate solvent polarity using solvatochromic dyes." Journal of Chemical Education **78**(5): 649.

Maier, T., S. Sanzenbacher, D. R. Kammerer, N. Berardini, J. Conrad, U. Beifuss, R. Carle and A. Schieber (2006). "Isolation of hydroxycinnamoyltartaric acids from grape pomace by high-speed counter-current chromatography." Journal of Chromatography A **1128**(1-2): 61-67.

Malongane, F., L. J. McGaw and F. N. Mudau "The synergistic potential of various teas, herbs and therapeutic drugs in health improvement: a review." Journal of the Science of Food and Agriculture **97**(14):4679-4689.

Mariappan, R., P. Ayyappan and R. Uthandakalaipandian (2015). "Natural deep eutectic solvent extraction media for *Zingiber officinale* Roscoe: The study of chemical compositions, antioxidants and antimicrobial activities." The Natural Products Journal **5**(1): 3-13.

Marston, A. and K. Hostettmann (2006). "Developments in the application of counter-current chromatography to plant analysis." Journal of Chromatography A **1112**(1): 181-194.

Martinez, R., L. Berbegal, G. Guillena and D. J. Ramon (2016). "Bio-renewable enantioselective aldol reaction in natural deep eutectic solvents." Green Chemistry **18**(6): 1724-1730.

Moriguchi, I., S. Hirono, Q. Liu, I. Nakagome and Y. Matsushita (1992). "Simple method of calculating octanol/water partition coefficient." Chemical and Pharmaceutical Bulletin **40**(1): 127-130.

Mulia, K., E. Krisanti, F. Terahadi and S. Putri (2015). "Selected natural deep eutectic solvents for the extraction of α-mangostin from mangosteen (*Garcinia mangostana* L.) Pericarp." International Journal of Technology **6**(7): 1211-1220.

Na, M., T. M. Hung, W. K. Oh, B. S. Min, S. H. Lee and K. Bae (2010). "Fatty acid synthase inhibitory activity of dibenzocyclooctadiene lignans isolated from *Schisandra chinensis*." Phytotherapy Research **24**(S2): S225-S228.

Neves Costa, F. d. and G. G. Leitão (2010). "Strategies of solvent system selection for the isolation of flavonoids by countercurrent chromatography." Journal of Separation Science **33**(3): 336-347.

Okuniewski, M., K. Paduszyński and U. Domańska (2016). "Thermodynamic study of

molecular interactions in eutectic mixtures containing camphene." Journal of Physical Chemistry B **120**(50): 12928-12936.

Oreagba, I. A., K. A. Oshikoya and M. Amachree (2011). "Herbal medicine use among urban residents in Lagos, Nigeria." BMC Complementary and Alternative Medicine **11**(117): 1-8.

Osterby, B. R. and R. D. McKelvey (1996). "Convergent synthesis of betaine-30, a solvatochromic dye: An advanced undergraduate project and demonstration." Journal of Chemical Education **73**(3): 260.

Paiva, A., R. Craveiro, I. Aroso, M. Martins, R. L. Reis and A. R. C. Duarte (2014). "Natural deep eutectic solvents – Solvents for the 21st century." ACS Sustainable Chemistry and Engineering **2**(5): 1063-1071.

Pandey, A., Bhawna, D. Dhingra and S. Pandey (2017). "Hydrogen bond donor/acceptor cosolvent-modified choline chloride-based deep eutectic solvents." Journal of Physical Chemistry B **121**(16): 4202-4212.

Paradiso, V. M., A. Clemente, C. Summo, A. Pasqualone and F. Caponio (2016). "Towards green analysis of virgin olive oil phenolic compounds: Extraction by a natural deep eutectic solvent and direct spectrophotometric detection." Food Chemistry **212**: 43-47.

Pauli, G. F., T. Gödecke, B. U. Jaki and D. C. Lankin (2012). "Quantitative ^{1}H NMR. development and potential of an analytical method: An Update." Journal of Natural Products **75**(4): 834-851.

Pauli, G. F., B. U. Jaki and D. C. Lankin (2005). "Quantitative ^{1}H NMR: Development and potential of a method for natural products analysis." Journal of Natural Products **68**(1): 133-149.

Pauli, G. F., S. M. Pro, L. R. Chadwick, T. Burdick, L. Pro, W. Friedl, N. Novak, J. Maltby, F. Qiu and J. B. Friesen (2015). "Real-time volumetric phase monitoring: Advancing chemical analysis by countercurrent separation." Analytical Chemistry **87**(14): 7418-7425.

Pauli, G. F., S. M. Pro and J. B. Friesen (2008). "Countercurrent separation of natural products." Journal of Natural Products **71**(8): 1489-1508.

Peng, A., R. Li, J. Hu, L. Chen, X. Zhao, H. Luo, H. Ye, Y. Yuan and Y. Wei (2008). "Flow rate gradient high-speed counter-current chromatography separation of five diterpenoids from *Triperygium wilfordii* and scale-up." Journal of Chromatography A **1200**(2): 129-135.

Qian, J. and C. F. Poole (2007). "Distribution model for Folch partition." Journal of Separation Science **30**(14): 2326-2331.

Qiu, F., J. B. Friesen, J. B. McAlpine and G. F. Pauli (2012). "Design of countercurrent separation of *Ginkgo biloba* terpene lactones by nuclear magnetic resonance." Journal of Chromatography A **1242**: 26-34.

Radošević, K., N. Ćurko, V. Gaurina Srček, M. Cvjetko Bubalo, M. Tomašević, K. Kovačević Ganić and I. Radojčić Redovniković (2016). "Natural deep eutectic solvents as beneficial extractants for enhancement of plant extracts bioactivity." LWT - Food Science and Technology **73**: 45-51.

Ramos Alvarenga, R. F., J. B. Friesen, D. Nikolić, C. Simmler, J. G. Napolitano, R. van Breemen, D. C. Lankin, J. B. McAlpine, G. F. Pauli and S.-N. Chen (2014). "K-targeted metabolomic analysis extends chemical subtraction to DESIGNER extracts: Selective depletion of extracts of hops (*Humulus lupulus*)." Journal of Natural Products **77**(12): 2595-2604.

Reichardt, C. (1994). "Solvatochromic dyes as solvent polarity indicators." Chemical Reviews **94**(8): 2319-2358.

Ren, D.-B., Y.-H. Qin, Y.-H. Yun, H.-M. Lu, X.-Q. Chen and Y.-Z. Liang (2014). "Using nonrandom two-liquid model for solvent system selection in counter-current chromatography." Journal of Chromatography A **1355**: 80-85.

Ren, D.-B., Z.-H. Yang, Y.-Z. Liang, Q. Ding, C. Chen and M.-L. Ouyang (2013). "Correlation and prediction of partition coefficient using nonrandom two-liquid segment activity coefficient model for solvent system selection in counter-current chromatography separation." Journal of Chromatography A **1301**: 10-18.

Renon, H. and J. M. Prausnitz (1968). "Local compositions in thermodynamic excess functions for liquid mixtures." AIChE Journal **14**(1): 135-144.

Ribeiro, B. D., C. Florindo, L. C. Iff, M. A. Z. Coelho and I. M. Marrucho (2015). "Menthol-based eutectic mixtures: Hydrophobic low viscosity solvents." ACS Sustainable Chemistry and Engineering **3**(10): 2469-2477.

Roehrer, S., F. Bezold, E. M. García and M. Minceva (2016). "Deep eutectic solvents in countercurrent and centrifugal partition chromatography." Journal of Chromatography A **1434**: 102-110.

Rossum, T. G. J. V., Vulto, R. A. D. Man, Brouwer and Schalm (1998). "Glycyrrhizin as a potential treatment for chronic hepatitis C." Alimentary Pharmacology and Therapeutics **12**(3): 199-205.

Rozema, E., A. D. van Dam, H. C. M. Sips, R. Verpoorte, O. C. Meijer, S. Kooijman and Y. H. Choi (2015). "Extending pharmacological dose-response curves for salsalate with natural deep eutectic solvents." RSC Advances **5**(75): 61398-61401.

Ru and B. König (2012). "Low melting mixtures in organic synthesis - an alternative to ionic liquids?" Green Chemistry **14**(11): 2969-2982.

Ruesgas-Ramón, M., M. C. Figueroa-Espinoza and E. Durand (2017). "Application of deep eutectic solvents (DES) for phenolic compounds extraction: Overview, challenges, and opportunities." Journal of Agricultural and Food Chemistry **65**(18): 3591-3601.

Ryu, E. Y., S. Y. Park, S. G. Kim, D. J. Park, J. S. Kang, Y. H. Kim, R. Seetharaman, Y.-W. Choi and S.-J. Lee (2011). "Anti-inflammatory effect of heme oxygenase-1 toward *Porphyromonas gingivalis* lipopolysaccharide in macrophages exposed to gomisins A, G, and J." Journal of Medicinal Food **14**(12): 1519-1526.

San José, J., M. A. Sanz-Tejedor and Y. Arroyo (2015). "Effect of fatty acid composition in vegetable oils on combustion processes in an emulsion burner." Fuel Processing Technology **130**: 20-30.

Sanchez-Leija, R. J., J. A. Pojman, G. Luna-Barcenas and J. D. Mota-Morales (2014). "Controlled release of lidocaine hydrochloride from polymerized drug-based deep-eutectic solvents." Journal of Materials Chemistry B **2**(43): 7495-7501.

Sanhueza, L., R. Melo, R. Montero, K. Maisey, L. Mendoza and M. Wilkens (2017). "Synergistic interactions between phenolic compounds identified in grape pomace extract with antibiotics of different classes against *Staphylococcus aureus* and *Escherichia coli*." PLoS ONE **12**(2): e0172273.

Schinkovitz, A., S. M. Pro, M. Main, S.-N. Chen, B. U. Jaki, D. C. Lankin and G. F. Pauli (2008). "Dynamic nature of the ligustilide complex." Journal of Natural Products **71**(9): 1604-1611.

Schr öder, M. and W. Vetter (2011). "High-speed counter-current chromatographic separation of phytosterols." Analytical and Bioanalytical Chemistry **400**(10): 3615-3623.

Shibusawa, Y., A. Yanagida, M. Isozaki, H. Shindo and Y. Ito (2001). "Separation of apple procyanidins into different degrees of polymerization by high-speed counter-current chromatography." Journal of Chromatography A **915**(1): 253-257.

Simmler, C., J. R. Anderson, L. Gauthier, D. C. Lankin, J. B. McAlpine, S.-N. Chen and G. F. Pauli (2015). "Metabolite profiling and classification of DNA-authenticated licorice botanicals." Journal of Natural Products **78**(8): 2007-2022.

Simmler, C., D. Nikolić, D. C. Lankin, Y. Yu, J. B. Friesen, R. B. van Breemen, A. Lecomte, C. Le Quémener, G. Audo and G. F. Pauli (2014). "Orthogonal analysis underscores the relevance of primary and secondary metabolites in licorice." Journal of Natural Products **77**(8): 1806-1816.

Skalicka-Wozniak, K., T. Mroczek, I. Garrard and K. Glowniak (2012). "Isolation of the minor and rare constituents from fruits of *Peucedanum alsaticum* L. using high-performance counter-current chromatography." Journal of Separation Science **35**(7): 790-797.

Skalicka-Wozniak, K., M. Walasek, A. Ludwiczuk and K. Glowniak (2013). "Isolation of terpenoids from *Pimpinella anisum* essential oil by high-performance counter-current chromatography." Journal of Separation Science **36**(16): 2611-2614.

Sporna-Kucab, A., S. Ignatova, I. Garrard and S. Wybraniec (2013). "Versatile solvent systems for the separation of betalains from processed *Beta vulgaris* L. juice using counter-current chromatography." Journal of Chromatography B **941**: 54-61.

Stefanovic, R., M. Ludwig, G. B. Webber, R. Atkin and A. J. Page (2017). "Nanostructure, hydrogen bonding and rheology in choline chloride deep eutectic solvents as a function of the hydrogen bond donor." Physical Chemistry Chemical Physics **19**(4): 3297-3306.

Stewart, J. J. P. (1990). "MOPAC: A semiempirical molecular orbital program." Journal of Computer-Aided Molecular Design **4**(1): 1-103.

Stott, P. W., A. C. Williams and B. W. Barry (1998). "Transdermal delivery from eutectic systems: enhanced permeation of a model drug, ibuprofen." Journal of Controlled Release **50**(1): 297-308.

Sutherland, I. A., A. J. Booth, L. Brown, B. Kemp, H. Kidwell, D. Games, A. S. Graham, G. G. Guillon, D. Hawes, M. Hayes, L. Janaway, G. J. Lye, P. Massey, C. Preston, P. Shering, T. Shoulder, C. Strawson and P. Wood (2001). "Industrial scale-up of countercurrent chromatography." Journal of Liquid Chromatography and Related Technologies **24**(11-12): 1533-1553.

Sutherland, I. A. and D. Fisher (2009). "Role of counter-current chromatography in the modernisation of Chinese herbal medicines." Journal of Chromatography A **1216**(4): 740-753.

Sze, L. L., S. Pandey, S. Ravula, S. Pandey, H. Zhao, G. A. Baker and S. N. Baker (2014). "Ternary deep eutectic solvents tasked for carbon dioxide capture." ACS Sustainable Chemistry and Engineering **2**(9): 2117-2123.

Dunlap, T. L., C. E. Howell, N. Mukand, S.N. Chen, G. F. Pauli, B. M. Dietz and J. L. Bolton (2017). "Red Clover Aryl Hydrocarbon Receptor (AhR) and Estrogen Receptor (ER) Agonists Enhance Genotoxic Estrogen Metabolism." Chemical Research in Toxicology **30**(11): 2084-2092.

Chemical Research in Toxicology 2017 30 (11), 2084-2092

Tong, S., J. Yan, Y. X. Guan, Y. Fu and Y. Ito (2010). "Separation of α-cyclohexylmandelic acid enantiomers using biphasic chiral recognition high-speed counter-current chromatography." Journal of Chromatography A **1217**(18): 3044-3052.

Torelli-Souza, R. R., L. A. Cavalcante Bastos, H. G. L. Nunes, C. A. Camara and R. V. S. Amorim (2012). "Sustained release of an antitumoral drug from alginate-chitosan

hydrogel beads and its potential use as colonic drug delivery." Journal of Applied Polymer Science **126**(S1): E409-E418.

Trivedi, T. J., J. H. Lee, H. J. Lee, Y. K. Jeong and J. W. Choi (2016). "Deep eutectic solvents as attractive media for CO_2 capture." Green Chemistry **18**(9): 2834-2842.

Uma Maheswari, A. and K. Palanivelu (2015). "Carbon dioxide capture and utilization by alkanolamines in deep eutectic solvent medium." Industrial and Engineering Chemistry Research **54**(45): 11383-11392.

van Osch, D. J. G. P., L. F. Zubeir, A. van den Bruinhorst, M. A. A. Rocha and M. C. Kroon (2015). "Hydrophobic deep eutectic solvents as water-immiscible extractants." Green Chemistry **17**(9): 4518-4521.

Vitale, S. A. and J. L. Katz (2003). "Liquid droplet dispersions formed by homogeneous liquid−liquid nucleation: "The Ouzo Effect"." Langmuir **19**(10): 4105-4110.

Vuong, T. V. and D. B. Wilson (2010). "Glycoside hydrolases: Catalytic base/nucleophile diversity." Biotechnology and Bioengineering **107**(2): 195-205.

Wagenaar, F. L., J. E. Hochlowski, J. Y. Pan, N. P. Tu and P. A. Searle (2009). "Purification of high-throughput organic synthesis libraries by counter-current chromatography." Journal of Chromatography A **1216**(19): 4154-4160.

Wang, X., D. Hu, L. Zhang, G. Lian, S. Zhao, C. Wang, J. Yin, C. Wu and J. Yang (2014). "Gomisin A inhibits lipopolysaccharide-induced inflammatory responses in N9 microglia via blocking the NF-κB/MAPKs pathway." Food and Chemical Toxicology **63**: 119-127.

Wang, X., Y. Wang, Y. Geng, F. Li and C. Zheng (2004). "Isolation and purification of honokiol and magnolol from *cortex Magnoliae officinalis* by high-speed counter-current chromatography." Journal of Chromatography A **1036**(2): 171-175.

Webster, G. K. and S. Kumar (2014). "Expanding the analytical toolbox: Pharmaceutical application of quantitative NMR." Analytical Chemistry **86**(23): 11474-11480.

Wei, W.-L., R. Zeng, C.-M. Gu, Y. Qu and L.-F. Huang (2016). "*Angelica sinensis* in China-A review of botanical profile, ethnopharmacology, phytochemistry and chemical analysis." Journal of Ethnopharmacology **190**: 116-141.

Wei, Y. and Y. Ito (2006). "Preparative isolation of imperatorin, oxypeucedanin and isoimperatorin from traditional Chinese herb "bai zhi" *Angelica dahurica* (Fisch. ex Hoffm) Benth. et Hook using multidimensional high-speed counter-current chromatography." Journal of Chromatography A **1115**(1-2): 112-117.

Wei, Y., Q. Xie, D. Fisher and I. A. Sutherland (2011). "Separation of patuletin-3-*O*-

glucoside, astragalin, quercetin, kaempferol and isorhamnetin from *Flaveria bidentis* (L.) Kuntze by elution-pump-out high-performance counter-current chromatography." Journal of Chromatography A **1218**(36): 6206-6211.

Wei, Y., Q. Xie and Y. Ito (2009). "Preparative separation of axifolin-3-glucoside, hyperoside and amygdalin from plant extracts by high-speed countercurrent chromatography." Journal of Liquid Chromatography and Related Technologies **32**(7): 1010-1022.

Wei, Y., T. Zhang and Y. Ito (2003). "Preparative separation of rhein from Chinese traditional herb by repeated high-speed counter-current chromatography." Journal of Chromatography A **1017**(1-2): 125-130.

Wei, Y., T. Zhang, G. Xu and Y. Ito (2001). "Application of analytical and preparative high-speed counter-current chromatography for separation of lycopene from crude extract of tomato paste." Journal of Chromatography A **929**(1-2): 169-173.

Wei, Y., T. Y. Zhang and K. Y. Wu (2002). "Separation of eleutheroside E from crude extract of *Radix Acanthopanacis senticosus* by analytical and preparative high-speed countercurrent chromatography." Se Pu **20**(6): 543-545.

WHO executive board (2013). "Traditional medicine " **134**: 1-4.

Wikene, K. O., E. Bruzell and H. H. Tønnesen (2015). "Characterization and antimicrobial phototoxicity of curcumin dissolved in natural deep eutectic solvents." European Journal of Pharmaceutical Sciences **80**: 26-32.

Wikene, K. O., E. Bruzell and H. H. Tønnesen (2015). "Improved antibacterial phototoxicity of a neutral porphyrin in natural deep eutectic solvents." Journal of Photochemistry and Photobiology B: Biology **148**: 188-196.

Wikene, K. O., H. V. Rukke, E. Bruzell and H. H. Tønnesen (2016). "Physicochemical characterisation and antimicrobial phototoxicity of an anionic porphyrin in natural deep eutectic solvents." European Journal of Pharmaceutics and Biopharmaceutics **105**: 75-84.

Wilson, A. (1915). "The value of salicylic acid in the treatment of wounds and typhoid fever." British Medical Journal **1**(2825): 331-332.

Wood, P., S. Ignatova, L. Janaway, D. Keay, D. Hawes, I. Garrard and I. A. Sutherland (2007). "Counter-current chromatography separation scaled up from an analytical column to a production column." Journal of Chromatography A **1151**(1): 25-30.

Xin, R., S. Qi, C. Zeng, F. I. Khan, B. Yang and Y. Wang (2017). "A functional natural deep eutectic solvent based on trehalose: Structural and physicochemical properties." Food Chemistry **217**: 560-567.

Yanagida, A., A. Shoji, Y. Shibusawa, H. Shindo, M. Tagashira, M. Ikeda and Y. Ito

(2006). "Analytical separation of tea catechins and food-related polyphenols by high-speed counter-current chromatography." Journal of Chromatography A **1112**(1): 195-201.

Yang, C., Y. Yang, H. A. Aisa, X. Xin, H. Ma, A. Yili and Y. Zhao (2012). "Bioassay-guided isolation of antioxidants from *Astragalus altaicus* by combination of chromatographic techniques." Journal of Separation Science **35**(8): 977-983.

Yang, F. and Y. Ito (2002). "Preparative separation of lappaconitine, ranaconitine, *N*-deacetyllappaconitine and *N*-deacetylranaconitine from crude alkaloids of sample *Aconitum sinomontanum* Nakai by high-speed counter-current chromatography." Journal of Chromatography A **943**(2): 219-225.

Yao, Y., Z. Cheng, H. Ye, Y. Xie, J. He, M. Tang, T. Shen, J. Wang, Y. Zhou, Z. Lu, F. Luo, L. Chen, L. Yu, J.-L. Yang, A. Peng and Y. Wei (2010). "Preparative isolation and purification of anti-tumor agent ansamitocin P-3 from fermentation broth of *Actinosynnema pretiosum* using high-performance counter-current chromatography." Journal of Separation Science **33**(9): 1331-1337.

Ye, H., L. Chen, Y. Li, A. Peng, A. Fu, H. Song, M. Tang, H. Luo, Y. Luo, Y. Xu, J. Shi and Y. Wei (2008). "Preparative isolation and purification of three rotenoids and one isoflavone from the seeds of *Millettia pachycarpa* Benth by high-speed counter-current chromatography." Journal of Chromatography A **1178**(1-2): 101-107.

Yeh, J.-C., I. J. Garrard, C.-W. C. Cho, S. W. Annie Bligh, G.-h. Lu, T.-P. Fan and D. Fisher (2012). "Bioactivity-guided fractionation of the volatile oil of *Angelica sinensis* radix designed to preserve the synergistic effects of the mixture followed by identification of the active principles." Journal of Chromatography A **1236**: 132-138.

Yuan, Y., B. Wang, L. Chen, H. Luo, D. Fisher, I. A. Sutherland and Y. Wei (2008). "How to realize the linear scale-up process for rapid purification using high-performance counter-current chromatography." Journal of Chromatography A **1194**(2): 192-198.

Zhang, M., S. Ignatova, P. Hu, Q. Liang, Y. Wang, G. Luo, F. Wu Jun and I. Sutherland (2011). "Development of a strategy and process parameters for a green process in counter-current chromatography: Purification of tanshinone IIA and cryptotanshinone from *Salvia miltiorrhiza* Bunge as a case study." Journal of Chromatography A **1218**(36): 6031-6037.

Zhang, M., S. Ignatova, Q. Liang, F. Wu Jun, I. Sutherland, Y. Wang and G. Luo (2009). "Rapid and high-throughput purification of salvianolic acid B from *Salvia miltiorrhiza* Bunge by high-performance counter-current chromatography." Journal of Chromatography A **1216**(18): 3869-3873.

Zhang, S., X. Wang, F. Ouyang, Z. Su, C. Wang and M. Gu (2008). "Separation and purification of dl-tetrahydropalmatine from *Corydalis yanhusuo* W. T. Wang by HSCCC with a new solvents system screening method." Journal of Liquid

Chromatography and Related Technologies **31**(17): 2632-2642.

Zhao, B.-Y., P. Xu, F.-X. Yang, H. Wu, M.-H. Zong and W.-Y. Lou (2015). "Biocompatible deep eutectic solvents based on choline chloride: Characterization and application to the extraction of rutin from *Sophora japonica*." ACS Sustainable Chemistry and Engineering **3**(11): 2746-2755.

Zhou, T., G. Fan, Z. Hong, Y. Chai and Y. Wu (2005). "Large-scale isolation and purification of geniposide from the fruit of *Gardenia jasminoides* Ellis by high-speed counter-current chromatography." Journal of Chromatography A **1100**(1): 76-80.

8. APPENDICES

APPENDIX A

As qNMR represents a quantitative methodology that is performed electronically and can be stored digitally, it has unique potential for the implementation of electronic data (e-data). Importantly, because (q)NMR can yield qualitative and quantitative information simultaneously, e-data will be capable of covering both identity and purity/strength assays. The present study initiates the implement action of e-data by acquiring high-quality 1D NMR data sets of BDS marker compounds, interpreting the spectra using quantum mechanics and deconvolution methods, and generating electronic, instrument-independent e-data evaluation packages.

As an example, the qCNMR e-data were used in the Section 5.1, including for sucrose, citric acid, choline chloride, proline, and schisandrol A.

APPENDIX A (continued)

Sucrose

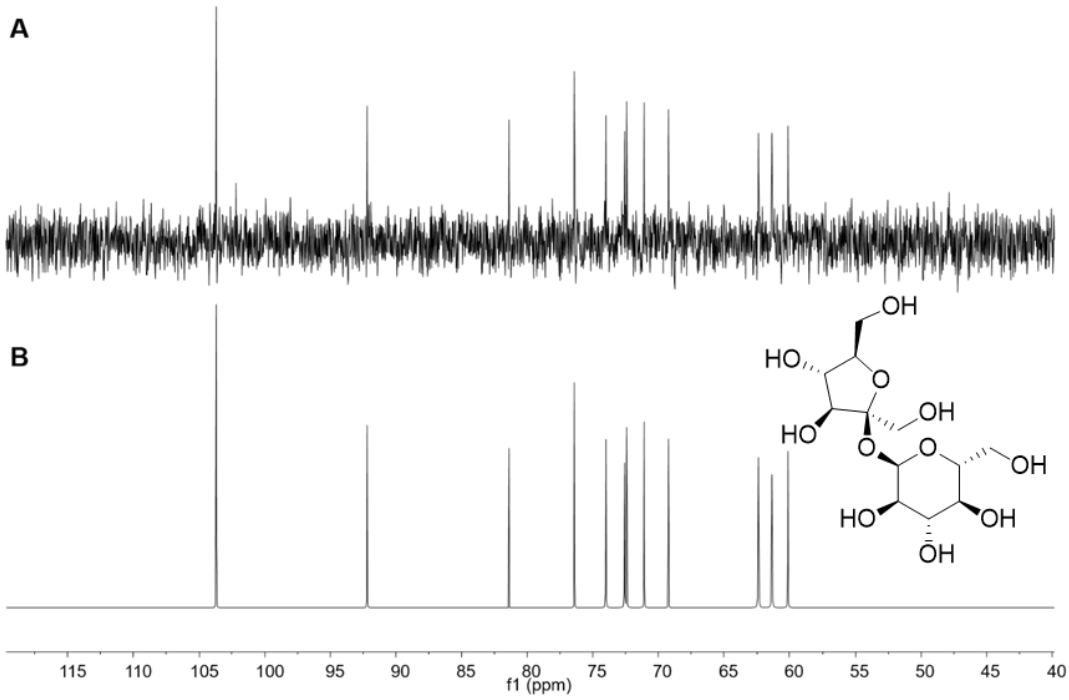

(A) qCNMR spectrum of sucrose; (B) MNova deconvolution filed spectrum of (A).

Citric acid

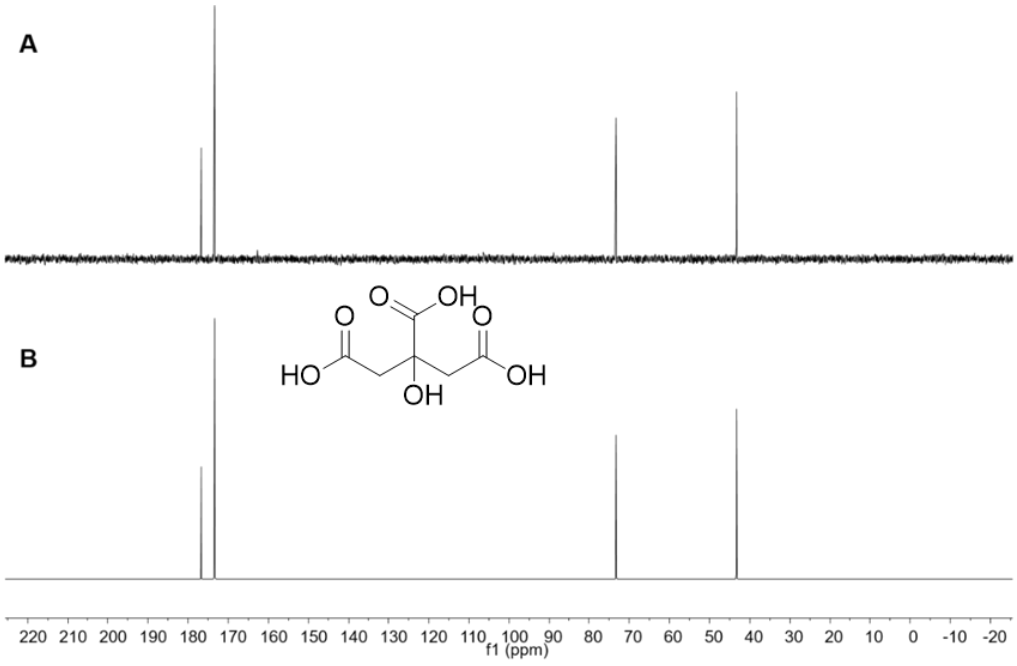

(A) qCNMR spectrum of citric acid; (B) MNova deconvolution filed spectrum of (A).

APPENDIX A (continued)

Choline chloride

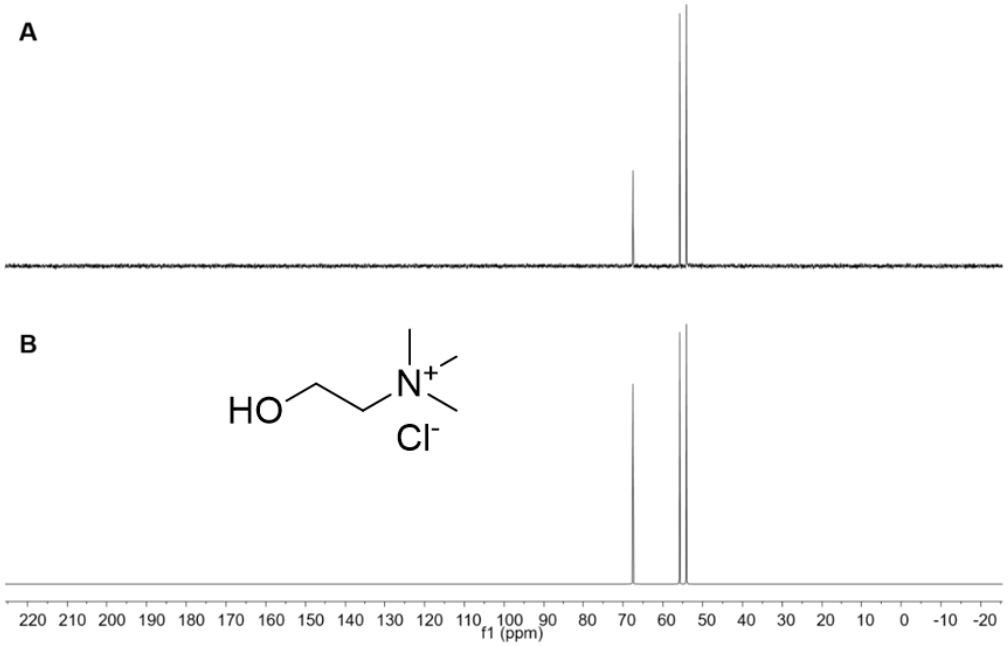

(A) qCNMR spectrum of choline Cl; (B) MNova deconvolution filed spectrum of (A).

Proline

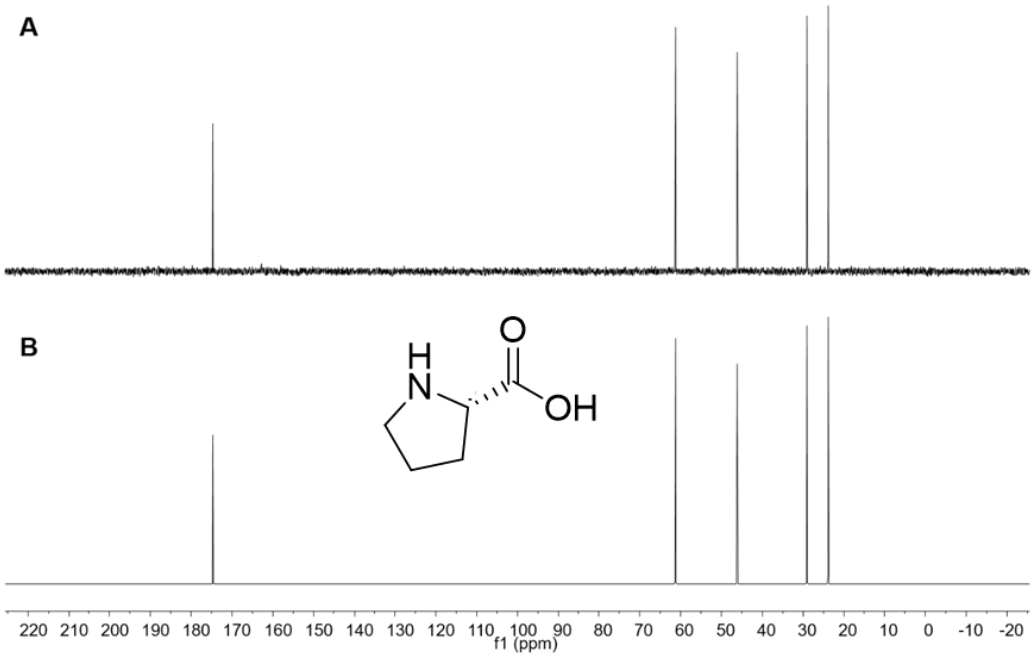

(A) qCNMR spectrum of proline; (B) MNova deconvolution filed spectrum of (A).

APPENDIX A (continued)

Schisandrol A

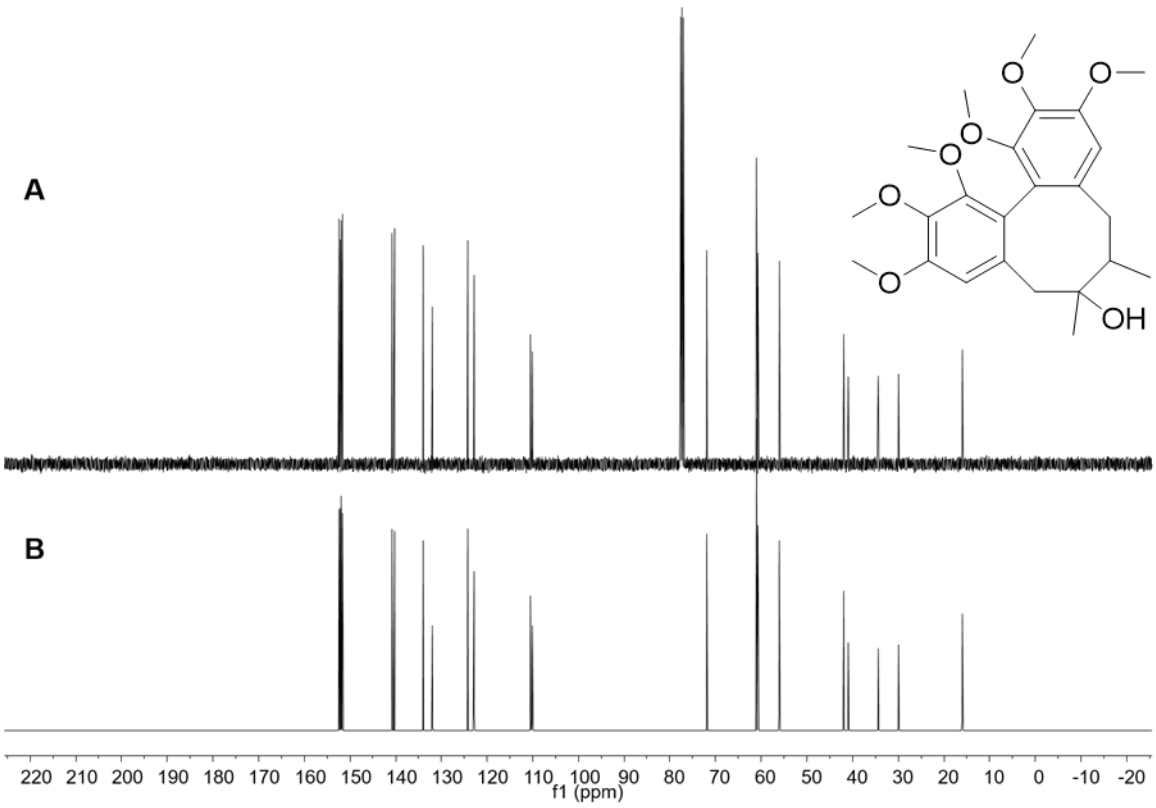

(A) qCNMR spectrum of schisandrol A; (B) MNova deconvolution filed spectrum of (A).

NADES Components and The Corresponding Frequency in References

Alcohol or sugar	F	Amino acid	F	Carboxylic acid	F	Carboxylates	F
Acetyl-glucosamine	1	Alanine	4	Aconitic acid	3	Acesulfamate	1
Adonitol	3	Arginine	1	Adipic acid	2	Acetate	1
Cyclodextrin	1	Asparic acid	1	Benzoic acid	2	Benzoate	1
Erythritol	1	Asparagine	1	Caffeic acid	1	Butanoate	1
Ethylene glycol	2	Glutamic acid	2	Citric acid	31	Decanoate	1
Fructose	19	Glutamine	1	Cinnamic acid	1	Fumarate	1
Galactose	3	Glycine	1	Coumaric acid	1	Glycolate	1
Deoxy-glucose	1	Histidine	1	Gallic acid	1	Hexanoate	1
Glucose	34	Isoleucine	1	Hyroxybenzoic acid	1	Isobutyrate	1
Glucosamine	1	Leucine	1	Itaconic acid	1	Maleate	1
Glycerol	8	Lysine	1	Lactic acid	4	Malate	1
Ethylene Glycol	1	Methionine	1	Levulinic acid	1	Octanoate	1
Meso-inositol	2	Phenylalanine	1	Maleic acid	5	Pivalate	1
Isomaltose	1	Proline	21	Malic acid	35	Propionate	1
Isosorbide	1	Serine	3	Mandelic acid	1	Tartarate	1
Lactose	25	Threonine	1	Malonic acid	6	Tiglate	1
Maltose	5	Tryptophan	1	Oxalic acid	3	Saccharinate	1
Mannitol	2	Valine	1	Phenylacetic acid	3	Succinate	1
Mannose	8			Phenylpropionic acid	1	Valeric acid	2
		Ammonium and					
Propanediol	2	other organic salts	F	Suberic acid	1		
Raffinose	4	Betaine	18	Succinic acid	2	Urea derivatives	F
Rhamnose	2	Betaine hydrochloride	2	Tartaric acid	5	Dimethylurea	15
Ribitol	2	Carnitine	1	Tricarballylic acid	2	Guanidinium HCl	1
Sorbitol	15	Choline bitartrate	1			Urea	16
Sorbose	2	Choline chloride	96				
Sucrose	22	Phytic acid sodium	6				
Trehalose	5	Glutamic salt	2				
Xylitol	6						
Xylose	3						
Vanillin	1						

Note: F represents frequency; References are (Choi et al. 2011 and 2013) and (Ru and Konig 2012).

Appendix B (continued)

Abbreviations of the Most Common Reported NADES Components (Reporting Frequency > 10)

NADES components	Abbreviation	Frequency
Choline chloride	Ch	96
Malic acid	M	35
Glucose	G	34
Citric acid	C	31
Lactose	L	25
Sucrose	S	22
Proline	P	21
Fructose	F	19
Betaine	B	18
Sorbitol	So	15

Appendix C

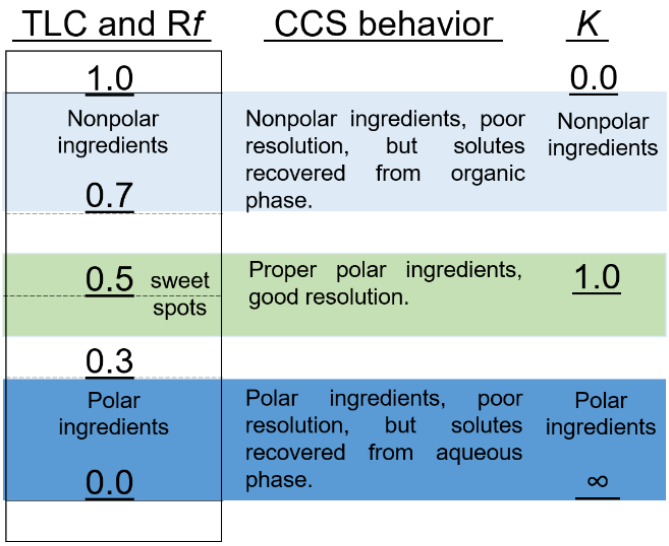

For some analytes investigated using the HEMWat family, TLC R*f* values near 0.5 and ranging from 0.3 to 0.7 typically correspond to the CCS K value sweet spot (see naringenin, reserpine, and umbelliferone in TABLE III). This demonstrated that the TLC R*f* sweet spots for CCS prediction may cover the range from 0.3 to 0.7, or even broader. The results also indicated that the actual R*f* sweet spot range can change on a case by case basis, depending on the analyte and/or the SS. These insights have to be considered for the general understanding of what constitutes R*f* sweet spots that correspond to CCS performance.

As a practical guide, three R*f* value zones are proposed as a result of the present study. They are: the R*f* value sweet spots where R*f* is close to 0; the effective separation zone, ranging from 0.3 to 0.7; and the non-effective zones, ranging from 0 to 0.3 and 0.7 to 1. Regardless of how the R*f* sweet spot range is changed, they always cover the point at R*f* = 0.5 (in Figures 13 and 14). Thus, R*f* values near 0.5, consider as an accepted Rf sweet spot range, reliably predict K value sweet spots

Appendix C (continued)

most reliably. As many factors including temperature, atmospheric pressure, the quality of solvents, TLC chamber condition (saturated vs non-saturated), and even the TLC practitioner's spotting habits affect the TLC results in practice, these factors combined can lead to varying in results. Thus, in practice, R*f* value sweet spots may shift slightly away from (but stay near) the point of 0.5.

Appendix D

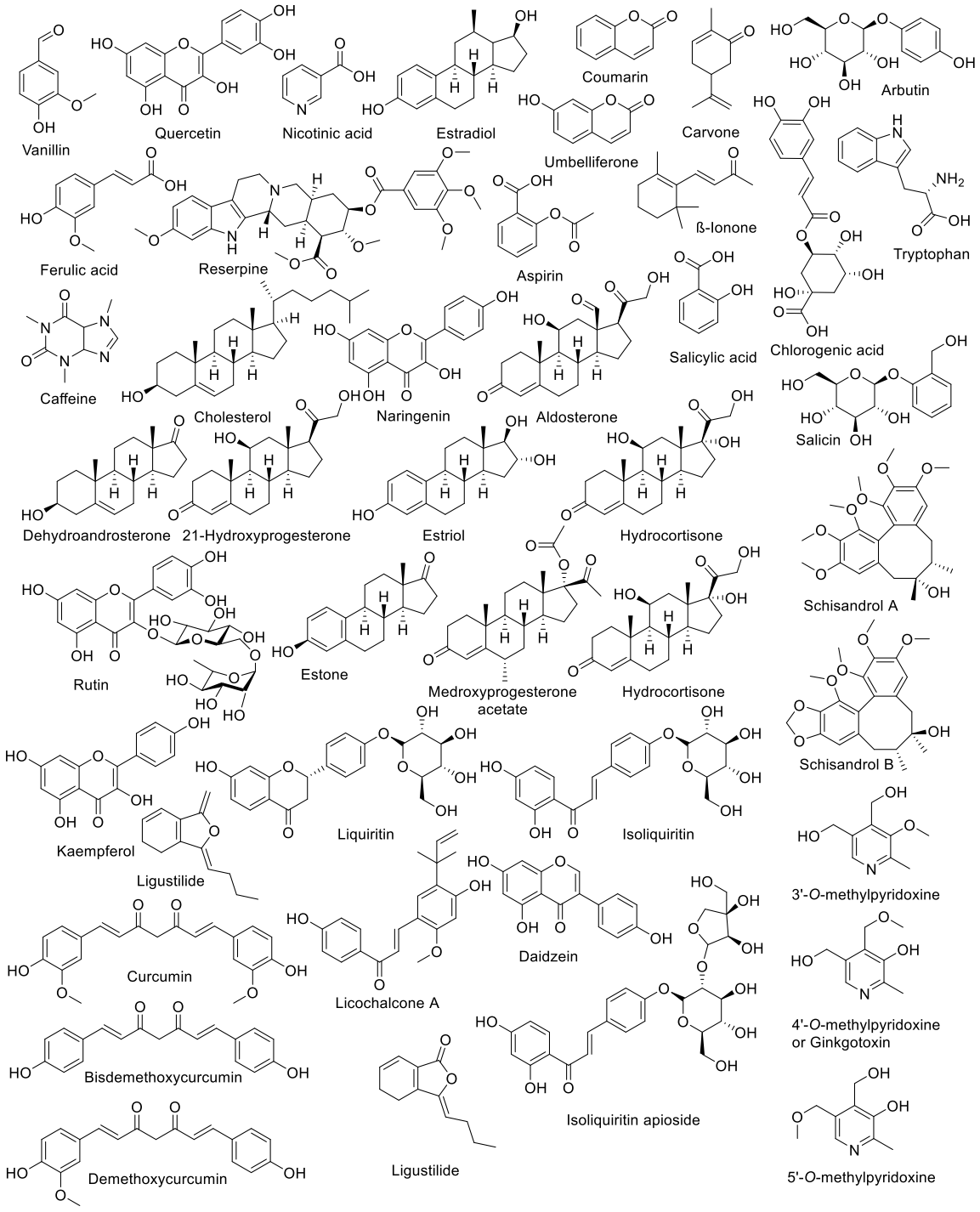
Vanillin
Quercetin
Nicotinic acid
Estradiol
Coumarin
Umbelliferone
Carvone
Arbutin
Ferulic acid
Reserpine
Aspirin
ß-Ionone
Tryptophan
Caffeine
Cholesterol
Naringenin
Aldosterone
Salicylic acid
Chlorogenic acid
Salicin
Dehydroandrosterone
21-Hydroxyprogesterone
Estriol
Hydrocortisone
Schisandrol A
Rutin
Estone
Medroxyprogesterone acetate
Hydrocortisone
Schisandrol B
Kaempferol
Ligustilide
Liquiritin
Isoliquiritin
3'-O-methylpyridoxine
Curcumin
Licochalcone A
Daidzein
Bisdemethoxycurcumin
4'-O-methylpyridoxine or Ginkgotoxin
Isoliquiritin apioside
Demethoxycurcumin
Ligustilide
5'-O-methylpyridoxine

Appendix E

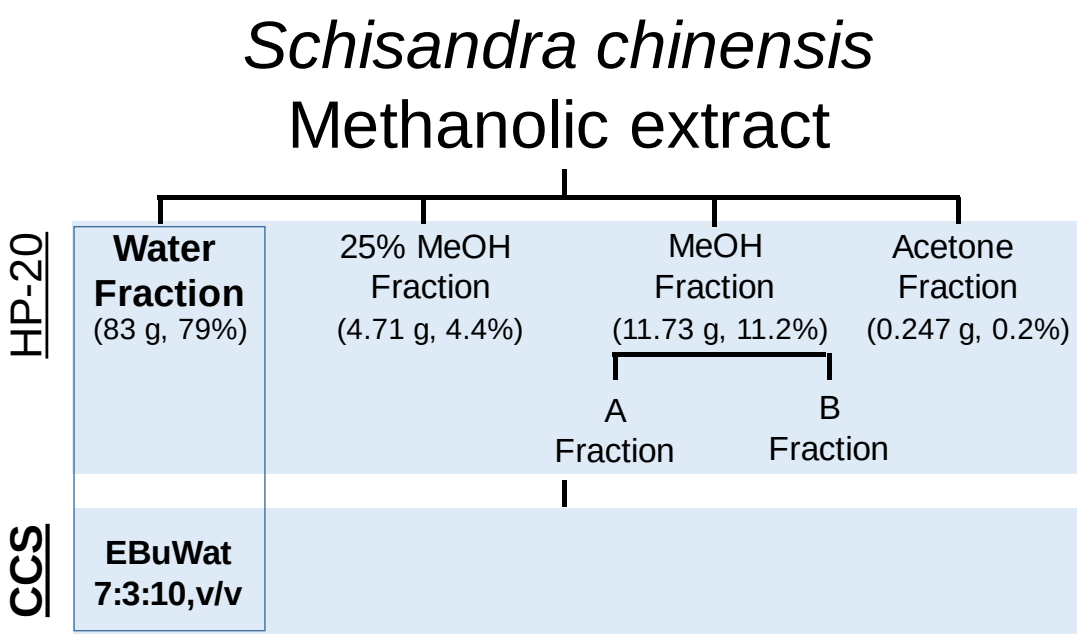

Scheme of the sub-fractionation procedure of the *S. chinensis* HP-20 water fraction

The water fraction mostly contains highly polar ingredients.
EBWat (7:3:10, v/v) was selected as CCS SS.

HSCCC (16 mL) Sf = 0.5, flow rate 0.3 mL/min, 30 mg of water fraction, 3 min/tube;

HSCCC (320 mL) Sf = 0.78, flow rate 1 mL/min, 332 mg of water fraction, 12 min/tube.

Lower phase as mobile phase.

Citric acid (eluted in K value range, 0.25-0.63) and malic acid (eluted in K value range, 0.58-0.67) were identified from the resulting fractions.

Appendix E (continued)

Citric acid

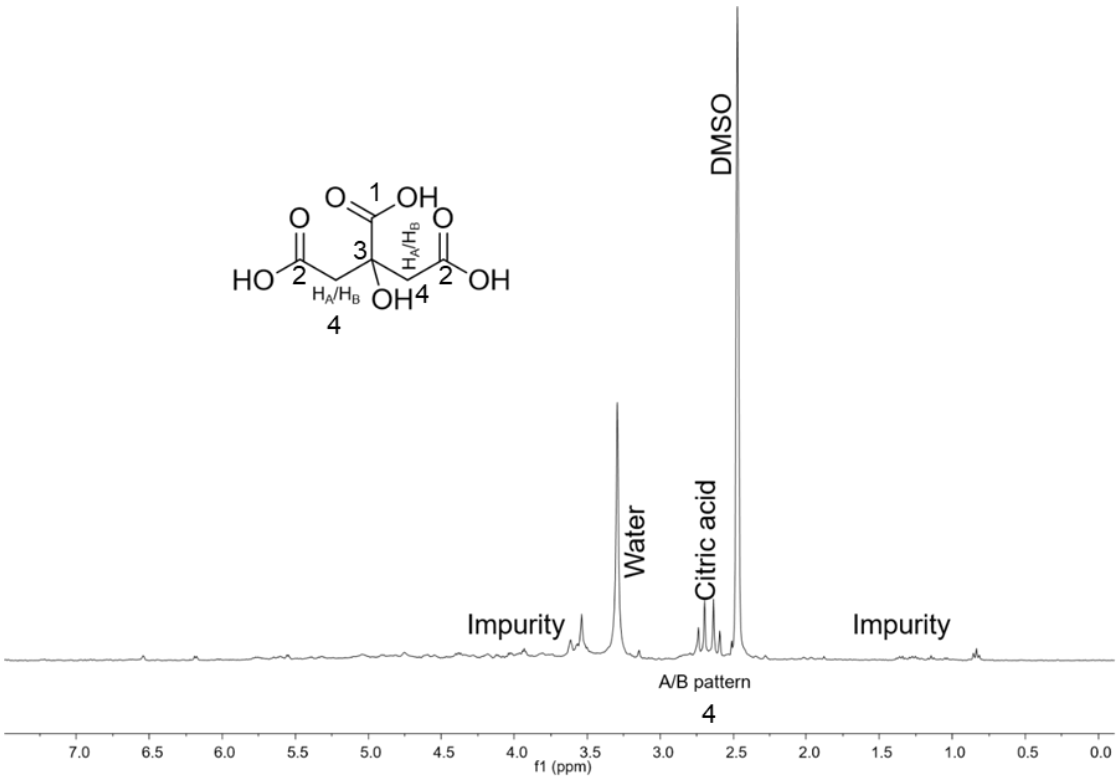

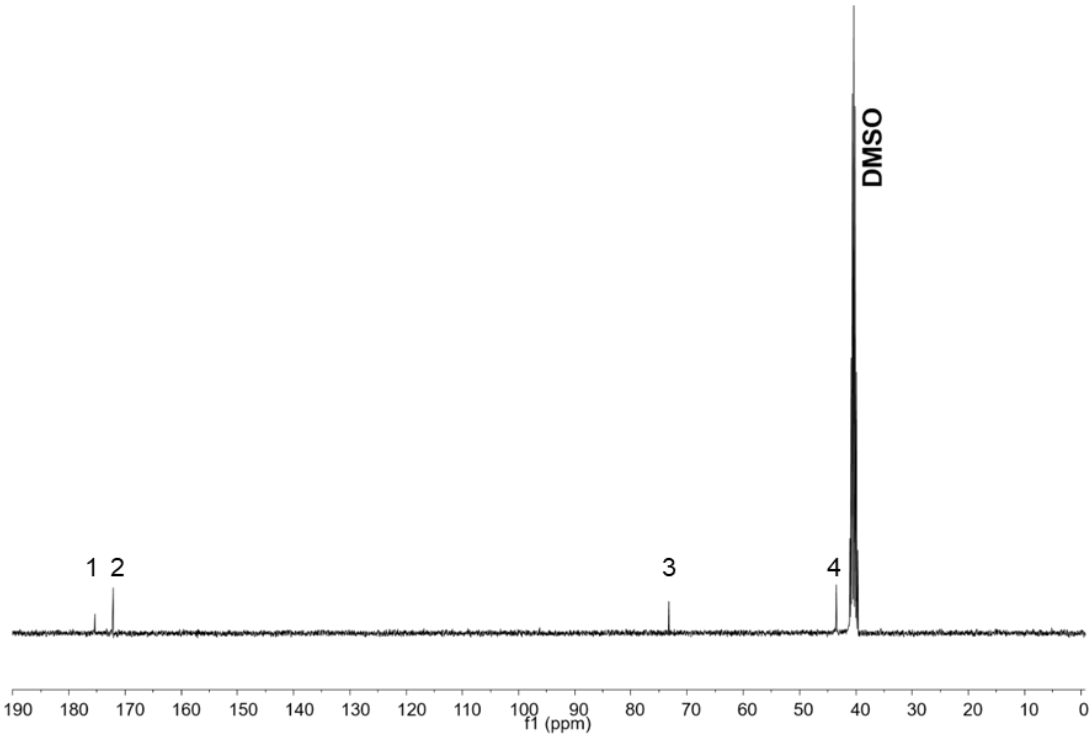

Appendix E (continued)

Malic acid

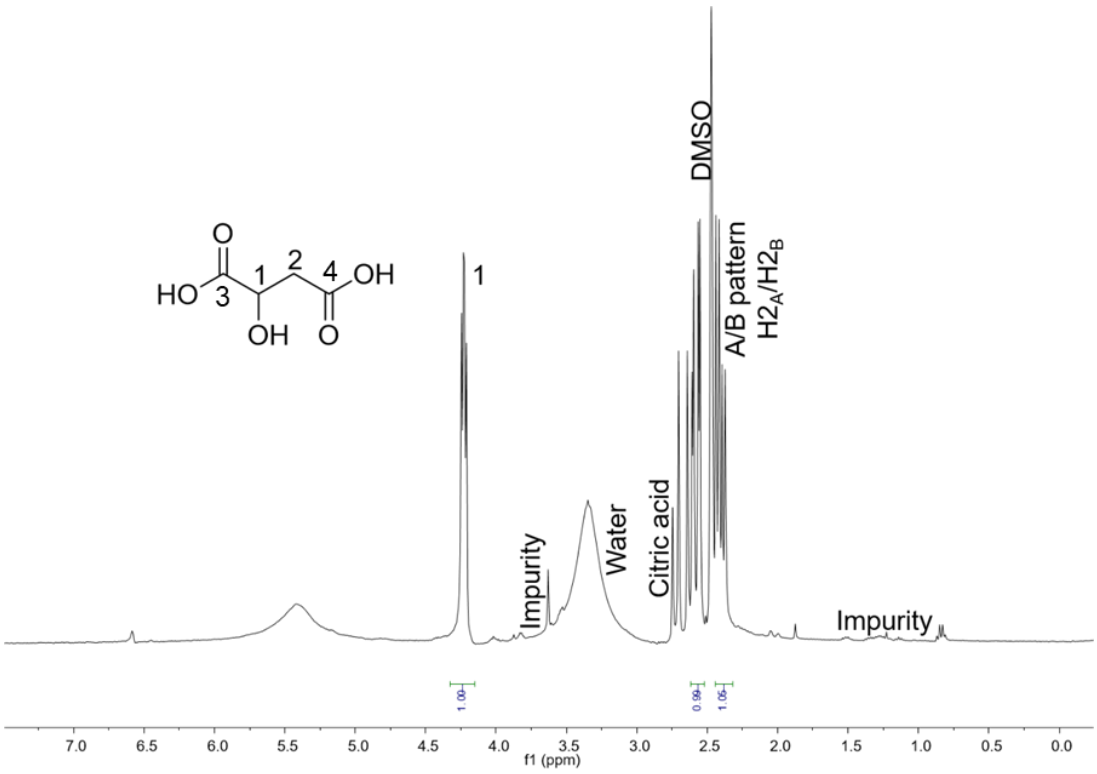

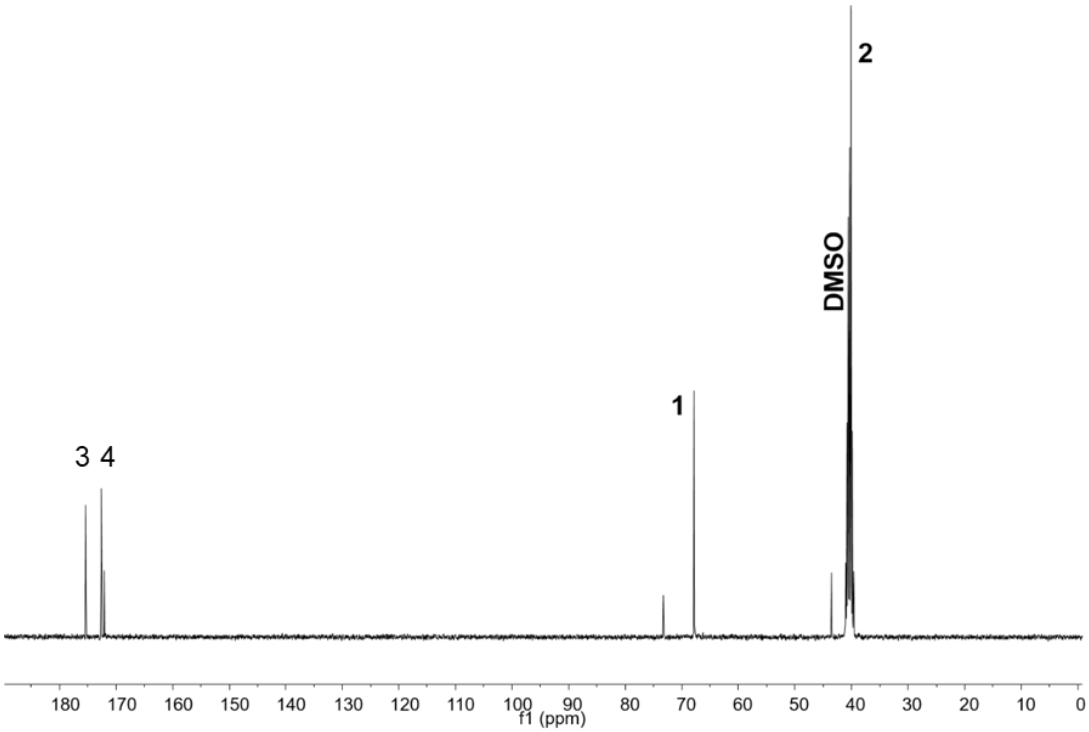

Appendix F

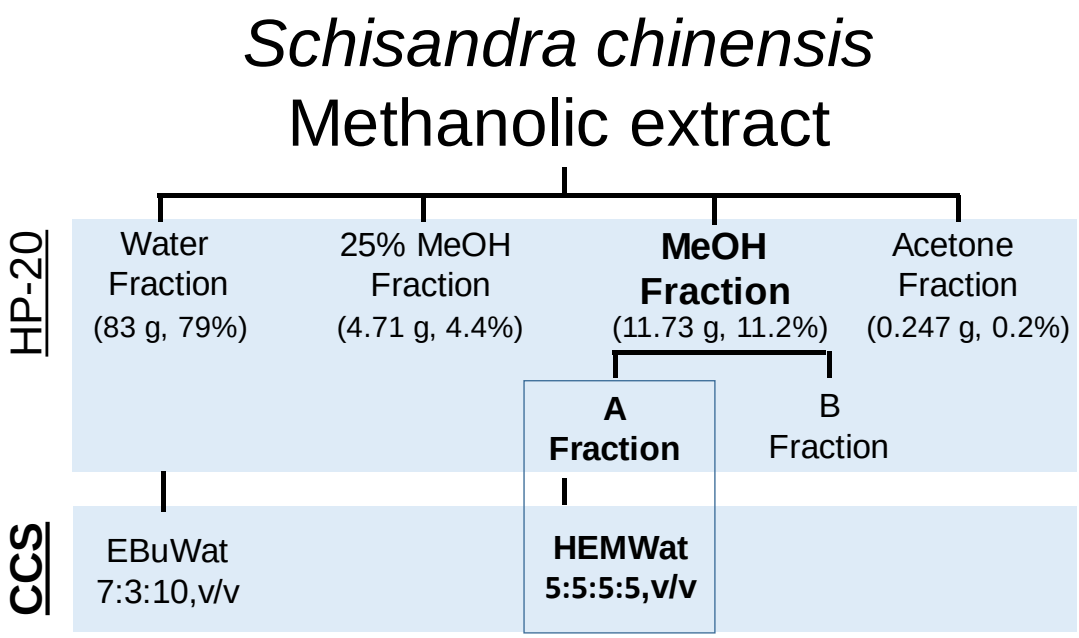

Scheme of the sub-fractionation procedure of *S. chinensis* methanol fraction

HEMWat (5:5:5:5, v/v) was selected for CCS. HSCCC (320 mL) Sf=0.78, flow rate 1 mL/min, 100 mg of MeOH fraction, collecting 12 min/tube. Lower phase as mobile phase.

According to TLC matching results, F26 (schisandrol A) and F42 (schisandrol B, gomisin J, and angeloylgomisin H) were purified further by prep-HPLC. All proton assignment can be found in Figure 43. ^{13}C assignments of schisandrol A can be found in Figure 6.

Appendix F (continued)

Schisandrol A or Schizandrin

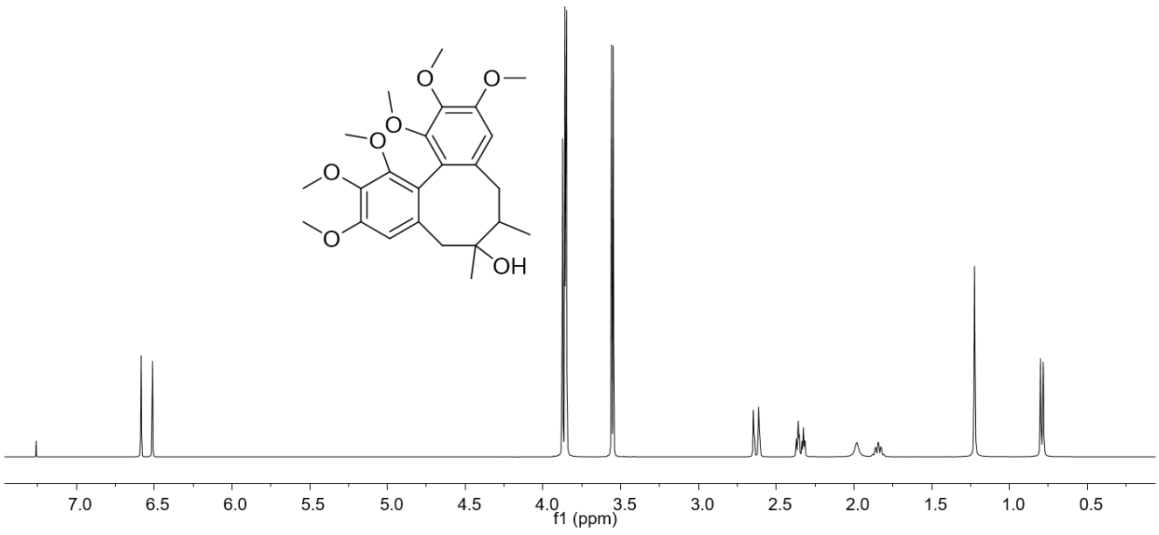

^{1}H NMR spectrum of schisandrol A

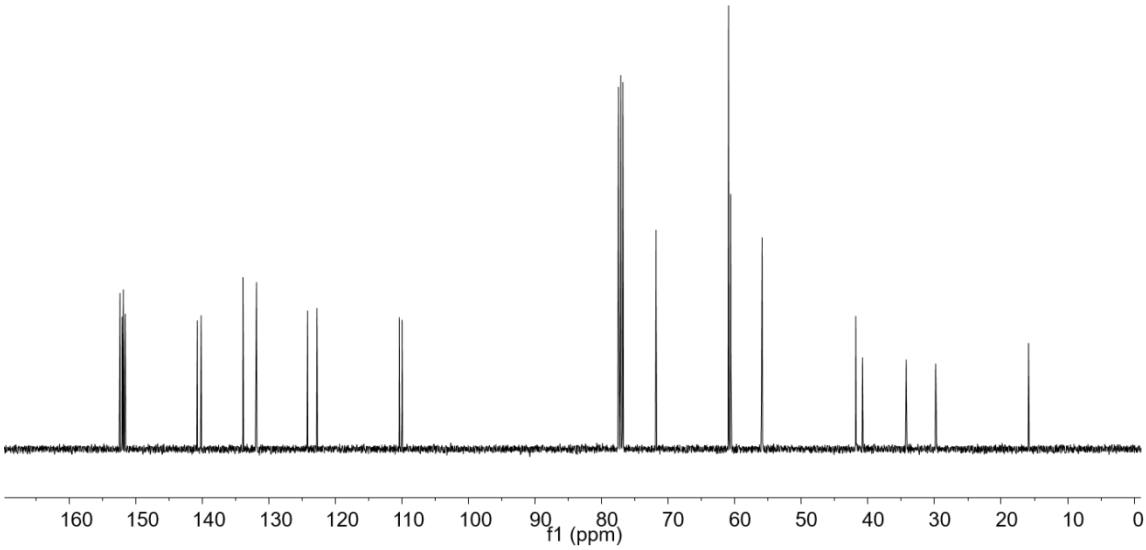

^{13}C NMR spectrum of schisandrol A

Appendix F (continued)

Gomisin J

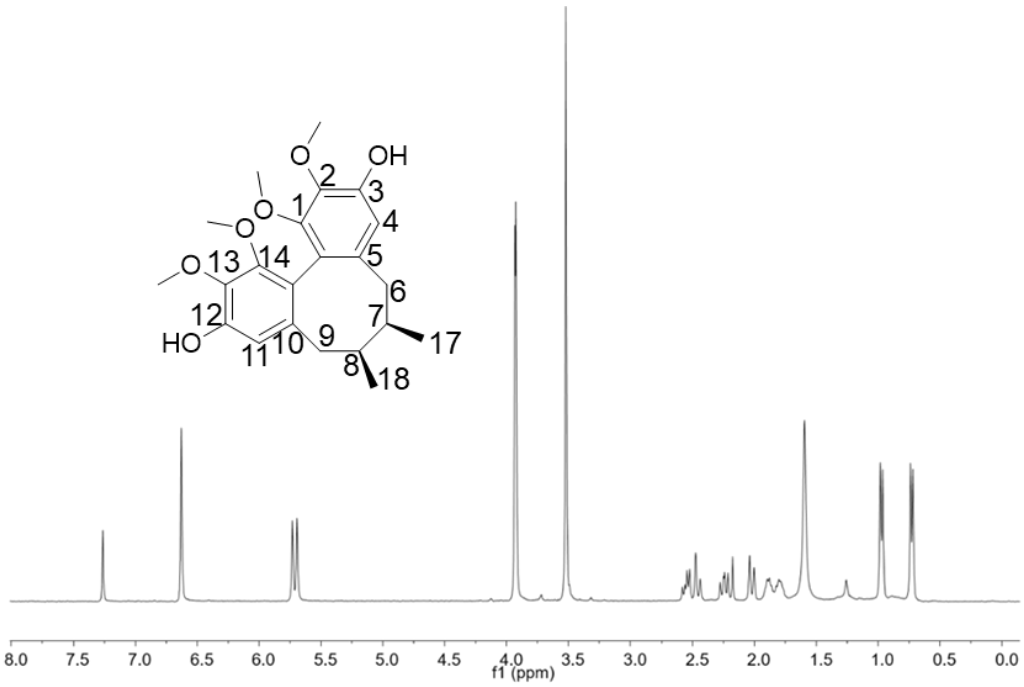

^{1}H NMR spectrum of gomisin J

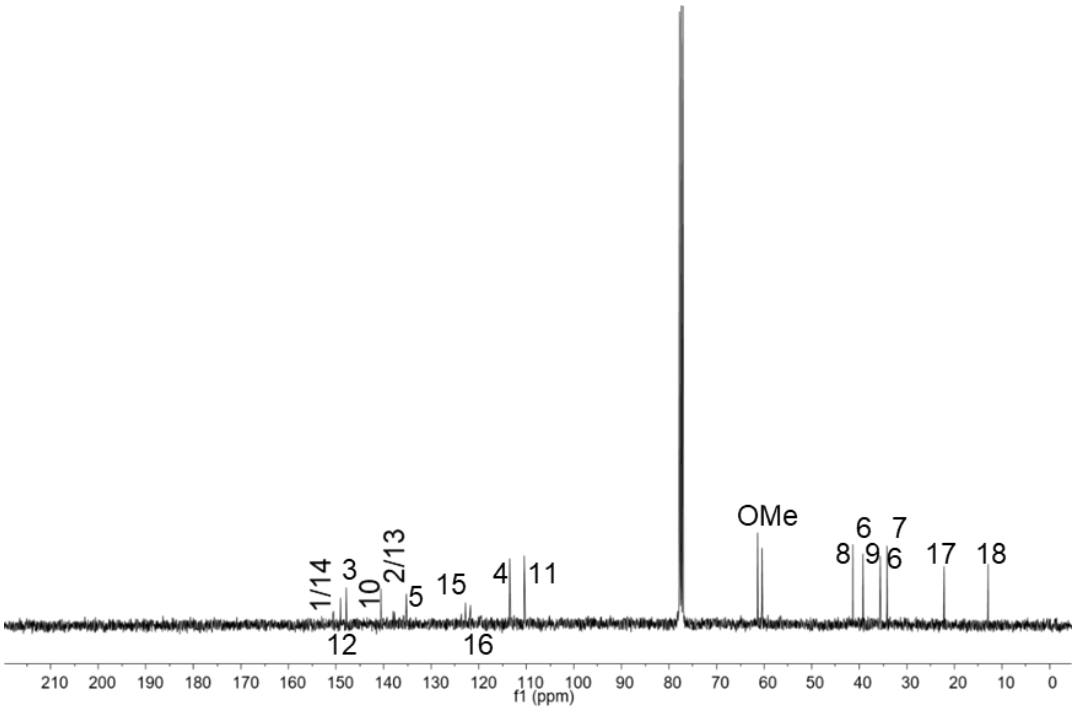

^{13}C NMR spectrum of gomisin J

Appendix F (continued)

Schisandrol B or Gomisin A

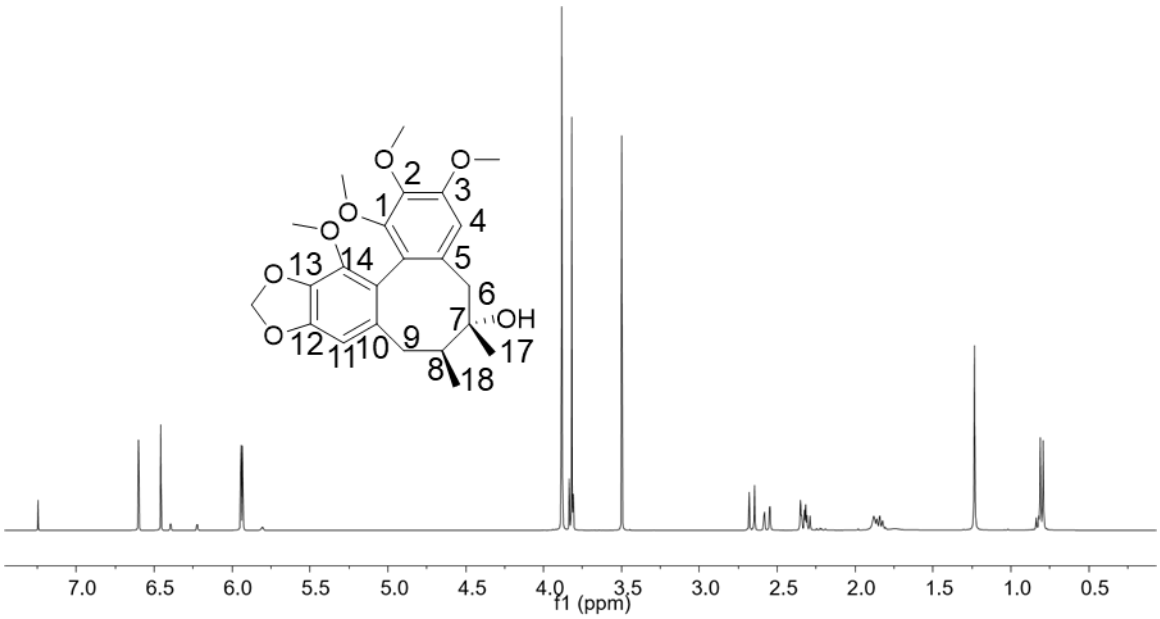

^{1}H NMR spectrum of schisandrol B

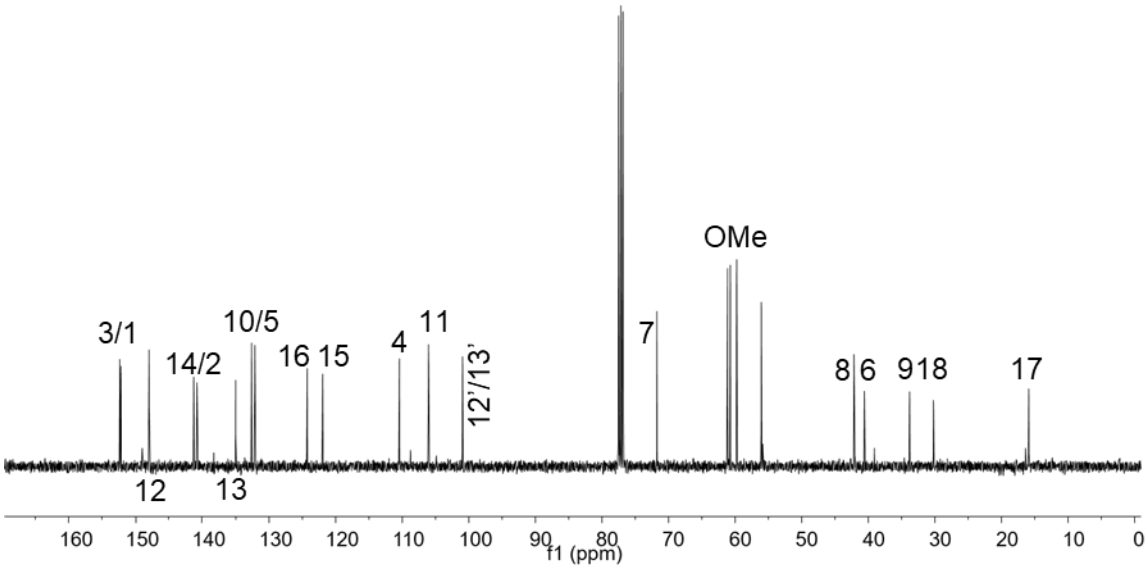

^{13}C NMR spectrum of schisandrol B

Appendix F (continued)

Angeloylgomisin H

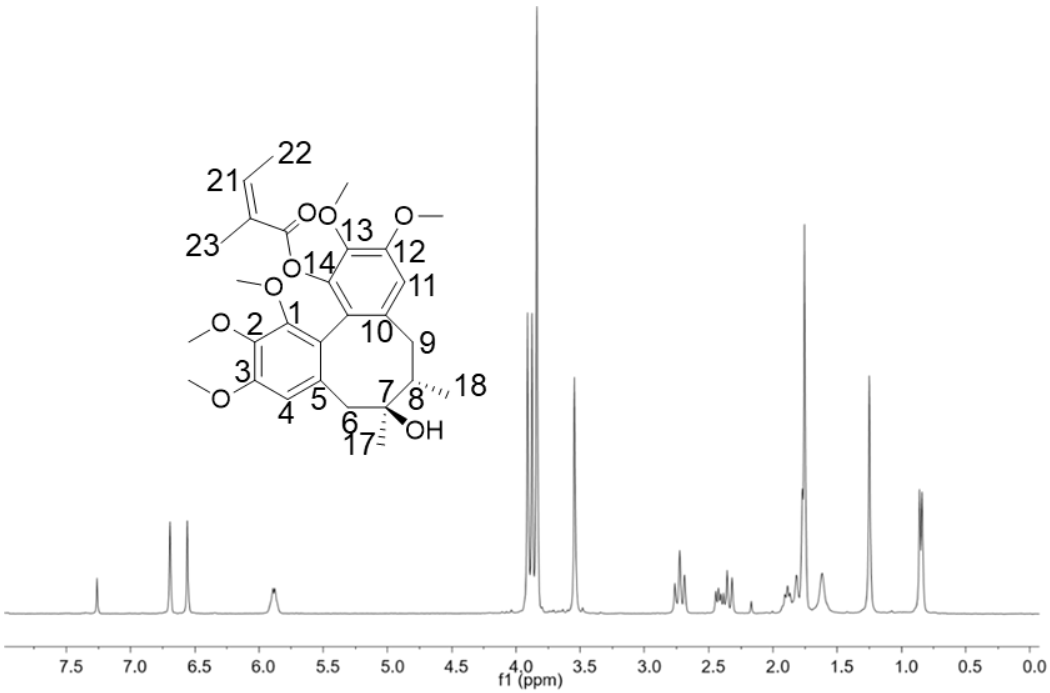

^{1}H NMR spectrum of Angeloylgomisin H

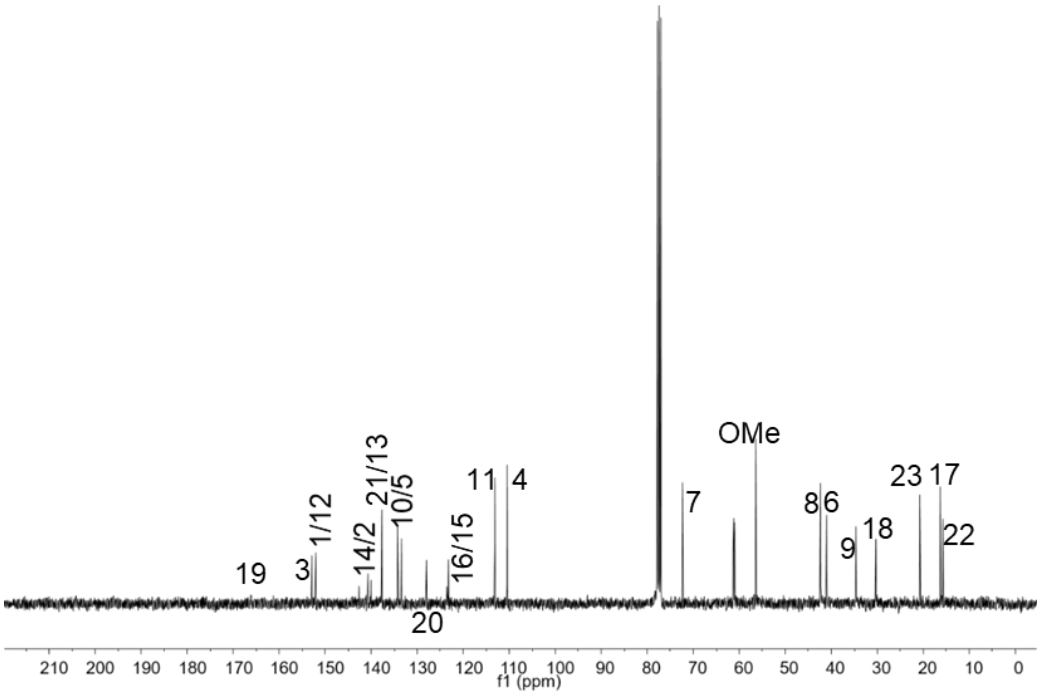

^{13}C NMR spectrum of Angeloylgomisin H

Appendix G

Liu, Y., S. N. Chen, J. B. McAlpine, L. L. Klein, J. B. Friesen, D. C. Lankin and G. F. Pauli (2014). "Quantification of a botanical negative marker without an identical standard: ginkgotoxin in Ginkgo biloba." J Nat Prod **77**(3): 611 -617.

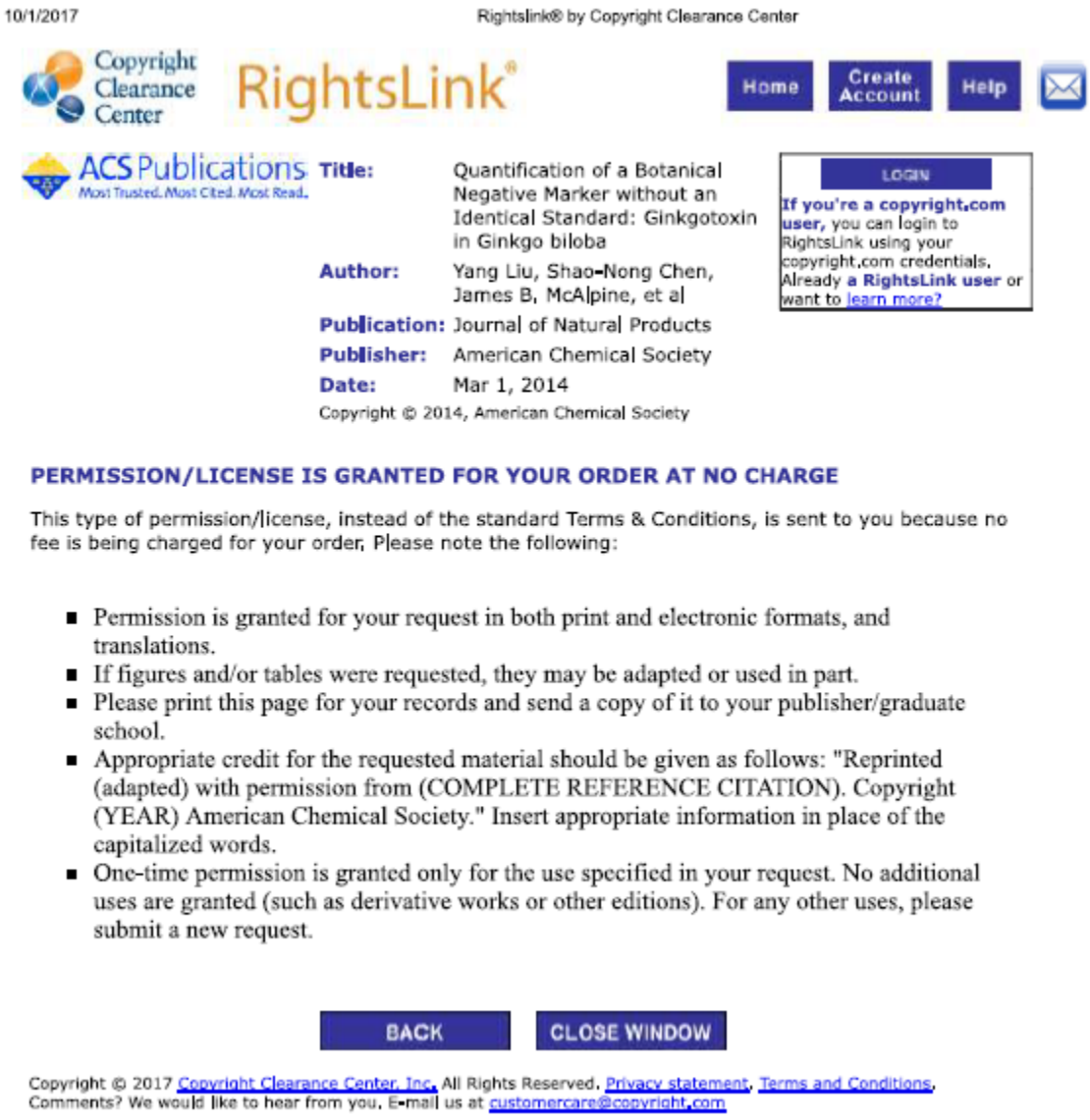

10/1/2017 Rightslink® by Copyright Clearance Center

Copyright Clearance Center RightsLink® Home Create Account Help

ACS Publications Most Trusted. Most Cited. Most Read.

Title: Quantification of a Botanical Negative Marker without an Identical Standard: Ginkgotoxin in Ginkgo biloba
Author: Yang Liu, Shao-Nong Chen, James B. McAlpine, et al
Publication: Journal of Natural Products
Publisher: American Chemical Society
Date: Mar 1, 2014
Copyright © 2014, American Chemical Society

LOGIN
If you're a copyright.com user, you can login to RightsLink using your copyright.com credentials. Already a RightsLink user or want to learn more?

PERMISSION/LICENSE IS GRANTED FOR YOUR ORDER AT NO CHARGE

This type of permission/license, instead of the standard Terms & Conditions, is sent to you because no fee is being charged for your order. Please note the following:

- Permission is granted for your request in both print and electronic formats, and translations.
- If figures and/or tables were requested, they may be adapted or used in part.
- Please print this page for your records and send a copy of it to your publisher/graduate school.
- Appropriate credit for the requested material should be given as follows: "Reprinted (adapted) with permission from (COMPLETE REFERENCE CITATION). Copyright (YEAR) American Chemical Society." Insert appropriate information in place of the capitalized words.
- One-time permission is granted only for the use specified in your request. No additional uses are granted (such as derivative works or other editions). For any other uses, please submit a new request.

BACK CLOSE WINDOW

Copyright © 2017 Copyright Clearance Center, Inc. All Rights Reserved. Privacy statement. Terms and Conditions.
Comments? We would like to hear from you. E-mail us at customercare@copyright.com

Appendix G (continued)

Liu, Y., J. B. Friesen, L. L. Klein, J. B. McAlpine, D. C. Lankin, G. F. Pauli and S. N. Chen (2015). "The Generally Useful Estimate of Solvent Systems (GUESS) method enables the rapid purification of methylpyridoxine regioisomers by countercurrent chromatography." J Chromatogr A **1426**: 248-251.

Copyright Clearance Center RightsLink®

Home | Account Info | Help

Title: The Generally Useful Estimate of Solvent Systems (GUESS) method enables the rapid purification of methylpyridoxine regioisomers by countercurrent chromatography

Author: Yang Liu,J. Brent Friesen,Larry L. Klein,James B. McAlpine,David C. Lankin,Guido F. Pauli,Shao-Nong Chen

Publication: Journal of Chromatography A

Publisher: Elsevier

Date: 24 December 2015

Copyright © 2015 Elsevier B.V. All rights reserved.

Logged in as:
Yang Liu
LOGOUT

Order Completed

Thank you for your order.

This Agreement between University of Illinois, at Chicago ("You") and Elsevier ("Elsevier") consists of your license details and the terms and conditions provided by Elsevier and Copyright Clearance Center.

Your confirmation email will contain your order number for future reference.

printable details

License Number	4200430863335
License date	Oct 01, 2017
Licensed Content Publisher	Elsevier
Licensed Content Publication	Journal of Chromatography A
Licensed Content Title	The Generally Useful Estimate of Solvent Systems (GUESS) method enables the rapid purification of methylpyridoxine regioisomers by countercurrent chromatography
Licensed Content Author	Yang Liu,J. Brent Friesen,Larry L. Klein,James B. McAlpine,David C. Lankin,Guido F. Pauli,Shao-Nong Chen
Licensed Content Date	Dec 24, 2015
Licensed Content Volume	1426
Licensed Content Issue	n/a
Licensed Content Pages	4
Type of Use	reuse in a thesis/dissertation
Portion	full article
Format	electronic

Appendix G (continued)

Liu, Y., J. B. Friesen, J. B. McAlpine and G. F. Pauli (2015). "Solvent System Selection Strategies in Countercurrent Separation." Planta Med **81**(17): 1582-1591.

Copyright Clearance Center RightsLink®

Home | Account Info | Help

Thieme

Title: Solvent System Selection Strategies in Countercurrent Separation

Author: Yang Liu, J. Brent Friesen, James B, McAlpine, Guido F, Pauli

Publication: Planta Medica

Publisher: Thieme

Date: Jan 1, 2015

Copyright © 2015, Rights Managed by Georg Thieme Verlag KG Stuttgart • New York

Logged in as:
Yang Liu
LOGOUT

Permission Request Submitted

Your request is now under review.
You will be notified of the decision via email.
Please print this request for your records.

printable details

Order Number	501316038
Order Date	Oct 01, 2017
Licensed Content Publisher	Thieme
Licensed Content Publication	Planta Medica
Licensed Content Title	Solvent System Selection Strategies in Countercurrent Separation
Licensed Content Author	Yang Liu, J. Brent Friesen, James B. McAlpine, Guido F. Pauli
Licensed Content Date	Jan 1, 2015
Licensed Content Volume	81
Licensed Content Issue	17
Type of Use	Dissertation/Thesis
Requestor type	author of the original Thieme publication
Format	electronic
Portion	full article/document
Will you be translating?	no
Distribution quantity	1
Specified additional information	Use the content in my dissertation.

Appendix G (continued)

Liu, Y., J. Garzon, J. B. Friesen, Y. Zhang, J. B. McAlpine, D. C. Lankin, S. N. Chen and G. F. Pauli (2016). "Countercurrent assisted quantitative recovery of metabolites from plant-associated natural deep eutectic solvents." Fitoterapia **112**: 30-37.

Copyright Clearance Center RightsLink®

Home | Account Info | Help

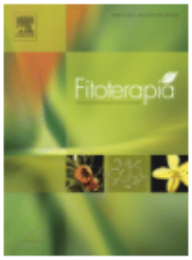

Title: Countercurrent assisted quantitative recovery of metabolites from plant-associated natural deep eutectic solvents

Author: Yang Liu,Jahir Garzon,J. Brent Friesen,Yu Zhang,James B. McAlpine,David C. Lankin,Shao-Nong Chen,Guido F. Pauli

Publication: Fitoterapia

Publisher: Elsevier

Date: July 2016

Logged in as:
Yang Liu
LOGOUT

Order Completed

Thank you for your order.

This Agreement between University of Illinois, at Chicago ("You") and Elsevier ("Elsevier") consists of your license details and the terms and conditions provided by Elsevier and Copyright Clearance Center.

Your confirmation email will contain your order number for future reference.

printable details

License Number	4200440470327
License date	Oct 01, 2017
Licensed Content Publisher	Elsevier
Licensed Content Publication	Fitoterapia
Licensed Content Title	Countercurrent assisted quantitative recovery of metabolites from plant-associated natural deep eutectic solvents
Licensed Content Author	Yang Liu,Jahir Garzon,J. Brent Friesen,Yu Zhang,James B. McAlpine,David C. Lankin,Shao-Nong Chen,Guido F. Pauli
Licensed Content Date	Jul 1, 2016
Licensed Content Volume	112
Licensed Content Issue	n/a
Licensed Content Pages	8
Type of Use	reuse in a thesis/dissertation
Portion	full article
Format	electronic

Appendix G (continued)

Liu, Y., J. B. Friesen, E. M. Grzelak, Q. Fan, T. Tang, K. Duric, B. U. Jaki, J. B. McAlpine, S. G. Franzblau, S. N. Chen and G. F. Pauli (2017). " Sweet spot matching: A thin-layer chromatography-based countercurrent solvent system selection strategy." J Chromatogr A **1504**: 46-54.

Copyright Clearance Center RightsLink®

Home | Account Info | Help

Title: Sweet spot matching: A thin-layer chromatography-based countercurrent solvent system selection strategy

Author: Yang Liu,J. Brent Friesen,Edyta M. Grzelak,Qingfei Fan,Ting Tang,Kemal Durić,Birgit U. Jaki,James B. McAlpine,Scott G. Franzblau,Shao-Nong Chen,Guido F. Pauli

Publication: Journal of Chromatography A

Publisher: Elsevier

Date: 30 June 2017

Logged in as:
Yang Liu
LOGOUT

Review Order

Please review the order details and the associated terms and conditions.

No royalties will be charged for this reuse request although you are required to obtain a license and comply with the license terms and conditions. To obtain the license, click the Accept button below.

Licensed Content Publisher	Elsevier
Licensed Content Publication	Journal of Chromatography A
Licensed Content Title	Sweet spot matching: A thin-layer chromatography-based countercurrent solvent system selection strategy
Licensed Content Author	Yang Liu,J. Brent Friesen,Edyta M. Grzelak,Qingfei Fan,Ting Tang,Kemal Durić,Birgit U. Jaki,James B. McAlpine,Scott G. Franzblau,Shao-Nong Chen,Guido F. Pauli
Licensed Content Date	30 June 2017
Licensed Content Volume	1504
Licensed Content Issue	n/a
Licensed Content Pages	9
Type of Use	reuse in a thesis/dissertation
Portion	full article
Format	electronic

Appendix G (continued)

Liu Y., Friesen J.B., McAlpine, Lankin, D.C., Chen, S.N., and Pauli, G.F. "Natural Deep Eutectic Solvents: Properties, Applications, and Perspectives" (2018). Journal of Natural Products, **81**: 679–690.

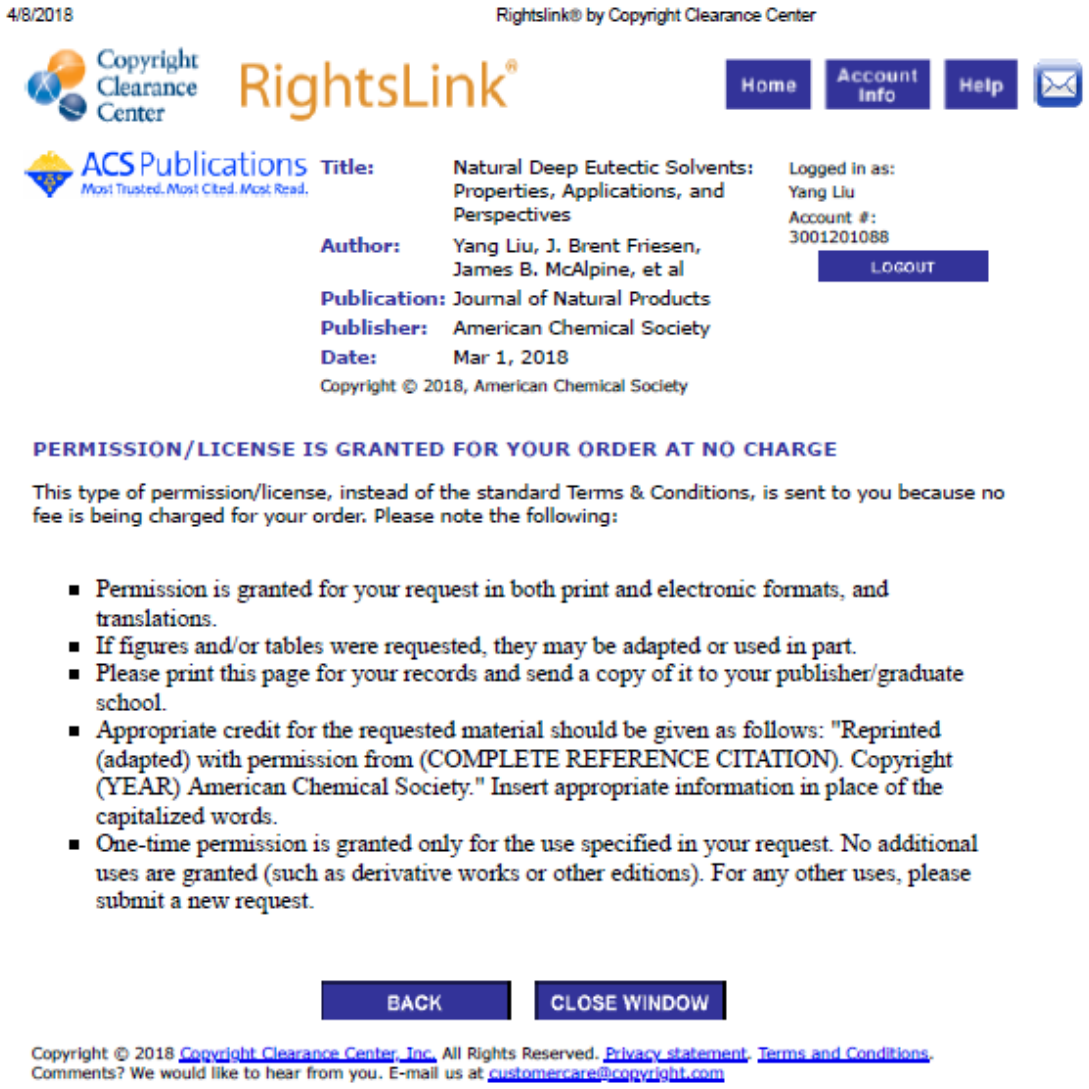

4/8/2018 Rightslink® by Copyright Clearance Center

Copyright Clearance Center RightsLink®

Home | Account Info | Help

ACS Publications Most Trusted. Most Cited. Most Read.

Title: Natural Deep Eutectic Solvents: Properties, Applications, and Perspectives

Author: Yang Liu, J. Brent Friesen, James B. McAlpine, et al

Publication: Journal of Natural Products

Publisher: American Chemical Society

Date: Mar 1, 2018

Copyright © 2018, American Chemical Society

Logged in as: Yang Liu
Account #: 3001201088
LOGOUT

PERMISSION/LICENSE IS GRANTED FOR YOUR ORDER AT NO CHARGE

This type of permission/license, instead of the standard Terms & Conditions, is sent to you because no fee is being charged for your order. Please note the following:

- Permission is granted for your request in both print and electronic formats, and translations.
- If figures and/or tables were requested, they may be adapted or used in part.
- Please print this page for your records and send a copy of it to your publisher/graduate school.
- Appropriate credit for the requested material should be given as follows: "Reprinted (adapted) with permission from (COMPLETE REFERENCE CITATION). Copyright (YEAR) American Chemical Society." Insert appropriate information in place of the capitalized words.
- One-time permission is granted only for the use specified in your request. No additional uses are granted (such as derivative works or other editions). For any other uses, please submit a new request.

BACK | CLOSE WINDOW

Copyright © 2018 Copyright Clearance Center, Inc. All Rights Reserved. Privacy statement. Terms and Conditions.
Comments? We would like to hear from you. E-mail us at customercare@copyright.com

Appendix H

Angelica sinensis (Oliver) Diels (Apiaceae)

Artemisia annua Linnaeus (Asteraceae)

Carthamus tinctorius Linnaeus (Asteraceae)

Catharanthus roseus (Linnaeus) George Don (Apocynaceae)

Corydalis yanhusuo W.T. Wang. (Papaveraceae)

Curcuma longa Linnaeus (Zingiberaceae)

Erythroxylum coca Lam (Erythroxylaceae)

Garcinia mangostana Linnaeus (Clusiaceae)

Ginkgo biloba Linnaeus (Ginkgoaceae)

Glycyrrhiza glabra Linnaeus. (Fabaceae)

Pseudolarix kaempferi (Lindl.) Gordon (Pinaceae)

Salix cinerea Linnaeus (Salicaceae)

Schisandra chinensis Turczaninow (Schisandraceae)

Trifolium pratense Linnaeus (Fabaceae)

Zingiber officinale Roscoe (Zingiberaceae)

10. VITA

NAME: Yang Liu

EDUCATION: Master of Science, Botany, Key Laboratory of Forest Plant Ecology, Ministry of Education, Harbin, China, 2010

Bachelor of Science, Biological Science, College of Life Sciences, Northeast Forestry University, Harbin, China, 2007

TEACHING: Teaching Assistant, College of Pharmacy, University of Illinois at Chicago, 2012 – 2014

PROFESSIONAL MEMBERSHIPS: American Society of Pharmacognosy member, 2014-present

Controlled Release Society–Illinois Student Chapter, 2014-present

AAAS/Science member, 2015-present

HONORS: USP Global Fellowship (United States Pharmacopeial Convention)

Jerry McLaughlin Student Travel Award (American Society of Pharmacognosy)

W.E. van Doren Scholar (University of Illinois Foundation)

Myron Goldsmith Scholar (University of Illinois at Chicago)

UIC Student Travel Presenter's Award (UIC Graduate College)

UIC Graduate Student Council Travel Award (UIC Graduate Student Council)

ABSTRACTS: **Liu, Y.**, Friesen, J.B., Grzelak, E.M., Fan, Q.F., Tang, T., Durić, K., Simmler, C., McAlpine, J.B., Chen, S.N., and Pauli, G.F.**,

Matching Sweet Spots: Refining a TLC-Based Countercurrent Solvent system selection Strategy. 9th International Conference on Countercurrent Chromatography, Chicago, IL. 2016.

Duric, K., **Liu, Y.**, Phansalkar R., McAlpine, J.B., Friesen, J.B., Pauli, G.**, and Chen, S.N., Mass Balance and Stability Study of Ligustilide as bioactive Marker of *Angelica sinensis* and Other Apiaceaous Botanicals, American Society of Pharmacognosy 2016 Annual Meeting, Copenhagen, Denmark. 2016.

Grzelak, E.M., **Liu, Y.**, Lankin D.C., Nam, J.W., Friesen, J.B., Chen, S.N., McAlpine J.B., Chen, S.N., Suh, J.W., Yang, S.H., Cheng, J., Lee H., Kim, J.Y., Cho, S.H., Pauli, G.F., Franzblau, S.G., and Jaki, B.U., Rapid Detection and Targeted Isolation of Anti-Tuberculosis Lead Compounds from Actinomycetes by (HP)TLC-Bioautography - MS/NMR., 10th International Symposium on Chromatography of Natural Products, Lublin, Poland. 2016.

Liu, Y. *, Garzon, J. *, Friesen, J.B., Lankin D.C., McAlpine, J.B., Chen, S.N., and Pauli, G.**, Recovery of Metabolites from Natural Deep Eutectic Solvent Matrices by Countercurrent Separation, American Society of Pharmacognosy 2015 Annual Meeting, Copper Mountain, CO. 2015.

Liu, Y., Friesen, J.B., McAlpine, J.B., Chen, S.N., and Pauli, G.**, The Generally Useful Estimate of Solvent Systems Method Enables the Rapid Separation of Curcuminoids by Countercurrent Separation, American Society of Pharmacognosy 2015 Annual Meeting, Copper Mountain, CO. 2015.

Grzelak, E.M.*, **Liu, Y.***, Nam, J.W., Friesen, J.B., Chen, S.N., Lankin D.C., McAlpine J.B., Suh, J.W., Yang, S.H., Cheng, J., Lee H., Kim, J.Y., Cho, S.H., Pauli, G.F., Franzblau, S.G., and Jaki, B.U. TLC-Bioautography Linked with GUESS: A Truly Targeted Active Compound Isolation Process, American Society of Pharmacognosy 2015 Annual Meeting, Copper Mountain, CO. 2015.

Liu, Y., Chen, S.N., McAlpine, J.B., Klein L.L., Friesen, J.B., Lankin, D.C., and Pauli, G.**, Quantification of a Botanical Negative Marker without an Identical Standard: Ginkgotoxin in *Ginkgo Biloba*, American Society of Pharmacognosy 2014 Annual Meeting, Oxford, MS. 2014.

Liu, Y., Klein L., Friesen, J.B., McAlpine, J.B, Lankin, D.C., Chen, S.N., and Pauli, G.F.**, Guess Again: Development of a Countercurrent-based Threshold Assay for Ginkgotoxin Isomers. 8th International Conference on Countercurrent Chromatography, London, UK. 2014.

Zhang, Y., **Liu, Y.**, Buhrman, J. and Gemeinhart, R.A.*. Exploring Redox Responsive Polymeric Drug Delivery System for Codelivery of Hydrophobic Drug and Silencing RNAs. College of Pharmacy Research Day, Chicago, IL. 2014.

Liu, Y., Klein, L., Chen, S.N., Dong, S.H., McAlpine, J.B., Lankin, D.C., Friesen, J.B., Napolitano, J., and Pauli, G.F.**, Synthesis of Ginkgotoxin – toward a Pharmacopeial Safety Assay. 51st MIKI Meeting, Twin Cities, MN. 2013.

Senyuk, V.*, Zhang, Y.*, **Liu, Y.**, Ming, M., Premanand, K., Zhou, L., Chen, P., Chen, J., Rowley, J., Nucifora, G., and Qian, Z.**. A Critical Role of Mir-9 in Myelopoesis and EVI1-Induced Leukemogenesis. 54th ASH Annual Meeting and Exposition, Atlanta, GA. 2012.

PUBLICATIONS: **1 Liu Y.**, Zhang Y., Chen, S.N., Friesen J.B., Nikolić D., Choules M.P., McAlpine J.B., Lankin, D.C., Gemeinhart R.A., and Pauli, G.F. The influence of natural deep eutectic solvents on bioactive natural products: studying interactions between a hydrogel model and *Schisandra chinensis* metabolites. Fitoterapia. 2018, In Press.

2 Liu Y., Friesen J.B., McAlpine, J.B. Lankin, D.C., Chen, S.N., and Pauli, G.F. Natural Deep Eutectic Solvents: Properties, Applications, and Perspectives. Journal of Natural Products, 2018, 81 (3): 679–690.

3 Liu Y., Friesen J.B., Grzelak, E.M., Fan, Q., Tang, T., Durić, K., Jaki, B.U., McAlpine, J.B., Franzblau, S.G., Chen, S.N., and Pauli, G.F. Sweet Spot Matching: A TLC-based Countercurrent Solvent System Selection Strategy. Journal of Chromatography A, 2016 CCC special issue, 2017, 1504:46-54.

4 Liu Y., Garzon, J., Friesen, J.B., Zhang, Y., McAlpine, J.B., Lankin, D.C., Chen, S.N., Pauli, G.F. Countercurrent assisted quantitative recovery of metabolites from plant-associated natural deep eutectic solvents. Fitoterapia. 2016, 112:30-37.

5 Liu, Y., Friesen, J.B., Klein, L.L., McAlpine, J.B., Lankin, D.C., Pauli, G.F., and Chen, S.N. The Generally Useful Estimate of Solvent Systems (GUESS) method enables the rapid purification of methylpyridoxine regioisomers by countercurrent chromatography, Journal of Chromatography A, 2015, 1426: 248-251.

6 Liu, Y., Friesen, J.B., McAlpine, J.B., and Pauli, G.F. Solvent System Selection Strategies in Countercurrent Separation, Planta Medica, 2015, 81: 1-10.

7 Liu, Y., Chen, S.N., McAlpine, J.B., Klein, L.L., Friesen, J.B., Lankin, D.C., and Pauli, G.F. Quantification of a botanical negative marker without an identical standard: ginkgotoxin in *Ginkgo biloba*, Journal of Natural Products, 2014, 77(3):611-617.

8 Fan Q.F., **Liu Y.,** Kulakowski D., Chen, S.N., Friesen, J.B., Pauli, G.F., Song Q.S. Countercurrent separation assisted identification of two mammalian steroid hormones in *Vitex negundo.* Journal of Chromatography A, 2018, 1553: 108-115.

9 Zhang, Y., Buhrman, J.S., **Liu, Y.**, Rayahin, J.E., Gemeinhart, R.A. Reducible Micelleplexes are Stable Systems for Anti-miRNA Delivery in Cerebrospinal Fluid. Molecular Pharmaceutics. Molecular Pharmaceutics. 2016;13(6):1791-1799.

10 Zhang, Y., **Liu, Y.**, Sen, S., Rálcd, P and Gemeinhart, R.A. Charged Group Surface Accessibility Determines Micelleplexes Formation and Cellular Interaction, Nanoscale, 2015, 17(7):7559-7564.

11 Senyuk, V., Zhang, Y., **Liu, Y.**, Ming, M., Premanand, K., Zhou, L., Chen, P., Chen, J., Rowley, J., Nucifora, G., and Qian, Z. A critical role of miR-9 in myelopoesis and EVI1-induced leukemogenesis, Proceedings of the National Academy of Sciences, 2013, 110 (14): 5594-5599.